MECHANICAL BEHAVIOR OF MATERIALS

B.TECH, 5th SEMESTER

LECTURES NOTE

BY

Mrs. SAHUKARI NAGAMANI

DEPARTMENT OF METALLURGICAL AND MATERIALS ENGINEERING

PARALA MAHARAJA ENGINEERING COLLEGE, BERHAMPUR

Disclaimer

This document does not claim any originality and cannot be used as a substitute for prescribed textbooks. The information presented here is merely a collection by the committee faculty members for their respective teaching assignments as an additional tool for the teaching-learning process. Various sources as mentioned at the reference of the document as well as freely available material from internet were consulted for preparing this document. The ownership of the information lies with the respective authors or institutions. Further, this document is not intended to be used for commercial purpose and the committee faculty members are not accountable for any issues, legal or otherwise, arising out of use of this document. The committee faculty members make no representations or warranties with respect to the accuracy or completeness of the contents of this document and specifically disclaim any implied warranties of merchantability or fitness for a particular purpose.

MTPC3002 MECHANICAL BEHAVIOUR OF MATERIALS (3-0-0)

Course Objective:

To obtain knowledge of the various mechanical properties exhibited by various materials, namely strength, fracture, fatigue and creep. To obtain insight into the different mechanical properties of materials under engineering applications.

Module-I (06 hrs)

Theory of elasticity and plasticity, stress-strain relationship,Types of dislocations, their geometrical and elastic properties, Application of dislocation theory to strengthening mechanism and yield point, Strain ageing and work hardening phenomena.

Module-II (06 hrs)

Fracture: Fracture behaviour, Griffith`s theory, linear elastic fracture mechanics, fractography, Ductile to brittle transition, Transition temperature phenomena, Factors affecting transition temperature, fracture toughness, strain energy release rate, Stress concentration, stress intensity factor, Crack growth criteria, Mode of deformation, Environment-assisted fracture.

Module-III (06 hrs)

Fatigue: Introduction to Fatigue, stress cycles, Cyclic stress-strain behaviour - low and high cycle fatigue, S-N curve, structure feature of fatigue, Fatigue crack propagation, Paris law, Effect of mean stress, stress concentration, size, surface, metallurgical variables and temperature on fatigue.

Module-IV (06 hrs)

Creep: Introduction to creep, Creep Curve, Stress Rupture Test, Structural Changes During Creep, Mechanism of Creep deformation, Power Law, Deformation Mechanism Maps, Effect of temperature on creep, Superplasticity, Parametric methods for Prediction of Long Time Properties.

Module-V (06 hrs)

Torsion Test: Mechanical Properties in Torsion, Torsional Stresses for Large Plastic Strains, Types of Torsion Failure, Tension Test Vs. Torsion Test, Hot Torsion Testing.

Impact Test: Notched Bar Impact Tests, Instrumented Charpy Test, Significance of Transition Temperature Curve, Metallurgical Factors affecting Transition Temperature Fracture.

Text Books:

1. Mechanical Metallurgy, G.W. Dieter
2. Mechanical Behaviour of Materials, M. A. Meyers and K. K. Chawla

Reference Books:

1. Mechanical Behaviour of Materials, William F. Hosford
2. Introduction to Dislocations, D. Hull and D.J. Bacon
3. Deformation Behaviour and Fracture Mechanics of Engineering Materials, R. W. Hertzberg
4. Mechanical Behaviour of Materials, Courtney

Strengthening mechanisms

Subjects of interest

- *Introduction/Objectives*
- *Grain boundary strengthening*
- *Yield-point phenomenon*
- *Strain ageing*
- *Solid-solution strengthening*
- *Strengthening from second phase particles*
- *Martensitic strengthening*
- *Strain hardening or cold working*
- *Bauschinger effect*
- *Preferred orientation (texture)*

Objectives

- Different types of strengthening mechanisms in metals which improve mechanical properties will be highlighted in this chapter.
- This also includes the nature of grain boundaries and their effects on the strengthening mechanisms, the influences of solute atoms, second phase particles, and fibre on the strengthening mechanisms.
- Other strengthening mechanisms such as strain hardening, martensitic hardening and cold working on the mechanical properties of the materials will also be discussed.

Introduction

The ability of a metal to plastically deform depends on the ability of dislocations to move.

Strengthening techniques rely on restricting dislocation motion to render a material harder and stronger.

To obtain material strength

Sometimes ductility or toughness are sacrificed.

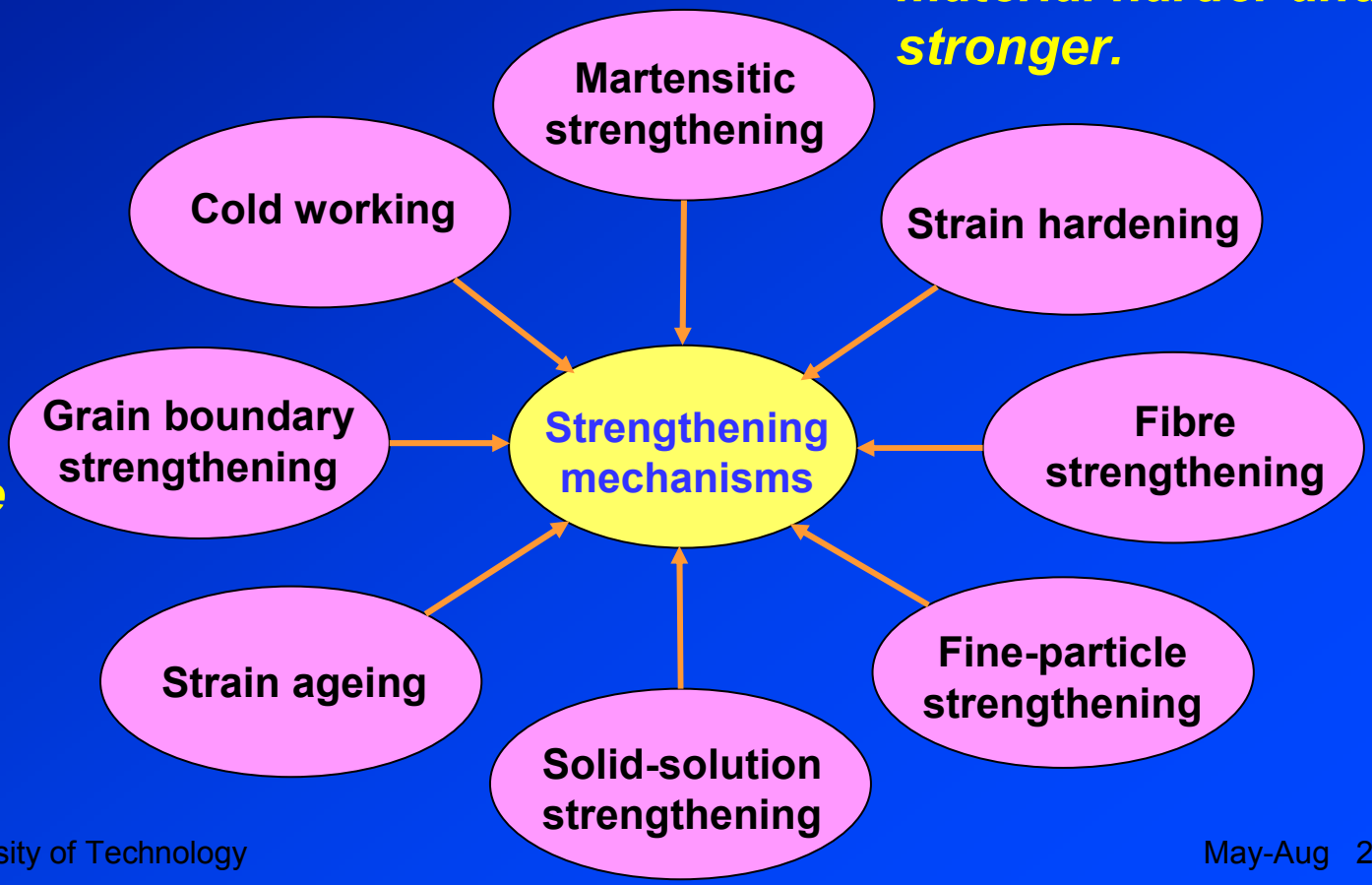

Grain boundary strengthening

Grain boundaries

*Grain boundary separates two grains having **different crystallographic orientations**.*

*Grain boundary structure contains **grain boundary dislocations**, which are not mobile and produce extensive slip.*

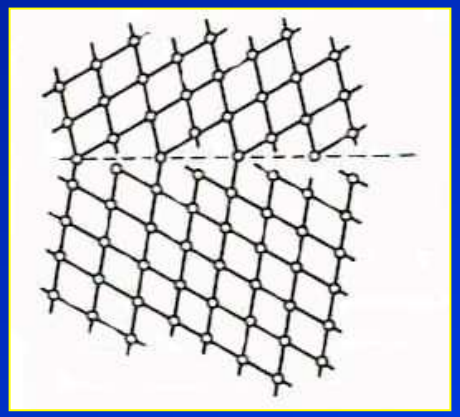

Schematic atomic model of a grain boundary

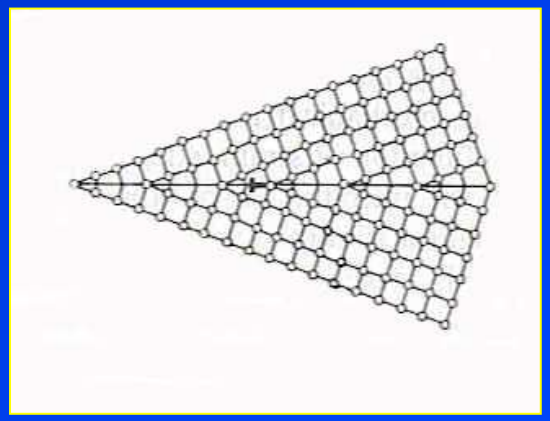

Dislocation model of grain boundary

High and low angle grain boundaries

High - angle grain boundary → high surface energy
Low - angle grain boundary → low surface energy

High energy grain boundary serves as ***preferential sites*** for solid state reactions;

1) Diffusion
2) Phase transformation
3) Precipitation

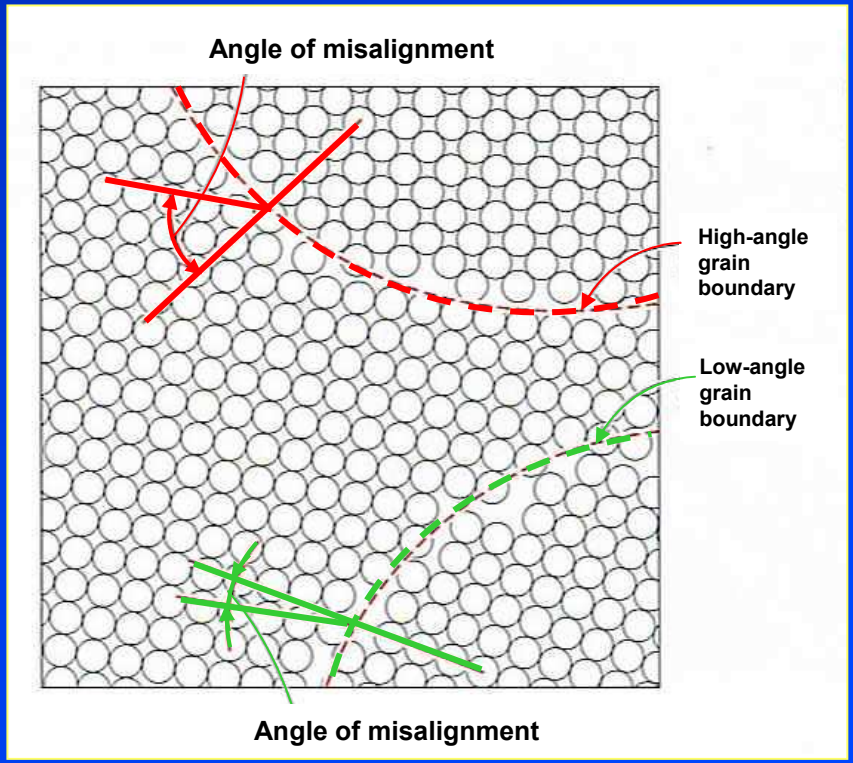

Schematic diagram showing low- and high-angle grain boundaries.

Low angle grain boundaries

- Along the boundary the ***atoms adjust their position*** by localised deformation to produce a smooth transition from one grain to the other.
- Where the atom planes end on the grain boundaries, it is therefore considered to have ***an array of dislocations***.
- The ***angular difference*** in orientation between the grain is θ.

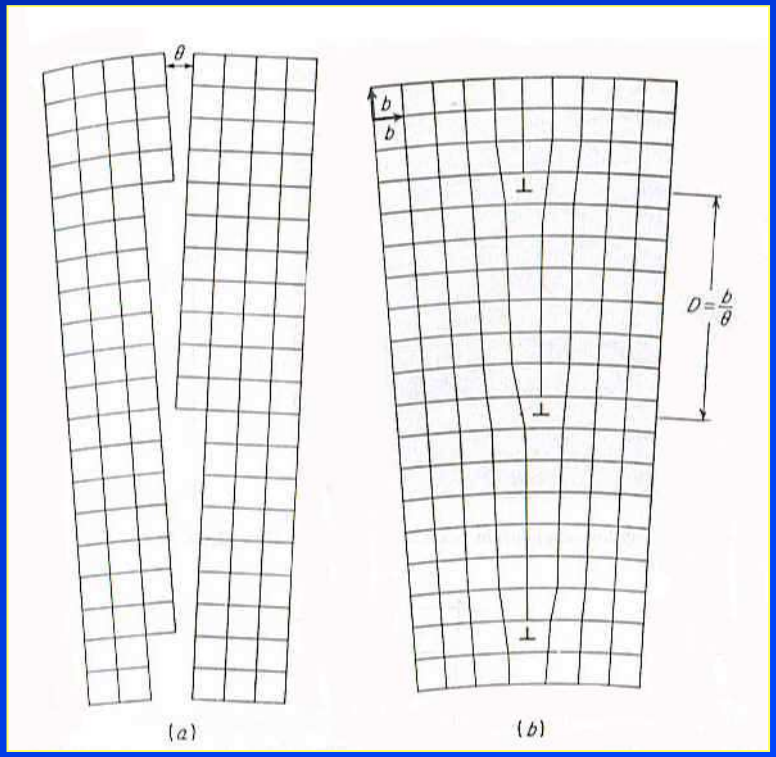

Diagram of low-angle grain boundary

Subgrain boundaries

Subgrain boundaries are ***low-angle boundaries***, with ***lower-energy boundaries*** than the grain boundaries. → therefore etch less readily than grain boundaries.

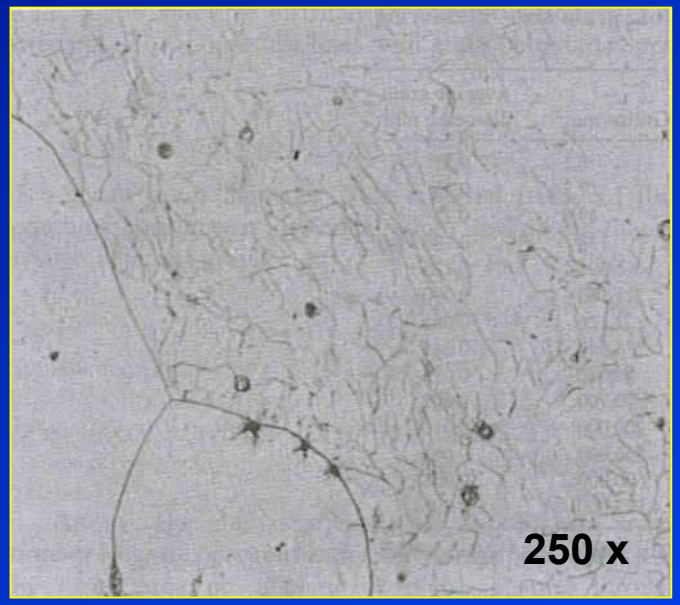

Subgrain boundary network in Fe-3% alloy.

If the angle θ is small the distance between dislocation is large. It is often possible to observe ***pits*** (corresponding to sites for ***edge dislocations***) along the boundaries, see *fig*.

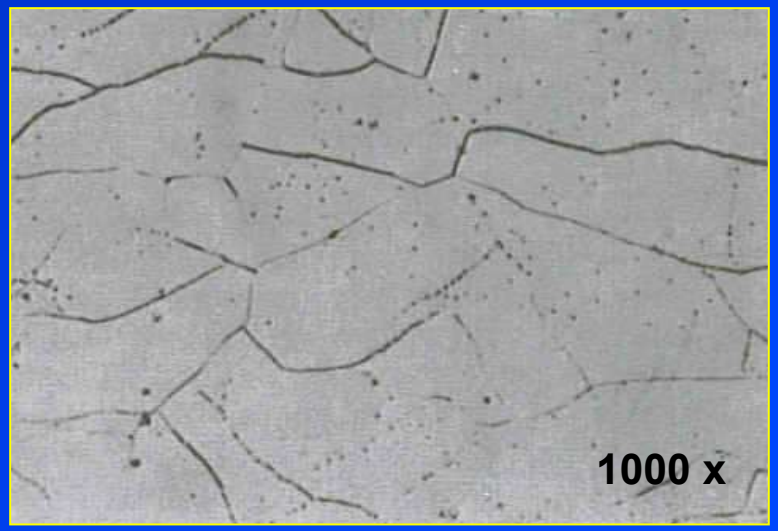

***Etch-pit structures along low-angle grain boundaries* in Fe-Si alloy.**

Polygonization

- ***Polygonization*** occurs when a single crystal is bent to a relatively small curvature and then annealed.
- Bending results in an excess number of dislocations of similar sign distributing along the bend-glide plane.
- After heating, dislocations group themselves into the lower-energy configuration of a low-angle boundary, forming a ***polygonlike network***.

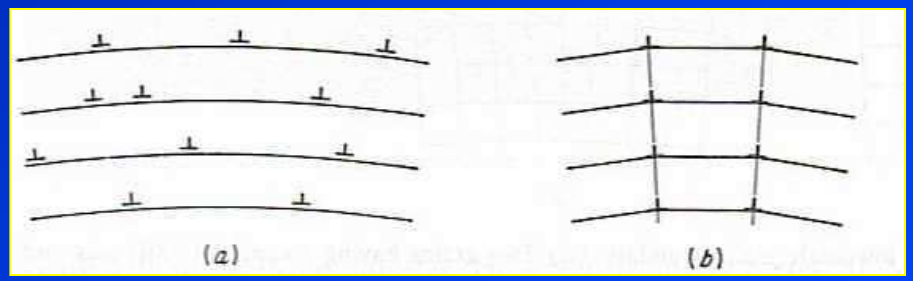

Movement of dislocations to produce polygonization.

Deformation of grain boundaries.

- Discontinuity due to grain boundaries leads to ***more complex deformation mode*** in polycrystals than in single crystals.
- Individual grain is constrained since mechanical integrity and coherency are maintained along the grain boundaries, causing different deformation between neighbouring grains.
- A polycrystal macroscopically deforms as the stress is applied. Slips operate in each grains which produces ***overlaps*** and ***voids*** at boundaries, *fig (a),(b).*
- These overlaps and voids can be corrected by introducing ***geometrically necessary dislocations*** at (c),(d).

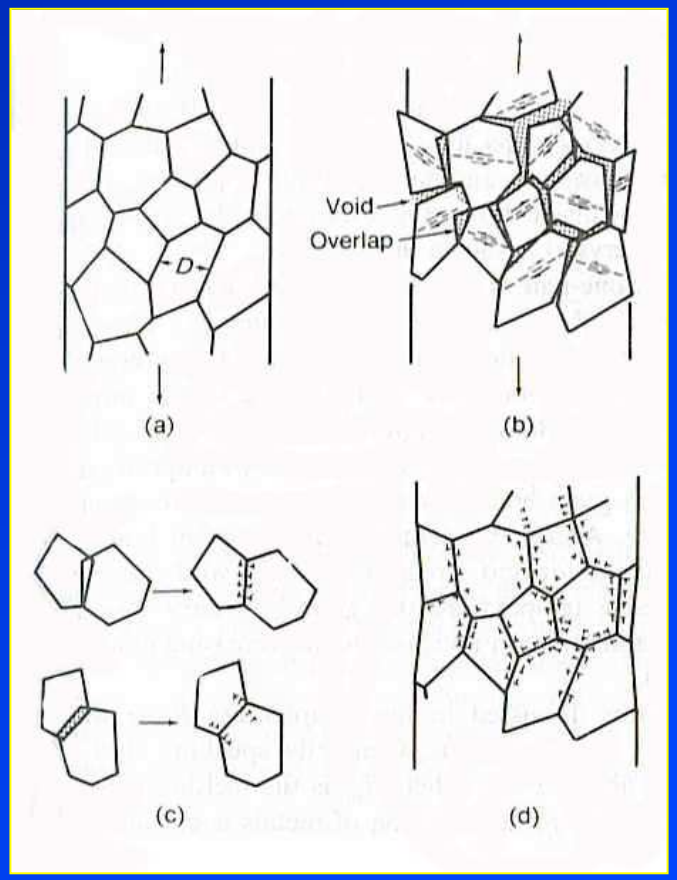

Ashby's model of deformation of a polycrystal.

Plastic deformation of polycrystalline metals

- Due to random crystallographic orientations of the numerous grains, the direction of ***slip varies from one gain to another***.
- *Fig.* shows two slip systems operate in each grain and variation in grain orientation is indicated by the ***different alignment of slip lines***.

<u>Note:</u> More slip systems are usually operate near the grain boundary, the material is usually harder near the boundary than the grain interior.

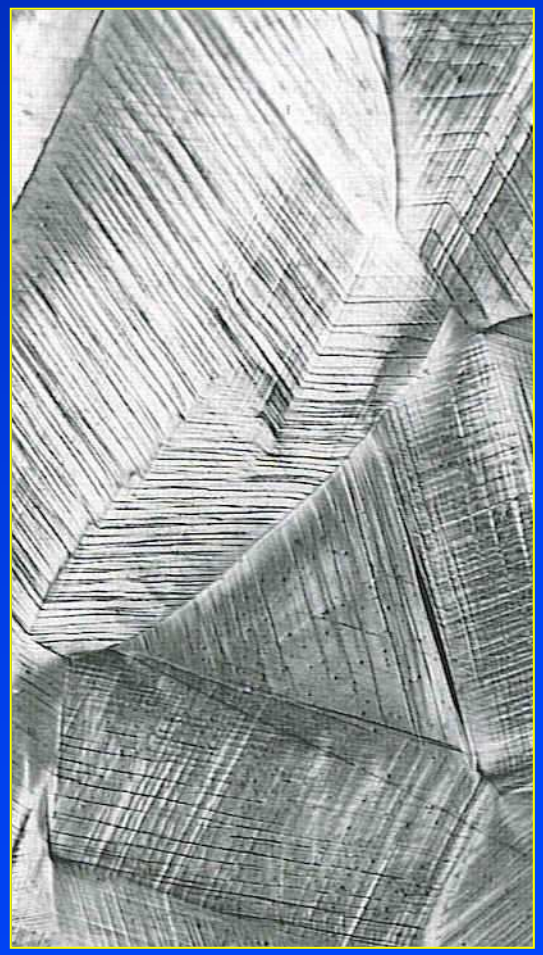

Slip lines on the surface of a deformed polycrystalline copper

Grain boundary sliding

At $T > 0.5T_m$, deformation can occur by sliding along the grain boundaries.

Temperature ↑

Strain rate ↓

→ ***Tendency for grain boundary sliding (as in creep).***

Equicohesive temperature

Above the ***equicohesive temperature***, the grain boundary region is weaker than the grain interior.

→ ***Strength increases with increasing grain size.***

Strengthening from grain boundaries

There are two important roles of the grain boundary which acts as a barrier to dislocation motion;

1) Difficulty for a dislocation to pass through ***two different grain orientations*** (need to change direction).
2) The atomic disorder within a grain boundary region contributes to a ***discontinuity of slip planes from one grain to another***.

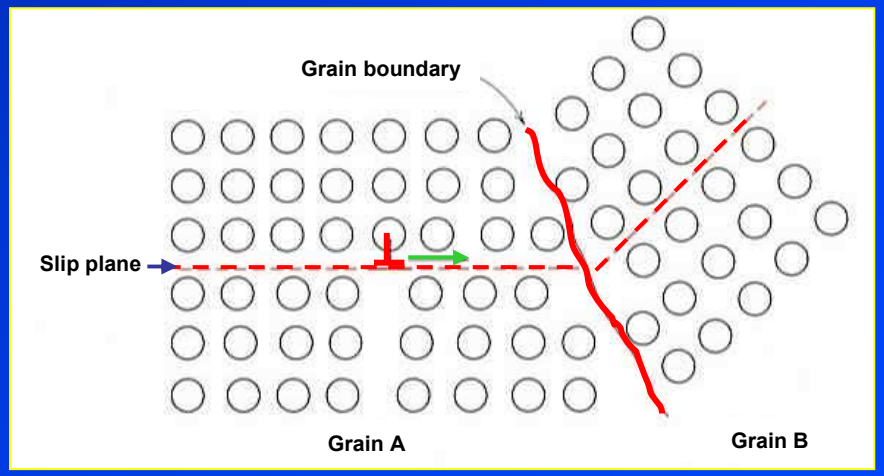

The motion of a dislocation as it encounters a grain boundary.

Hall-Petch relation

A fine-grained material is harder and stronger than one that is coarse grained since greater amounts of grain boundaries in the fine-grained material impede dislocation motion.

The general relationship between the ***yield stress*** (tensile strength) and ***grain size*** was proposed by ***Hall*** and ***Petch***.

$$\sigma_o = \sigma_i + kD^{-1/2} \qquad \text{...Eq. 1}$$

Where σ_o = the yield stress

σ_i = the 'friction stress' or resistance to dislocation movement

k = the 'locking parameter' or hardening contribution from grain boundary.

D = grain diameter

Hall - Petch relation and dislocation pile-up model

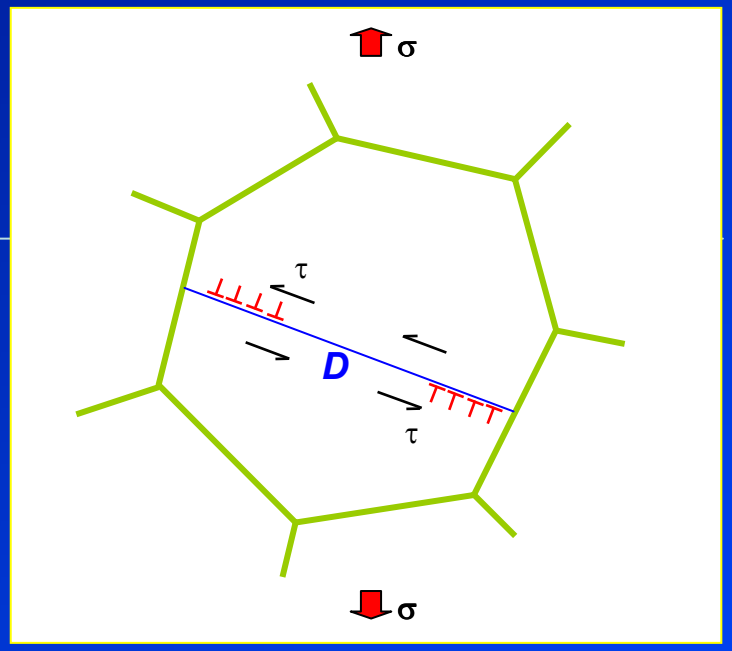

- The ***dislocation model*** for the ***Hall-Petch equation*** was originally based on the idea that grain boundaries act as ***barriers*** to dislocation motion.
- Dislocations will be sent out from the source at the centre of a grain of ***D*** diameter to ***pile up*** at grain boundary.
- The number of dislocations at the pile-up is

$$n = \frac{k\pi\tau_s D}{4Gb} \qquad \ldots Eq.\ 2$$

Where τ_s is the average resolved shear stress

k is a factor close to unity

The ***stress at the tip of the pile-up*** must exceed some critical shear stress τ_c to continue slip past the grain-boundary barrier

Then

$$\tau_c = n\tau_s = \frac{\pi\tau_s^2 D}{4Gb}, \quad \tau_s = \tau - \tau_i$$

$$\tau = \tau_i + \left(\frac{\tau_c 4Gb}{\pi D}\right)^{1/2}$$

$$\tau = \tau_i + kD^{-1/2} \qquad \ldots Eq.\ 3$$

Note: for large pile-ups

Grain size determination

• Since the size of the grain is usually associated with mechanical properties of the materials, determination of the grain size is therefore of importance.

• ***There are a number of techniques utilised for grain size measurement;***

1) Intercept method
2) ASTM standard comparison charts (grain number)
3) Image analyser

• ***The obtained parameters can be specified in terms of;***

1) Average grain volume
2) Average grain diameter
3) Average area
4) Maximum diameter
5) Minimum diameter
6) Aspect ratio

Intercept method

Intercept method *is carried out by measuring the mean number of intercepts of random test lines with grain boundaries per unit length of test line* N_L.

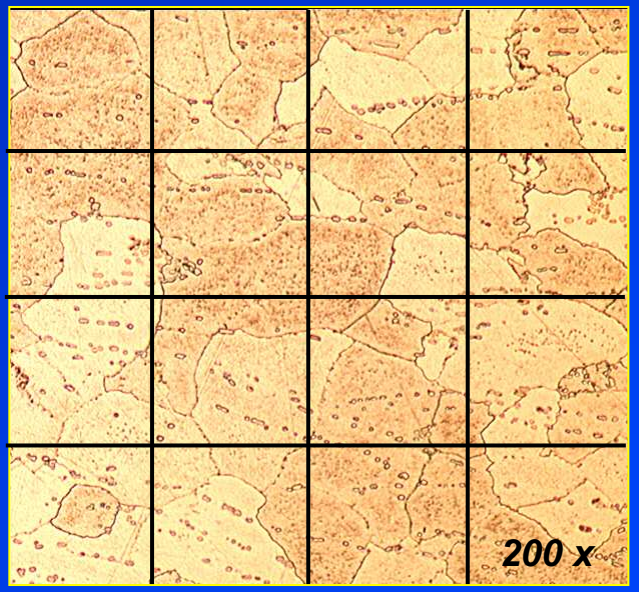

- Strength lines of the same length ***L*** are drawn though several photomicrograph with a known scale.
- The grain intersected N_L by each line segment are counted.
- The ***average grain diameter*** is obtained by

$$D = \frac{L}{N_L M}$$

…Eq. 4

Where ***M*** is a ***linear magnification*** of the photomicrograph.

<u>Note:</u> The grain size obtained by this method will be somewhat ***smaller*** *than the actual grain size. In some case, a factor 2/3 is used.*

ASTM standard comparison chart

Comparison of the grains at a fixed magnification with the ***American Society for Testing and Materials (ASTM)*** *grain size charts.*

The ***ASTM*** grain-size number ***G*** is related to n_a, the number of grains per mm^2 at a magnification of 1 x by the relationship

$$G = -2.9542 + 1.4427 \ln n_a$$

…Eq. 5

Table 6-1 Comparison of grain-size measuring systems†

ASTM no.	Grains/mm²	Grains/mm³	Average grain diameter, mm
−1	3.9	6.1	0.51
0	7.8	17.3	0.36
1	15.5	49.0	0.25
2	31.0	138	0.18
3	62.0	391	0.125
4	124	1,105	0.090
5	248	3,126	0.065
6	496	8,842	0.045
7	992	25,010	0.032
8	1,980	70,700	0.022
9	3,970	200,000	0.016
10	7,940	566,000	0.011
11	15,870	1,600,000	0.008
12	31,700	4,527,000	0.006

† "Determining the Standard Grain Size," ASTM Standard E112, 1985.

Example: *If a steel has a value of σ_i = 150 MPa and **k** = 0.70 MPa.m$^{1/2}$, what is the value of the yield stress if the grain size is ASTM no.6.*

From *Eq.6*

$$\ln n_a = (G + 2.9542)/1.4427$$

$$n_a = \exp\left(\frac{6 + 2.9524}{1.4427}\right) = 496 \ \ mm^{-2} \ \ = 496 \times 10^6 \ \ m^{-2}$$

Grain diameter

$$D \approx \sqrt{1/n_a} \ \ or \ \ D^2 \approx 1/n_a$$

$$D^2 \approx 20 \times 10^{-10} \ \ m^2, \ \ D \approx 44.7 \times 10^{-6} m$$

$$\frac{1}{\sqrt{D}} = 149 \ \ m^{-1/2}$$

$$\sigma_o = \sigma_i + kD^{-1/2} = 150 + (0.70)(149) = 254.3 \ \ MPa$$

Yield point phenomenon

*Metals, particularly **low-carbon steel**, show a localised heterogeneous transition from elastic to plastic deformation. → **Yield point elongation**.*

- The load after the ***upper yield point*** suddenly drop to approximately constant value (***lower yield point***) and then rises with further strain.
- The elongation which occurs at constant load is called the ***yield-point elongation***, which are heterogeneous deformation.
- ***Lüder bands*** or stretcher strains are formed at approximately 45° to the tensile axis during yield point elongation and propagate over the specimen.

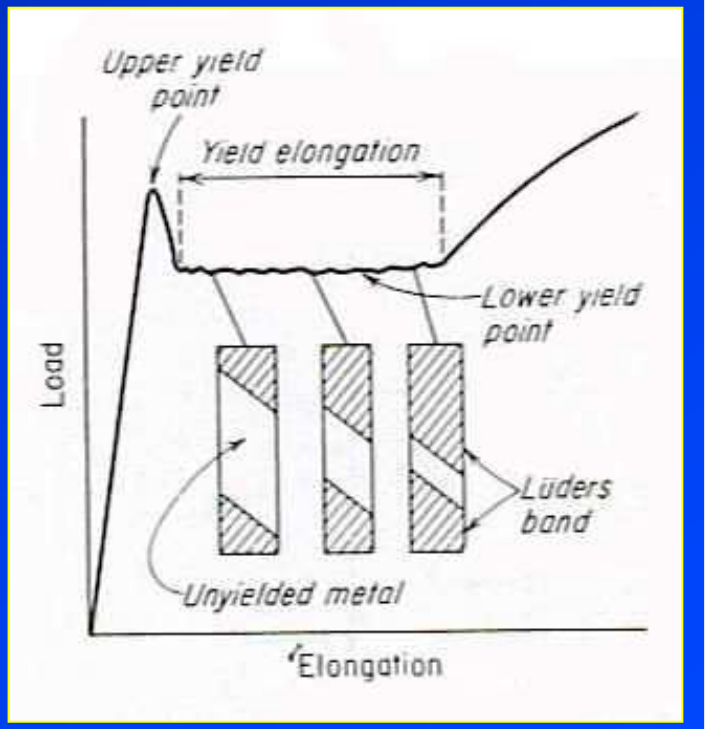

Yield point behaviour in BCC metals

<u>Note:</u> The yield point phenomenon has also been observed in other metals such as Fe, Ti, Mo, Cd, Zn, Al alloys.

The upper yield point

*The **upper yield point** is associated with small amounts of **interstitial** or **substitutional** impurities.*

- The solute atoms (***C*** or ***N***) in low carbon steel, ***lock*** the dislocations, → ***raise the initial yield stress***.
- The breakaway stress required to pull a dislocation line away from a line of solute atoms is

$$\sigma \approx \frac{A}{b^2 r_o^2} \qquad \text{...Eq. 6}$$

Where ***A*** is $4Gba^3\varepsilon$, a is atomic radius
r_o is the distance from the dislocation core to the line of solute atoms ~ 0.2 nm.

- When the dislocation is ***pulled free*** from the solute atoms, slip can occur at lower stress. → the ***lower yield point***.
- The magnitude of the yield-point effect depends on ***interaction energy***, ***concentration of solute atoms***.

Note: Upper yield point is promoted by using elastically rigid machine, careful axial alignment of specimen (free from stress concentrations, high strain rate, low temperature.)

Strain ageing

Strain ageing *is a phenomenon in which the metal* ***increase in strength while losing ductility*** *after being heated at relatively low temperature or cold-working.*

The ***reappearing of the (higher) yield point*** after ageing is obtained, see *fig*.

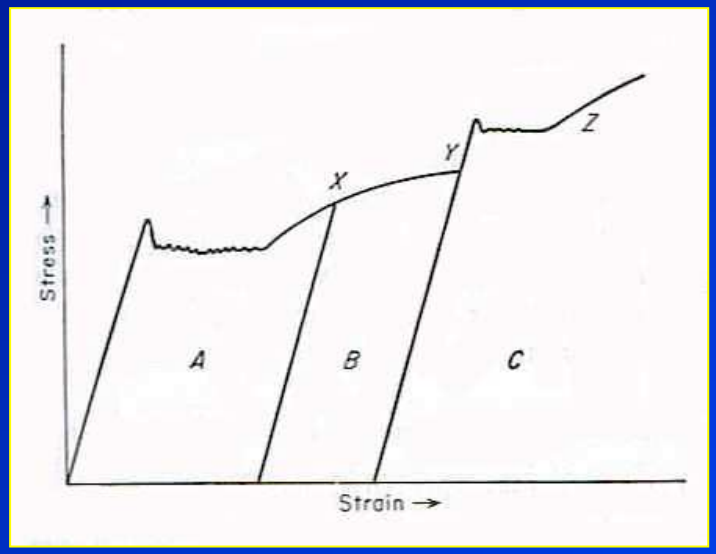

Strain ageing in low-carbon steel.

- Reloading at ***X*** and straining to ***Y*** does not produce yield point.
- After this point if the specimen is reloading after ageing (RT or ageing temp) the ***yield point will reappear*** at a higher value.
- This reappearance of the yield point is due to the ***diffusion of C and N atoms to anchor the dislocations***.
- ***N*** has more strain ageing effect in iron than ***C*** due to a higher ***solubility*** and ***diffusion coefficient***.

Stretcher strains

- **Strain ageing** should be eliminated in **deep drawing steel** since it leads to surface marking or **stretcher strains**.
- To solve the problem, the amount of ***C*** and ***N*** should be lowered by adding elements such as ***Al, V, Ti, B*** to form ***carbides*** or ***nitrides***.

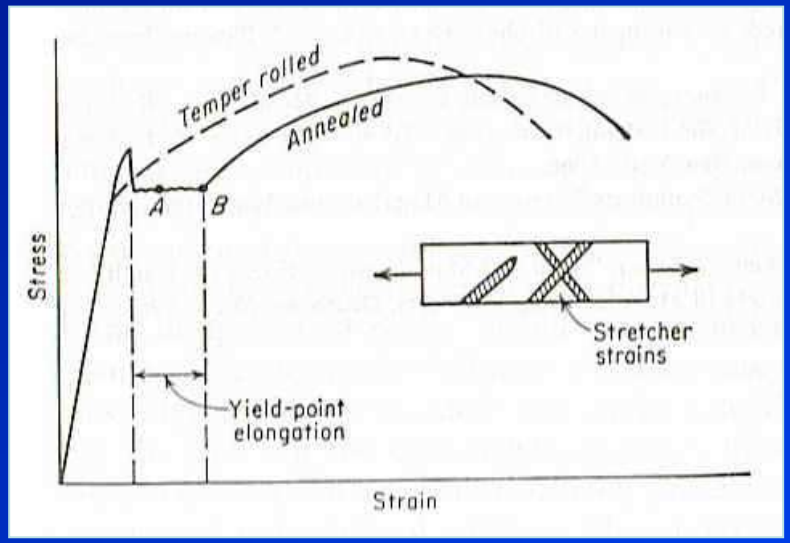

Relation of stretcher strain in stress-strain curve

Stretcher strain in low-carbon steel

Serrated stress strain curves

- Strain ageing increases yield point but ***lower ductility***.
- Strain ageing is also associated with ***serrated stress-strain curves*** or ***repeated yielding***, due to high speed of diffusion of solute atoms to catch and lock dislocations.
- This dynamic strain ageing is also called ***Portevin-LeChatelier effect***.

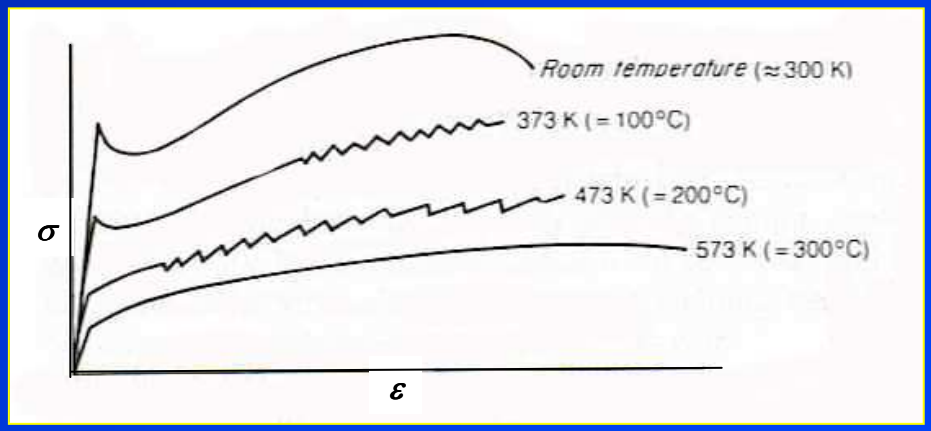

Portevin-LeChaterier effect.

Blue brittleness

Blue brittleness *occurs in plain carbon steel in which* ***discontinuous yielding*** *appears in the temperature range 500 to 650 K.*

During this blue brittleness region, steels show

- Decreased tensile ductility.
- Decreased notched-impact resistance.
- Minimum strain rate sensitivity.

<u>Note:</u> This is just an accelerated strain aging by temperature.

Solid-solution strengthening

Solute atoms are introduced into the matrix (solvent atoms).

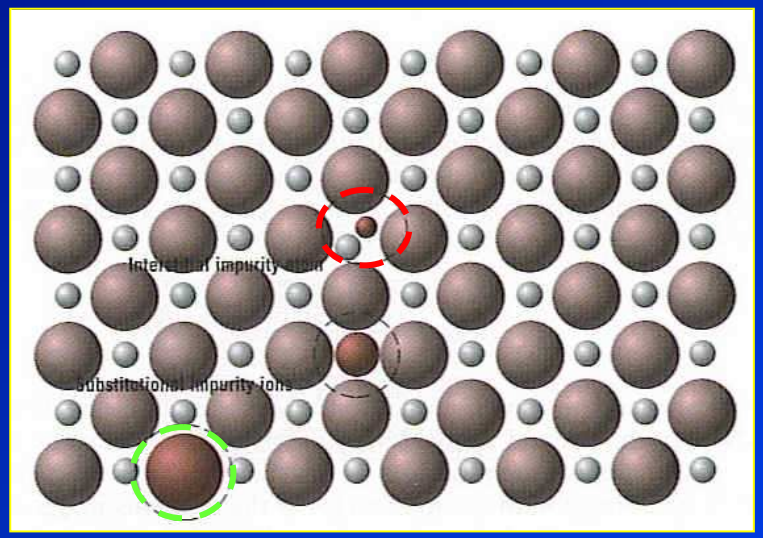

There are two types of solid solutions;

1) ***Substitutional solid solution***: the solute and solvent atoms are ***similar in size***, rendering the solute atoms to occupy lattice point of the solvent atoms.

2) ***Interstitial solid solution:*** The solute atoms are of ***smaller size*** than the solvent atom, rendering the solute atoms to occupy the interstitial sites in the solvent lattice.

Note: solid solution is compositionally homogeneous, the solute (impurity) atoms are randomly distributed throughout the matrix.

Factors affecting solubility of solute atoms

The ***solubility of the solute atoms*** in the host matrix (solvent) can be determined by several factors;

1) ***Atomic size factors :*** Solid solution is appreciable when the difference in atomic radii between the tow atoms is < ***~15%,*** otherwise → creating substantial lattice distortion.
2) ***Crystal structure :*** ***Similar crystal structure*** of metals of both atom types types are preferred.
3) ***Electronegativity :*** The more ***electropositive*** one element and the more ***electronegative*** the other, the more tendency to form an intermetallic compound than solid solution.
4) ***Valences :*** A metal will have more of a tendency to dissolve another metal of ***higher valency*** than one of a lower valency.

Effects of solute alloy additions on stress-stain curve

- The addition of ***solute atoms*** raises the ***yield stress*** and the ***stress-stain curve*** as a whole.
- Therefore from *Eq.1*

$$\sigma_o = \sigma_i + kD^{-1/2}$$

- The ***solute atoms*** should have more influence on the ***frictional resistance to dislocation motion*** σ_i than the locking of dislocation ***k***.

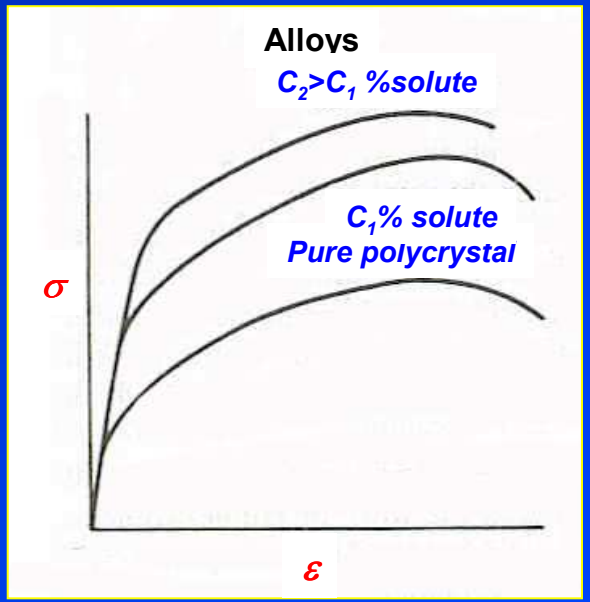

Effects of solute atoms on stress-strain curves.

Solute atoms ⬆ ***Strengthening effect*** ⬆

Effects of solute alloy additions on tensile properties

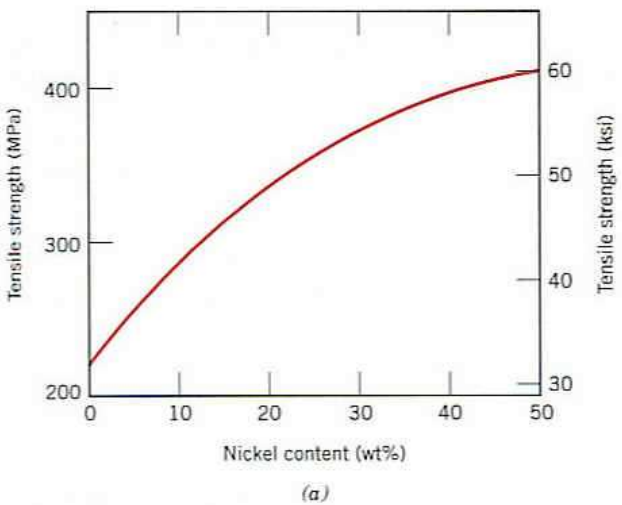

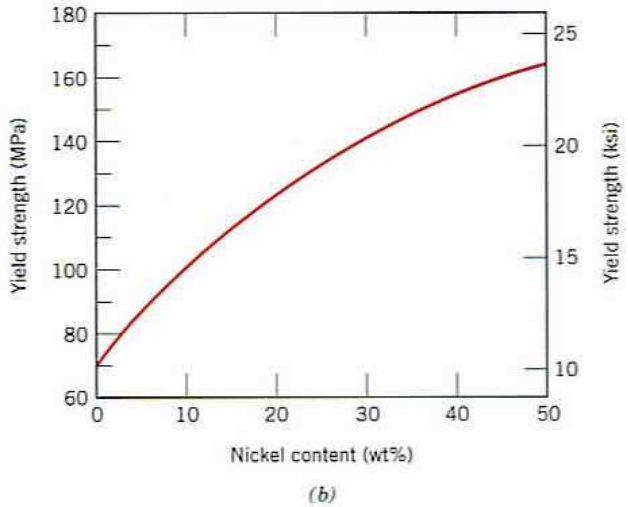

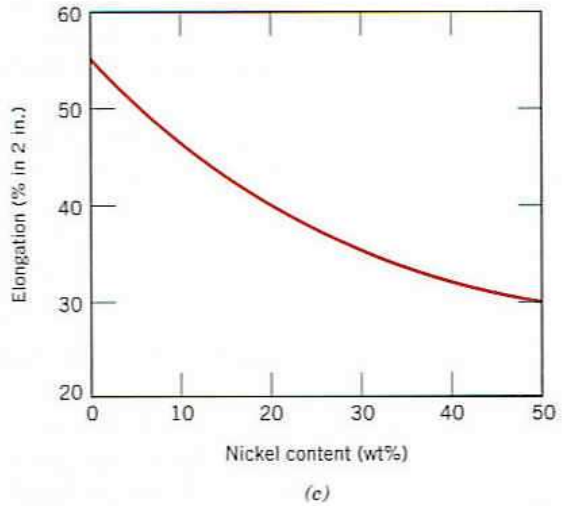

Impurity atoms ⬆

Tensile strength ⬆
Yield stress

Ductility ⬇

Variation with nickel content of (*a*) tensile strength, (*b*) yield strength, and (*c*) ductility (%EL) for copper-nickel alloys, showing strengthening.

Lattice strain due to solute atoms

Lattice strains *produced by the introduction of solute atoms can be divided into:*

1) Tensile lattice strain

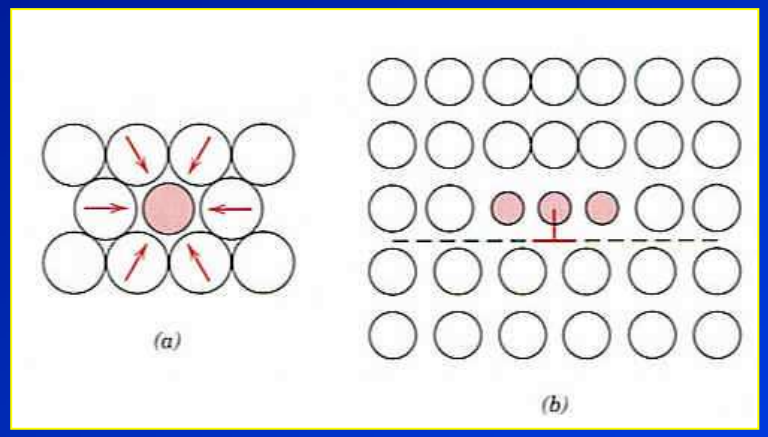

Smaller solute atoms are introduced, imposing tensile lattice strain to the host atoms.

2) Compressive lattice strain

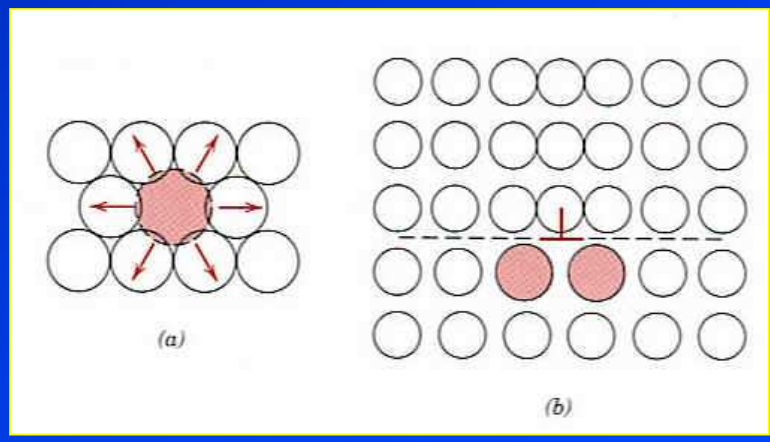

Larger solute atoms are introduced, imposing compressive lattice strain to the host atoms.

Interactions between solute atoms and dislocations

Solute atoms can interact with dislocations by the following mechanisms:

1) ***Elastic interaction***
2) ***Modulus interaction***
3) ***Stacking-fault interaction***
4) ***Electrical interaction***
5) ***Short-range order interaction***
6) ***Long-range order interaction***

<u>Note:</u> 1, 2, 6 are insensitive to temperature and influence at about $0.6T_m$.

Elastic interaction

• Strengthening due to elastic interaction is proportional to the ***misfit between solute atoms and dislocations*** giving elastic field around surrounding them.

Modulus interaction

• The presence of the solute atom locally alter the modulus of the crystal. Solute atom with ***small shear modulus*** will reduce the energy of the strain field.

Stacking-fault interaction

Solute atoms within the stacking fault ↑

Stacking fault energy ↓

Separation between partial dislocations ↑

Electrical interaction

• The solute atoms having charge can interact with dislocation which have electrical dipoles. → ***weak***.

Short-range order interaction

• Strengthening by short-range order interaction is due to more work which has to put in when dislocations try to move pass through the short range ordered atoms.

Long-range order interaction

• Alloys having a long-range periodic arrangement of dissimilar atoms develop ***superlattice***. The stress required to move a dislocation through a long-range region is high and the rate of ***strain hardening*** is higher in the ordered condition than the disordered state.

Strengthening from second phase

Many commercial alloys are composed of two or more metallurgical phases which provide strengthening effects:

- **Two phase aggregates**
- **Second phase/intermetallic particles**
- **Precipitation hardening**
- **Fibering structure**

Note: *1)These are heterogeneous on a microscopic scale or maybe homogeneous on a macroscopic scale.*

2) Strengthening from second phases is normally additive to the solid solution strengthening produced in the matrix.

Strengthening by two-phase aggregates

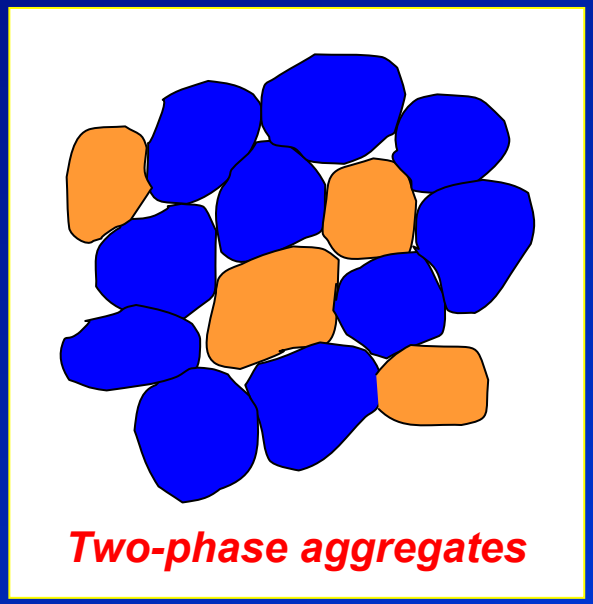

Two-phase aggregates

The size of the second phase particles are of similar size to that of the matrix.

Examples ;

- Beta brass particles in an alpha brass matrix
- Pearlite colonies in the ferrite matrix in annealed steels

Strengthening by second phase particles

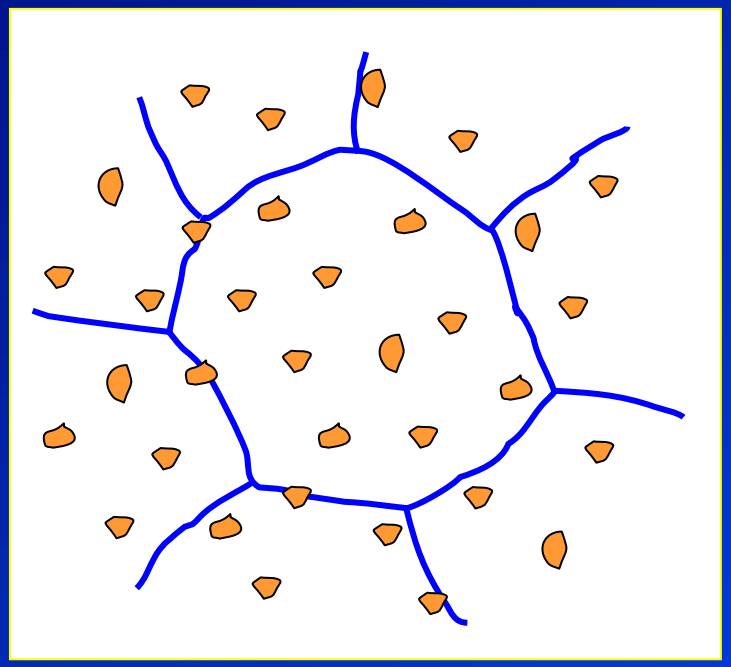

Dispersed second-phase particles in the matrix.

- The ***second phase or intermetallic particles*** are much finer (down to submicroscopic dimensions) than the grain size of the matrix.
- The second phase particles produce ***localised internal stresses*** which alter the ***plastic properties*** of the matrix.

Examples ;

- Second phase particles in matrix.

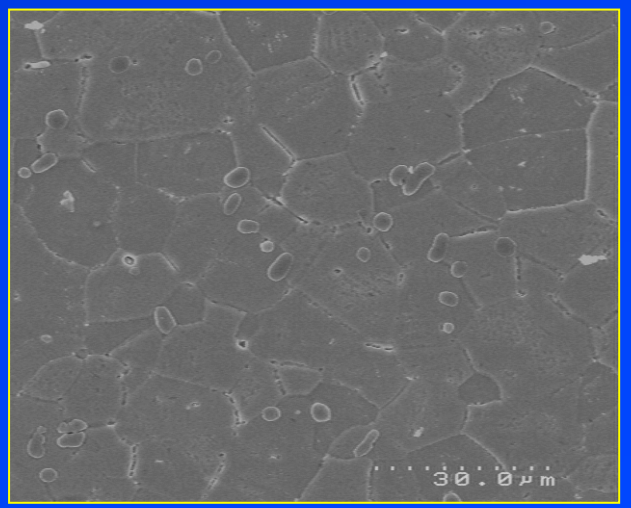

Factors influencing second-phase particle strengthening

Particle size

Particle shape

Number (V_f)

Distribution (interparticle spacing)

Strength

Ductility

Strain hardening

<u>Note:</u> Its almost impossible to vary these factors independently in experiments.

If the contributions of each phase are independent, the properties of the multiple phase alloy is the summation of a weighted average of individual phases.

For example;

Stress $\sigma_{avg} = V_1\sigma_1 + V_2\sigma_2 + ...V_n\sigma_n$ *…Eq. 7*

Strain $\varepsilon_{avg} = V_1\varepsilon_1 + V_2\varepsilon_2 + ...V_n\varepsilon_n$ *…Eq. 8*

Where the volume fraction ***V***

$V_1 + V_2 + ... + V_n = 1$

Estimate flow stress of two-phase alloy

• The average property in the ***two-phase alloy*** will increase with the volume fraction V_f of the strong phase.

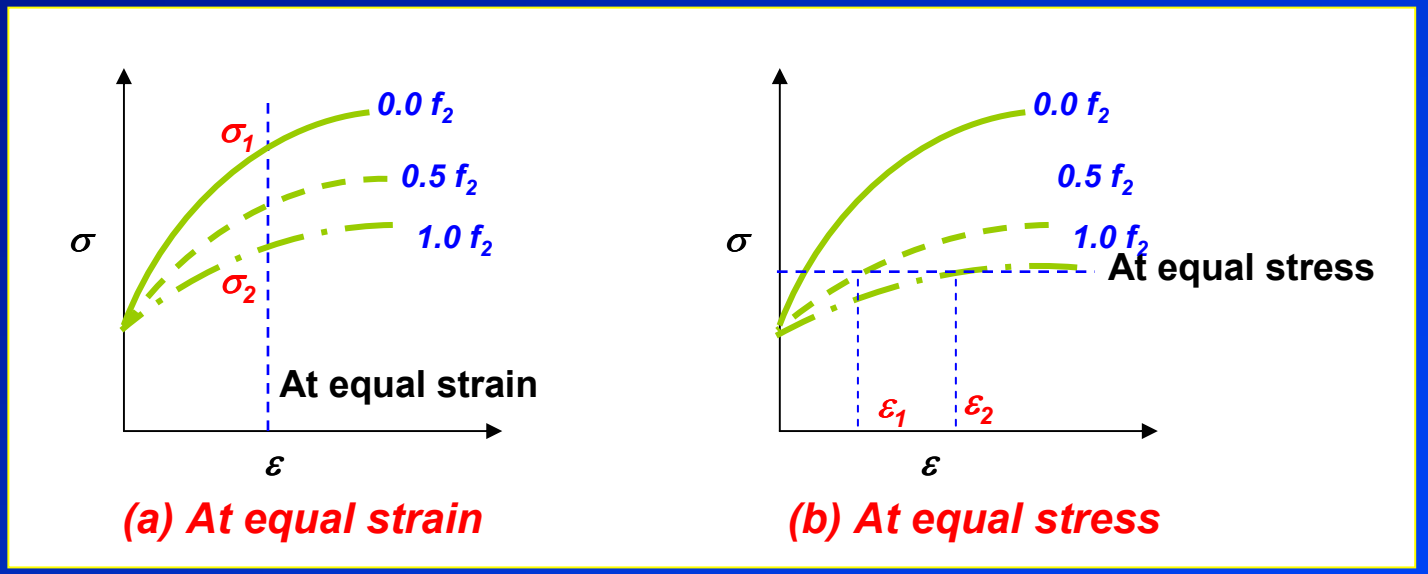

• It is more often that the ***second phase is stronger than the matrix*** but not all second-phase particles produce strengthening effects.

• The ***strong bonding between particles*** and matrix is required to be able to produce strengthening effects.

Deformation in two ductile phase alloys

- Depending on the V_f of the two phases and the total deformation.
- Slip will occur first in the weaker phase
- Not all second phase particles produce strengthening effects.

Deformation in alloy of a ductile and brittle phase

- Mechanical properties depends on how the hard brittle phase distribute throughout the softer matrix.
- Homogeneously distributed hard particles promote strength.
- Continuously distributed along the grain boundaries leads to brittle fracture.→ ***reduce strength***.

Microstructure dependence of yield stress in steels

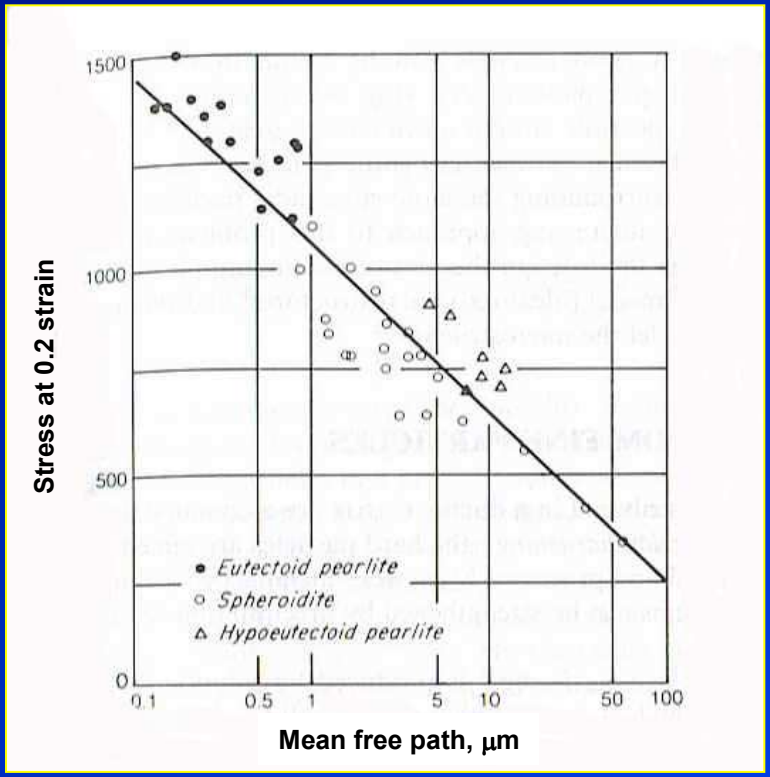

Flow stress vs. log of mean free ferrite path in steels.

- ***Gensamer et al*** studied the influence of different microstructures obtained from ***annealed, normalised and spheroidized steels*** (aggregates of ***cementites*** and ***ferrite***).
- The $\sigma_{0.2\%}$ was inversely proportional to the logarithm of ***mean free ferrite path*** (interparticle spacing).

Interparticle spacing ⬇ **Yield stress** ⬆

Precipitation hardening

Precipitation hardening or age hardening requires the second phase which is ***soluble at high temperature*** but has ***a limited solubility at lower temperatures***.

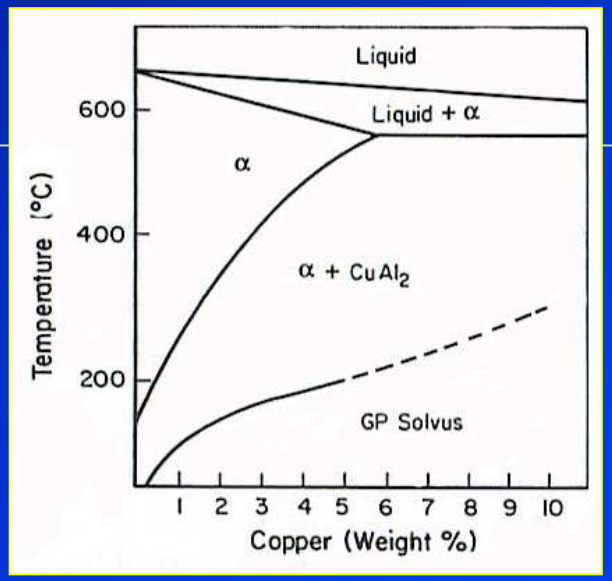

Al-Cu phase diagram

Solution treating at high temperature, then quenching → **Second phase is in solid solution.**

Ageing at low temperature → **Precipitation of the second phase, giving strengthening effect.**

Example: Age hardening aluminium alloys
Copper-beryllium alloys

Note: In precipitate-hardened system, there is coherency between the second-phase particle and the matrix.
But in dispersion-hardened system, there is no coherency.

The formation of coherency precipitate

A number of steps occurs during precipitation hardening.

- After quenching from solid solution the alloy contains ***areas of solute segregation or clustering.*** → ***GP zone.*** This clustering is GP[1] produces local strain giving higher hardness than the matrix.

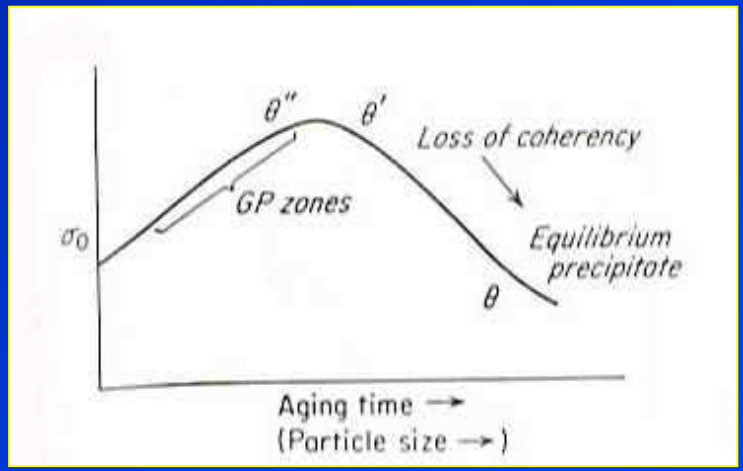

Variation of yield stress with ageing time.

- The hardness of the ***GP zone*** increases with ageing time, developing GP[2] or ***θ″.***
- Precipitate ***θ′*** is ***coherent*** with the matrix. → further ***increase in hardness.***
- Further ageing produces ***θ***, (***not coherent*** with the matrix). → ***lowering the hardness***.

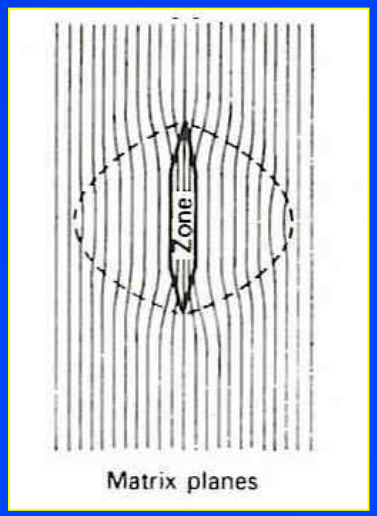

Deformation of alloys with fine particle strengthening

Case study in deformation of Al-4.5%Cu single crystal

- After solution treated and quenched, ***copper is in supersaturated solid solution***, giving ***higher yield stress*** than pure aluminium.
- The yield stress increases when the crystal is aged to form coherent ***GP zone***. Yield drop and low strain hardening suggest that dislocations cut through the zone once the stress reaches a high enough value.
- ***Strain hardening*** significantly increase when the crystal is aged to ***peak hardness***. Dislocations are short and move around particles.

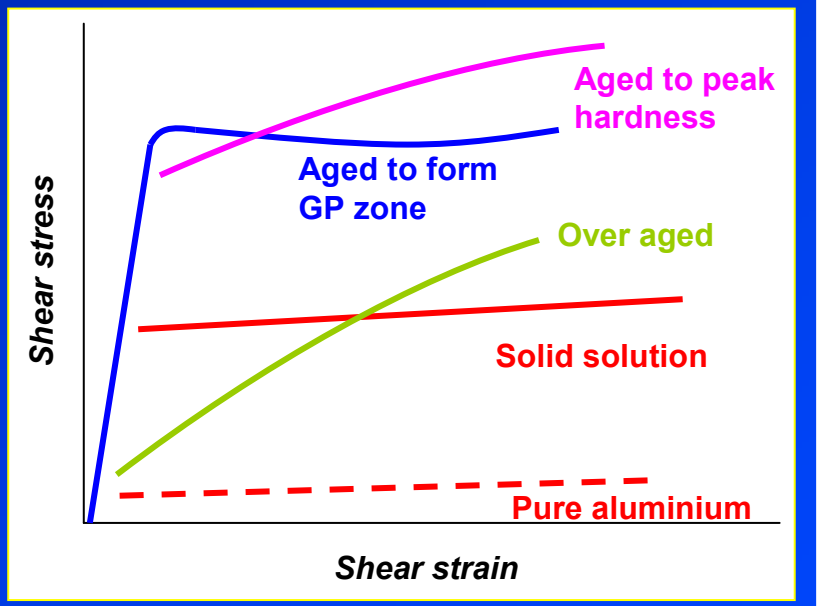

- ***Over-aged condition*** produces coarse noncoherent particles, giving low yield stress, high strain hardening.

Factors affecting precipitation hardening

Particle size, shape, volume fraction and distribution are ***key factors*** in improving precipitation hardening (cannot vary independently).

Example: For a given V_f

Particle size ↑ ***Interparticle spacing*** ↑

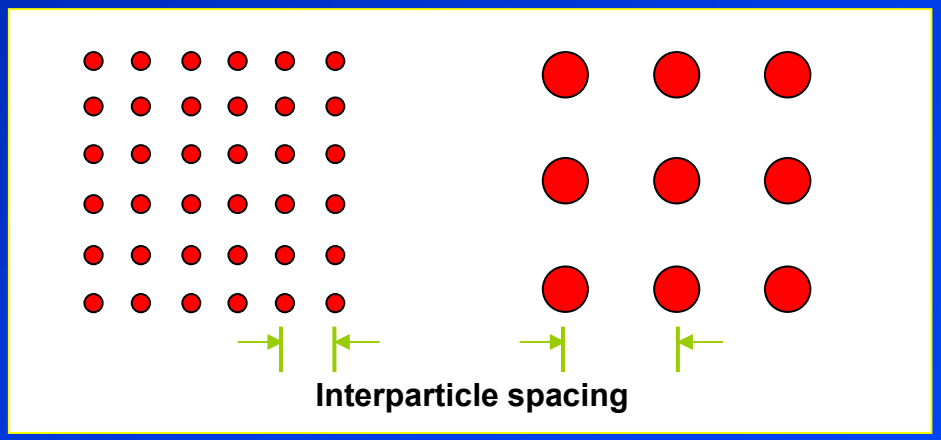

- High strength alloys seem to consist of ***fine strong particles well distributed in deformed matrix.***
- Fine hard particles increase strength by cutting dislocations → dislocation tangles → increasing strain hardening.
- Deformed matrix bares the load which makes fracture more difficult.

Interparticle spacing λ

$$\lambda = \frac{4(1-V_f)r}{3V_f} \qquad \text{...Eq. 9}$$

Where V_f is the volume fraction of spherical particles of radius r.

Properties affecting strengthening mechanisms by particles

Coherency strain

• Misfit between particles and matrix produces strain field → improving strength.

Stacking-fault energy

• Yield stress increases with the difference in stacking fault energy between the particle and the matrix.

Ordered structure

• introduce anti-phase boundaries.
• good high temperature strength.

Modulus effect

• Modulus difference between the matrix and the particles produces strength but it is not the case in most alloys.

Interfacial energy and morphology

• High particle-matrix surface energy leads to higher strength. (rely on surface-to-volume ratio or morphology)

Lattice friction stress

• Peierls stress in particle and matrix produce strengthening effect.

Interaction between fine particles and dislocations

Second phase particles *act in two distinct ways to retard the motion of dislocations.*

1) Particles maybe cut by dislocation

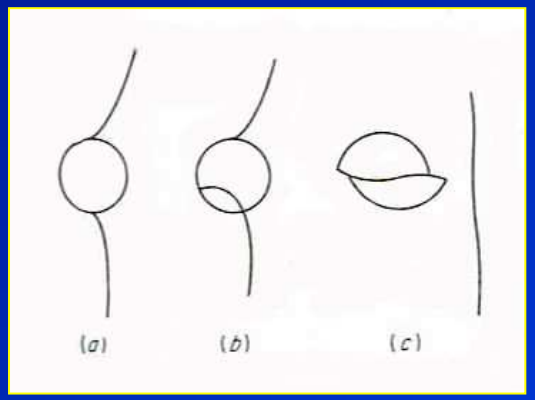

- When the particles are small / soft.

2) Particles allow dislocation to bypass/bow around them.

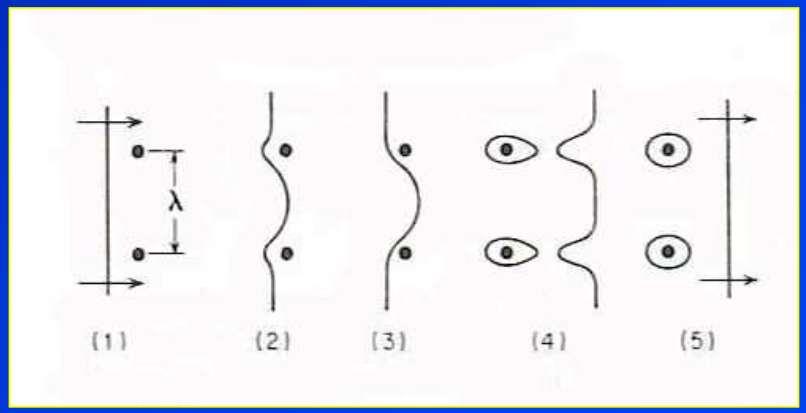

Orawan's mechanism of dispersion hardening.

- In over aged noncoherent precipitates. Bowing of dislocations around particles leaving dislocation loops behind.
- *Stress required to force dislocation between particles;*

$$\tau_o = \frac{Gb}{\lambda}$$ *…Eq. 10*

Role of slip character

The slip character can be characterised in to;

- ***Planar or wavy***
- ***Coarse or fine***

- ***Coarse planar slip*** → promotes brittle failure. Particles which is easily sheared by dislocations tend to produce coarse planar slips.

- ***Fine wavy slip*** → homogeneous deformation, giving best ductility at a given strength level. Particles which are by passed by dislocations lead to fine wavy slip.

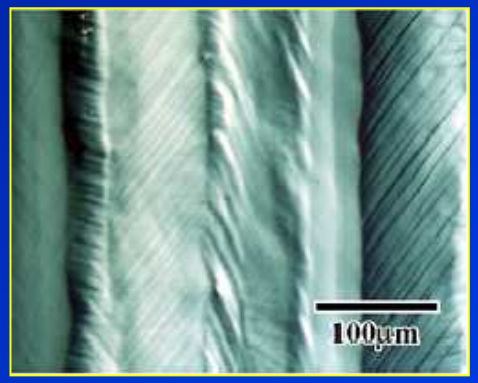

Planar slips in aged hardenable Al alloy.

Coplanar bands in warm rolled nitrogen-alloyed austenistic stainless steel

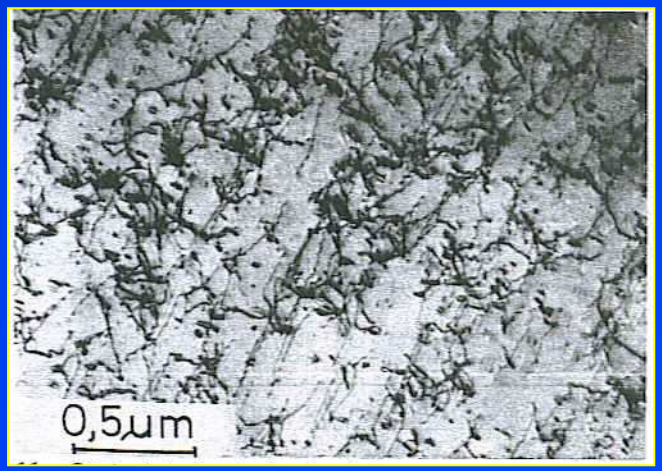

Wavy slips

Fibre strengthening

- ***Ductile metals*** can be reinforced using relatively ***stronger fibres***.
- Very high strength whiskers of Al_2O_3, or ***SiC*** fibres have been used for this purpose.
- ***Fibre-reinforced materials*** (metal or polymer as matrix) are also known as composite materials.

- The matrix transmits the load to the fibres.
- protect fibres from surface damage.
- separate individual fibres and blunt crack from fibre breakage.

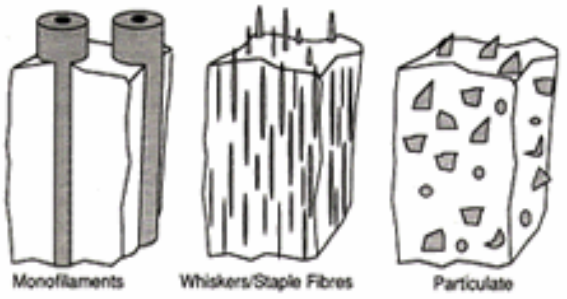

- High modulus fibres in Fibre-reinforced metals carry more load than dispersion-reinforced metals.
- Fibre-reinforced materials are highly anisotropic.

<u>Note:</u> Variation of stress between fibres and matrix is complex.

Strength and moduli of composites

The ***rule of mixtures*** is used to approximate the modulus and strength of a fibre-reinforced composite.

If a tensile force ***P*** is applied in the direction of the fibre, and assuming that the strain of fibre and matrix are similar, $e_f = e_m = e_c$.

$$P = \sigma_f A_f + \sigma_m A_m \quad \text{...Eq. 11}$$

Where A_f and A_m are the cross-sectional areas of fibre and matrix.

The average composite strength σ_c is

$$\sigma_c = \frac{P}{A_c} = \frac{\sigma_f A_f}{A_c} + \frac{\sigma_m A_m}{A_c}$$

$$\sigma_c = \sigma_f V_f + \sigma_m V_m \quad \text{...Eq. 12}$$

where

$$A_c = A_f + A_m$$

$$V_f + V_m = 1$$

Likewise

$$E_c = E_f V_f + E_m V_m \quad \text{...Eq. 13}$$

Example: *Boron fibre, E_f = 380 GPa, are made into a unidirectional composite with an aluminium matrix, E_m = 60 GPa. What is the modulus parallel to the fibres for 10 and 60 volume%.*

$$E_c = E_f V_f - (1 - V_f) E_m$$

$$V_f = 0.10 \ , E_c = 380(0.10) + 0.9(60) = 92 \ \ GPa$$

$$V_f = 0.60 \ , E_c = 380(0.60) + 0.4(60) = 252 \ \ GPa$$

Stress-strain curves of the fibre, matrix and fibre-reinforced composite

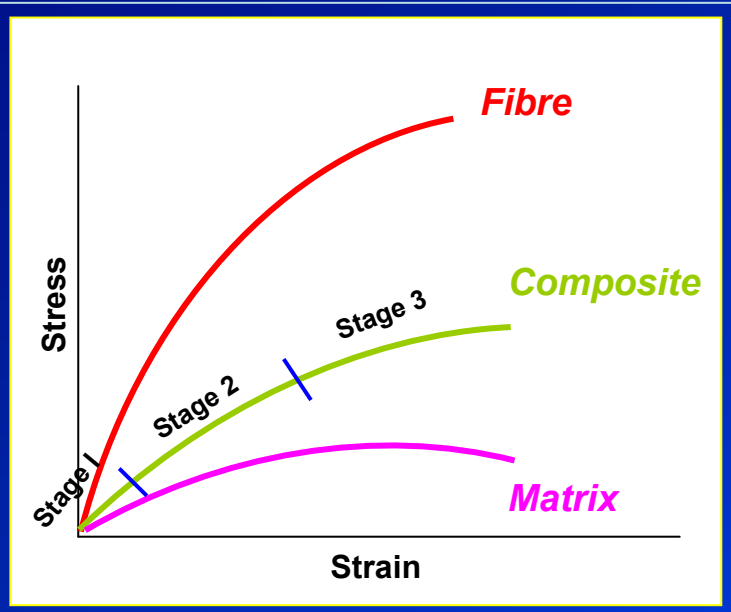

- ***Stage 1 :*** Both fibres and matrix undergo elastic deformation.
- ***Stage 2 :*** Matrix deforms plastically but fibres deform elastically.
- ***Stage 3 :*** Both matrix and fibres undergo plastic deformation.

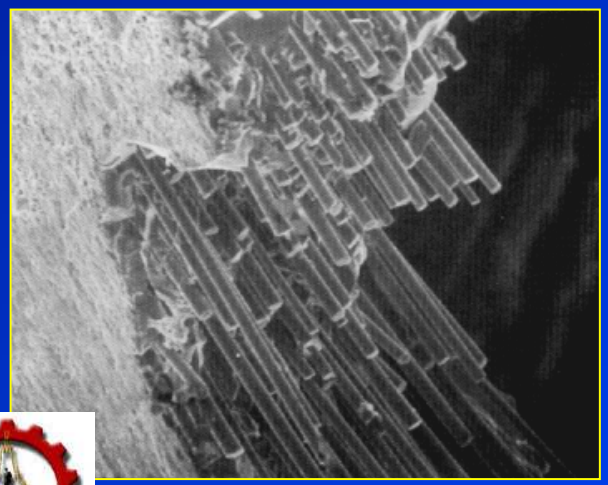

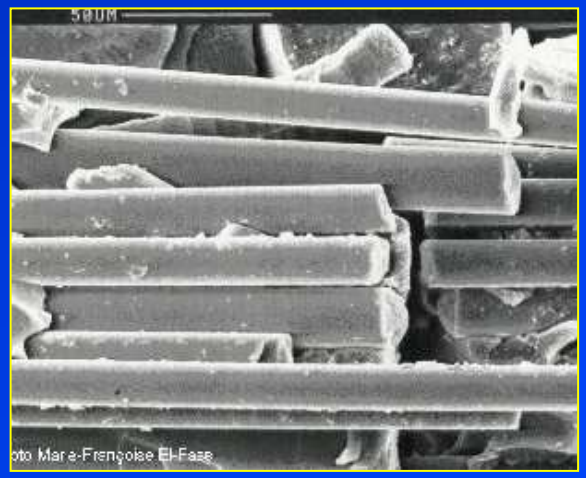

- The load is transferred from ductile matrix to strong fibres.
- Breakage or pull-out of fibres increase the strength.

Theoretical variation of composite strength with volume fraction of fibres

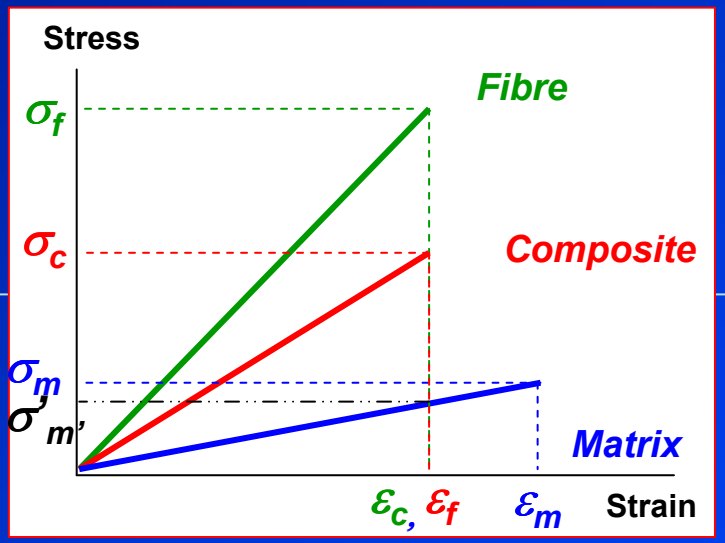

• The ***critical fibre volume*** which must be exceeded for fibre strengthening to occur.

$$V_{f\,(crit)} = \frac{\sigma_{mu} - \sigma'_m}{\sigma_{fu} - \sigma'_m} \qquad \ldots Eq.\ 14$$

• The ***minimum volume fraction*** of fibre which must be exceeded to have real reinforcement.

$$V_{f\,(\min)} = \frac{\sigma_{mu} - \sigma'_m}{\sigma_{fu} + \sigma_{mu} - \sigma'_m} \qquad \ldots Eq.\ 15$$

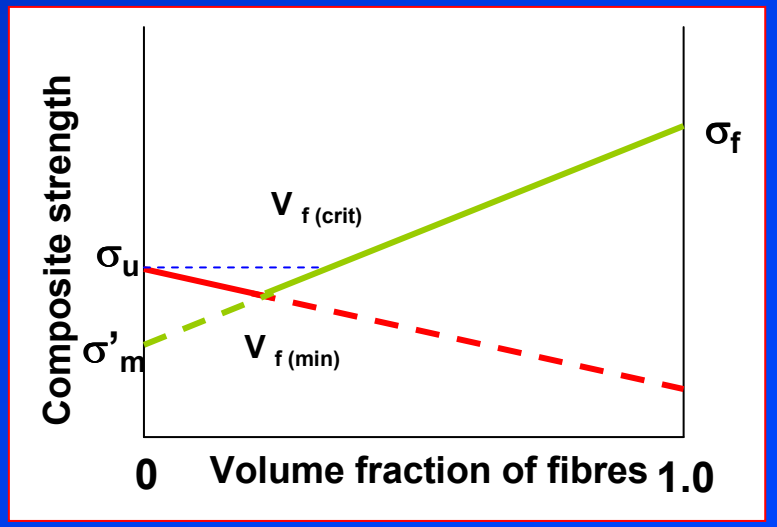

σ_u is the ultimate tensile strength of the composite

σ_f is the strength of the fibre

σ'_m is the flow stress in the matrix

Martensite strengthening

• ***Martensitic strengthening*** is obtained when austenite is transformed into martensite by a ***diffusionless shear-type process*** in quenching.

• ***Martensitic transformation*** occurs in many alloy systems but ***steels*** has shown the most pronounced effect.

High strength of martensite is due to two main contributions;

• ***Slip barriers*** *from (1) conventional* ***plate martensite structure*** *with a unique habit plane and an internal parallel twins of each 0.1 mm thick within the plate and (2)* ***Block martensite structure*** *containing a high dislocation density of* 10^{9} *to* 10^{10} mm^{-2}.

• ***Carbon contents*** *(<0.4%) lead to carbon atom clustering and dislocation interaction → increased strength and hardness, see fig.*

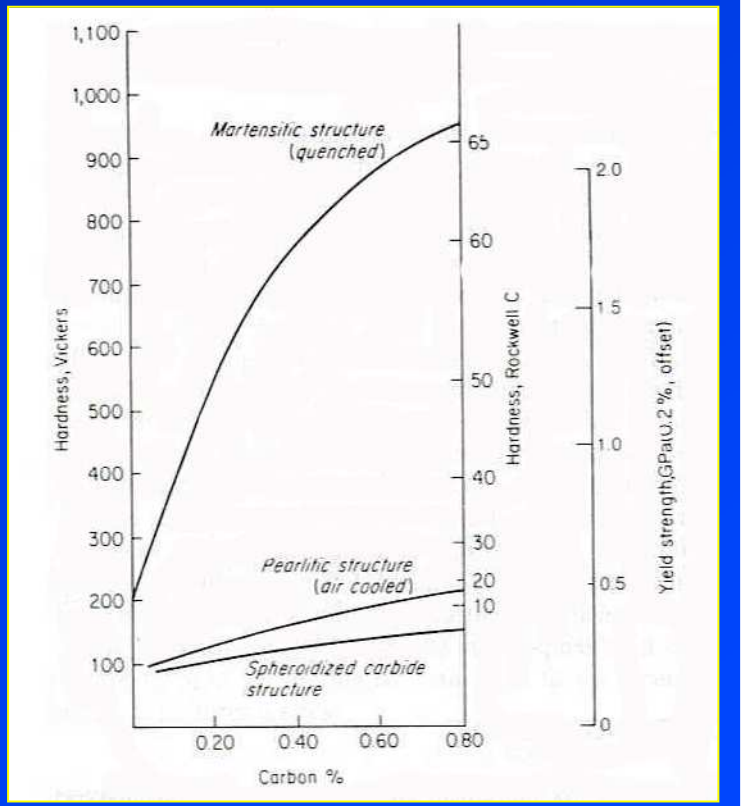

Hardness in various products in steel.

Ausforming process

Ausforming *is a thermo-mechanical process where steel is plastically deformed (>50%) usually rolling and then quenched to below the* M_s *to form* ***martensite****.*

• Plastic deformation of austenite should be done ***without transformation to pearlite or bainite***.

• ***Highest strengths*** are achieved by the greatest possible deformation at the lowest temperature at transformation does not occur.

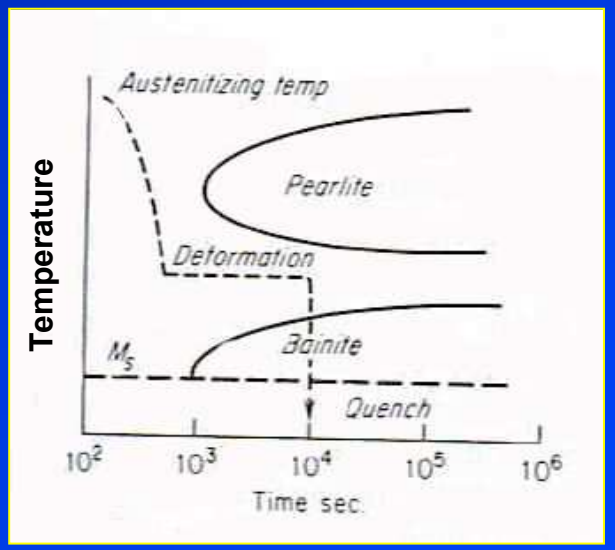

TTT diagram showing steps in ausforming process.

• Uniformly distributed dislocations of high density (10^{11} mm^{-2}) and precipitation provides sites for ***dislocation multiplication*** and ***pinning***, contribute to very high strength (2-3 GPa) with 40-20% RA.

Strain hardening or cold working

Cold-work structure *occurs when plastic deformation carried out at in a temperature region and over a time interval such that the strain hardening is not relieved.*

- ***Cold worked structure*** contains dislocation ~ 10^{11} mm^{-2}, while annealed structure possesses ~10^{4} to 10^{6} mm^{-2}.
- As the deformation proceeds, the high density dislocations tangles form the ***cell walls***.
- About 10% of energy input in cold work process is stored in the lattice.

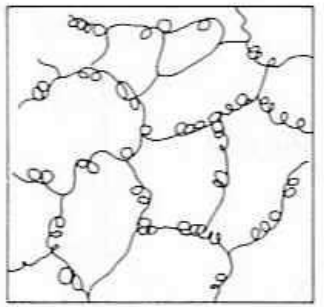

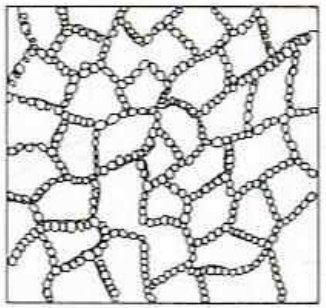

(a) Deformed to 10% ***(b) Deformed to 50%***

Dislocations in cell walls.

Temp ↓ **Strain rate** ↑

Stored energy ↑

Strain hardening

• Strain hardening or cold working is used to harden alloys that do not respond to heat treatment.

Cold work ↑ **Strength** ↑

Ductility ↓

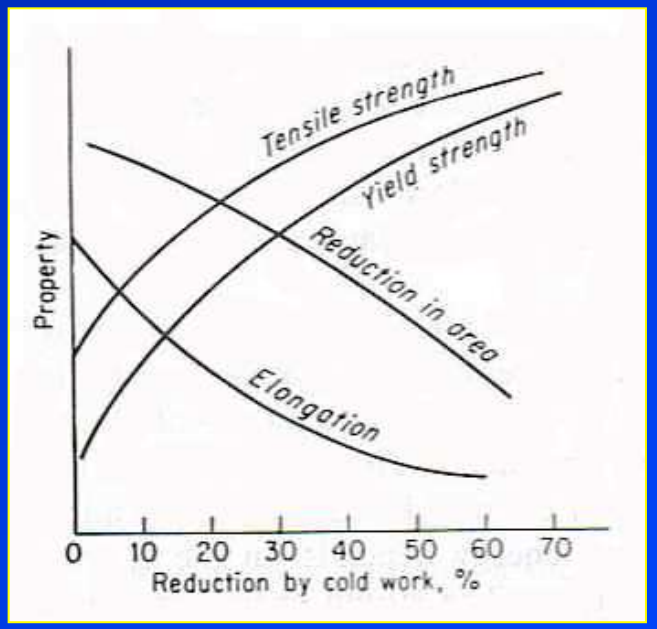

Variation of tensile properties with amount of cold-work.

• The rate of strain hardening is lower in ***HCP*** than in ***cubic metals***.

• The final strength of ***cold-worked solid solution alloy*** is almost always greater than that of the ***pure metal cold-worked to the same extent***.

Annealing of cold-worked metal

- ***Annealing*** of the cold worked structure at high temperature ***softens the metal*** and reverts to a strain-free condition.
- Annealing restores the ductility to a metal that has been severely strain hardened.
- Annealing can be divided into ***three distinct processes;***

1) **Recovery**
2) **Recrystallisation**
3) **Grain growth**

Recovery, recrystallisation, grain growth

• ***Recovery*** : the restoration of the physical properties of the cold-worked metal without any observable change in microstructure. *Strength is not affected*.

• ***Recrystallisation*** : the cold-worked structure is replaced by a new set of strain-free grains. *Hardness and strength decrease but ductility increases.*

• ***Grain growth*** : occurs at higher temperature where some of the recrystallised fine grains start to grow rapidly. *Grain growth is inhibited by second phase particles to pin the grain boundaries*.

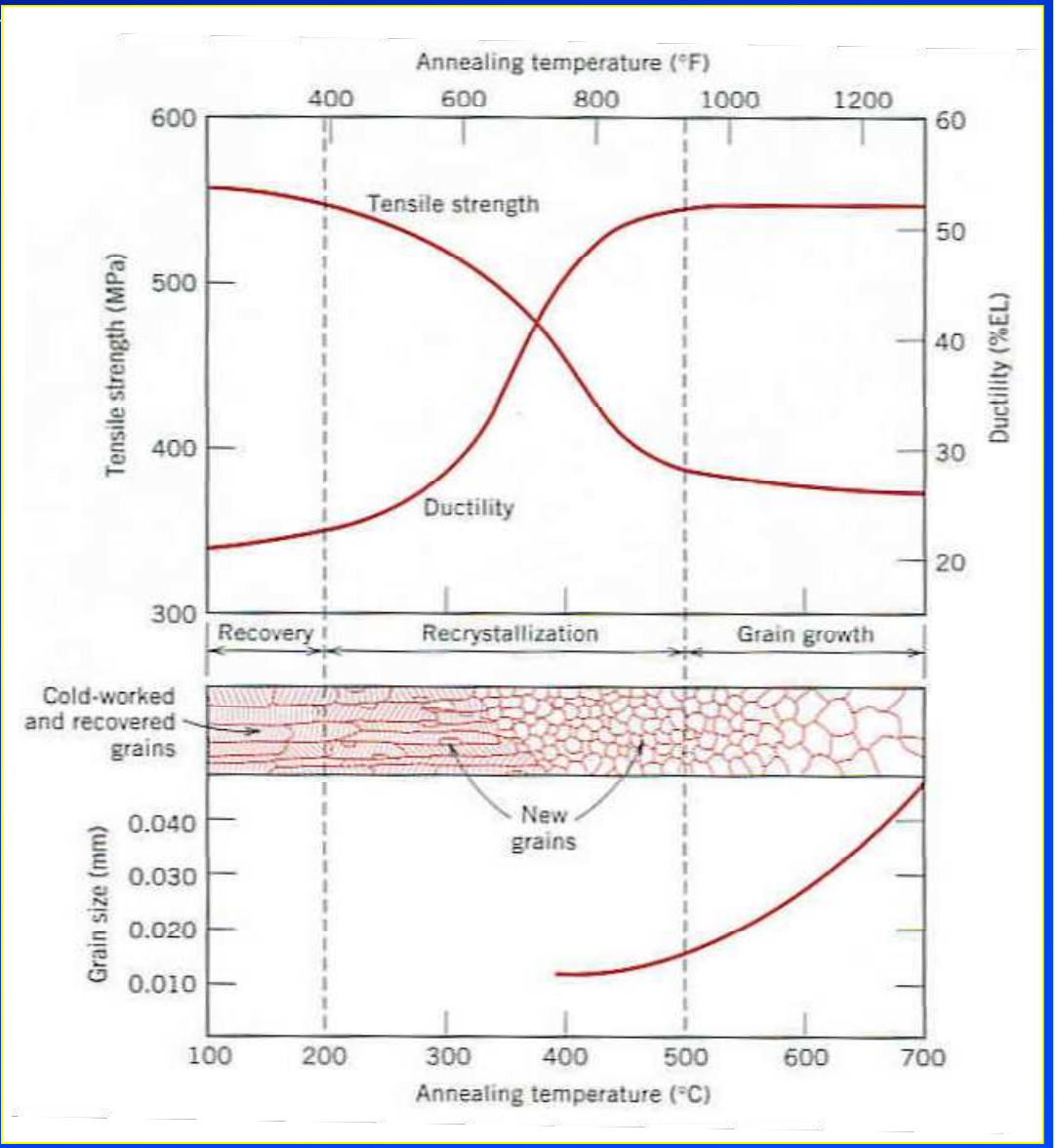

Properties change during recovery, recrystallisation and grain growth

Variables affecting recrystallisation behaviour

There are six variables affecting recrystallisation behaviour.

1) The amount of prior deformation
2) Temperature
3) Time
4) Initial grain size
5) Composition
6) Amount of recovery prior to start the recrystallisation.

- ***Impurity*** *decrease recrystallisation temperature.*
- ***Solid solution alloying*** *additions raise the recrystallisation temperature.*

Degree of deformation ⬇ T_{recrys} ⬆

Degree of deformation ⬆
T_{anneal} ⬇ , GS_{recrys} ⬇

$GS_{original}$ ⬆ ***Cold work*** ⬆

Preferred orientation (texture)

- *Severe deformation produces a **reorientation of the grains** into a **preferred orientation**. Certain crystallographic planes tend to orient themselves in a preferred manner with respect to the maximum strain direction.*

- The ***preferred orientation*** resulting from plastic deformation is ***strongly dependent on the available slip and twining systems***, but not affected by processing variable such as die angle, roll diameter, roll speed, etc.

Table 7.3 Deformation textures in metals with common crystal structures

Structure	*Wire (fibre texture)*	*Sheet (rolling texture)*
bcc	[1 1 0]	{1 1 2} ⟨1 $\bar{1}$ 0⟩ to {1 0 0} ⟨0 1 1⟩
fcc	[1 1 1], [1 0 0] double fibre	{1 1 0} ⟨1 1 2⟩ to {3 $\bar{5}$ 1} ⟨1 1 2⟩
cph	[2 1 0]	{0 0 0 1} ⟨1 0 0 0⟩

<u>Note:</u> the deformation texture cannot in general be eliminated by an annealing operations

Grain orientation by EBSD analysis

• EBSD analysis employs ***back scattered electrons*** to give grain orientation information.

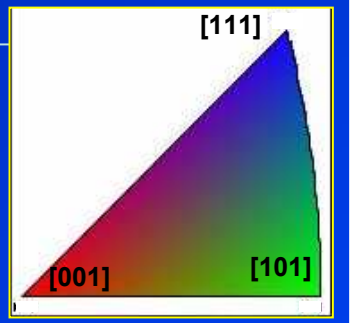

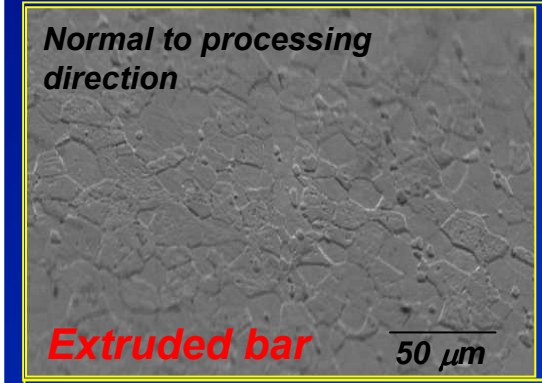

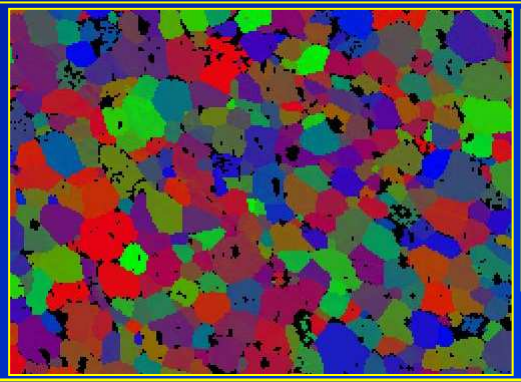

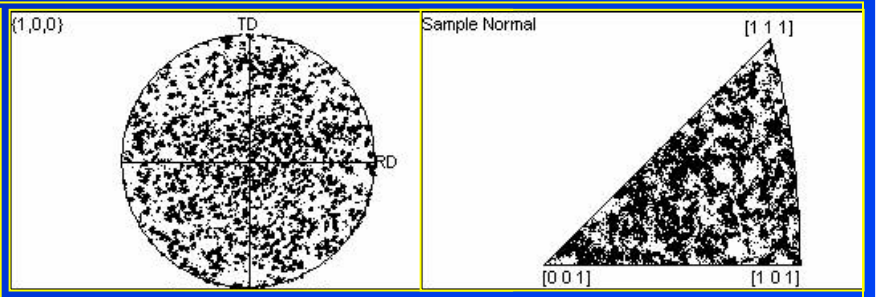

Homogeneously distributed.

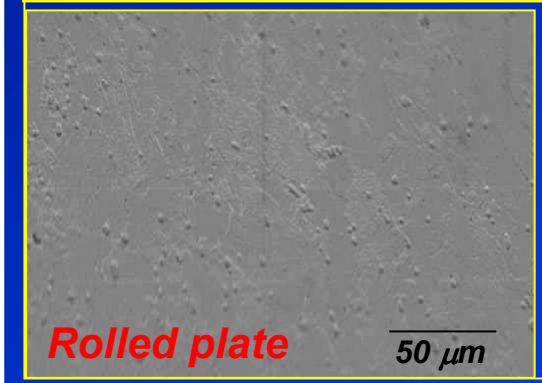

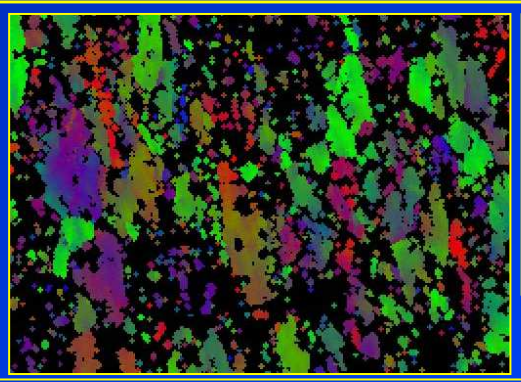

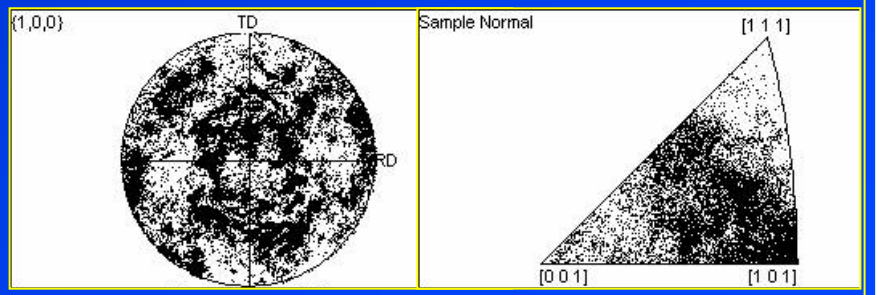

Preferred orientation.

SEM micrograph ***Orientation map*** ***Pole figure*** ***Inverse pole figure***

Mechanical fibering (fibrous texture)

- ***Fibrous texture*** *is produced along the maximum stress direction acting on the materials.*

- Inclusions, cavities and second phase constituents are aligned in the main direction of mechanical working.

- The ***geometry of the flow*** and the ***amount of the deformation*** are the most important variables.

- Mechanical fibering increases ***mechanical properties*** along the working (fibre) direction, with the transverse direction having inferior properties. → ***anisotropic properties.***

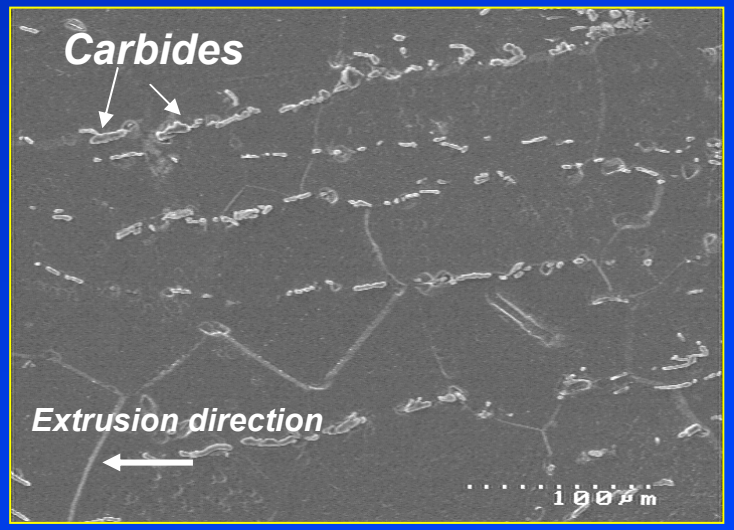

Alignment of carbides along the extrusion direction in β-Ti alloy.

References

- Dieter, G.E., ***Mechanical metallurgy***, 1988, SI metric edition, McGraw-Hill, ISBN 0-07-100406-8.
- Sanford, R.J., ***Principles of fracture mechanics***, 2003, Prentice Hall, ISBN 0-13-192992-1.
- W.D. Callister, ***Fundamental of materials science and engineering/ an interactive e. text.***, 2001, John Willey & Sons, Inc., New York, ISBN 0-471-39551-x.
- Hull, D., Bacon, D.J., ***Introduction to dislocations***, 2001, Forth edition, Butterworth-Heinemann, ISBN 0-7506-4681-0.
- Smallman, R.E., Bishop, R.J., ***Modern physical metallurgy & materials engineering***, 1999, sixth edition, Butterworth-Heinemann, ISBN 0-7506-4564-4.
- www.composite-bydesign.com
- www.mdi.espci.fr
- www.mtm.kuleuven.ac.be

References

• Aladar A. Csontos and Edgar A. Starke, ***The effect of inhomogeneous plastic deformation on the ductility and fracture behavior of age hardenable aluminum alloys***, International Journal of Plasticity, Vol. 21, Issue 6, June 2005, p. 1097-1118.

• S. Fréchard, A. Redjaïmia, E. Lach and A. Lichtenberger, ***Mechanical behaviour of nitrogen-alloyed austenitic stainless steel hardened by warm rolling,*** Materials Science and Engineering: A, Vol. 415, Issues 1-2, 2006, p. 219-224.

Fracture

Subjects of interest

- Introduction/ objectives
- Types of fracture in metals
- Theoretical cohesive strength of metals
- The development in theories of brittle fracture
- Fractographic observation in brittle fracture
- Ductile fracture
- Ductile to brittle transition behaviour
- Intergranular fracture
- Factors affecting modes of fracture
- Concept of the fracture curve

Objectives

- This chapter provides the development in the theories of brittle fractures together with mechanisms of fracture that might occur in metallic materials.
- Factors affecting different types of fracture processes such as brittle cleavage fracture, ductile failure or intergranular fracture will be discussed.

Introduction

Failure in structures leads to lost of properties and sometimes lost of human lives unfortunately.

Failure of Liberty Ships during services in World War II.

Failed fuselage of the Aloha 737 aircraft in 1988.

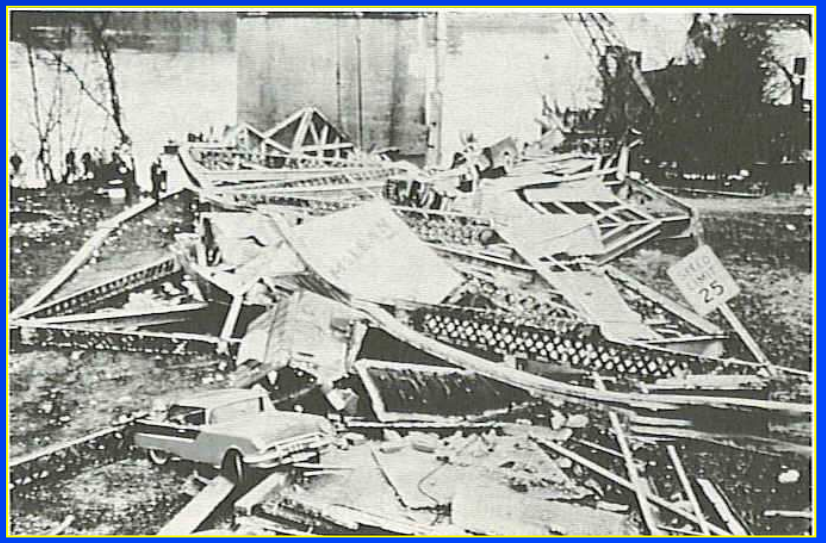

Collapse of Point Pleasant suspension bridge, West Virginia, 1967.

Types of fracture in metals

- *The concept of material strength and fractures has long been studied to overcome failures.*
- *The introduction of malleable irons during the revolution of material construction led to the perception of brittle and ductile fractures as well as fatigue failure in metals.*

Failure in metallic materials can be divided into two main categories;

Ductile failure

Ductile fracture involves a large amount of plastic deformation and can be detected beforehand.

Brittle failure

Brittle fracture is more catastrophic and has been intensively studied.

Theories of brittle fracture

Failure modes

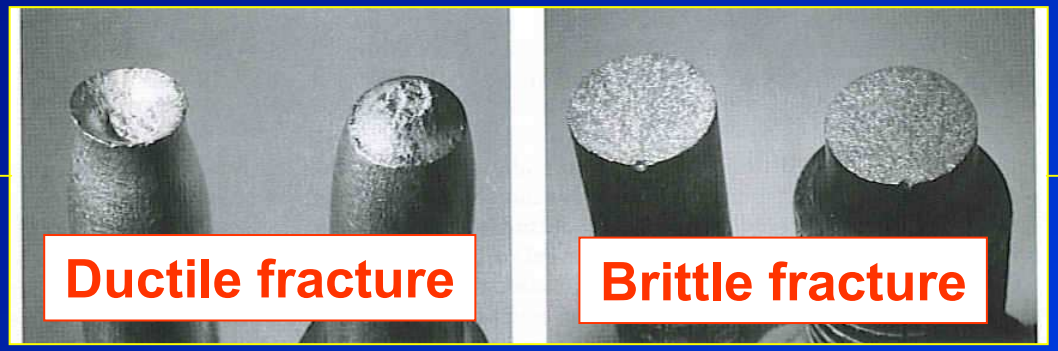

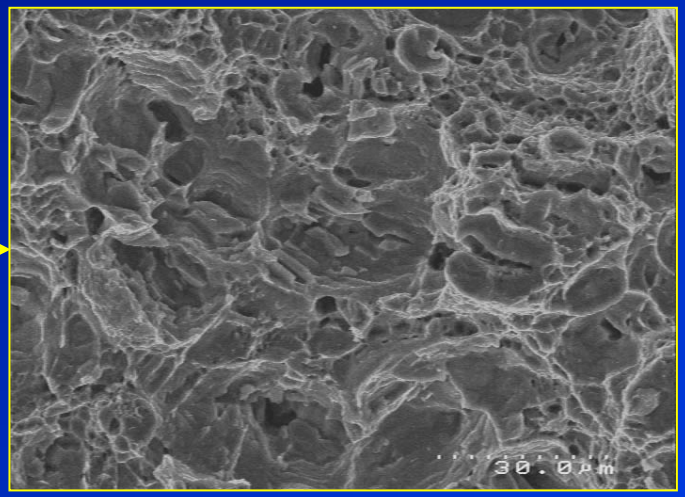

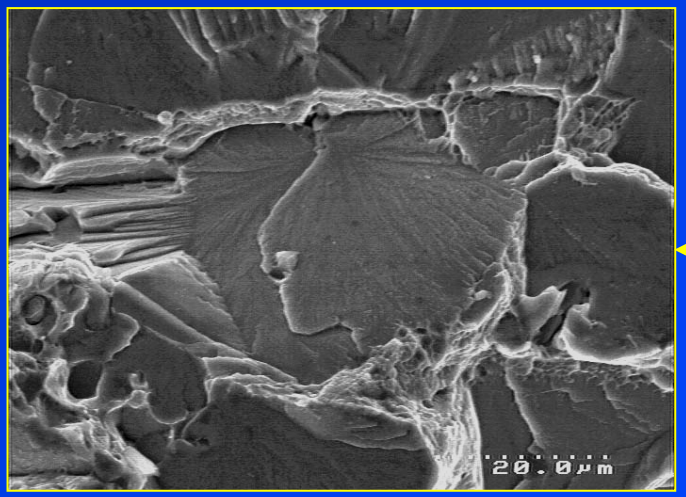

• ***High energy*** *is absorbed by microvoid coalescence during ductile failure (high energy fracture mode)*

Less catastrophic

• ***Low energy*** *is absorbed during transgranular cleavage fracture (low energy fracture mode)*

More catastrophic

Theoretical cohesive strength of metal

- In the most basic term, strength is due to the ***cohesive forces between atoms***.
- The ***attractive*** and ***repulsive*** force acting on the two atoms lead to ***cohesive force*** between two atoms which varies in relation to the separation between these atoms, see *fig*.

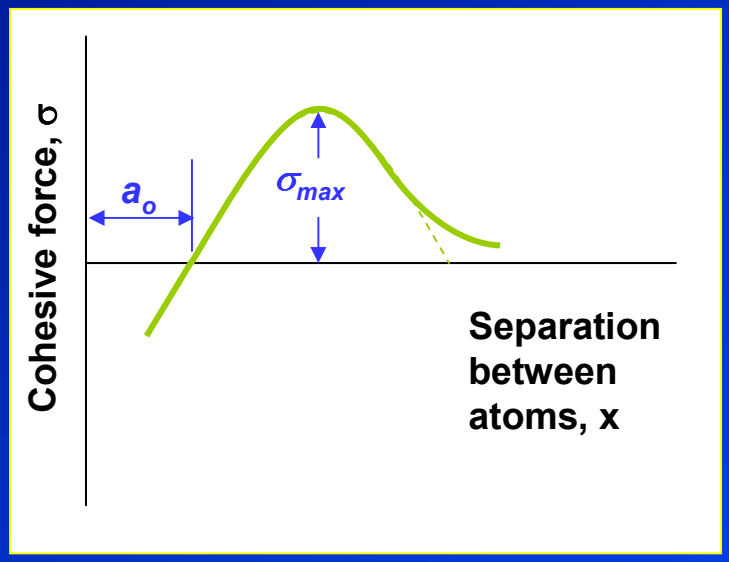

Cohesive force as a function of the separation between atoms.

The ***theoretical cohesive strength*** σ_{max} can be obtained in relation to the sine curve and become.

$$\sigma_{\max} = \left(\frac{E\gamma_s}{a_o} \right)^{1/2} \quad \text{...Eq. 1}$$

Where

γ_s is the surface energy

a_o is the unstrained interatomic spacing.

Note: Convenient estimates of σ_{max} ~ ***E/10***.

Fracture in single crystals

The ***brittle fracture*** of single crystals is related to the resolved normal stress on the cleavage plane.

Sohncke's law *states that fracture occurs when the* ***resolved normal stress*** *reaches a critical value.*

From the critical resolved shear stress τ_R for slip

$$\tau_R = \frac{P\cos\lambda}{A/\cos\phi} = \frac{P}{A}\cos\phi\cos\lambda \qquad \text{...Eq. 2}$$

The critical normal stress σ_c for brittle fracture

$$\sigma_c = \frac{P\cos\phi}{A/\cos\phi} = \frac{P}{A}\cos^2\phi \qquad \text{...Eq. 3}$$

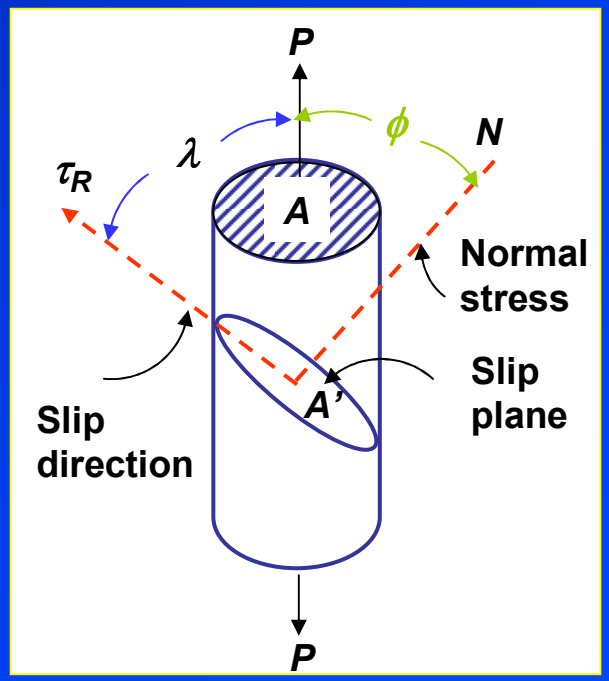

Note: shear stress → slip
tensile stress → crack propagation → fracture.

Example: *Determine the cohesive strength of a silica fibre, if* $E = 95$ *GPa,* $\gamma_s = 1\ J.m^{-2}$, *and* $a_o = 0.16$ *nm.*

$$\sigma_{\max} = \left(\frac{E\gamma_s}{a_o}\right)^{1/2} = \left(\frac{95\times10^{9}\times1}{0.16\times10^{-9}}\right)^{1/2} = 24.4\ GPa$$

- This ***theoretical cohesive strength*** is exceptionally higher than the fracture strength of engineering materials.
- This difference between cohesive and fracture strength is due to ***inherent flaws or defects*** in the materials which lower the fracture strength in engineering materials.
- ***Griffith*** explained the discrepancy between the ***fracture strength*** and theoretical cohesive strength using the ***concept of energy balance***.

Theories of brittle fracture

Griffith theory of brittle fracture

The first analysis on cleavage fracture was initiated by ***Griffith*** using ***the concept of energy balance*** in order to explain discrepancy between the theoretical cohesive strength and observed fracture strength of ideally brittle material.

The development in cleavage fracture models

- ***Modified Griffith theory*** *by Irwin and Orowan.*
- ***Zener's model*** *of microcrack formation at a pile-up of edge dislocations.*
- ***Stroh's model*** *of cleavage crack formation by dislocation pile-up.*
- ***Cottrell's model*** *of cleavage crack initiation in BCC metals*
- ***Smith's model*** *of microcrack formation in grain boundary carbide film.*

Griffith theory of brittle fracture

Observed fracture strength is always lower than theoretical cohesive strength

Griffith explained that the discrepancy is due to the ***inherent defects*** in brittle materials leading to stress concentration. → lower the fracture strength of the materials

Crack propagation criterion:

Consider a through thickness crack of length ***2a,*** subjected to a uniform tensile stress σ, at infinity.

Crack propagation occurs when the released elastic strain energy is at least equal to the energy required to generate new crack surface.

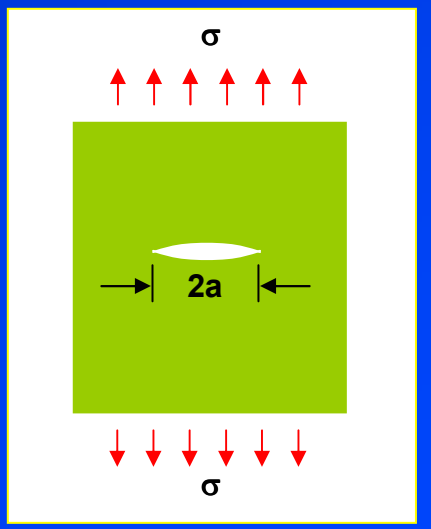

Griffith crack model

- The stress required to create the new crack surface is given as follows;

$$\sigma = \left(\frac{2E\gamma_s}{\pi a} \right)^{1/2} \quad \text{...Eq. 4}$$

- In plane strain condition, *Eq.4* becomes

$$\sigma = \left(\frac{2E\gamma_s}{(1-\upsilon^2)\pi a} \right)^{1/2} \quad \text{...Eq. 5}$$

The Griffith's equation

Modified Griffith equation

• The ***Griffith equation*** is strongly dependent on the crack size ***a***, and satisfies only ***ideally brittle materials*** like glass.

• However, ***metals*** are not ideally brittle and normally fail with certain amounts of plastic deformation, the fracture stress is increased due to ***blunting of the crack tip***.

• ***Irwin*** and ***Orowan*** suggested ***Griffith's equation*** can be applied to ***brittle materials*** undergone plastic deformation before fracture by including the plastic work, γ_p, into the total elastic surface energy required to extend the crack wall, giving the ***modified Griffith's equation*** as follows

$$\sigma_f = \left[\frac{2E(\gamma_s + \gamma_p)}{\pi(1-\upsilon^2)a}\right]^{1/2} \approx \left(\frac{E\gamma_p}{(1-\upsilon^2)a}\right)^{1/2}, when\ \gamma_p >> \gamma_2 \qquad ...Eq.\ 6$$

Zener's model of microcrack formation at a pile-up of edge dislocations

The ***Griffith theory*** only indicated the stress required for crack propagation of an existing crack of length ***2a*** but did not explain the ***nucleation of the crack***.

Zener and ***Stroh*** showed that the crack nucleation of length ***2c*** occurs when the shear stress τ_s created by ***pile-up*** of ***n*** dislocations of ***Burgers vector*** **b** at a grain boundary reaches the value of

$$\tau_s \approx \tau_i + \left(\frac{2\gamma_s}{nb}\right) \qquad \text{...Eq. 7}$$

Where τ_i is the lattice friction stress in the slip plane.

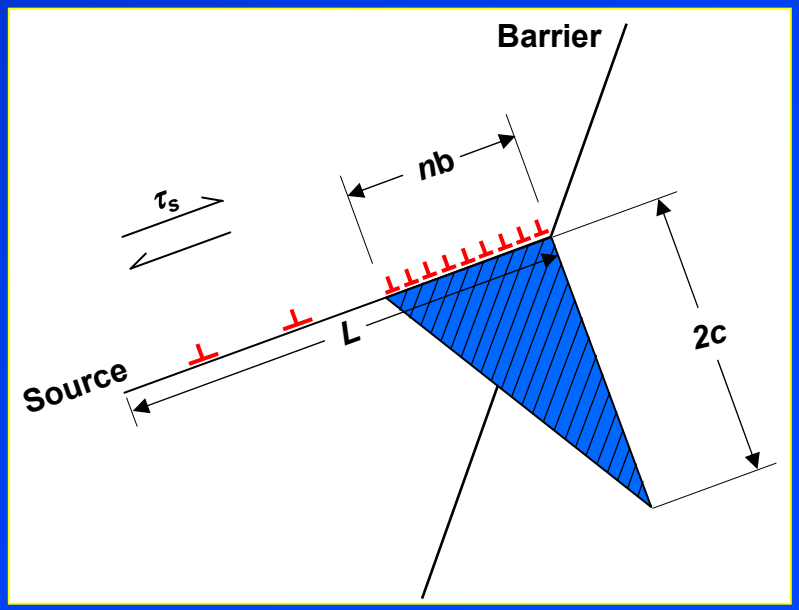

Dislocation pile-ups at barrier.

Stroh's model of cleavage crack formation by dislocation pile-up

Stroh included the effect of the grain size ***d*** in a model, suggesting the condition of the shear stress created by ***dislocation pile-up*** of the length ***d/2*** to nucleate a ***microcrack*** as follows

$$\tau_{eff} = \tau_y - \tau_i \sqrt{\frac{E\pi\gamma}{4(1-\upsilon^2)d}} \qquad \text{...Eq. 8}$$

where

τ_{eff} is the effective shear stress

τ_y is the yield stress

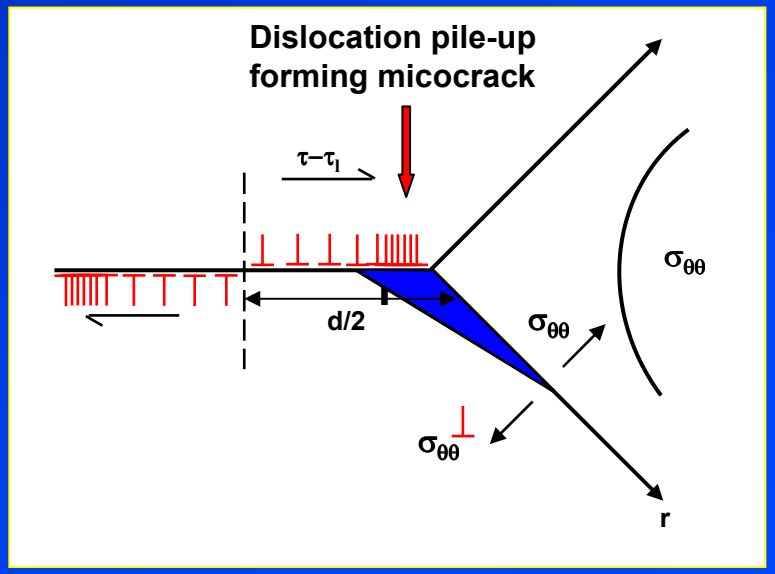

Stroh's model of cleavage crack formation by dislocation pile-up.

Note: This model indicates that the fracture of the material should depend only on the ***shear stress*** acting on the slip band.

Cottrell's model of cleavage crack initiation in BCC metals

Cottrell later suggested that the fracture process should be controlled by ***the critical crack growth stage*** under the applied tensile stress, which required higher stress than the ***crack nucleation*** itself as suggested by ***Stroh***.

Cottrell also showed that the ***crack nucleation stress*** can be small if the microcrack is initiated by ***intersecting of two low energy slip planes*** to provide a preferable cleavage plane.

$$\frac{a}{2}[\bar{1}\bar{1}1]+\frac{a}{2}[111]\rightarrow a[001] \qquad \text{...Eq. 9}$$

This results in a wedge cleavage crack on the (001) plane. Further propagation of this crack is then controlled by the applied tensile stress.

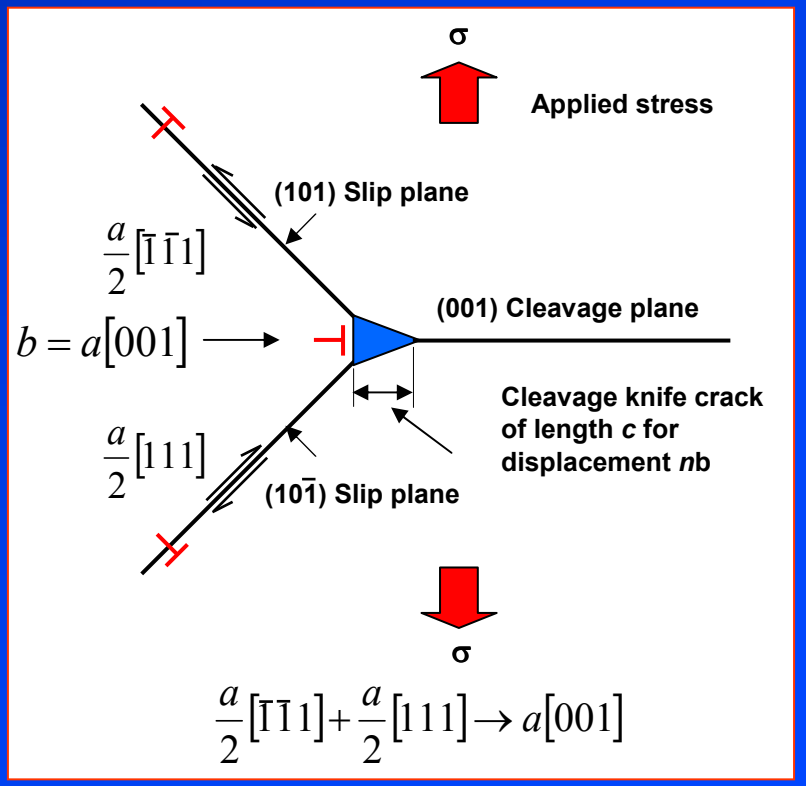

Cottrell's model of cleavage crack initiation in BCC metals

Smith's model of microcrack formation in grain boundary carbide film

Models proposed by ***Stroh*** and ***Cottrell*** involve ***crack initiation by dislocation pile-up*** of length ***D/2,*** but exclude the effect of ***second phase particles***.

Smith then proposed ***a model for cleavage fracture in mild steel*** concerning microcracking of grain boundary carbide by dislocation pile-up of length equal to half of the grain diameter ***D/2***.

Microcrack is initiated when sufficiently high applied stress causes local plastic strain within the ***ferrite grains*** to nucleate microcrack in brittle grain boundary carbide of thickness C_o.

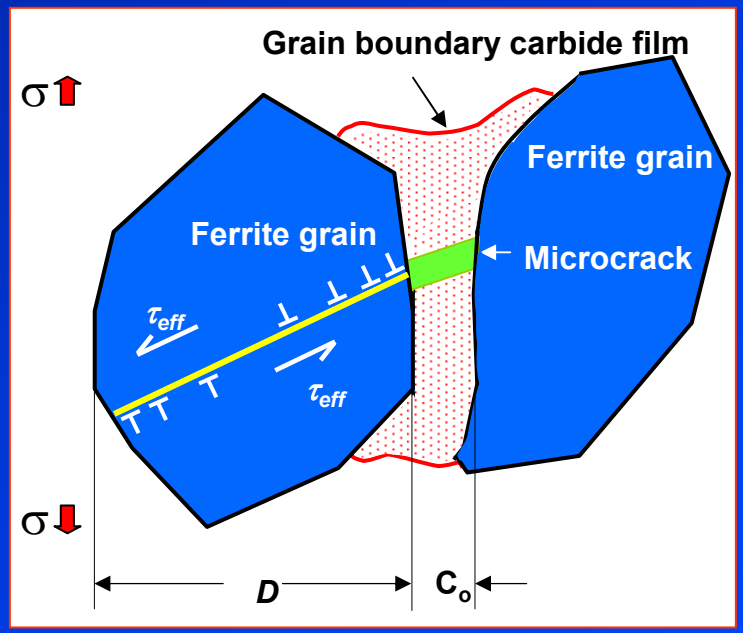

Smith's model of microcrack formation in grain boundary carbide film

...Eq. 10

$$\sigma_f^2\left(\frac{c_o}{d}\right)+\tau_{eff}^2\left\{1+\frac{4}{\pi}\left(\frac{C_o}{d}\right)^{1/2}\frac{\tau_i}{\tau_{eff}}\right\}^2 \geq \frac{4E\gamma_p}{(1-\upsilon^2)\pi d}$$

*Note: Further propagation of the GB carbide crack follows the **Griffith theory**.*

Fractographic observation in brittle fracture

The process of cleavage fracture consists of three steps:

1) Plastic deformation to produce dislocation pile-ups.

2) Crack initiation.

3) Crack propagation to failure.

Distinct characteristics of brittle fracture surfaces:

1) The absence of gross plastic deformation.

2) Grainy or Faceted texture.

3) River marking or stress lines.

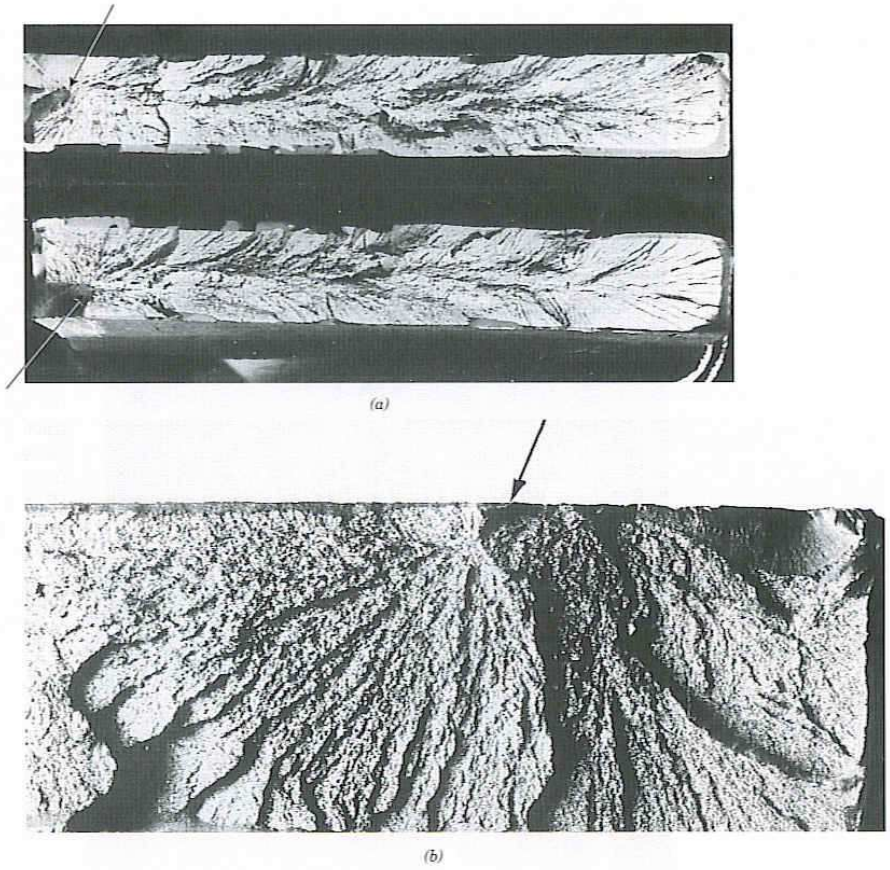

Brittle fracture indicating the origin of the crack and crack propagation path

Brittle fracture surface

- ***Cleavage fracture surface*** is characterised by flat facets (with its size normally similar to the grain size).
- ***River lines*** or the ***stress lines*** are steps between cleavage on parallel planes and always converge in the direction of local crack propagation.

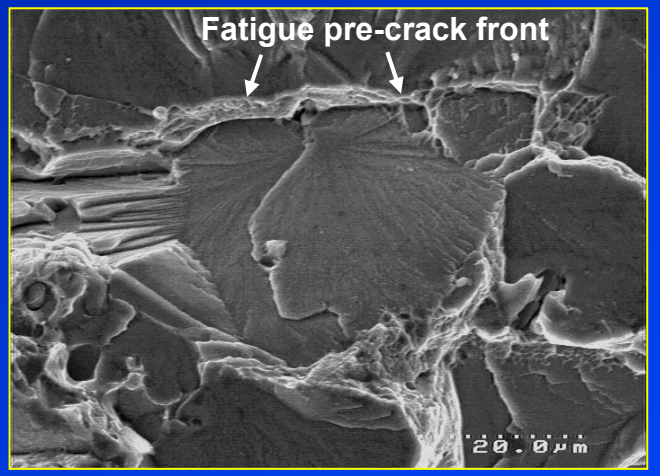

Cleavage facet

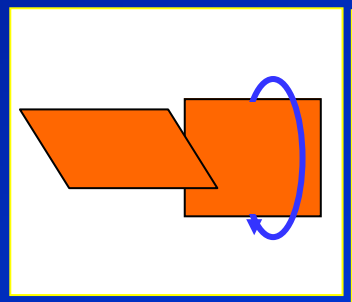

Twist boundary

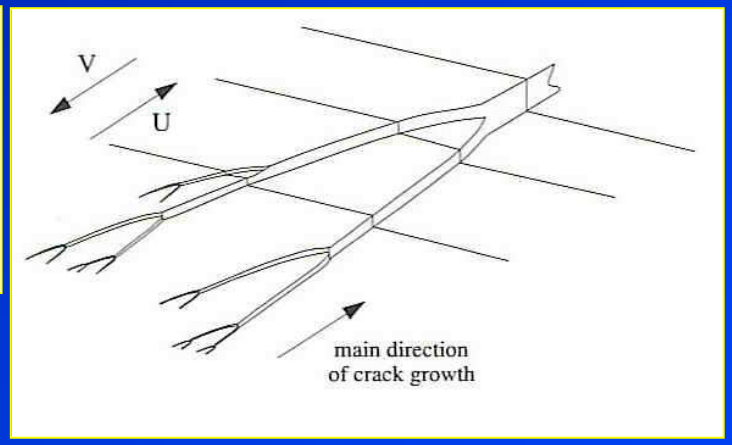

Schematic of river-line pattern.

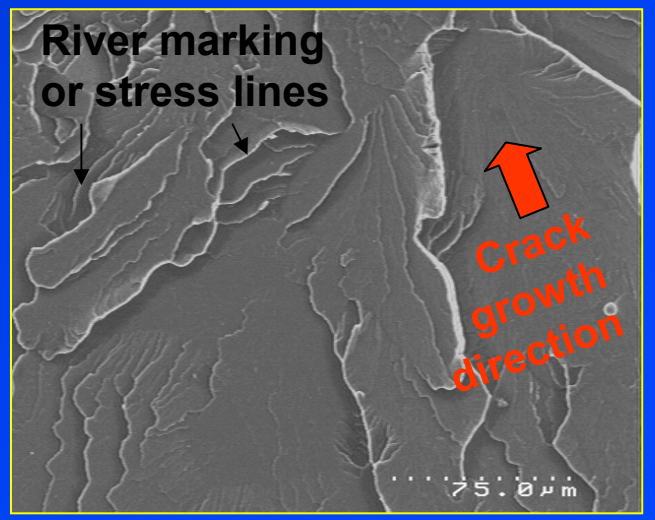

Brittle cleavage facet

Initiation of microcracks from deformation and twins

• ***Microcracks*** can be produced by the deformation process, see *fig*.

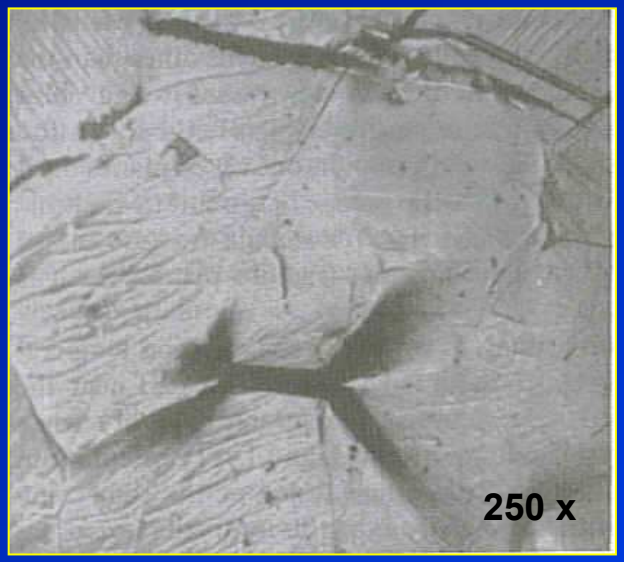

Microcracks produced in iron by tensile deformation at 133 K.

• ***Microcracks*** can also be initiated at ***mechanical twins***, especially in large grained bcc metals at low temperature.

• Crack initiation sites are due to the intersections of twins with other twins or intersection of twins with grain boundaries.

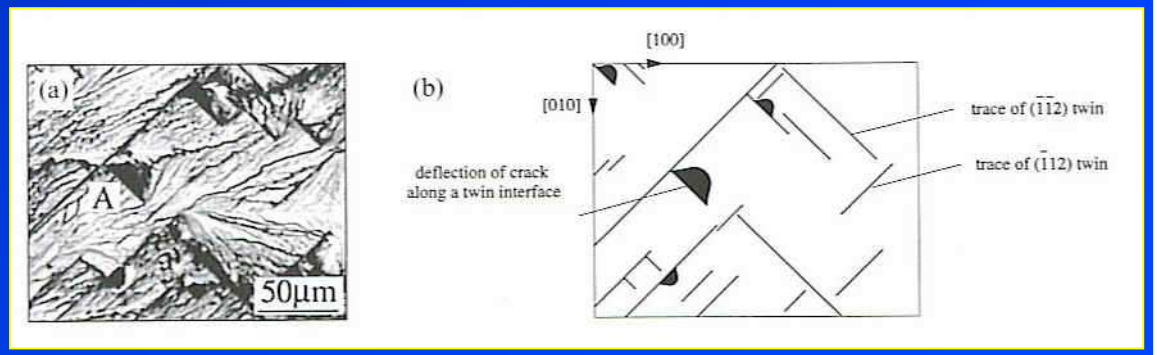

Cleavage along twin-matrix interfaces.

Crack initiation from particles in cleavage fracture

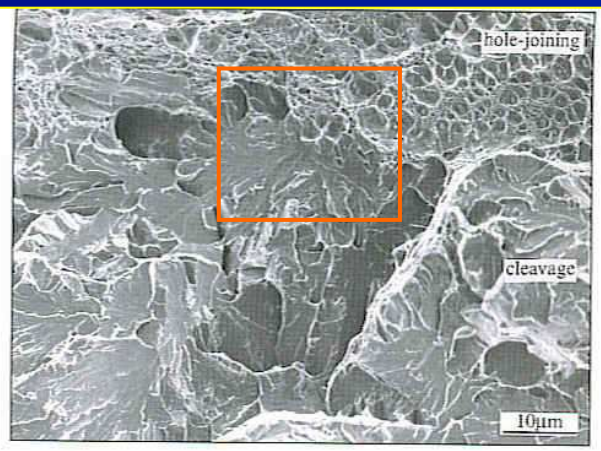

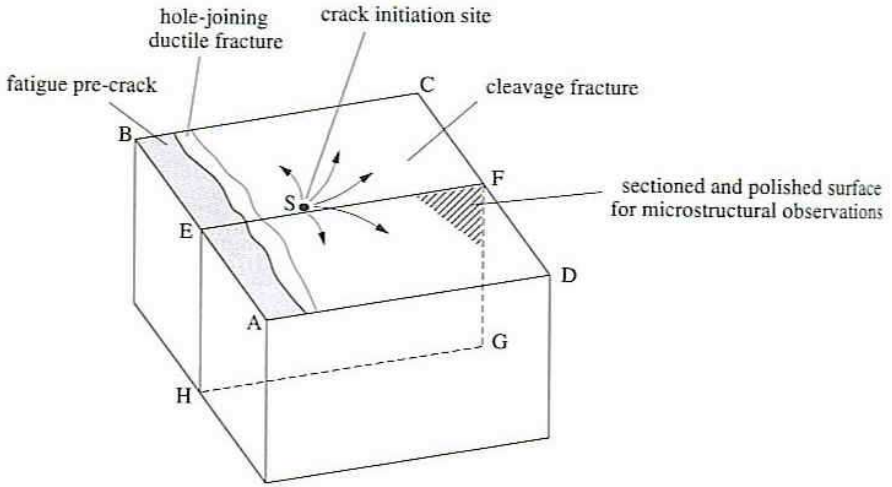

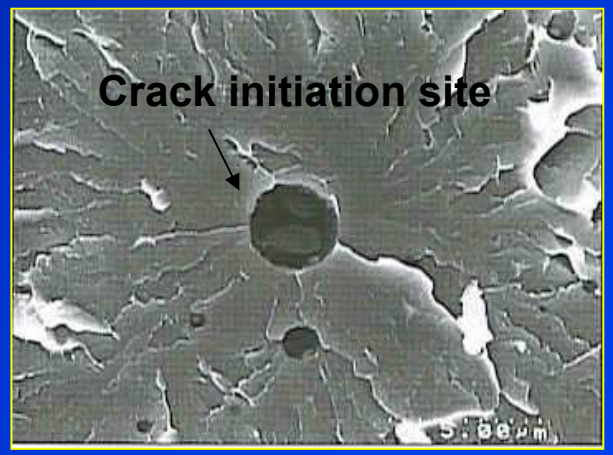

- Inclusions, porosity, second-phase particles or precipitates are preferential sites (***stress raiser***) for cleavage initiation.
- Fracture occurs along the ***crystallographic planes***.
- The direction of the river pattern represents the ***direction of the crack propagation***.

Example: *Crack initiation from carbide particles observed in β-Ti alloy.*

Titanium carbides act as ***stress raiser*** which are preferential site for transgranular cleavage fracture.

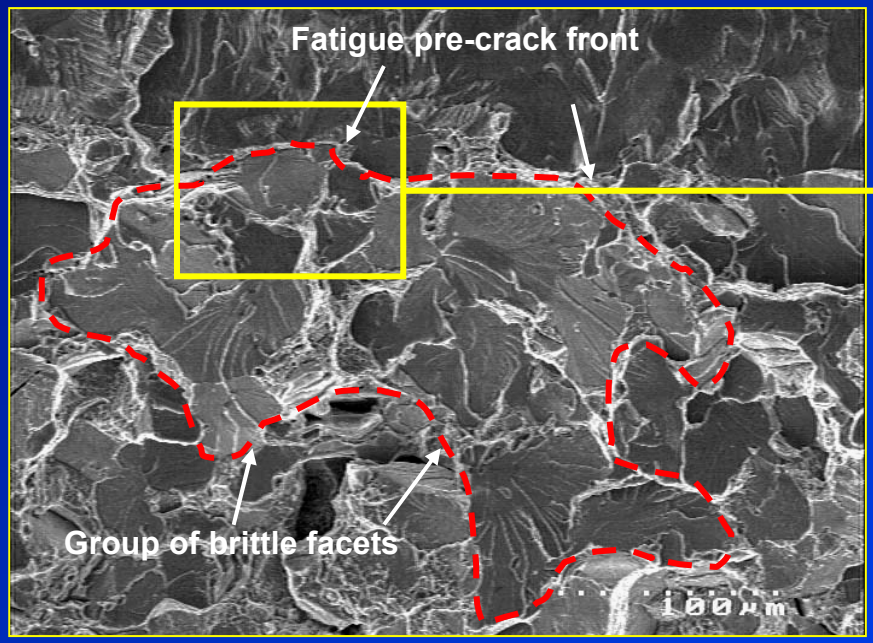

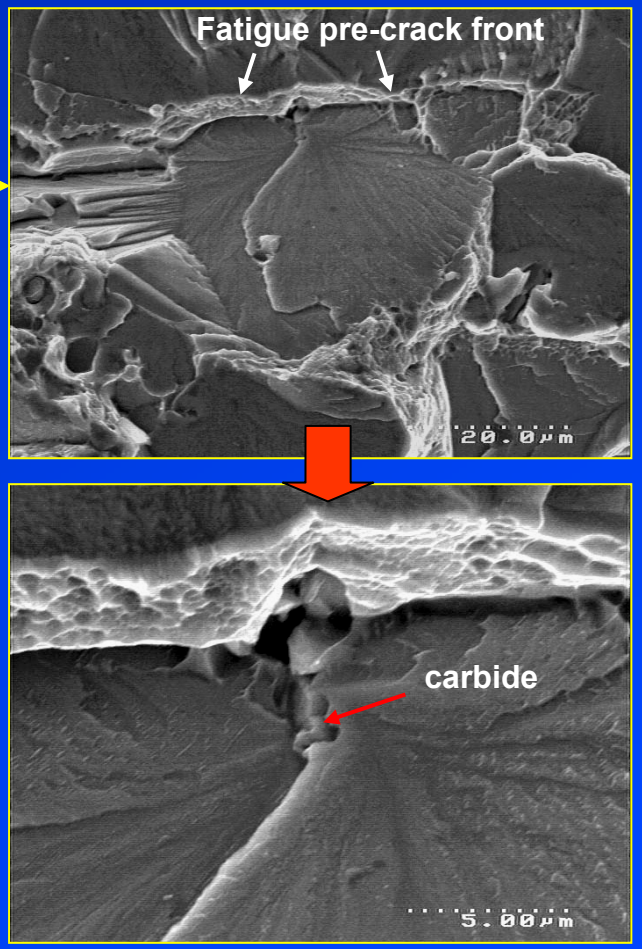

High local tensile stresses raised by dislocation pile-ups ahead of the carbide cause micro-cracking of carbide, which further propagate to cause global failure.

Effects of second phase particles on tensile ductility

• Second-phase particles which are ***readily cut by dislocation*** produce ***planar slips***, producing large dislocation pile-ups which are susceptible for brittle fracture.

• Second-phase particles which are ***impenetrable by dislocations***, greatly ***reduce the slip distance*** → the number of dislocations is sustained → reduce the pile-up.

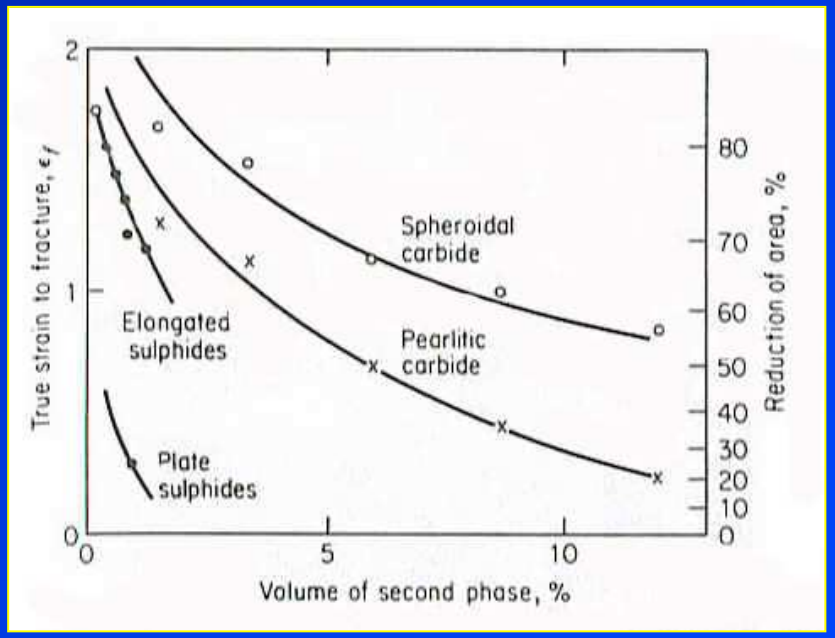

• Small spherical particles ***(r<1 μm)*** are more resistant to cracking.
• A soft ductile phase can also impart ductility to a brittle matrix.

Ductile fracture

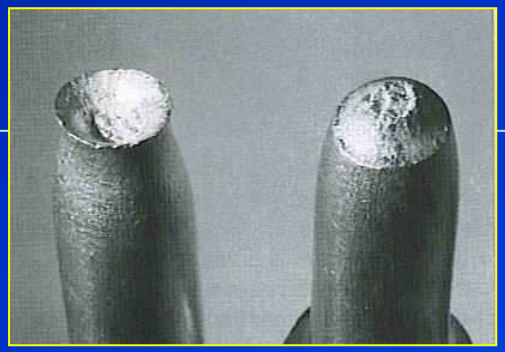

Ductile fracture *is a much less serious problem in engineering materials since failure can be detected beforehand due to observable* ***plastic deformation*** *prior to failure.*

- Under uniaxial tensile force, after necking, ***microvoids*** form and coalesce to form crack, which then propagate in the direction normal to the tensile axis.
- The crack then rapidly propagate through the periphery along the shear plane at 45^{o}, leaving the ***cub and cone fracture***.

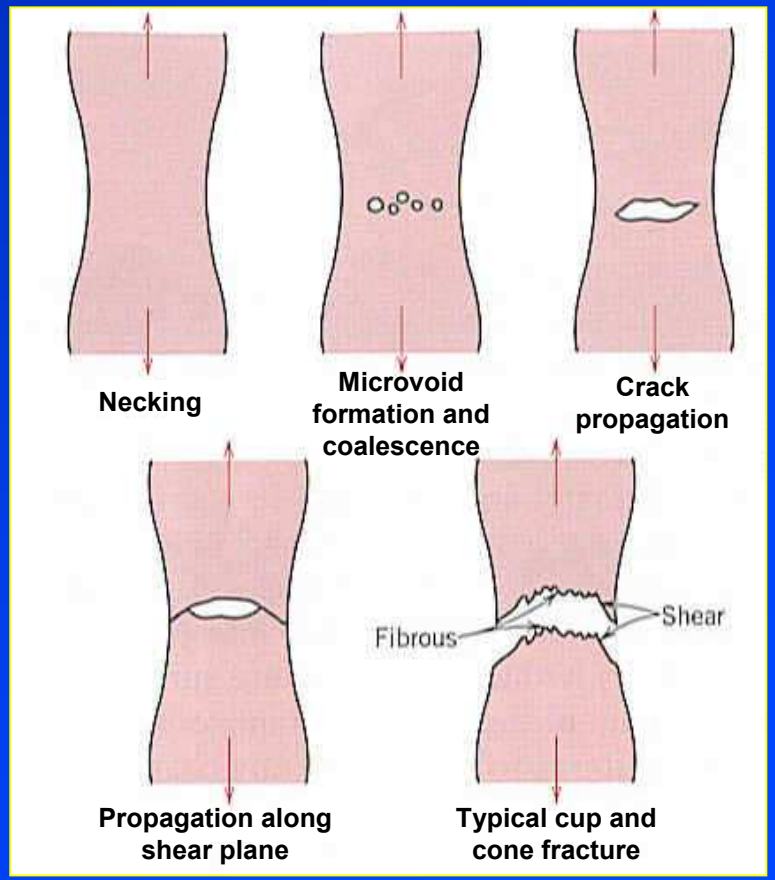

Stages in cup and cone fracture

Microvoid formation, growth and coalescence

- ***Microoids*** are easily formed at inclusions, intermetallic or second-phase particles and grain boundaries.
- ***Growth*** and ***coalescence*** of microvoids progress as the local applied load increases.

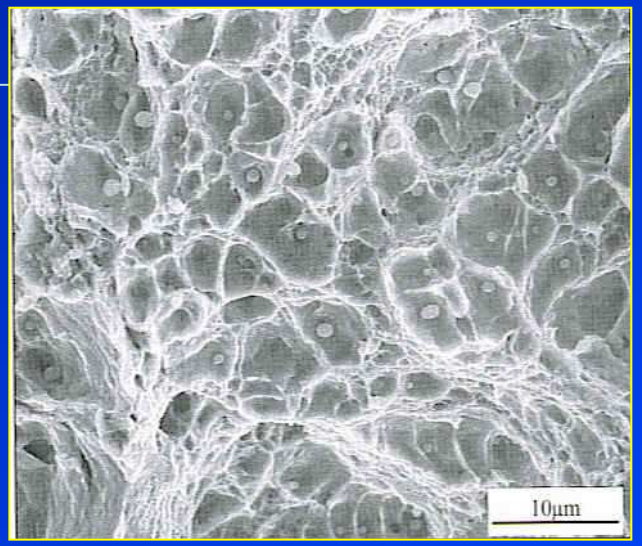

Ductile dimples centred on spherical particles

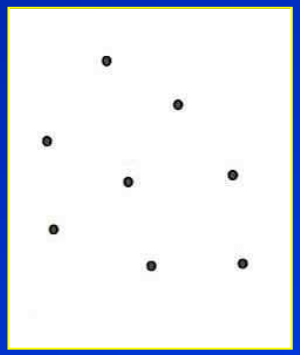

a) Random planar array of particles acting as void initiators.

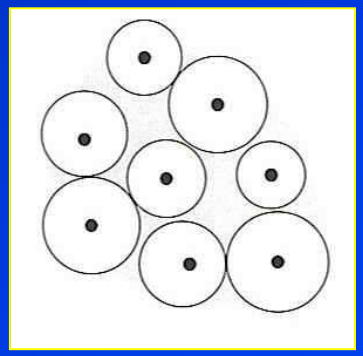

b) Growth of voids to join each other as the applied stress increases.

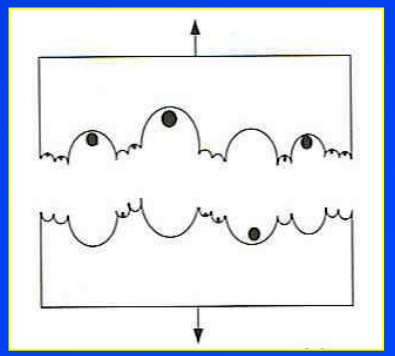

c) Linkage or coalescence of these voids to form free fracture surface.

Formation of microvoids from second phase particles

Microvoids are formed by

1) Decohesion at particle-matrix interface.
2) Fracture of brittle particle
3) Decohesion of an interface associated with shear deformation or grain boundary sliding.

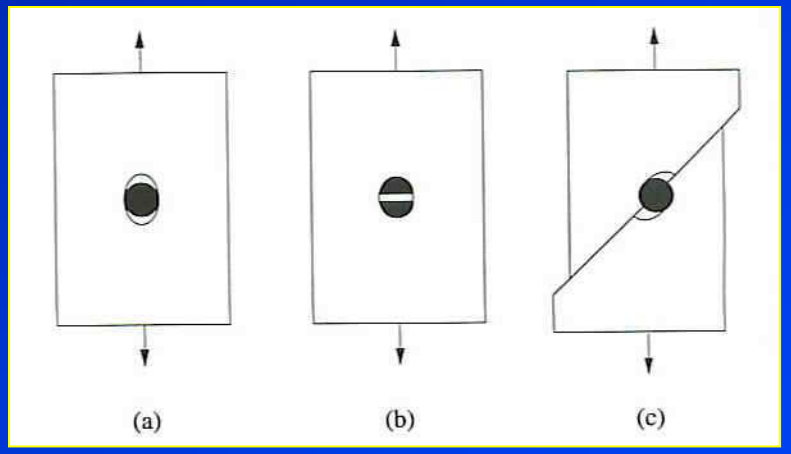

Mechanisms of microvoid formation

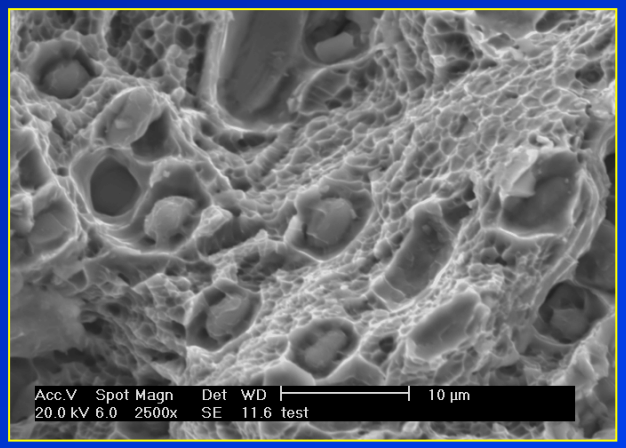

Decohesion of carbide particles from Ti matrix.

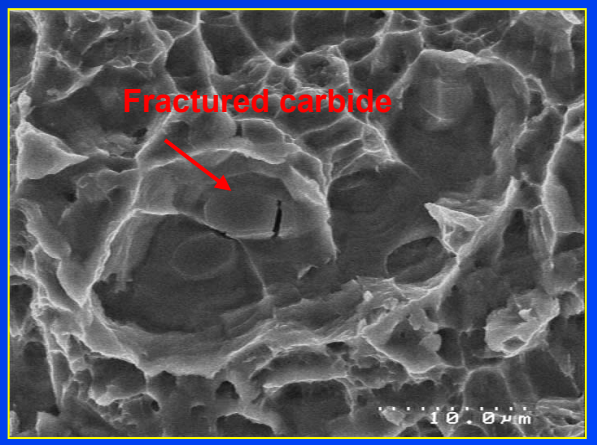

Fractured carbides aiding microvoid formation.

Microvoid shape

Microvoid shape is strongly influenced by the type of loading.

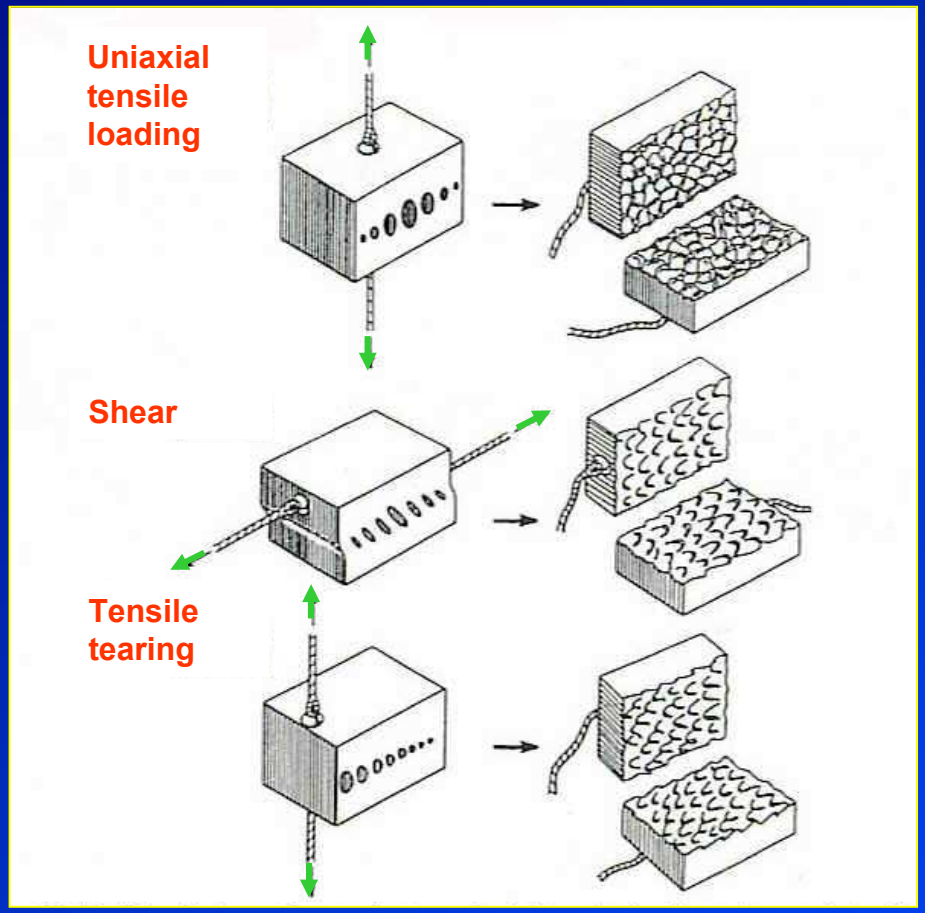

Uniaxial tensile loading

→ Equiaxed dimples.

Shear loading

→ Elongated and parabolic dimples pointing in the opposite directions on matching fracture surfaces.

Tensile tearing

→ Elongated dimples pointing in the same direction on matching fracture surface.

Formation of microvoids or dimples owing to uniaxial tensile loading, shear and tensile tearing

Ductile to brittle transition behaviour

BCC structure metals *experience* ***ductile-to-brittle transition behaviour*** *when subjected to decreasing temperature, resulting from a strong yield stress dependent on temperature.*

- ***BCC*** metals possess ***limited slip systems*** available at low temperature, ***minimising the plastic deformation*** during the fracture process.
- ***Increasing temperature*** allows more slip systems to operate, yielding ***general plastic deformation*** to occur prior to failure.

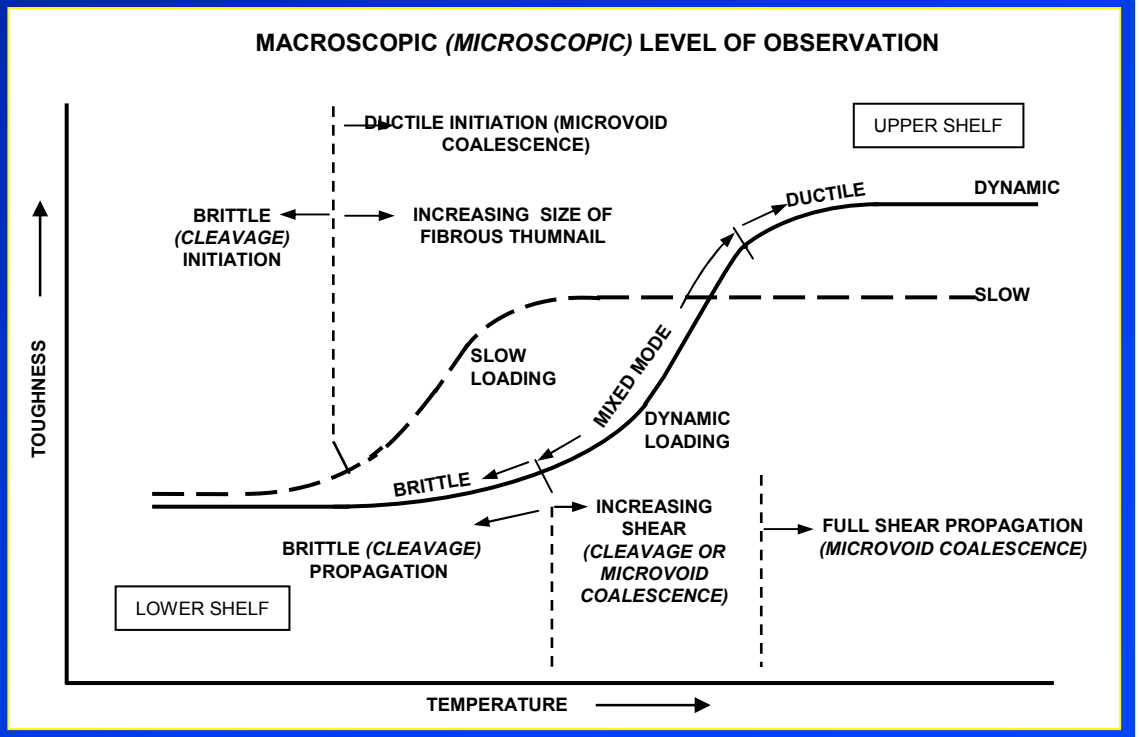

Low temperature → **Brittle cleavage fracture**

High temperature → **Ductile fracture**

Theory of the ductile to brittle transition

The ***criterion*** for a material to change its fracture behaviour from ***ductile to brittle mode*** is when the ***yield stress*** at the observed temperature is larger than the ***stress necessary for the growth of the microcrack*** indicated in the ***Griffith theory***.

Cottrell studied the role of parameters, which influence the ***ductile-to-brittle transition*** as follows;

...Eq. 11

$$\left(\tau_i D^{1/2} + k'\right)k' = G\gamma_s\beta$$

The criterion for ductile to brittle transition is when the term on the left hand side is greater than the right hand side.

where

τ_i is the lattice resistance to dislocation movement
k' is a parameter related to the release of dislocation into a pile-up
D is the grain diameter (associated with slip length).
G is the shear modulus
β is a constant depending on the stress system.

Factors affecting ductile to brittle transition

*From equation, materials having high lattice resistance τ_i, grain size **D** and **k'** has a high tendency to become brittle with decreasing temperature.*

$$\left(\tau_i D^{1/2} + k'\right)k' = G\gamma_s\beta$$

- The τ_i in **BCC** material is strongly dependent on temperature.
- Materials with high **k'** i.e., **Fe** and **Mo** are more susceptible for brittle fracture.
- Smaller grain sized metals can withstand brittle behaviour better.

Note: Alloy chemistry and microstructure also affect the ductile to brittle transition behaviour.

In mild steel Ni lowers DBTT
C, P, N, S, Mo raise DBTT

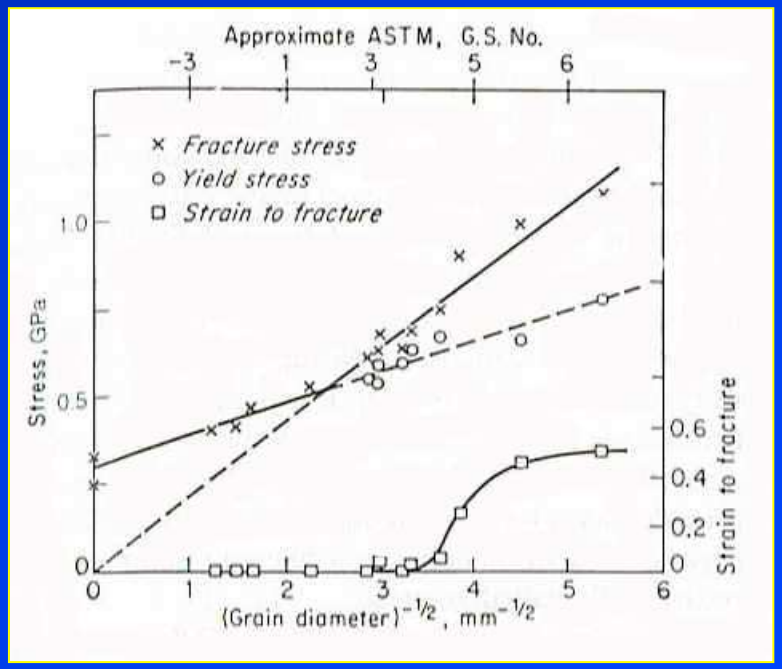

Effect of grain size on the yield and fracture stresses for a low-carbon steel tested in tension at -196°C.

Intergranular fracture

- ***Intergranular failure*** is a moderate to low energy brittle fracture mode resulting from ***grain boundary separation*** or segregation of embrittling particles or precipitates.
- ***Embrittling grain boundary particles*** are weakly bonded with the matrix, → high free energy and unstable, which leads to ***preferential crack propagation path***.

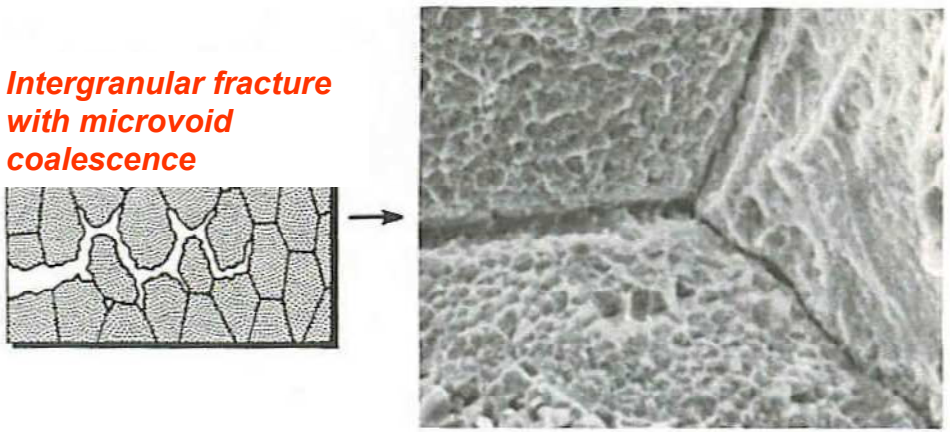

Intergranular fracture with and without microvoid coalescence.

Factors affecting modes of fracture

	Brittle fracture	Ductile fracture
Metallurgical aspect	Large grained materials with GB particles.	Fine grained material without GB particles.
Temperature	Low temperature	High temperature
State of stresses (notch effect)	Triaxial state of stresses (notch effect)	Absence of the notch
Strain rate	High strain rate	Low strain rate
Loading condition		Hydrostatic pressure (suppress crack initiation)

Metallurgical aspect of fracture

- Microstructure in metallic materials are highly complex.
- Various microstructural features affect how the materials fracture.

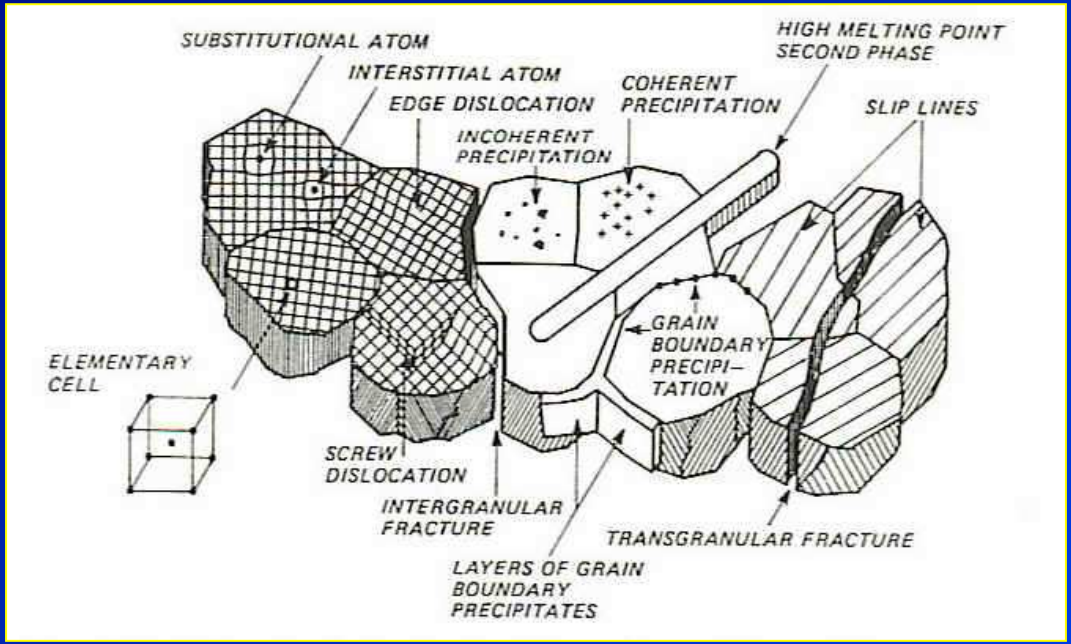

Microstructural features in metallic materials

There are microstructural features that can play a role in determining the fracture path, the most important are;

Second phase

Particles and precipitates

Grain size

Fibering and texturing

- ***High strength materials*** usually possess several microstructural features in order to optimise mechanical properties by ***influencing deformation behaviour / fracture paths***.

State of stresses (notch effect)

The difference in the state of stresses in the presence of a sharp crack or notch affects fracture in materials.

A notch or a sharp crack increases the ***tendency for brittle fracture*** in four important ways;

1) **Producing high local stresses**
2) **Introducing a triaxial state of stresses**
3) **Producing high local strain hardening and cracking**
4) **Producing a local magnification to the strain rate.**

Note: the notch also raises the ***plastic-constraint factor q,*** *which does not exceed the value of 2.75*

notch effect

The presence of the notch alters stress distribution

- In a thin plate, stress in the ***z*** (thickness) direction is absence, the specimen is not constrained.
- In thicker plate, σ_y (in the tensile direction) is constrained due to the reaction of σ_z and σ_x, leading to triaxial state of stresses.
- ***Triaxial stresses*** limit plastic deformation ahead of the crack tip → raising the general yield → material prone to brittle fracture

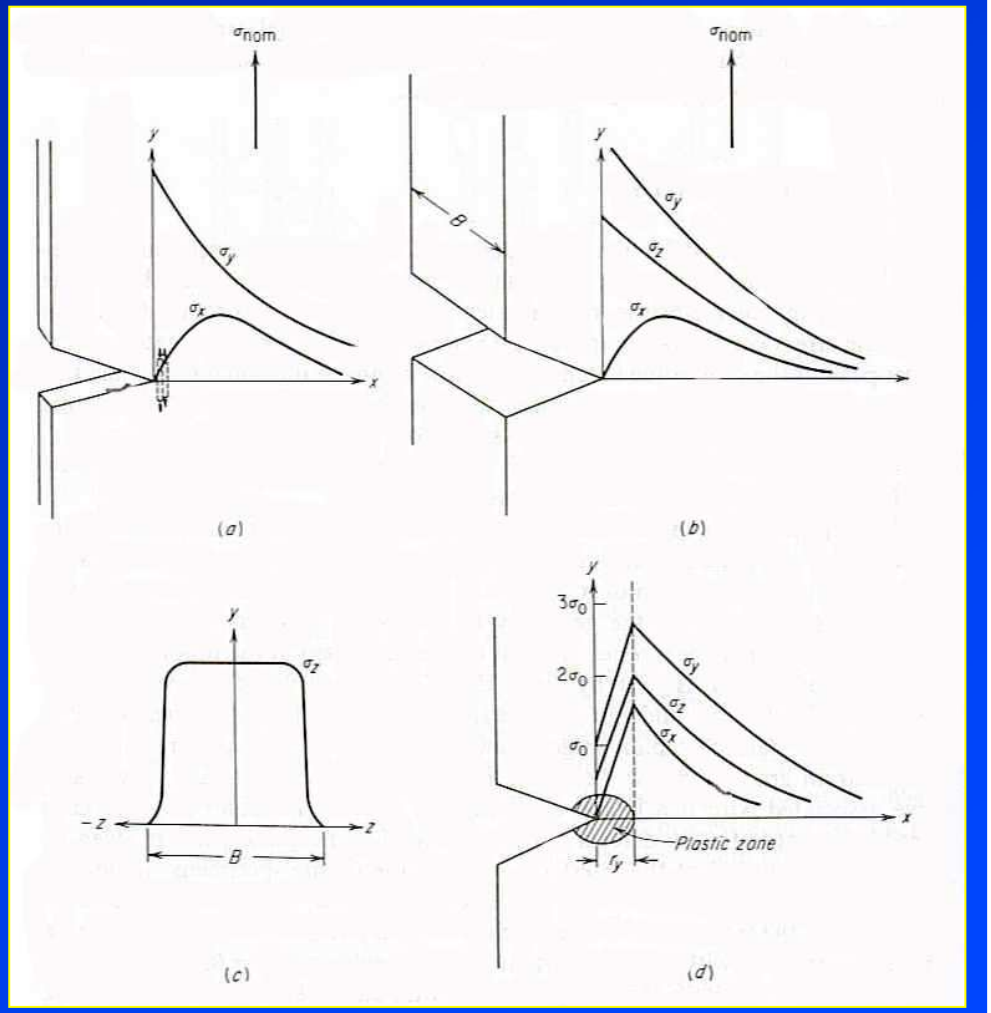

Elastic stresses beneath a notch in thin and thick plates

Effects of combined stress and hydrostatic pressure on fracture

Combined stress

- Yielding under complex states of stress is difficult to predict.
- Available data on ductile metals, i.e., ***Al*** and ***Mg*** alloys and ***steel*** indicate that the ***maximum-shear stress criterion*** for fracture are in the best agreement.

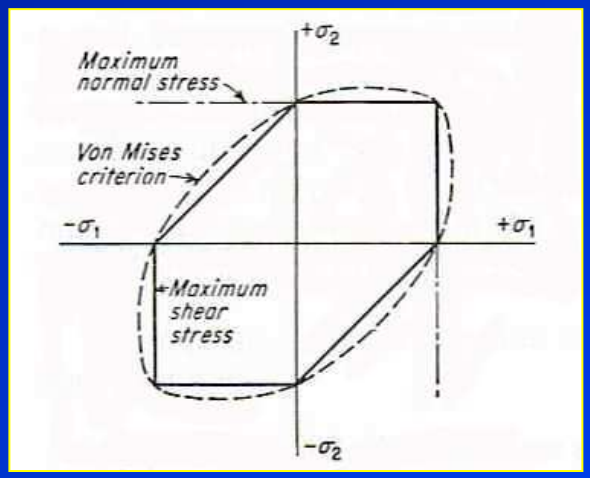

Proposed fracture criteria for biaxial state of stress in ductile metal

Hydrostatic pressure

- ***hydrostatic pressure*** is triaxial compressive stress resist fracture and increase ductility.
- ***Hydrostatic pressure*** exerts no shear stress, it therefore does not influence ***crack initiation*** but affects ***crack propagation***.

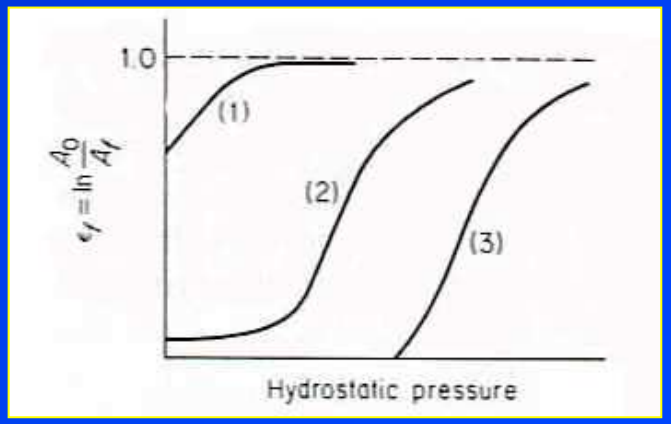

Effect of hydrostatic pressure on ductility in tension

Concept of the fracture curve

Ludwik proposed that a metal has a fracture stress curve in addition to a flow curve (true stress - true strain curve) and that ***fracture occurs when the flow curve intersects the fracture curve***.

- The plastic deformation is inhibited when strain hardening, triaxial stress, or high strain rate, causing sufficiently high stress to break the material.

- ***Fracture stress*** is difficult to measure since most metals exhibit small plastic deformation prior to failure even in the presence of the notch and at very low temperature.

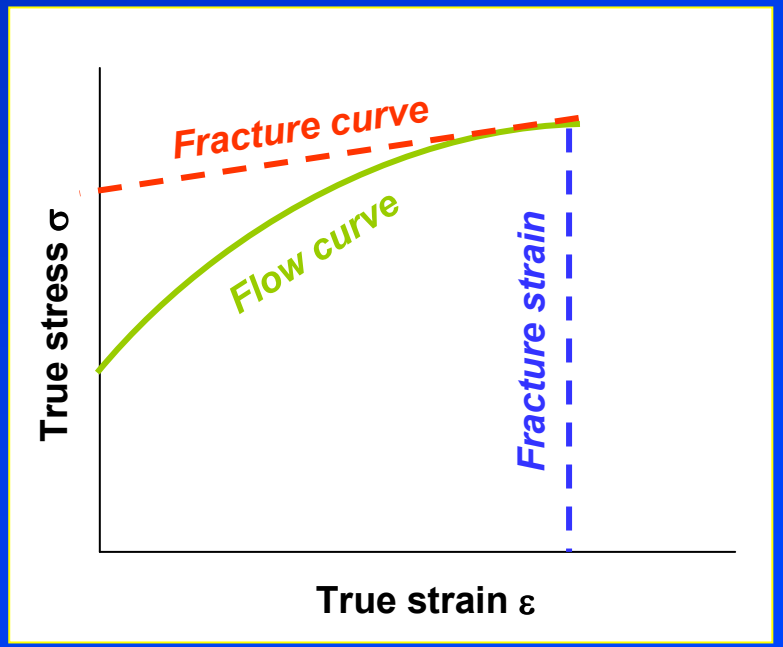

Intersection of flow curve and fracture curve.

Notch effect on transition temperature

The ***fracture stress*** σ_f is much less temperature sensitive than the ***flow stress*** σ_o.

- The σ_o of the ***unnotched specimen*** is lower than σ_f at temperatures above the transition temperature.
- The metal therefore deforms plastically before fracture. Below the transition temperature $\sigma_o > \sigma_f$, metal fails without plastic deformation.
- The ***presence of the notch*** raises the σ_o by the ***plastic-constraint factor*** ***q***. This shifts the transition temperature to the right hand side.

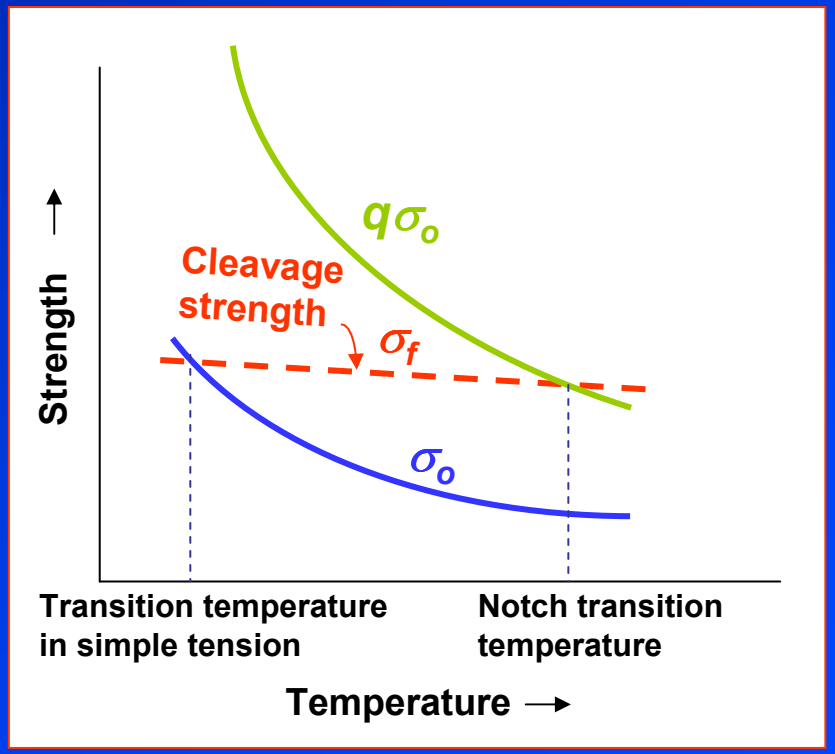

Description of transition temperature

References

- Dieter, G.E., ***Mechanical metallurgy***, 1988, SI metric edition, McGraw-Hill, ISBN 0-07-100406-8.
- Sanford, R.J., ***Principles of fracture mechanics***, 2003, Prentice Hall, ISBN 0-13-192992-1.
- W.D. Callister, ***Fundamental of materials science and engineering/ an interactive e. text***., 2001, John Willey & Sons, Inc., New York, ISBN 0-471-39551-x.
- Hull, D., Bacon, D.J., ***Introduction to dislocations***, 2001, Forth edition, Butterworth-Heinemann, ISBN 0-7506-4681-0.
- Smallman, R.E., Bishop, R.J., ***Modern physical metallurgy & materials engineering***, 1999, sixth edition, Butterworth-Heinemann, ISBN 0-7506-4564-4.

References

• Cottrell, A.H., ***Theory of brittle fracture in steel and similar metals***, 1958, Transactions of the metallurgical society of AIME, Vol. 212, p. 192-203.

• Stroh, A.N., Advanced Physics, 1957. Vol **6**: p. 418

Tension test

Subjects of interest

- *Introduction/Objectives*
- *Engineering stress-strain curve*
- *True stress-true strain curve*
- *Instability in tension*
- *Stress distribution at the neck*
- *Ductility measurement in tension tests*
- *Effect of strain rate on flow properties*
- *Effect of temperature on flow properties*

Tension test

Subjects of interest

- *Influence of testing machine on flow properties*
- *Thermally activated deformation*
- *Notch tensile test*
- *Tensile properties of steel*
- *Anisotropy of tensile properties*

Objectives

- This chapter provides fundamental backgrounds of tension tests where appropriate material parameters can be used for material selection.
- Differences between engineering stress-strain curve and true stress – true strain curve will be clearly understood.
- Effects of strain rate, test temperature, testing machine as well as notch and anisotropy on tensile properties will be highlighted.

Engineering stress-strain curve

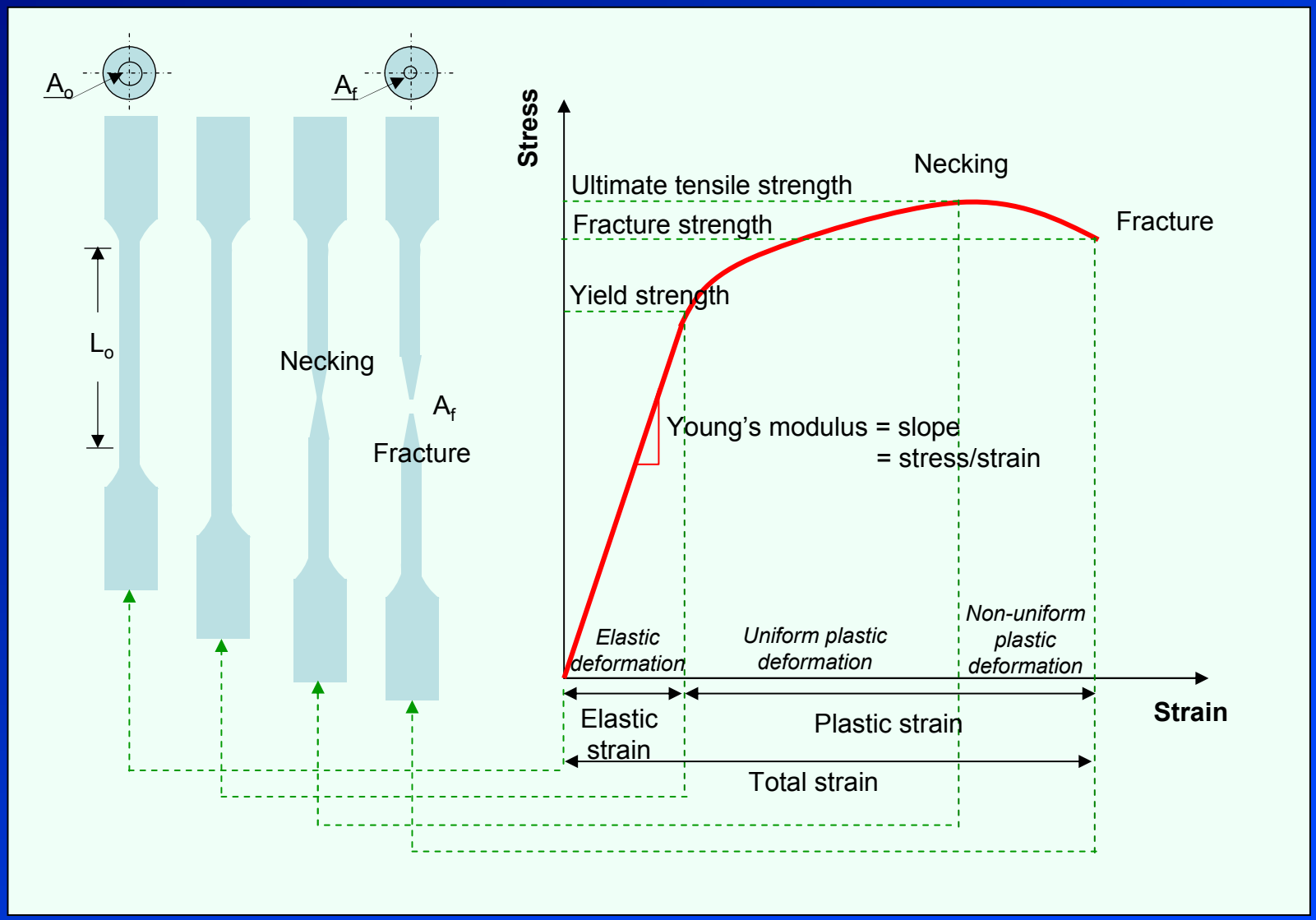

Engineering stress-strain curve

- Basic design information on the strength of materials.
- An acceptance test for the specification of materials.

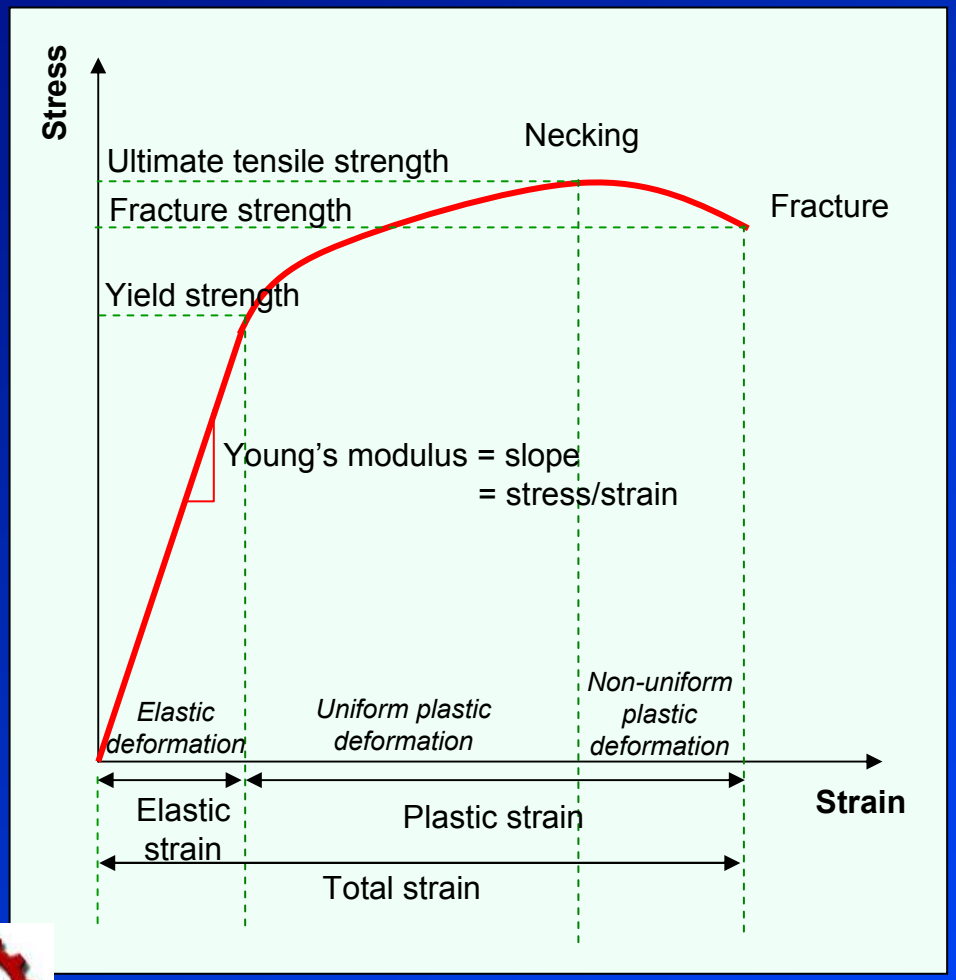

Average longitudinal tensile stress

$$s = \frac{P}{A_o}$$ *Eq.1*

Average linear strain

$$e = \frac{\delta}{L_o} = \frac{\Delta L}{L_o} = \frac{L - L_o}{L_o}$$ *Eq.2*

Factors affecting shape and magnitude of stress-strain curve

- Composition
- Heat treatment
- Prior history of plastic deformation

Metallurgical factors

- Strain rate
- Temperature
- State of stress

Test conditions

Recoverable elastic strain and plastic strain

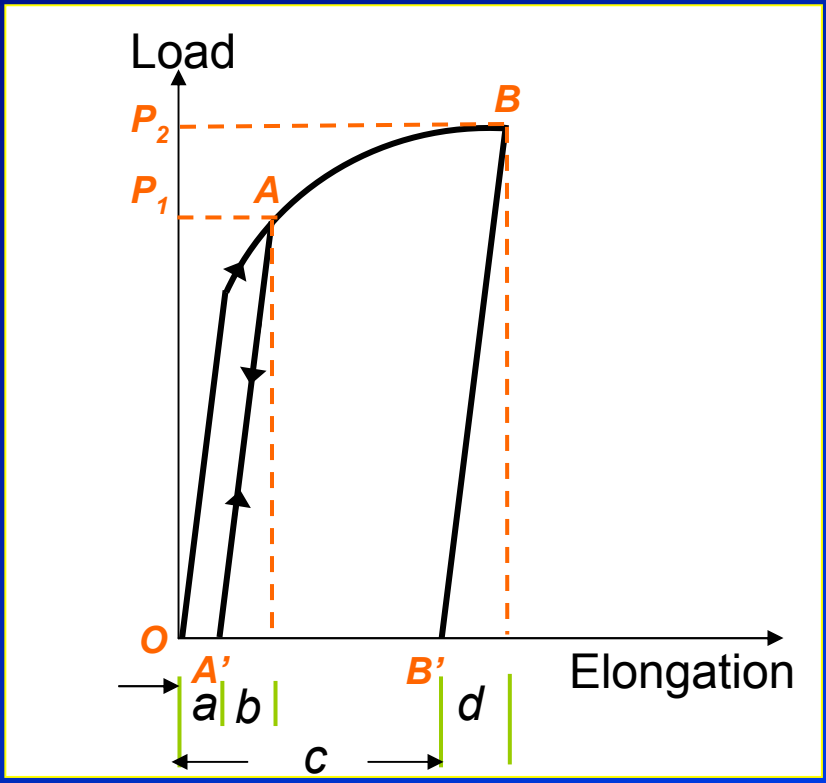

- Loading of tensile sample beyond yield point to ***A*** and then unloading give the unloading curve ***AA'*** with its slope parallel to the elastic Young's modulus.
- ***Recoverable elastic strain b*** on unloading is given by

$$b = \frac{\sigma_1}{E} = \frac{P_1 / A_o}{E}$$

Eq.3

- ***Permanent plastic strain a***
- Loading and unloading following ***OABB'*** gives ***plastic deformation c*** whereas ***elastic deformation*** under loading is ***d***.

Tensile strength

Tensile strength *or ultimate tensile strength (UTS)* s_u *is the maximum load* P_{max} *divided by the original cross-sectional area* A_o *of the specimen.*

$$s_u = \frac{P_{\max}}{A_o}$$

Eq.4

- Tensile strength is the most value quoted from tensile test results.
- Useful for ***specifications***, ***quality control*** of a product.
- In engineering design, ***safety factor*** should be applied.

Note: yield stress is more practical for ductile materials. But it has little relation to ***complex conditions of stress***.

Yielding

*Various criteria for the **initiation of yielding** are used depending on the sensitivity of the strain measurements and the intended use of the data.*

1) ***True elastic limit***: based on microstrain measurement at strains on order of 2×10^{-6}. Very low value and is related to the motion of a few hundred dislocations.

2) ***Proportional limit:*** the highest stress at which stress is directly proportional to strain.

3) ***Elastic limit:*** is the greatest stress the material can withstand without any measurable permanent strain after unloading. ***Elastic limit > proportional limit***.

4) ***Yield strength*** is the stress required to produce a small specific amount of deformation.

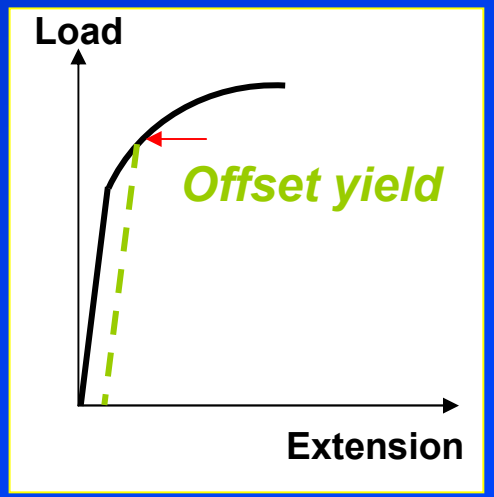

Yield strength of materials

The offset yield strength can be determined by the stress corresponding to the intersection of the stress-strain curve and a line parallel to the elastic line offset by a strain of 0.2 or 0.1%. (e = 0.002 or 0.001)

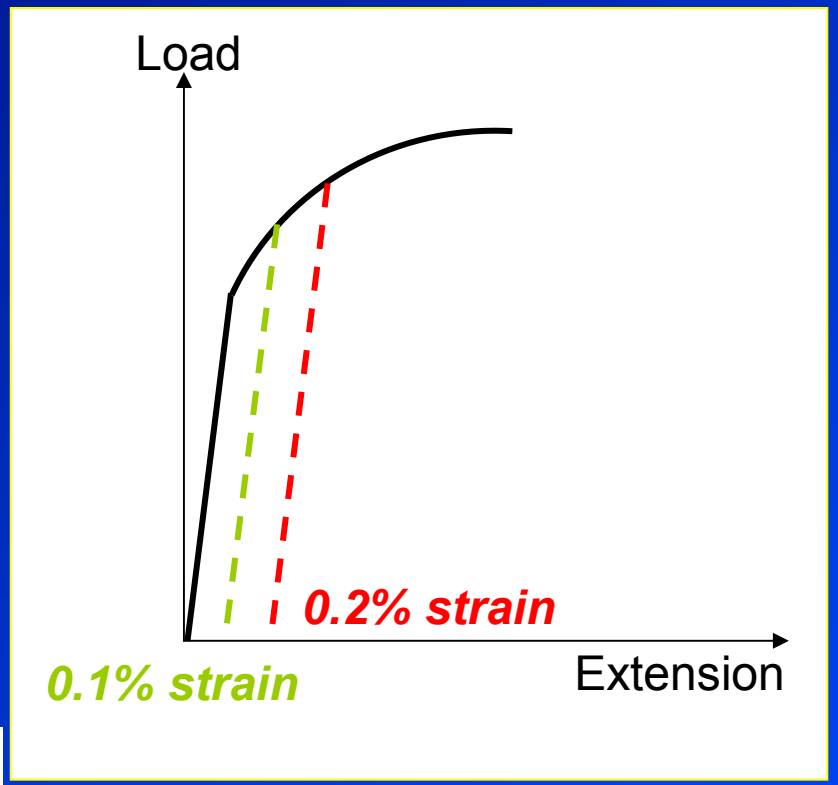

$$s_o = \frac{P_{(strain\ \ offset=0.002)}}{A_o}$$

Eq.5

In Great Britain, the offset yield stress is referred to ***proof stress*** either at 0.1 or 0.5%strain.

Used for design and specification purposes to avoid the practical difficulties of measuring the elastic limit or proportional limit.

Yield strength of materials

- ***FCC*** lattice materials (***Al, Cu***) have no definite yield point. The yield strength is therefore defined by the ***offset of yielding***.
- ***Yield strength*** can be improved by ***work hardening*** (cold working). → up to 300:1 stronger than original.
- Alloying of ***Al*** can improve ***elastic limit*** 1.5-2 times.

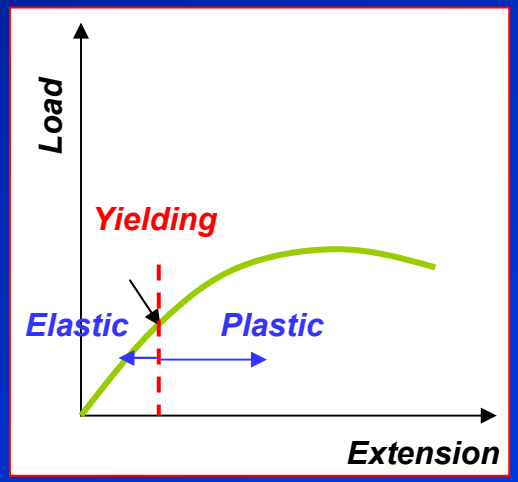

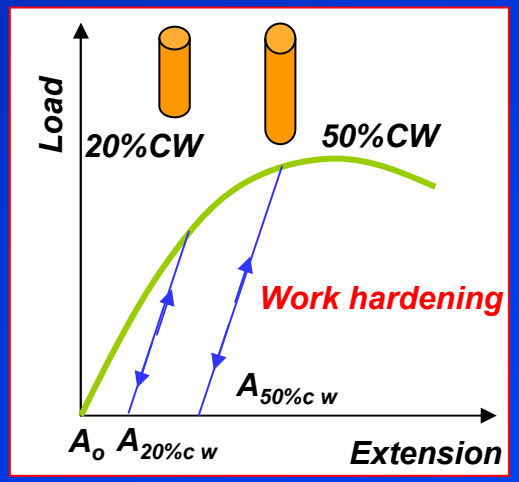

Improvement of yielding by cold working

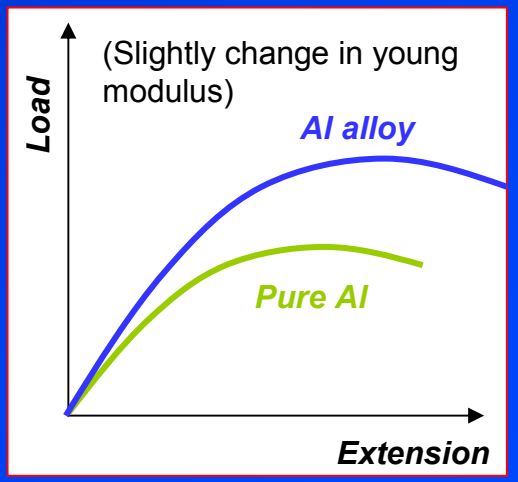

Improvement in elastic limit by alloying

Yield strength of materials

- ***BCC*** lattice materials (***Fe***) show a yield point phenomenon → ***Upper and lower yield points*** (depending on testing machine).
- ***Condition:*** Polycrystalline & small amounts of interstitial solute atoms.

Upper yield point $\frac{L_2}{A_o}$ **Lower yield point** $\frac{L_1}{A_o}$

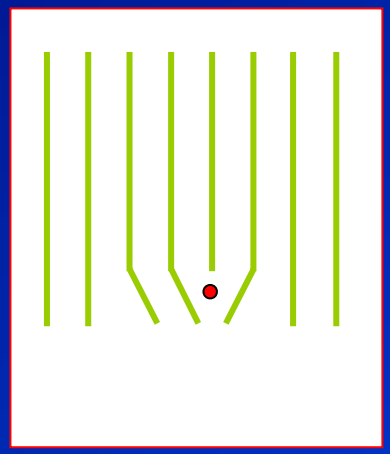

Interstitial solute atom

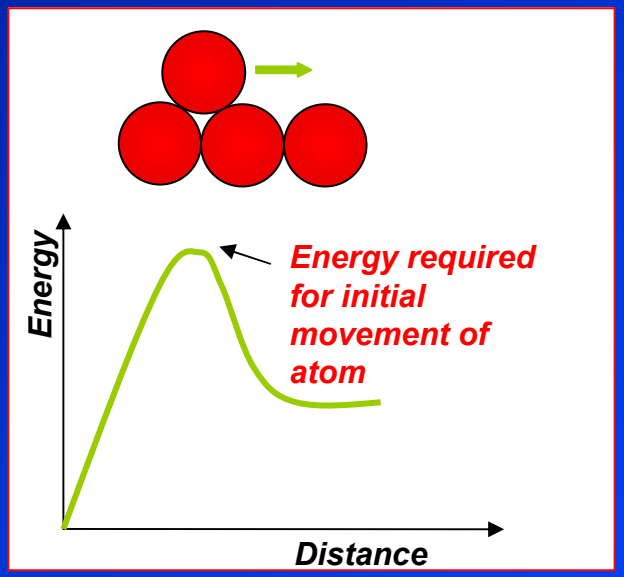

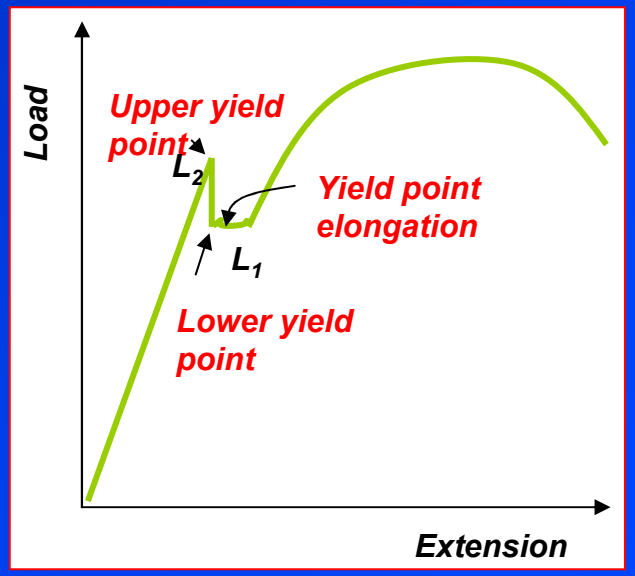

At yield point, localised internal friction requires more energy for interstitial atom to move dislocation, after that dislocation are free from interstitial atom (carbon, nitrogen).

Ductility

Ductility is a qualitative, subjective property of a material.

In general, ductility is of interest in three different ways

1) ***For metal working operation*** : indicating amount of deformation can be applied without failure.
2) ***For stress calculation or the prediction of severe load*** : indicating the ability of the metal to flow plastically before failure.
3) ***For indication of any changes in heat treatments or processing conditions in metal***.

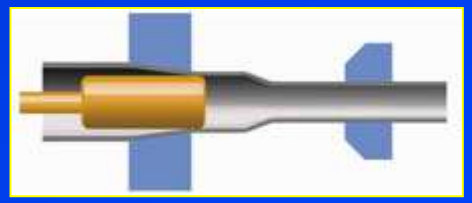

Measures of ductility

Elongation

$$e_f = \frac{L_f - L_o}{L_o}$$ *Eq.6*

Reduction of area, *q*

$$q = \frac{A_o - A_f}{A_o}$$ *Eq.7*

These ***parameters*** are obtained after fracture by putting specimen back together and taking the measurement.

Zero-gauge length elongation

$$e_o = \frac{L - L_o}{L_o} = \frac{A_o}{A} - 1 = \frac{1}{1-q} = \frac{q}{1-q}$$ *Eq.8*

Modulus of elasticity

Modulus of elasticity or ***Young's modulus*** is a measure of material stiffness (given by the slope of the stress-strain curve).

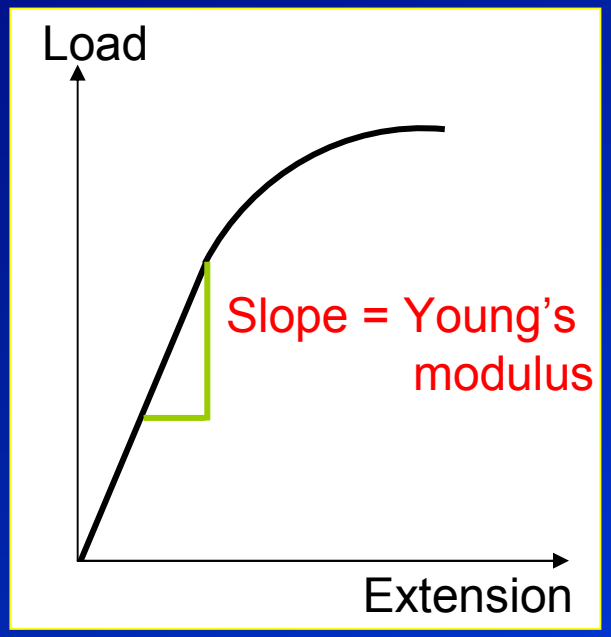

- Modulus of elasticity is determined by the binding forces between atoms (structure insensitive property)
- Cannot change ***E,*** but can improve by forming composites.
- Only slightly affected by alloying addition, heat treatment or cold work.

Temp ↑ ***Young's modulus*** ↓

Young's modulus ↑

Stiffness ↑

Deflection ↓

Table 8-1 Typical values of modulus of elasticity at different temperatures

Material	Modulus of elasticity, GPa				
	Room temp.	477 K	700 K	810 K	922 K
Carbon steel	207	186	155	134	124
Austenitic stainless steel	193	176	159	155	145
Titanium alloys	114	97	74	70	
Aluminum alloys	72	66	54		

Example: *A 13 mm diameter tensile specimen has a 50 mm gauge length. The load corresponding to the 0.2% offset is 6800 kg and the maximum load is 8400 kg. Fracture occurs at 7300 kg. The diameter after fracture is 8 mm and the gauge length at fracture is 65 mm. Calculate the standard properties of the material from the tension test.*

$$A_o = \frac{\pi}{4}(13)^2 = 132.7 \ mm^2 = 132.7 \times 10^{-6} \ m^2$$

$$A_f = \frac{\pi}{4}(8)^2 = 50.3 \ mm^2 = 50.3 \times 10^{-6} \ m^2$$

$$e_f = \frac{L - L_o}{L_o} = \frac{65 - 50}{50} = 30\%$$

$$q = \frac{A_o - A_f}{A_o} = \frac{132.7 - 50.3}{132.7} = 62\%$$

$$s_u = \frac{P_{\max}}{A_o} = \frac{8400 \times 9.8}{132.7 \times 10^{-6}} = 620 \ MPa$$

$$s_o = \frac{P_y}{A_o} = \frac{6800 \times 9.8}{132.7 \times 10^{-6}} = 502 \ MPa$$

$$s_f = \frac{P_f}{A_o} = \frac{7300 \times 9.8}{132.7 \times 10^{-6}} = 539 \ MPa$$

If ***E = 207 GPa***, the elastic recoverable strain at maximum load is

$$e_E = \frac{P_{\max} / A_o}{E} = \frac{620 \times 10^6}{207 \times 10^9} = 0.0030$$

If the elongation at maximum load (the uniform elongation) is 22%, what is the plastic strain at maximum load?

$$e_p = e_{total} - e_E = 0.2200 - 0.0030 = 0.2170$$

Resilience

- ***Resilience*** *is an ability of a material to* ***absorb energy when elastically deformed*** *and to return it when unloaded.*
- *Usually measured by* ***modulus of resilience*** *(strain energy per unit volume required to stress the material from zero to the yield stress,* σ_o*.*

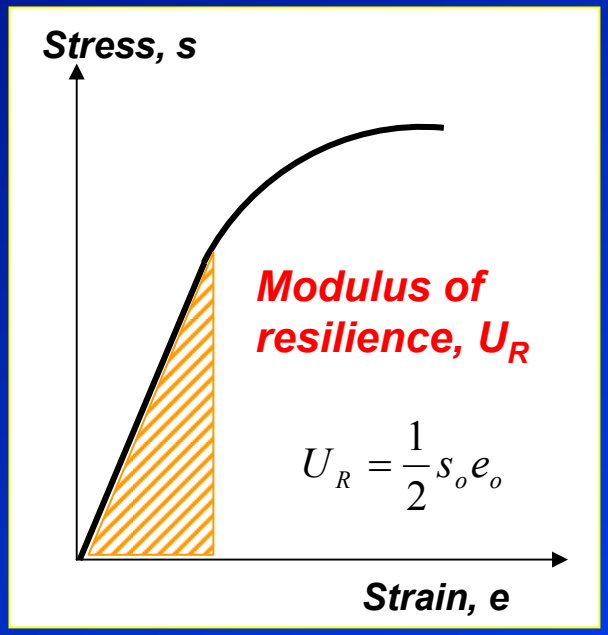

$$U_o = \frac{1}{2}\sigma_x e_x = U_R = \frac{1}{2} s_o e_o = \frac{s_o^2}{2E}$$ *Eq.9*

Table 8-2 Modulus of resilience for various materials

Material	E, GPa	s_0, MPa	Modulus of resilience, U_R, kPa
Medium-carbon steel	207	310	232
High-carbon spring steel	207	965	2250
Duralumin	72	124	107
Copper	110	28	3.5
Rubber	0.0010	2.1	2140
Acrylic polymer	3.4	14	28

Note: *for* ***mechanical springs*** *→ high yield stress and low modulus of elasticity.*

Toughness

- ***Toughness*** *is an ability to* ***absorb energy in the plastic range****.*
- *Or the ability to withstand occasional stresses above the yield stress without fracture.*
- *Can be simply defined by the* ***area under the stress-strain curve*** *(amount of work per unit volume that the material can withstand without failure.)*

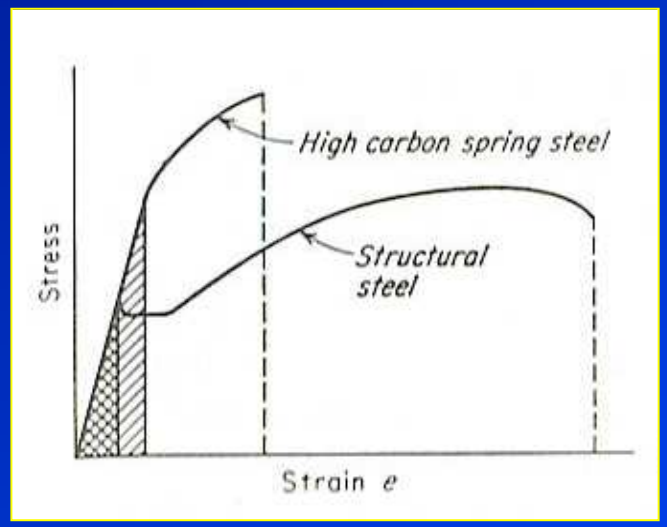

Comparison of stress-strain curves for high and low-toughness materials.

- The structural steel although has a lower yield point but more ductile than high carbon spring steel. → ***Structural steel is therefore tougher***.
- ***Toughness = strength + ductility***

Ductile materials

$$U_T \approx s_u e_f$$

$$U_T \approx \frac{s_o + s_u}{2} e_f$$

Eq.10

Brittle materials

$$U_T \approx \frac{2}{3} s_u e_f$$

Eq.11

(only approximation)

True-stress-true-strain curve

- ***True stress-strain curve*** gives a true indication of deformation characteristics because it is ***based on the instantaneous dimension*** of the specimen.
- The ***true stress-strain curve*** is also known as the ***flow curve***.

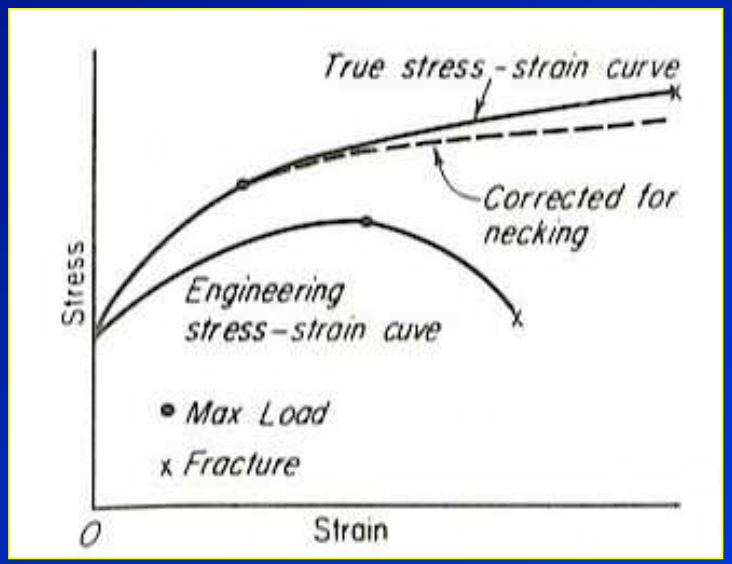

Comparison of engineering and the true stress-strain curves

- In ***engineering stress-strain curve***, stress drops down after necking since it is based on the original area.
- In ***true stress-strain curve***, the stress however increases after necking since the cross-sectional area of the specimen decreases rapidly after necking.

True stress

$$\sigma = \frac{P}{A_o}(e+1) = s(e+1)$$

Eq.12

True strain

$$\varepsilon = \ln(e+1)$$

Eq.13

Note: these equations are used for data upto the onset of necking. Beyond necking, use the actual measurements of load, cross-sectional area, diameter.

True stress at maximum load

- ***True stress at maximum load*** corresponds to the ***true tensile strength***.

The ultimate tensile strength

$$s_u = \frac{P_{\max}}{A_o}$$

The true stress at maximum load

$$\sigma_u = \frac{P_{\max}}{A_u}$$

And true strain at maximum load

$$\varepsilon_u = \ln \frac{A_o}{A_u}$$

Eliminating P_{max} gives

$$\sigma_u = s_u \frac{A_o}{A_u} = s_u e^{\varepsilon_u}$$

Eq.14

Where σ_u true stress at maximum load

ε_u true strain at maximum load

A_u cross-sectional area of the specimen at maximum load

True fracture stress

• The true fracture stress σ_f is the load at fracture $P_{fracture}$ divided by the cross sectional area at fracture A_f.

$$\sigma_f = \frac{P_{fracture}}{A_{fracture}}$$

Eq.15

Note: Need to be corrected for the triaxial state of stress existing in the tensile specimen at fracture. → Often error.

True fracture strain

• The true fracture strain ε_f is based on the original area A_o and the area after fracture A_f.

$$\varepsilon_f = \ln\frac{A_o}{A_f}$$

Eq.16

• After necking, the true fracture strain can be related to the area of reduction q.

$$\varepsilon_f = \ln\frac{1}{1-q}$$

Eq.17

True uniform strain

• The ***true uniform strain*** ε_u is the true strain based only on the strain up to the maximum load.

• Can either be measured from A_u or L_u at maximum load.

• The uniform strain is often used in ***estimating the formability of metals*** from the result of a tension test.

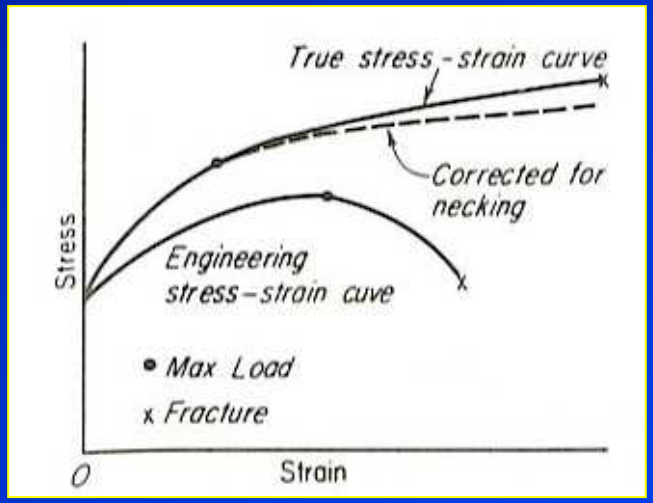

Engineering and true stress-strain curves

$$\varepsilon_u = \ln \frac{A_o}{A_u} \qquad \textit{Eq.18}$$

True local necking strain

• The true local necking strain is the strain required to deform the specimen from the maximum load to fracture.

$$\varepsilon_n = \ln \frac{A_u}{A_f} \qquad \textit{Eq.19}$$

Power-law flow curve

• The flow curve of many metals in the region of uniform plastic deformation can be expressed by the ***simple power law***.

$$\sigma = K\varepsilon^n \qquad \textit{Eq.20}$$

Where ***n*** is the strain hardening exponent
K is the strength coefficient

• ***Log-log plot of true stress-strain curve*** from yield point up to the maximum load will result in a straight line where ***n*** is the slope and ***K*** is the true stress at $\varepsilon = 1.0$.

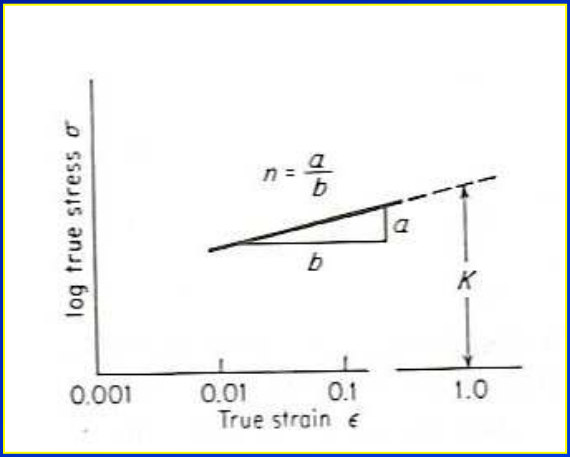

Log-log plot of true stress-strain curve

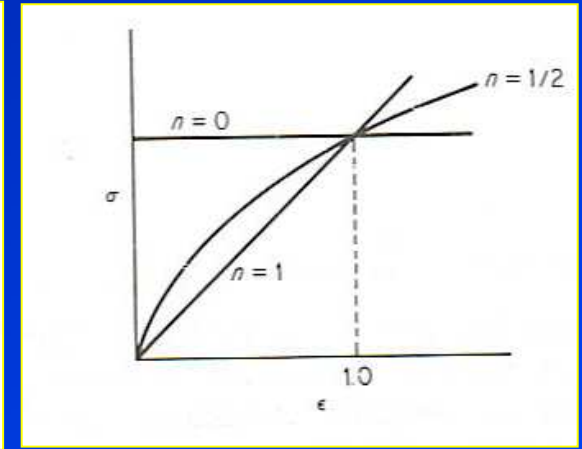

Different forms of power curve $\sigma = K\varepsilon^n$

n = 0 perfectly plastic solid
n = 1 elastic solid
For most metals, 0.1< ***n*** < 0.5

Variations of the power-law flow curve

Datsko showed that ε_o is considered as the amount of strain hardening of the material obtained prior to tension test.

$$\sigma = K(\varepsilon_o + \varepsilon)^n \qquad \text{Eq.21}$$

Ludwik equation relates the yield stress to the power law

$$\sigma = \sigma_o + K\varepsilon^n \qquad \text{Eq.22}$$

True stress-strain curve of ***austenistic stainless steel*** at low strain can be expressed by

$$\sigma = K\varepsilon^n + e^{K_1} e^{n_1 \varepsilon} \qquad \text{Eq.23}$$

Where $e^{K}{}_{1}$ ~ proportional limit
n is the slope of the curve

Example: *In the tension test of a metal fracture occurs at maximum load. The conditions at fracture were: A_f = 100 mm² and L_f = 60 mm. The initial values were: A_o = 150 mm² and L_o = 40 mm. Determine the true strain to fracture using changes in both length and area.*

$$\varepsilon_f = \ln\left(\frac{L_f}{L_o}\right) = \ln\left(\frac{60}{40}\right) = 0.405$$

$$\varepsilon_f = \ln\left(\frac{A_o}{A_f}\right) = \ln\left(\frac{150}{100}\right) = 0.405$$

At the maximum load, both area and gauge length can be used for a strain calculation.

If a more ductile metal is tested such that necking occurs and the final gauge length is 83 mm and the final diameter is 8 mm, while L_o = 40 mm and D_o = 12.8 mm.

$$\varepsilon_f = \ln\left(\frac{L_f}{L_o}\right) = \ln\left(\frac{83}{40}\right) = 0.730$$

$$\varepsilon_f = \ln\left(\frac{D_o}{D_f}\right)^2 = 2\ln\left(\frac{12.8}{8}\right) = 0.940$$

After necking, gauge length gives error but area of reduction can still be used for the calculation of true strain at fracture.

Instability in tension

Ideal plastic material → Undergo ***necking*** after yielding with no strain hardening

Most metal → ***Necking*** begins at maximum load with strain hardening → increasing load-carrying capacity

Necking *or localised deformation starts at the maximum load, which is opposed by a decrease in cross-sectional area of the specimen as it elongates.*

www.seas.upenn.edu

Instability occurs when

An increase in stress due to reduced cross-sectional area **>** The increase in load-carrying capability due to strain hardening

Instability in tension

The condition of instability, which leads to localised deformation is defined by

$$dP = 0, P = \sigma A$$

$$dP = \sigma dA + A d\sigma = 0$$

Because the volume is constant

$$\frac{dL}{L} = -\frac{dA}{A} = d\varepsilon$$

From the instability condition

$$-\frac{dA}{A} = \frac{d\sigma}{\sigma}$$

So that at a point of tensile instability

$$\frac{d\sigma}{d\varepsilon} = \sigma \qquad \textit{Eq.24}$$

Therefore the point of necking can be obtained from the true stress-strain curve by

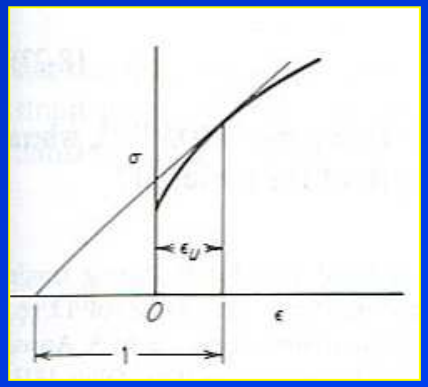

(a) Finding the point on the curve having a subtangent of unity.

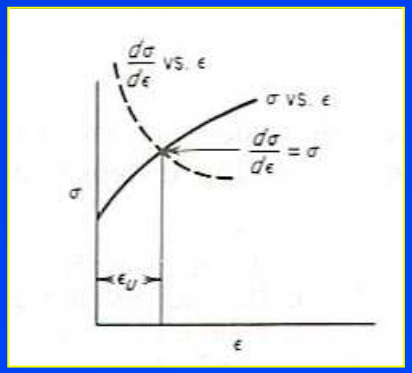

(b) The point where the rate of strain hardening $d\sigma/d\varepsilon$ equals the stress.

Considère's construction for the determination of maximum load

The ***maximum load*** can be determined from ***Considère's construction*** when the stress-strain curve is plotted in terms of true stress σ and conventional strain ***e***.

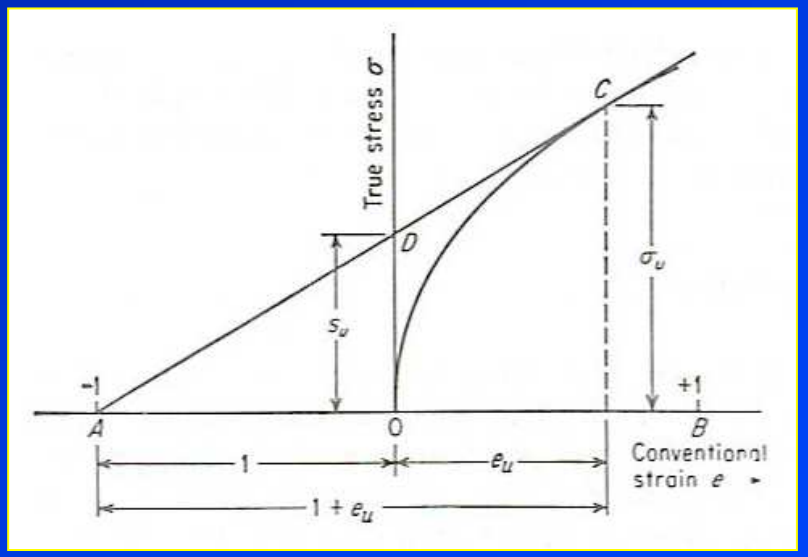

- Let point ***A*** represent a negative strain of 1.0.
- A line drawn from point ***A*** which is tangent to the stress-strain curve will give maximum load with the ***slope*** of ***$\sigma/(1+e)$.***
- The strain at which necking occurs is the true uniform strain ε_u

$$\varepsilon_u = n \qquad \text{Eq.25}$$

Table 8-3 Values for *n* and *K* for metals at room temperature

Metal	Condition	*n*	*K*, MPa
0.05% C steel	Annealed	0.26	530
SAE 4340 steel	Annealed	0.15	640
0.6% C steel	Quenched and tempered 540°C	0.10	1570
0.6% C steel	Quenched and tempered 705°C	0.19	1230
Copper	Annealed	0.54	320
70/30 brass	Annealed	0.49	900

Example: *If the true stress-strain curve is given by* $\sigma = 1400\varepsilon^{0.33}$*, where stress is in MPa, what is the ultimate tensile strength of the material?*

The uniform elongation to maximum load is

$$\varepsilon_u = n = 0.33$$

The true stress at maximum load is

$$\sigma_u = 1400(0.33)^{0.33} = 971 \ MPa$$

From *Eq.13*

$$e_u + 1 = \exp(\varepsilon_u) = \exp(0.33) = 1.391$$

Therefore the ultimate tensile strength is

From *Eq.12*

$$s_u = \frac{971}{e^{0.33}} = \frac{971}{1.391} = 698 \ MPa$$

Flow instability (necking) in biaxial tension

*Necking in a uniaxial cylindrical tensile specimen is isotropic. However in a **sheet specimen** where the width of the specimen is much higher than the thickness, there are two types of flow instability:*

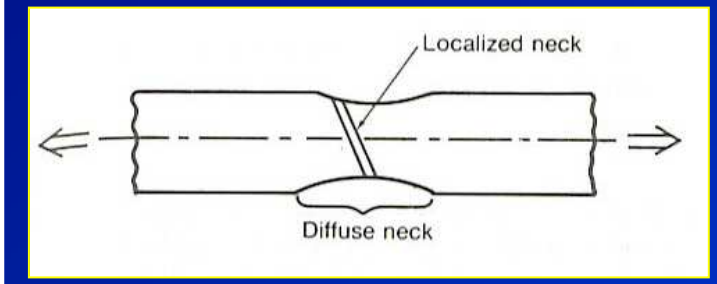

Diffuse and localised necking in a sheet tensile specimen.

1) Diffuse necking

- Provide ***a large extent of necking*** on the tensile specimen similar to necking from a cylindrical specimen.
- Diffuse necking might terminate in ***fracture*** but normally followed by localised necking.

2) Localised necking

- Localised necking is a ***narrow band*** with its size ~ specimen thickness, and inclined at an angle ϕ ~55°.
- Give no change in width through the localised neck → ***plain strain deformation***.

Power law flow curve for localised necking

$$\varepsilon_u = 2n \qquad \textit{Eq.26}$$

Stress distribution in necking

- ***Necking*** introduces a ***complex triaxial state of stress*** in the necked region ~ a mild notch.
- The ***average true stress at necking***, which is much higher than the stress would be required to cause a normal plastic flow due to stresses in width and thickness directions.

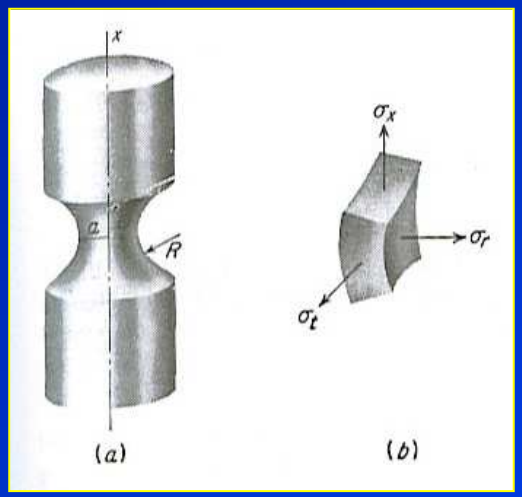

(a) Geometry of necked region, (b) stress acting on element at point O

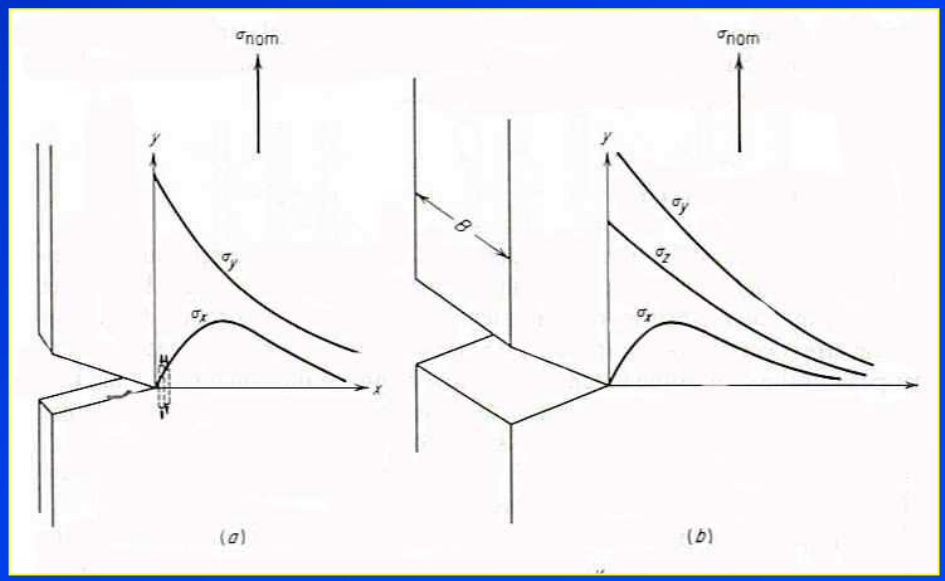

Elastic stresses beneath the notch in (a) plain stress, (b) plain strain

Ductility measurement in tension test

• ***Measured elongation*** in tension specimen depends on the ***gauge length*** or ***cross-sectional area***.

Total extension

Uniform extension up to necking

Depends on
• Metallurgical condition of the material (through ***n***)
• Specimen size and shape on the development of necking

Localised extension once necking begins

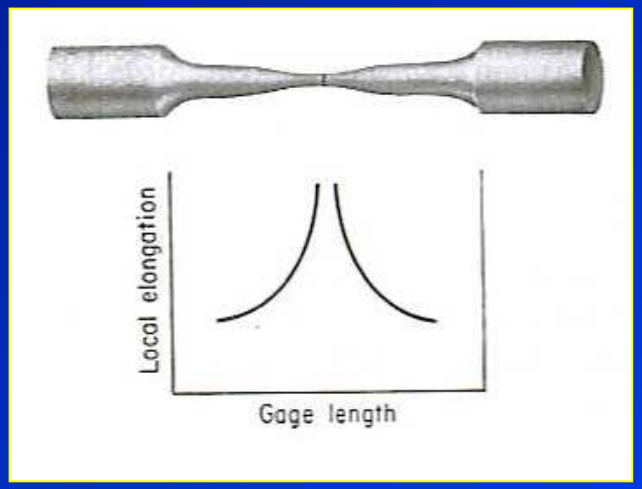

Variation of local elongation with position along gauge length of tensile specimen

The shorter the gauge length, the greater the effect of localised deformation at necking on total elongation.

Dimensional relationships of tensile specimens for sheet and round specimens

- Elongation depends on the original gauge length L_o. %elongation ↓ as L_o ↑

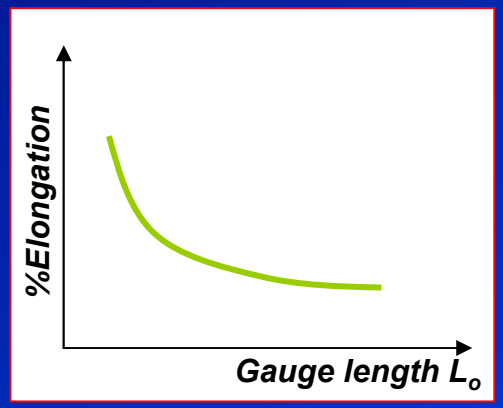

Example: Standard gauge length

$$L_o = 5.65\sqrt{A}$$ *Eq.27*

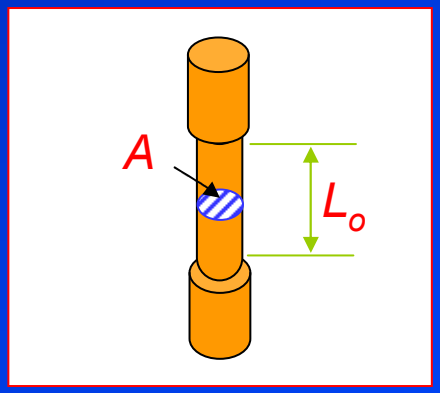

Table 8-4 Dimensional relationships of tensile specimens used in different countries

Type specimen	United States (ASTM)	Great Britain		Germany
		Before 1962	Current	
Sheet ($L_0/\sqrt{A_0}$)	4.5	4.0	5.65	11.3
Round (L_0/D_0)	4.0	3.54	5.0	10.0

Dimensional relationships for sheet and round tensile specimens used in different countries

Difference between % elongation and % reduction of area

% Elongation

• % Elongation is chiefly influenced by ***uniform elongation***, which is dependent on the ***strain-hardening capacity*** of the material.

Reduction of Area

• ***Reduction of area*** is more a measure of the deformation required to produce failure and its chief contribution results from the ***necking process***.

• Because of the ***complicated state of stress state*** in the neck, values of reduction of area are dependent on ***specimen geometry***, and ***deformation behaviour***, and they should not be taken as true material properties.

• ***RA*** is the most ***structure-sensitive ductility parameter*** and is useful in detecting ***quality changes in the materials***.

Effect of strain rate on flow properties

- Strain rate is defined as

$$\dot{\varepsilon} = \frac{d\varepsilon}{dt} \qquad \text{Eq.28}$$

- The unit is per second, s^{-1}.

Table 8-5 Spectrum of strain rate

Range of strain rate	Condition or type test
10^{-8} to 10^{-5} s^{-1}	Creep tests at constant load or stress
10^{-5} to 10^{-1} s^{-1}	"Static" tension tests with hydraulic or screw-driven machines
10^{-1} to 10^{2} s^{-1}	Dynamic tension or compression tests
10^{2} to 10^{4} s^{-1}	High-speed testing using impact bars (must consider wave propagation effects)
10^{4} to 10^{8} s^{-1}	Hypervelocity impact using gas guns or explosively driven projectiles (shock-wave propagation)

Spectrum of strain rate

Strain rate ↑ **Flow stress** ↑

Temperature ↑ **Strain rate dependence** ↑

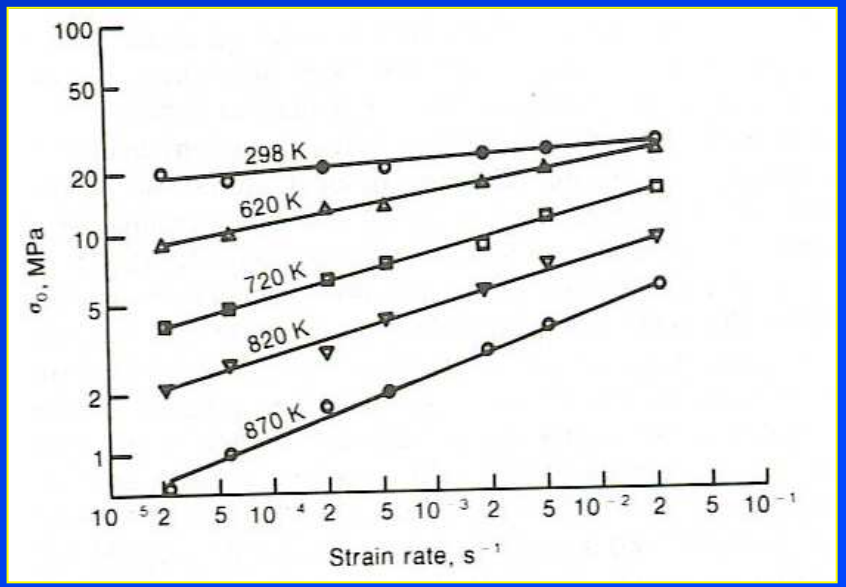

Flow stress dependence of strain rate and temperature

Strain rate sensitivity, m

- Strain rate sensitivity indicates any changes in ***deformation behaviour***.
- Measurement of strain rate sensitivity can be linked to ***dislocation concept*** (velocity of mobile dislocations).

- ***Strain rate sensitivity m*** can be obtained from

$$\sigma = C\left(\dot{\varepsilon}\right)^{m}\Big|_{\varepsilon,T} \qquad \textit{Eq.29}$$

- ***High strain rate sensitivity*** is a characteristic of ***superplastic*** metals and alloys.

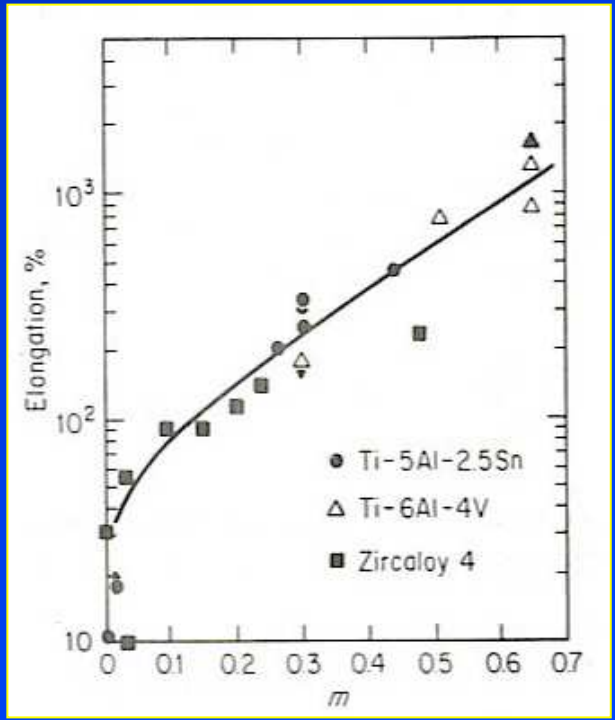

Dependence of tensile elongation on strain-rate sensitivity

Effect of temperature on flow properties

Temperature strongly affects the stress-strain curve and the flow and fracture properties.

Temperature ↑ **Strength** ↓

Ductility ↑

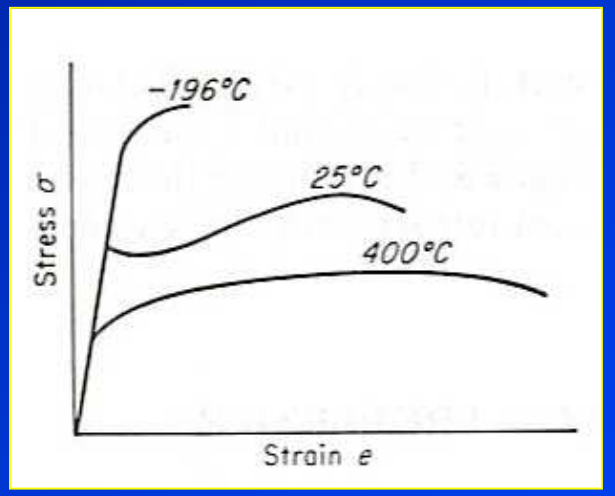

Changes in engineering stress-strain curves of mild steel with temperature

- ***Thermally activated processes*** assist deformation (dislocation motion) and reduce strength at elevated temperatures.
- ***Structural changes*** can occur at certain temperature ranges (high temp / long term exposure) to alter the general behaviour.

Effects of temperature on yield stress

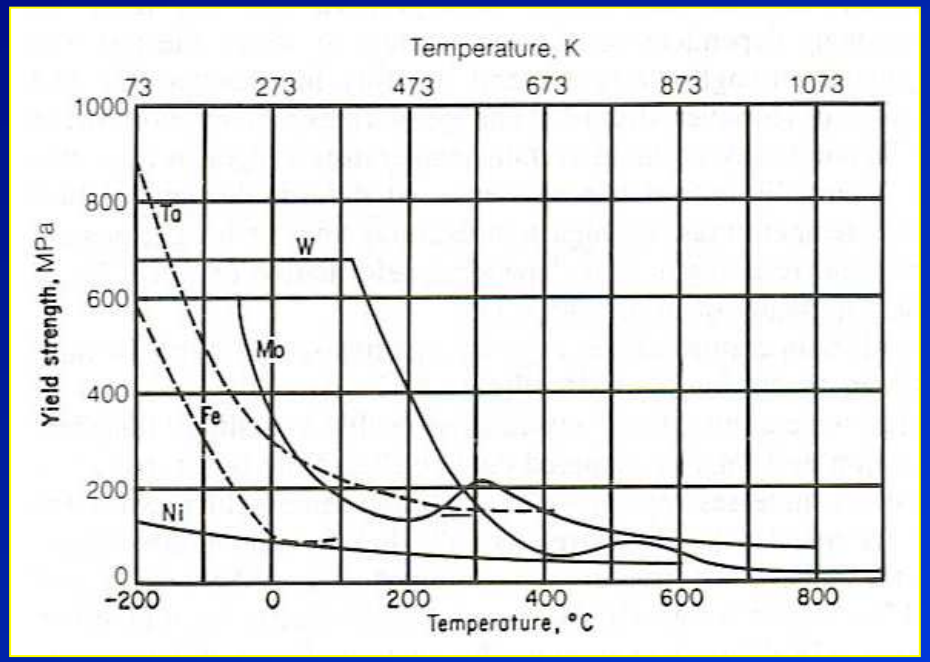

Effects of temperature on ductility

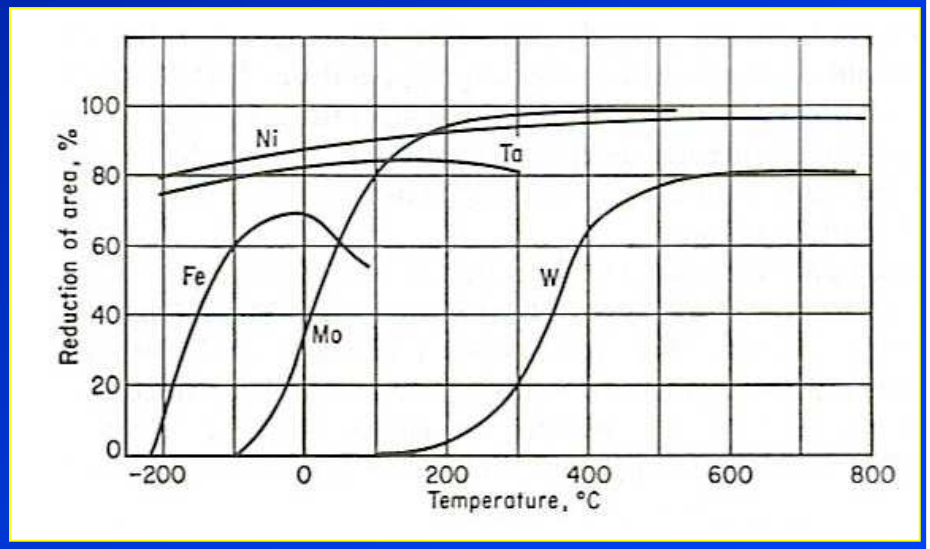

• For ***BCC*** metals, the ***yield stress*** is strongly dependent on temperature where as in ***FCC*** metals, the ***yield stress*** is only slightly dependent on temperature.

• ***W*** is brittle at 100°C, ***Fe*** at -225°C while ***Ni*** decreases little in ***ductility*** over the entire temperature interval.

Comparison of mechanical properties of different materials at various temperature

• Mechanical properties of different materials at various temperature can be compared in terms of ***homogeneous temperature*** (the ratio of the test temperature to the melting point, expressed in degree ***kelvin)***.

$$\text{Homogenous temperature} = \frac{\text{Testing temperature}}{\text{Melting temperature}}$$

• And this should be compared in terms of ratios of σ / E rather than simple ratios of flow stress.

Influence of testing machine on flow properties

Load controlled machine

• The ***operator adjusts the load precisely*** and leave with whatever displacement happens to be associated with the load.

Displacement controlled machine

• ***Displacement is controlled*** and the load adjusts itself to that position. Ex: Screw driven machine.

Currently we can have machines which can change from load control to displacement control.

Constant cross head velocity is the sum of

1) Elastic strain rate in specimen
2) Plastic strain rate in specimen
3) Strain rate resulting from elasticity of the machine.

Effect of the testing machine of the shape of the stress-strain curve and fracture behavior

Hard machine

- A rigid testing machine with a high spring constant.
- ***Ex:*** Screw driven machine.
- Will reproduce faithfully the upper and the lower yield point.

Soft machine

- Hydraulic testing machine.
- The effect of upper and lower yield point will be smeared out and only the extension at constant load will be recorded.

www.coronet.eu.com

Screw driven machine

solids.ame.arizona.edu

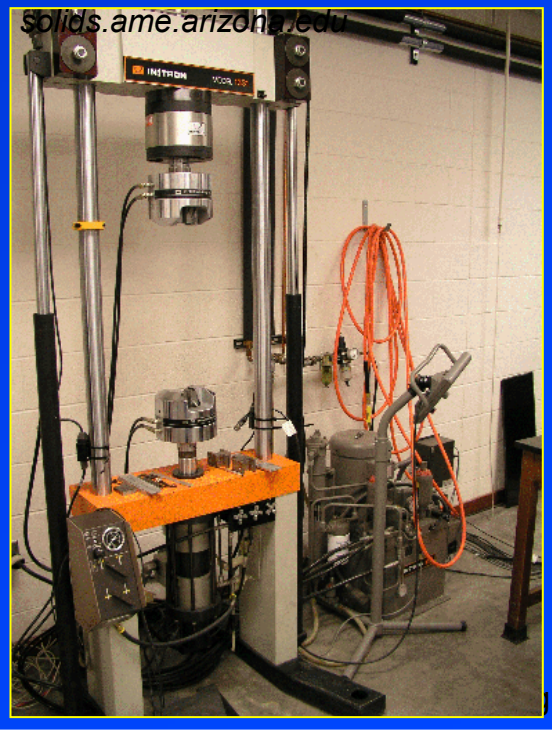

Hydraulic testing machine

Thermally activated deformation

Plastic deformation depends on

- **Stress**
- **Temperature**
- **Deformation**
- **Stain rate,**
- **Microstructure**
- **Composition**

The effective shear stress is τ-τ_i

Where τ is the applied shear stress
τ_i is the internal resisting stresses.

The τ_i can be grouped into;

1) ***Long-range obstacles*** : barriers too high and long the be surmounted by thermal fluctuation.
2) ***Short-range obstacles*** : (~10 atom diameters) thermal fluctuation can assist dislocations in surmounting these barriers. → ***thermal activation barrier***.

Thermal activation energy

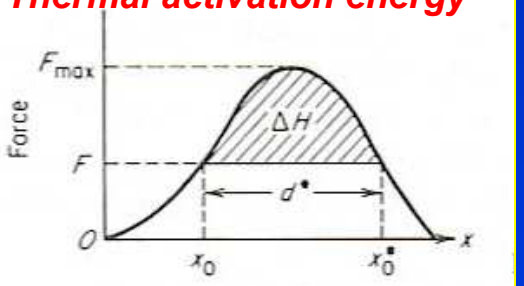

d* - distance the atom move during the process.
ΔH – Energy required to overcome the barrier.

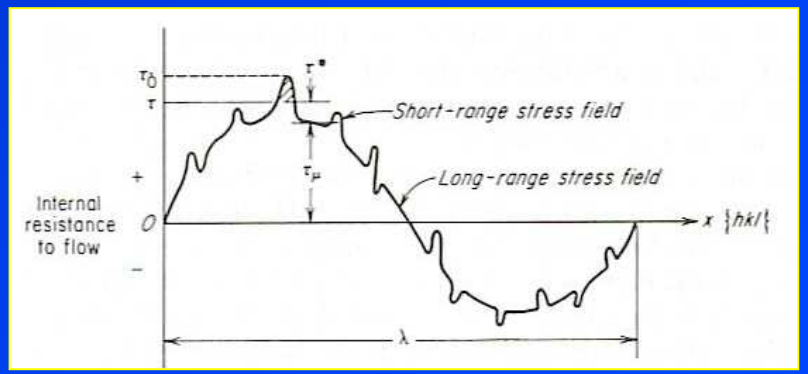

Long range and short range stress fields

Notch tensile test

Notch tensile test *is used to evaluate* ***notch sensitivity*** *(the tendency for reduced tensile ductility in the presence of a triaxial stress field and steep stress gradient. → express metallurgical or environmental changes.*

Notch tensile specimen

- ***60° notch*** with a ***root radius of 0.025 mm*** or less introduced into a round (circumferential notch) or a flat (double-edge notch) tensile specimen.
- The ***cross-sectional area*** under the notch root is ***one-half*** of the unnotched area.

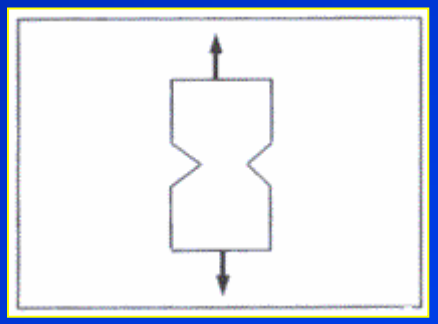

Notch tensile specimen.

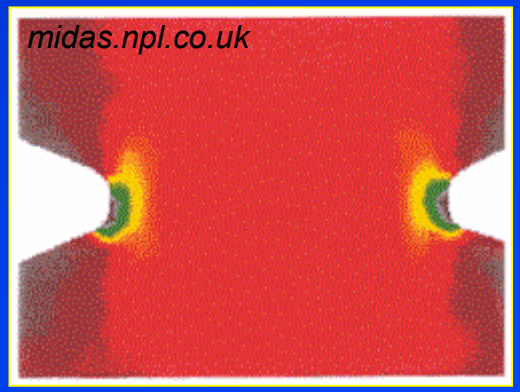

Stress distribution around tensile notches.

Notch strength

- ***Notch strength*** is defined as the ***maximum load*** divided by the ***original cross-sectional area at the notch***.

- Due to the ***constraint*** at the notch, the ***notch strength*** is higher than the tensile strength of the unnotched specimen.

- ***Notch-strength ratio NSR*** detects notch brittleness (high notch sensitivity) from;

$$\text{NSR} = \frac{S_{net}\ \text{(for notched specimen at maximum load)}}{S_u\ \text{(tensile strength for unnotched specimen)}}$$

- If the ***NSR*** is < 1, the metal is notch brittle.

Tensile properties of steel

Ferrous materials are of commercial importance. → Great deal of work is paid to relate microstructure, composition to properties.

Composition and more importantly microstructure are the chief variables which control the properties of steel.

The tensile properties of annealed and normalised steels are controlled by

1) Flow and fracture characteristics of the ferrite (strength ~ alloying elements, grain size)
2) Amount of ferrite
3) Shape of ferrite
4) Distribution and amount of cementite (***C*** content)

Tensile properties in steels with different microstructures

• ***Normalised steel*** has higher strength than ***annealed steel*** due to more rapid rate of cooling, resulting in ***pearlite.***

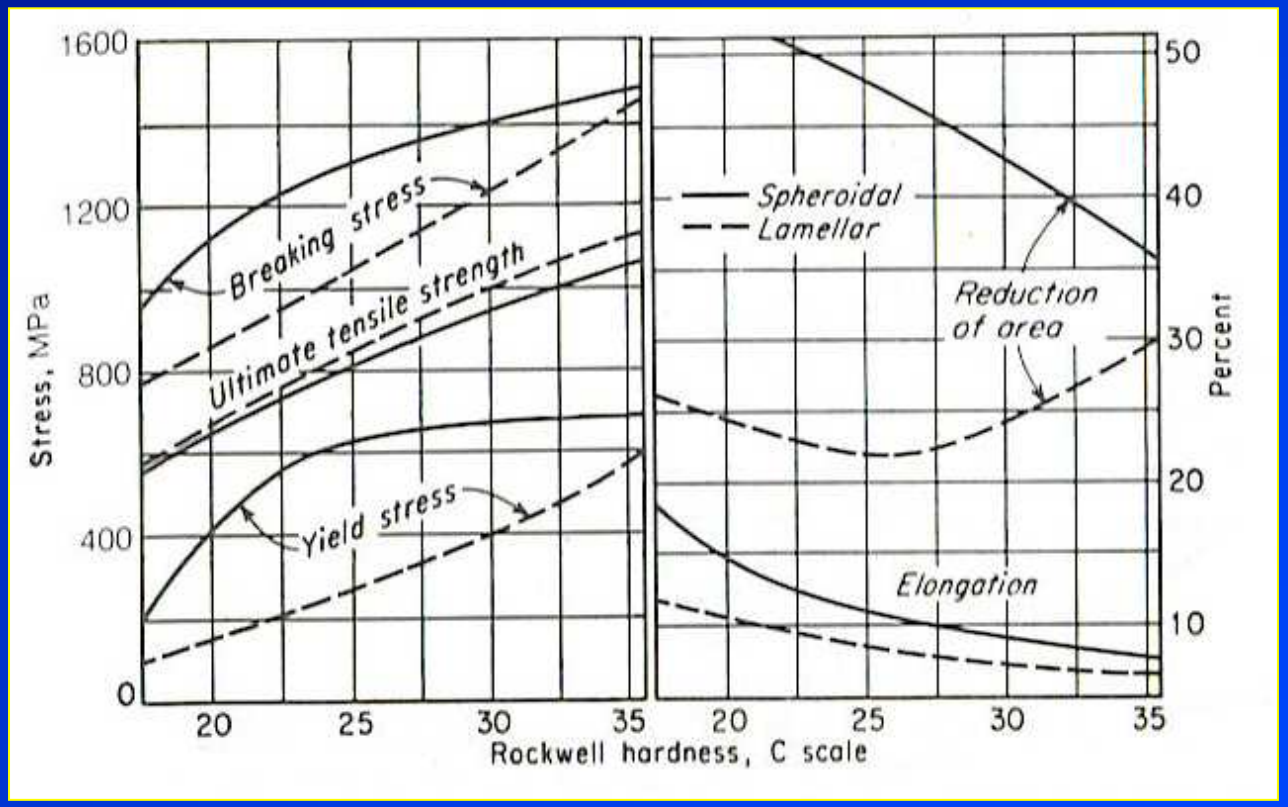

Tensile properties of pearlite and spheroidite in eutectoid steel

Tensile properties in steels with different microstructures

- Strength of ***annealed steel*** can be improved by ***cold working.***

Table 8-6 Effect of cold-drawing on tensile properties of SAE 1016 steel†

Reduction of area by drawing, %	Yield strength, MPa	Tensile strength, MPa	Elongation, in 50 mm, %	Reduction of area, %
0	276	455	34	70
10	496	517	20	65
20	565	579	17	63
40	593	655	16	60
60	607	703	14	54
80	662	793	7	26

† After L. J. Ebert, "A Handbook on the Properties of Cold Worked Steels," PB 121662, Office of Technical Services, U.S. Department of Commerce, 1955.

Tensile properties in steels with different microstructures

- ***Tensile properties of pearlitic steel*** can be best controlled by ***transforming the austenite to pearlite*** at a constant temperature on continuous cooling from above the critical temperature.
- The transformation product is ***lamellar pearlite***.

Pearlite microstructure

Transformation temperature ↑

↓

Spacing between cementite platelets ↓

Strength ↑

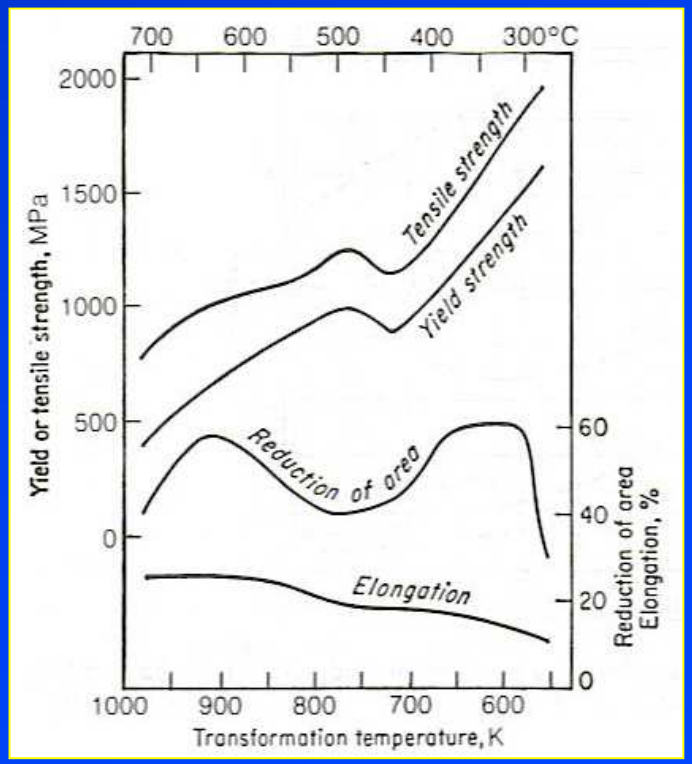

Relationship of tensile properties of Ni-Cr-Mo steel to isothermal transformation temperature.

Tensile properties in quenched and tempered steels

- ***The best combination of strength and ductility*** is obtained in steel which has been ***quenched*** to a fully martensitic structure and then ***tempered***.

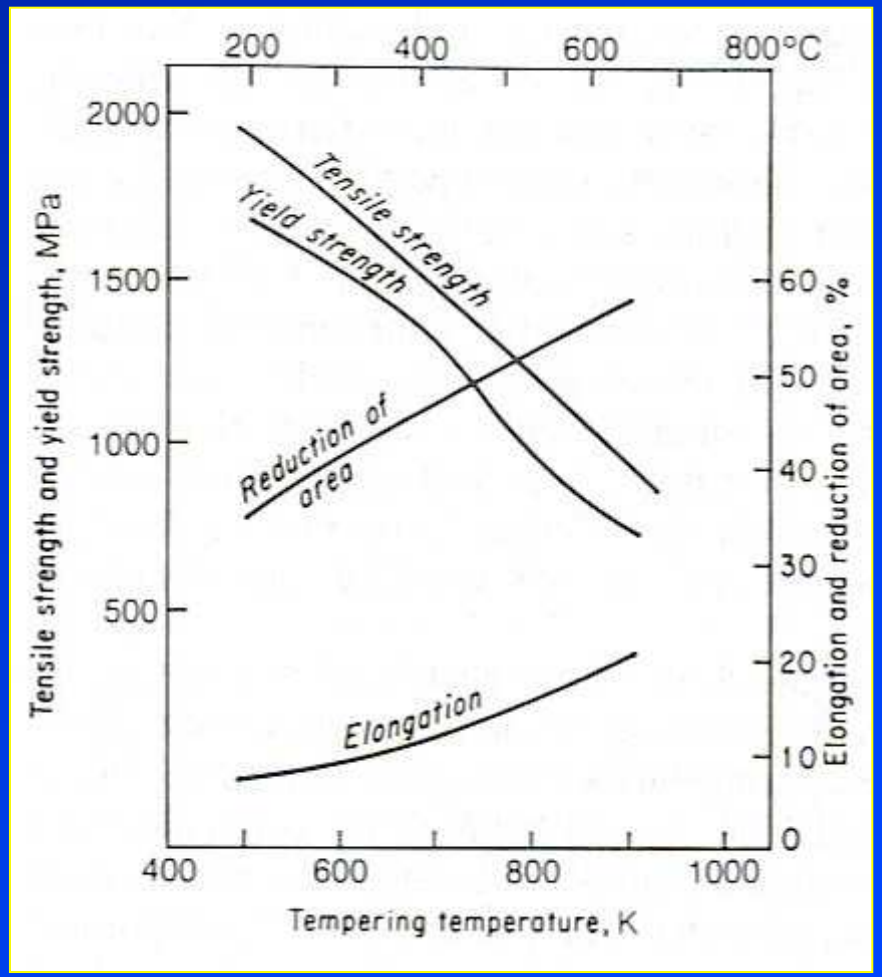

Tensile properties of quenched and tempered SAE-4340 steel as a function of tempering temperature

Tensile properties in quenched and tempered steels

- ***Martensitic structure*** provides ***hardness and strength.***
- Mechanical properties are changed by altering the tempering temperature.

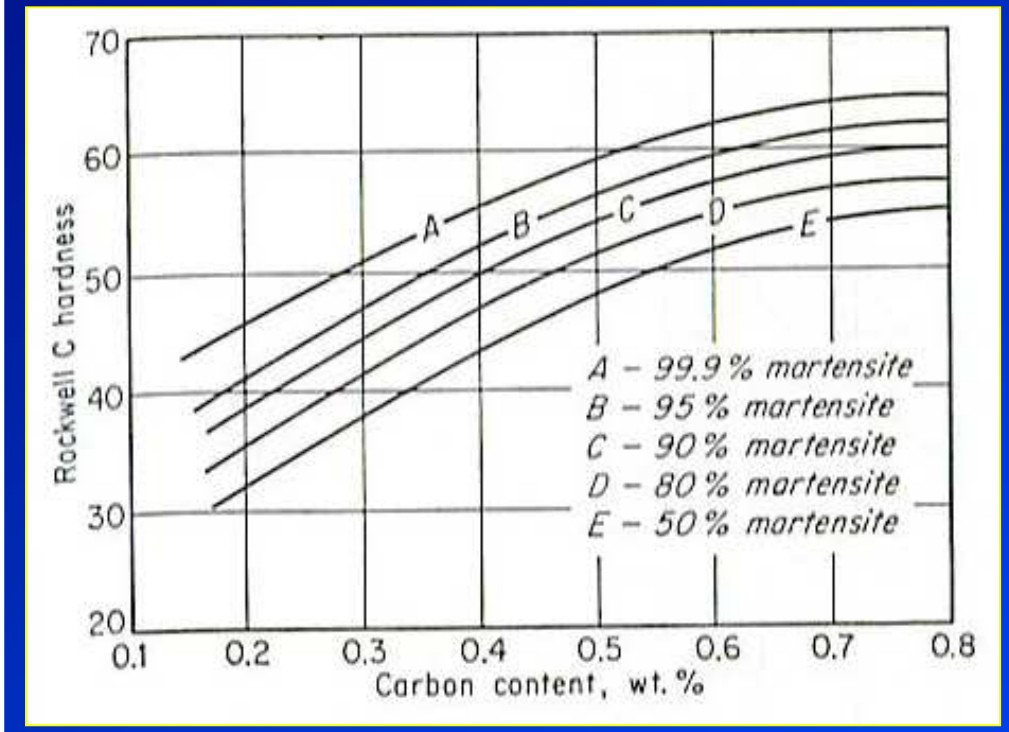

As-quenched hardness of steel as a function of carbon content

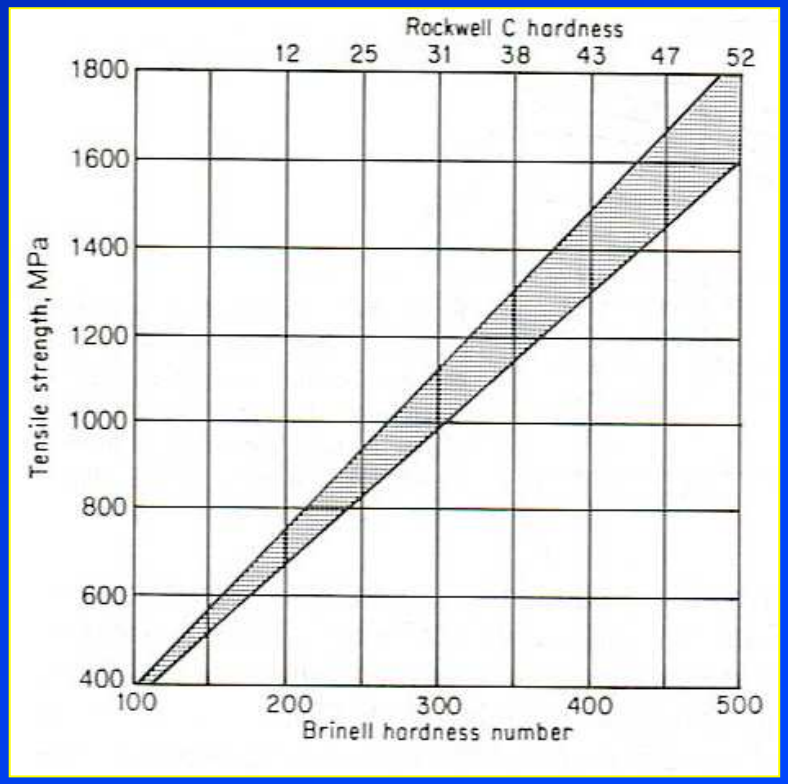

Relationship between tensile strength and hardness for quenched and tempered, annealed and normalised steel

Tensile properties in low-carbon steel

- Mechanical properties of ***low-carbon steels (0.3-0.5%C)*** do not depend basically on alloy content, carbon content or tempering temperature.
- Steels quenched to essentially 100% martensite and then tempered can give ***Tensile strength*** of in the range 700 – 1400 MPa. → a wide variety of alloyed steels are used.
- A range of specific properties can be obtained as appeared in ***shaded area***.
- in large steel sections, ***slack-quenched structure*** (non-100% martensitic structure-containing ferrite, pearlite, bainite interspersed with martensite) gives ***poorer properties***.

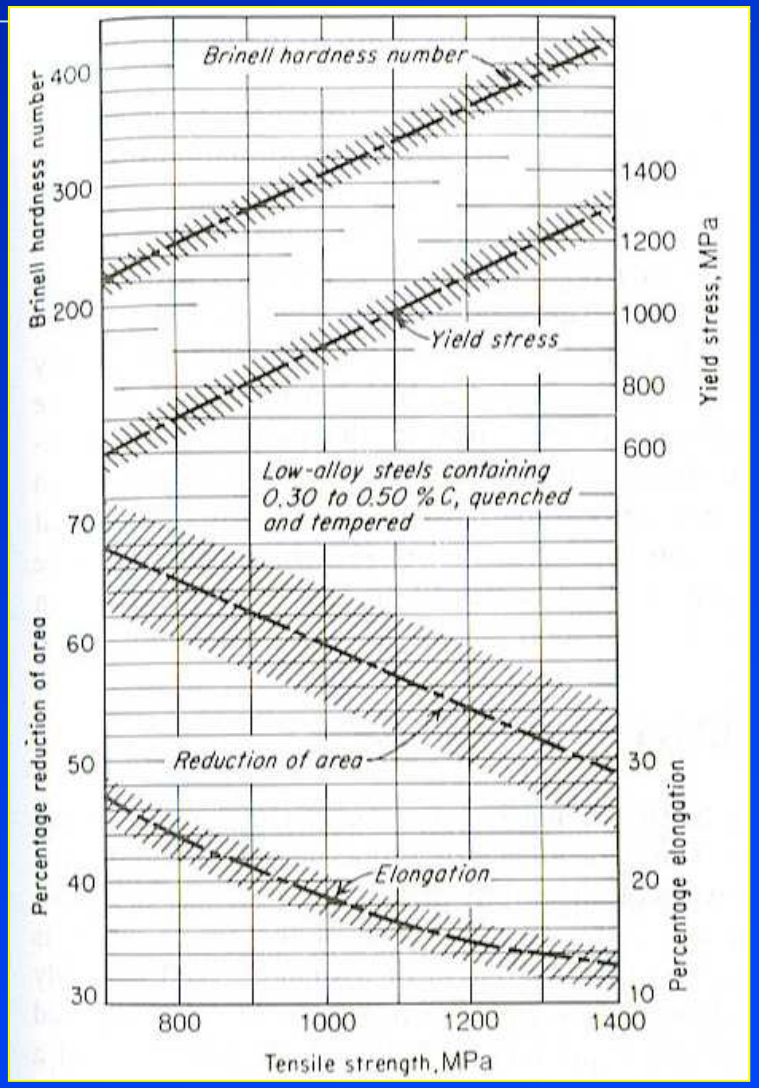

Relationships between tensile properties of quenched and tempered low-alloy steels

Anisotropy of tensile properties

Crystallographic anisotropy

- **Crystallographic anisotropy** results from the ***preferred orientation*** of the grains, which is produced by severe plastic deformation.
- ***Yield strength*** and ***tensile strength*** to a lesser extent, are the properties most affected.
- Crystallographic anisotropy can be eliminated by ***recrystallisation***.
- Example : ***Ears*** in deep-drawn cups.

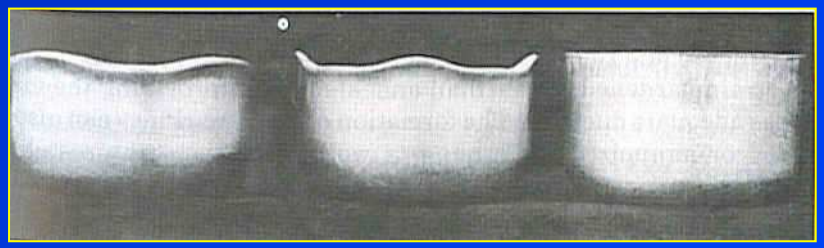

Ears in drawn cups.

Anisotropy of tensile properties

Mechanical fibering

- ***Mechanical fibering*** is due to ***preferred alignment*** of inclusions, voids, seggregation, and second phase in the ***working direction***. → important in forgings and plates.
- Ductility is the most affected.

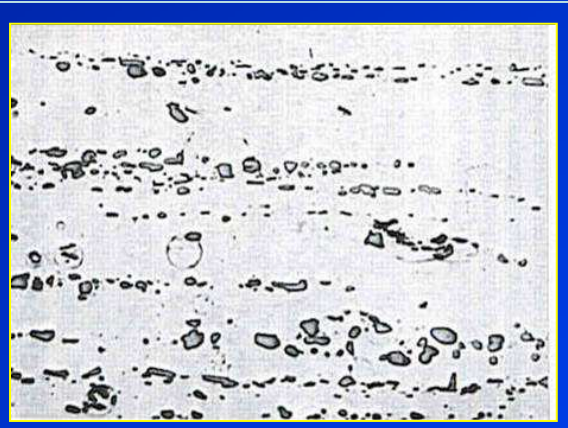

Alignment of particles or inclusions along the working direction

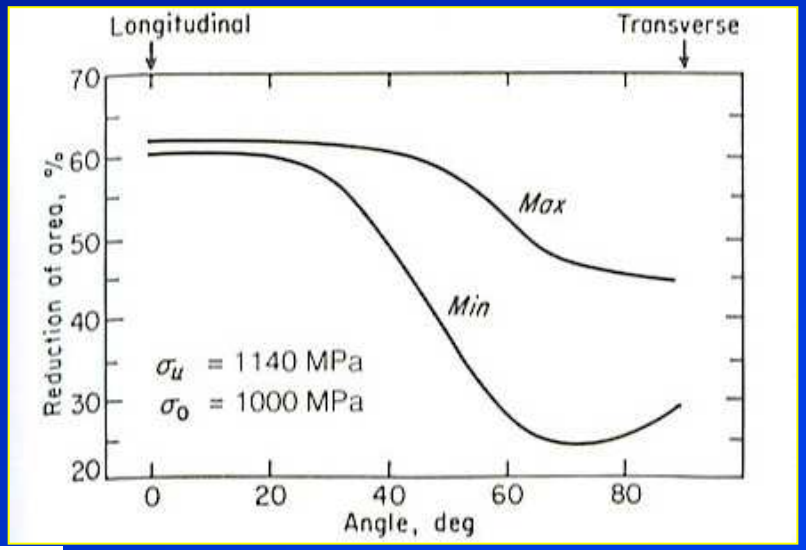

Reduction of area and angle between the longitudinal direction in forging and the specimen axis

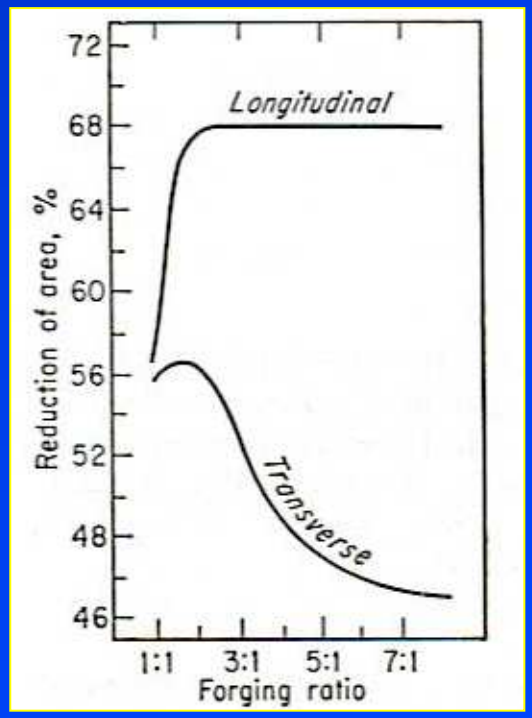

Effect of forging on longitudinal and transverse reduction of area

References

- Dieter, G.E., ***Mechanical metallurgy***, 1988, SI metric edition, McGraw-Hill, ISBN 0-07-100406-8.

Hardness Test

Subjects of interest

- *Introduction/objectives*
- *Brinell hardness*
- *Meyer hardness*
- *Vickers hardness*
- *Rockwell hardness*
- *Microhardness tests*
- *Relationship between hardness and the flow curve*
- *Hardness-conversion relationships*
- *Hardness at elevated temperatures*

Objectives

- This chapter provides fundamental knowledge of hardness of materials along with different methods of hardness measurements normally used.
- Relationships between hardness and tensile properties will be made and finally factors affecting hardness of metals will be discussed.

Introduction

Definition ***Hardness is a resistance to deformation***.

(for people who are concerned with mechanics of materials, hardness is more likely to mean the resistance to indentation)

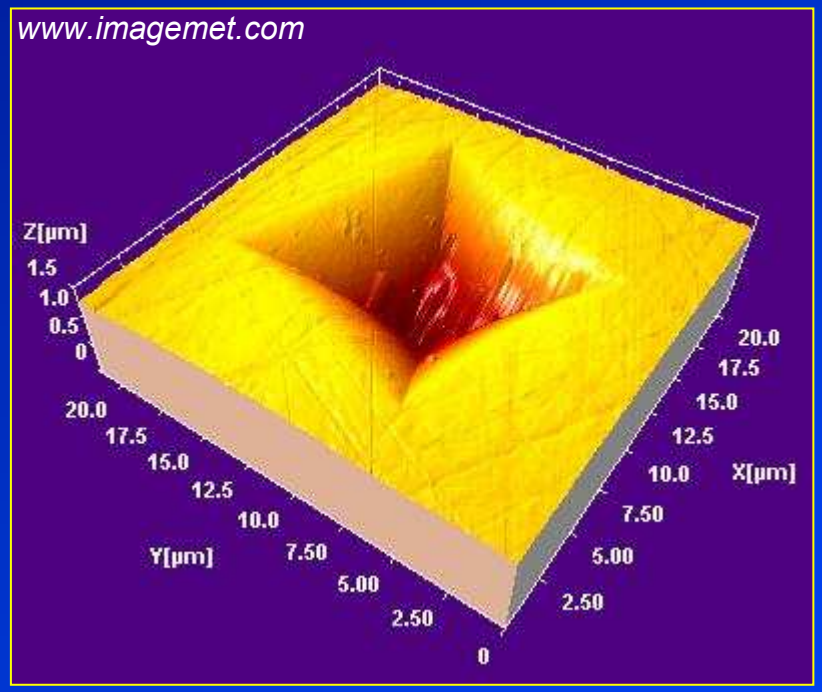

Hardness impression

Deeper or larger impression

Softer materials

Introduction

There are three general types of hardness measurements

1) Scratch hardness

- The ability of material to scratch on one another
- Important to mineralogists, using ***Mohs'scale*** 1= talc, 10 = diamond
- Not suited for metal → annealed copper = 3, martensite = 7.

2) Indentation hardness

- Major important engineering interest for metals.
- Different types : Brinell, Meyer, Vickers, Rockwell hardness tests.

3) Rebound or dynamic hardness

- The indentor is dropped onto the metal surface and the hardness is expressed as the energy of impact.

Introductions

• Hardness tests can be used for many engineering applications to achieve the basic requirement of mechanical property.

• ***For examples***

→ surface treatments where surface hardness has been much improved.

→ Powder metallurgy

→ Fabricated parts: forgings, rolled plates, extrusions, machined parts.

Nitrided part

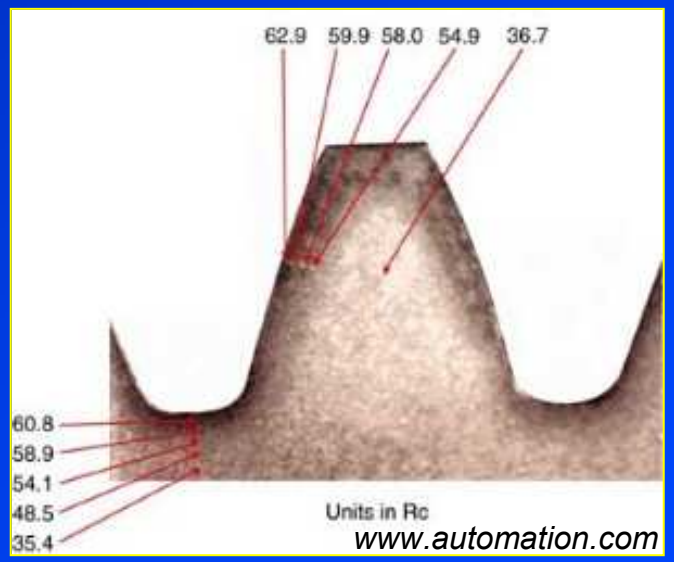

Hardness variation of nitrided part

Brinell hardness

• ***J.A. Brinell*** introduced the ***first standardised indentation-hardness*** test in 1900. The ***Brinell hardness test*** consists in indenting the metal surface with a ***10-mm diameter steel ball*** at a load range of 500-3000 kg, depending of hardness of particular materials.

• The load is applied for a standard time (~30 s), and the ***diameter of the indentation is measured***.
→giving an average value of two readings of the diameter of the indentation at right angle.

• The ***Brinell hardness number (BHN or H_B)*** is expressed as the load ***P*** divided by surface area of the indentation.

$$BHN = \frac{P}{(\pi D/2)\left(D - \sqrt{D^2 - d^2}\right)} = \frac{P}{\pi D t} \qquad \textit{Eq.1}$$

Where ***P*** is applied load, kg
D is diameter of ball, mm
d is diameter of indentation, mm
t is depth of the impression, mm

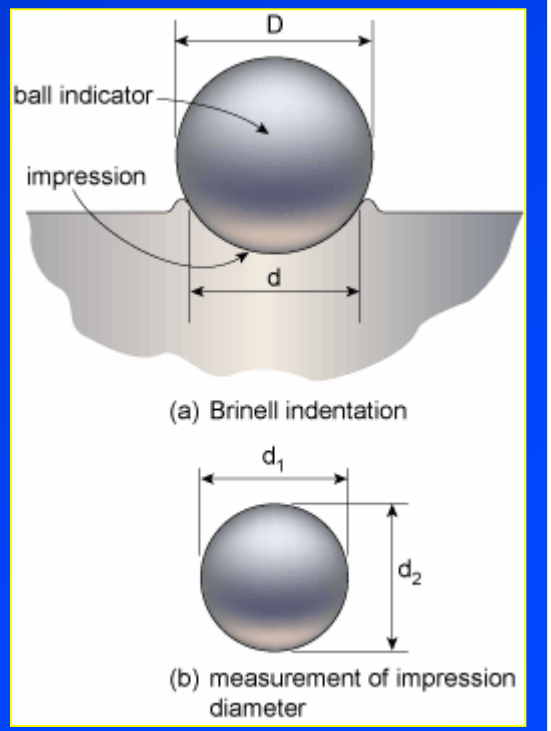

Unit $kgf.mm^{-2}$ =9.8 MPa

Advantages and disadvantages of Brinell hardness test

- Large indentation averages out ***local heterogeneities of microstructure***.
- Different loads are used to cover a wide rage of hardness of commercial metals.
- Brinell hardness test is ***less influenced by surface scratches and roughness*** than other hardness tests.
- The test has ***limitations*** on ***small specimens*** or in ***critically stressed parts*** where indentation could be a possible site of failure.

www.instron.com

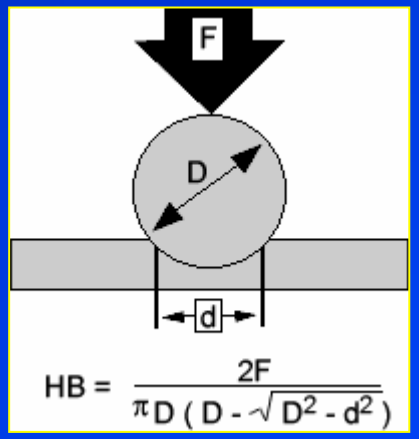

www.alexdenouden.nl

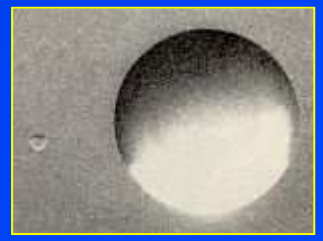

Brinell hardness impression

Brinell hardness test with nonstandard load or ball diameter

• From fig, ***d = Dsinϕ***, giving the alternative expression of ***Brinell hardness number*** as

$$BHN = \frac{P}{(\pi/2)D^2(1-\cos\phi)} \qquad \textit{Eq.2}$$

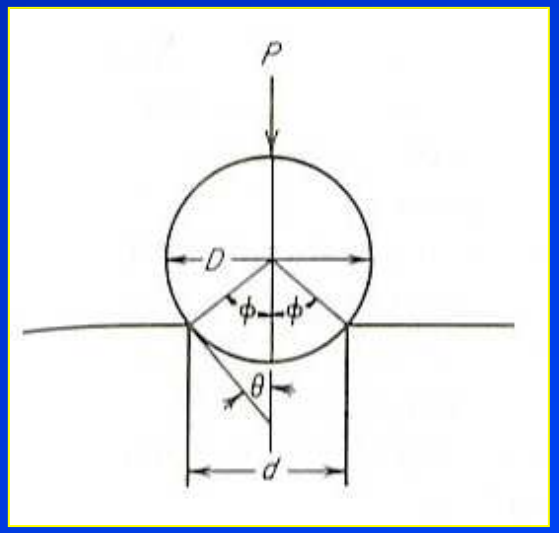

Basic parameter in Brinell test

• In order to obtain the same ***BHN*** with a non-standard load or ball diameter, it is necessary to produce a ***geometrical similar indentations***.

• The included angle ***2ϕ*** should remain constant and the ***load and the ball diameter*** must be varied in the ratio

$$\frac{P_1}{D_1^2} = \frac{P_2}{D_2^2} = \frac{P_3}{D_3^3} \qquad \textit{Eq.3}$$

Meyer hardness

• ***Meyer*** suggested that hardness should be expressed in terms of the ***mean pressure between the surface of the indenter and the indentation***, which is equal to the load divided by the projected area of the indentation.

$$p_m = \frac{P}{\pi r^2} \qquad \textit{Eq.4}$$

• ***Meyer hardness*** is therefore expressed as follows;

$$Meyer\ \ hardness = \frac{4P}{\pi d^2} \qquad \textit{Eq.5}$$

Note: *- Meyer hardness is less sensitive to the applied load than Brinell hardness.*

- Meyer hardness is a more fundamental measure of indentation hardness but it is rarely used for practical hardness measurement.

Vickers hardness

- ***Vickers hardness test*** uses a ***square-base diamond pyramid*** as the indenter with the included angle between opposite faces of the pyramid of 136°.
- The ***Vickers hardness number (VHN)*** is defined as the load divided by the surface area of the indentation.

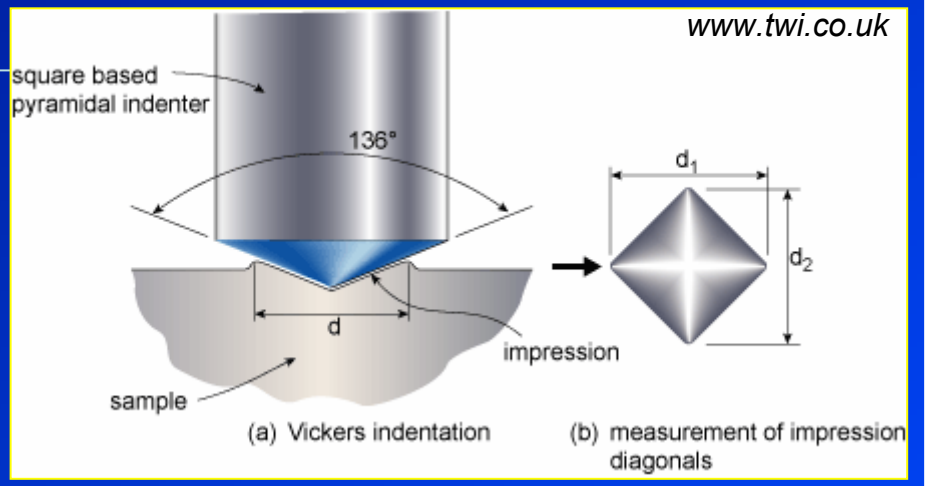

Note: not widely used for routine check due to a slower process and requires careful surface preparation.

$$VHN = \frac{2P\sin(\theta/2)}{L^2} = \frac{1.854P}{L^2}$$ *Eq.6*

Where ***P*** is the applied load, kg
L is the average length of diagonals, mm
θ is the angle between opposite faces of diamond = 136°.

Note: the unite can be VHN, DPH, H_v

Vickers hardness

- ***Vickers hardness test*** uses the loads ranging from 1-120 kgf, applied for between 10 and 15 seconds.
- Provide a fairly ***wide acceptance for research work*** because it provides a continuous scale of hardness, for a given load.
- ***VHN*** = 5-1,500 can be obtained at the same load level→ ***easy for comparison***).

ZHV30 micro and macro Vickers with automatic impression measurement

Impressions made by Vickers hardness

- ***A perfect square indentation (a)*** made with a perfect diamond-pyramid indenter would be a ***square***.
- ***The pincushion indentation (b)*** is the result of sinking in of the metal around the flat faces of the pyramid. This gives an overestimate of the diagonal length (observed in ***annealed metals***).
- ***The barrel-shaped indentation (c)*** is found in ***cold-worked metals***, resulting from ridging or piling up of the metal around the faces of the indenter. Produce a low value of contact area→ ***giving too high value***.

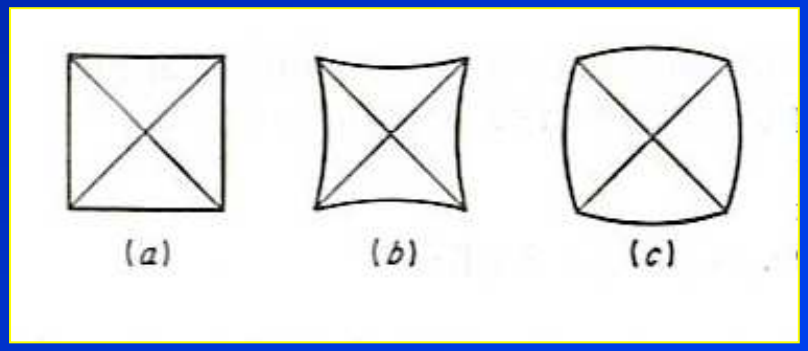

Types of diamond-pyramid indentation (a) perfect indentation (b) pincushion indentation due to sinking in (c) barrelled indentation due to ridging.

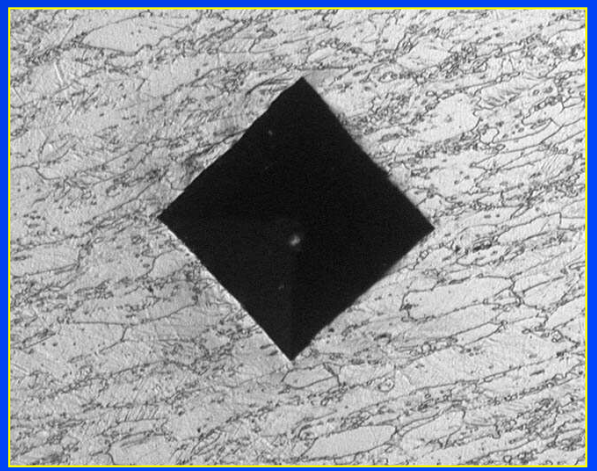

Vickers hardness values of materials

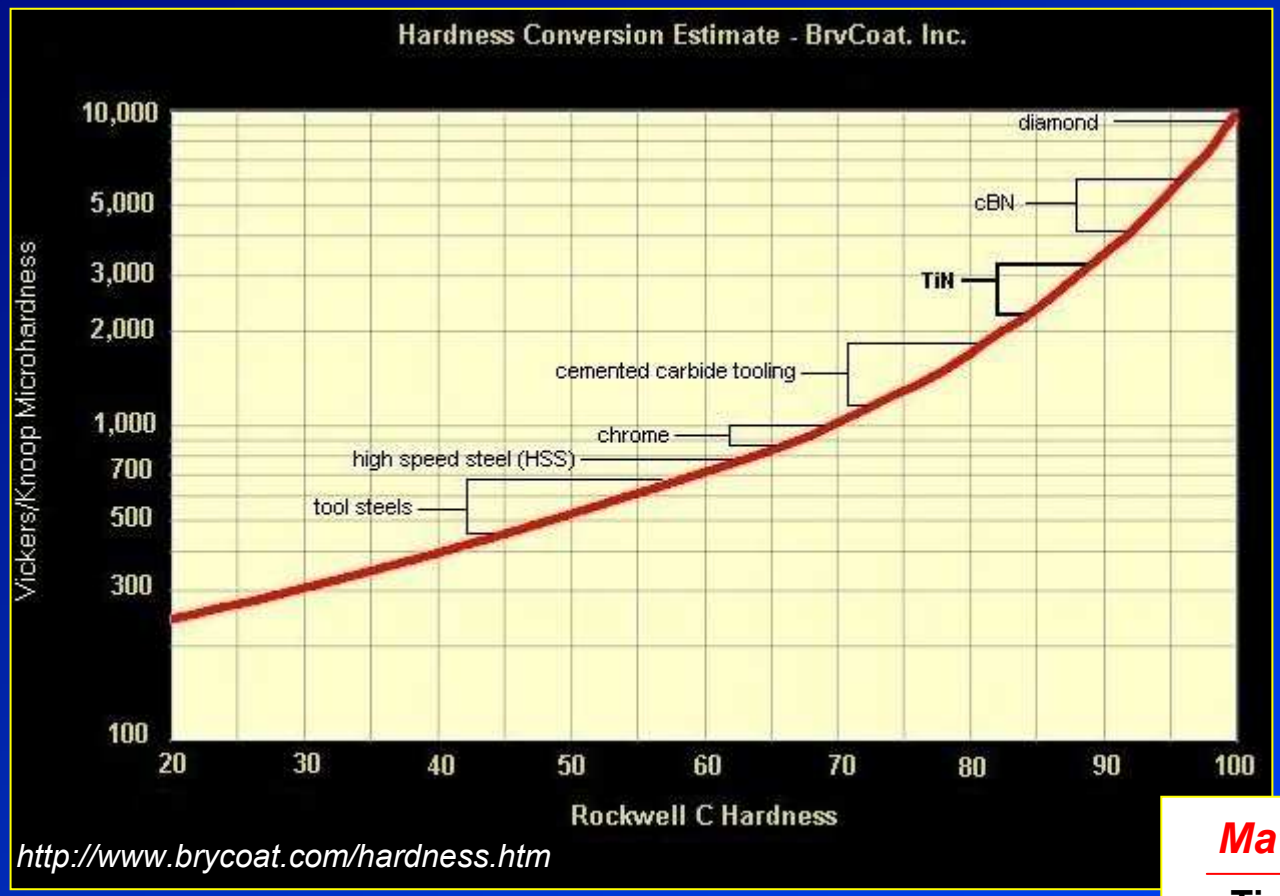

Materials	H_v
Tin	5
Aluminium	25
Gold	35
Copper	40
Iron	80
Mild steel	230
Full hard steel	1000
Tungsten carbide	2500

Rockwell hardness

- ***The most widely used hardness test in the US and generally accepted due to***
  1) Its speed
  2) Freedom from personal error.
  3) Ability to distinguish small hardness difference
  4) Small size of indentation.

- The hardness is measured according to the ***depth of indentation***, under a constant load.

8150 LK Combined Rockwell
Rockwell suprficial

Rockwell hardness test

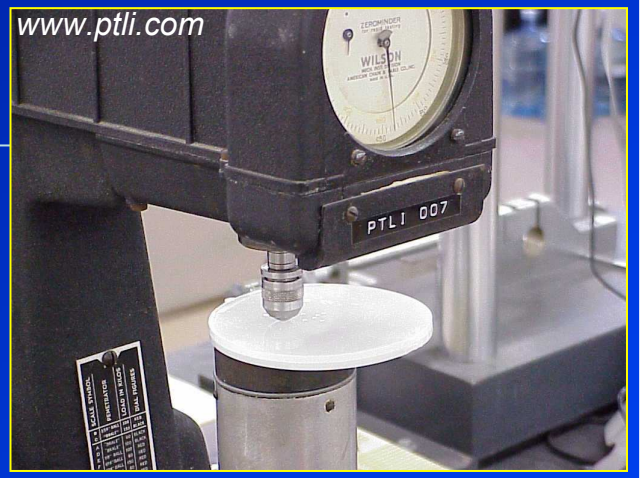

Principal of the Rockwell Test

- Position the surface area to be measured close to the indenter.
- Applied the ***minor load*** and a zero reference position is established
- The ***major load*** is applied for a specified time period (dwell time) beyond zero
- The ***major load*** is released leaving the minor load applied.

The dial contains 100 divisions, each division representing a penetration of 0.002 mm.

Deeper indentation

Softer material

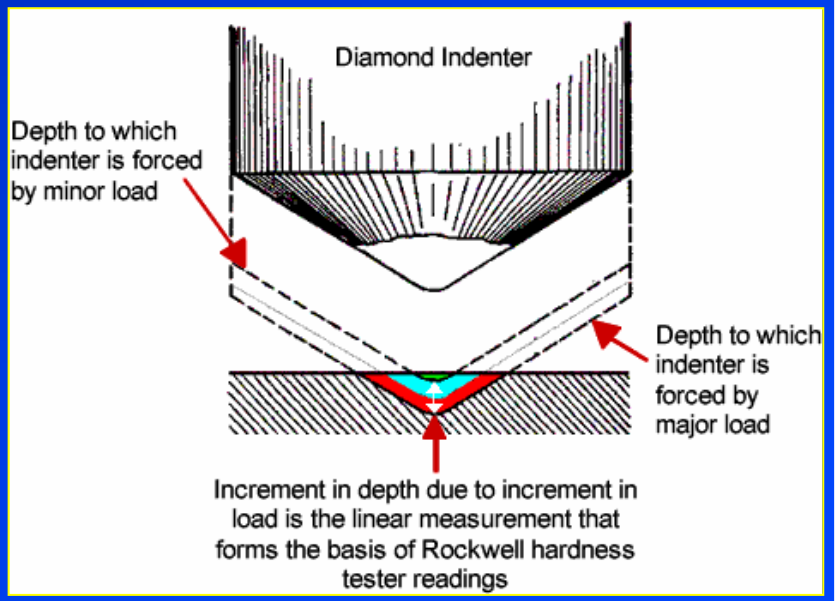

The Rockwell number represents the difference in depth from the zero reference position as a result of the applied major load.

Rockwell hardness scale

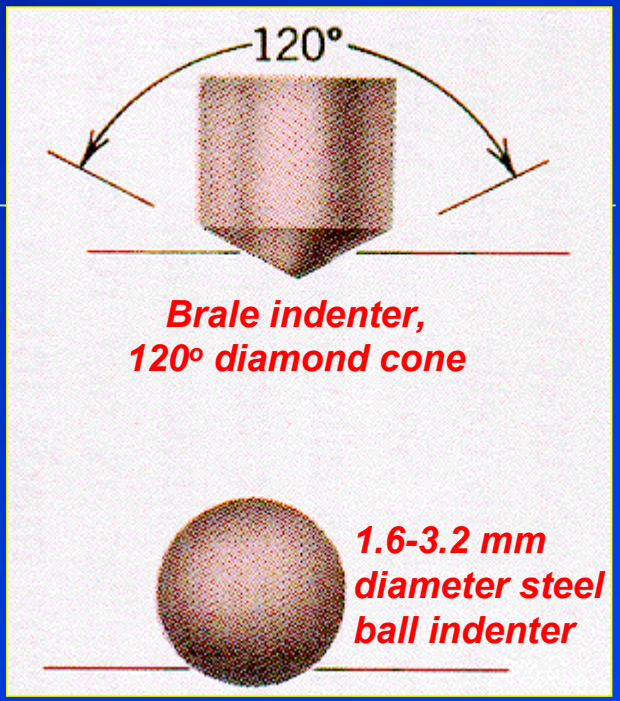

• ***Rockwell hardness number (RHN)*** represents in different scale, A, B, C,.. depending on types of indenters and major loads used.

EX:

Scale	Indenter	Load (kg.f)	Scale
A	Brale	60	HRA
B	1/16" steel ball	100	HRB
C	Brale	150	HRC

• The Hardened steel is tested on the ***C scale*** with R_c***20-70***.

• Softer materials are tested on the ***B scale*** with R_b***30-100***.

The scale is usable for materials from annealed brass to cemented carbides. Other scales are available for special purposes.

Rockwell hardness instruction

- Cleaned and well seated indenter and anvil.
- Surface which is clean and dry, smooth and free from oxide.
- ***Flat surface***, which is ***perpendicular to the indenter***.
- Cylindrical surface gives ***low readings***, depending on the curvature.
- ***Thickness*** should be 10 times higher that the depth of the indenter.
- The ***spacing between the indentations*** should be 3 or 5 times the diameter of the indentation.
- ***Loading speed*** should be standardised.

www.qualitymag.com

Microhardness

- Determination of hardness over very small areas for example individual constituents, phases, requires ***hardness testing machines in micro or sub-micro scales***.
- ***Vickers hardness*** can also be measured in a microscale, which is based on the same fundamental method as in a macroscale.

- The ***Knoop indenter*** (diamond-shape) is used for measuring in a small area, such as at the cross section of the heat-treated metal surface.

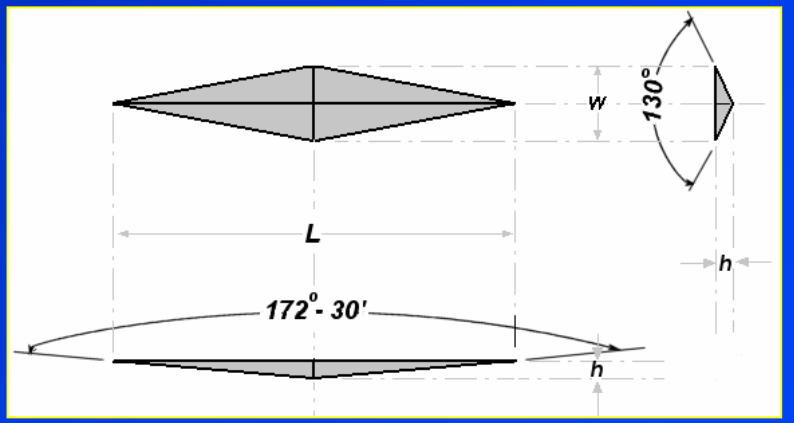

- The ***Knoop hardness number (KHN)*** is the applied load divided by the unrecovered projected area of the indentation.

$$KHN = \frac{P}{A_p} = \frac{P}{L^2 C} \qquad \text{Eq.7}$$

Where ***P*** = applied load, kg

A_p = unrecovered projected area of indentation, mm^2

L = length of long diagonal, mm

C = a constant for each indenter supplied by manufacturer.

Plastic zone underneath an indenter

- The ***plastic zone*** underneath a ***harness indentation*** is surrounded with elastic material, which acts to ***hinder plastic flow.***
- The material surrounding the deformed zone is rigid and ***upward flow*** of material compensates for the material displaced by the punch.
- The ***compressive stress*** required to cause ***plastic flow*** in the hardness test > that in the simple compression due to this ***constraint***.

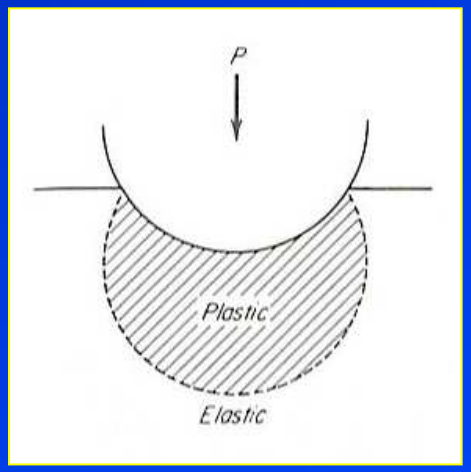

Plastic zone under a Brinell indenter.

Relationship between hardness and the flow curve

- ***Tabor*** suggested a method by which the ***plastic region of the true stress-strain curve*** may be determined from ***indentation hardness measurement***.
- This is under a condition such that the ***true strain*** was proportional to the ***d/D*** ratio (***ε = 0.2d/D***).

$$\sigma_o = \frac{VHN}{3}(0.1)^n \qquad \text{Eq.8}$$

Where σ_o is the 0.2% offset yield strength, kgf.mm^{-2}(=9.81 MPa)

VHN is the Vickers hardness number

n is the work hardening exponent.

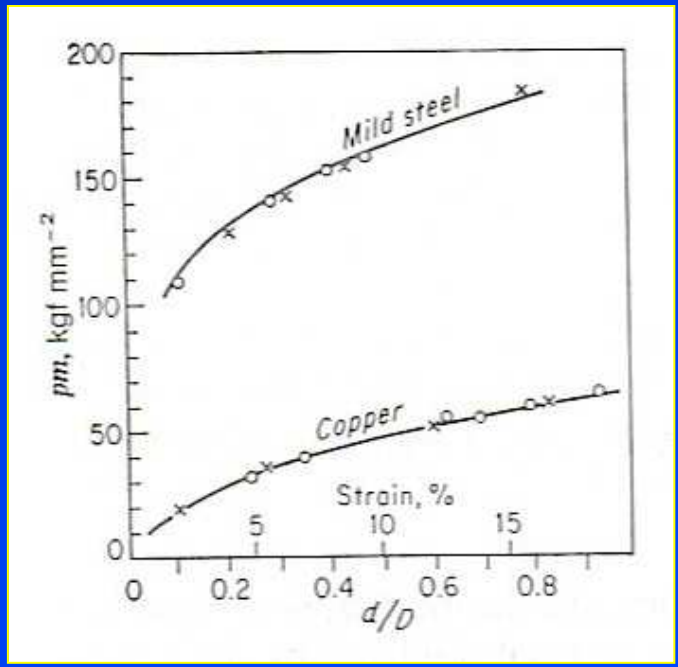

Comparison of flow curve determined from hardness measurements

Relationship between hardness and the flow curve

• For ***Brinell hardness,*** a very useful correlation has been used for heat-treated plain-carbon and medium-alloy steels as follows:

$$UTS(MPa) = 3.4(BHN) \qquad \textit{Eq.9}$$

• Furthermore, ***Young's modulus*** can also be given from the ***nano-hardness test***.

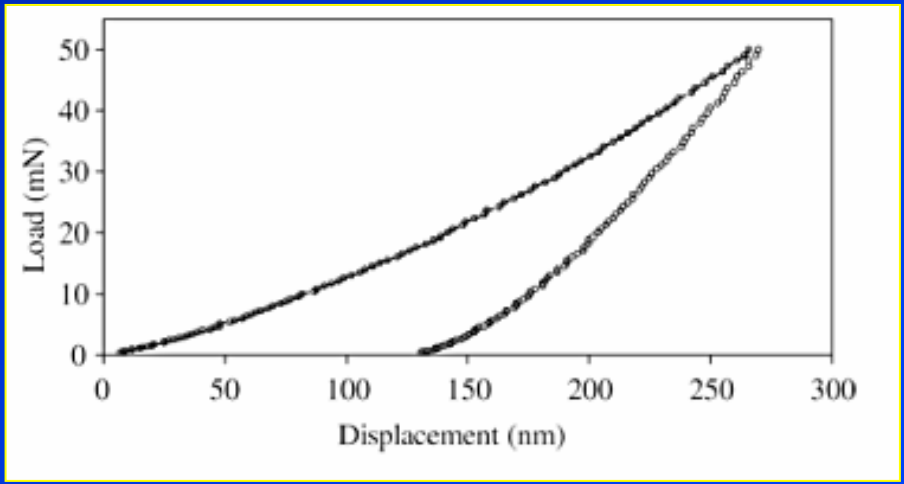

Load displacement curve obtained from hardness test

Hardness conversion relationships

- Hardness conversions are ***empirical relationships*** for Brinell, Rockwell and Vickers hardness values.
- This hardness conversions are applicable to heat-treated carbon and alloy steels in many heat treatment conditions. (or alloys with similar elastic moduli).
- For ***soft metals***, indentation of hardness depends on the strain hardening behaviour of the materials.
- Special hardness-conversion tables for cold-worked aluminium, copper, and 18-8 stainless steel are given in the ***ASM Metals Handbook***.

Hardness at elevated temperatures

- ***Hot hardness*** gives a good indication of potential usefulness of an alloy for ***high-temperature strength applications***.
- Hot hardness testers use a ***Vickers indenter*** made of sapphire and with provisions for testing in either vacuum or an inert atmosphere.
- The temperature dependence of hardness could be expressed as follows;

$$H = Ae^{-BT} \qquad \textit{Eq.10}$$

Where ***H*** = hardness, $kgf.mm^{-2}$
T = test temperature, ***K***
A,B = constants

Hardness at elevated temperatures

Log H VS temperature curve provides two slopes, having the turning point about one-half of the melting point of the material.

- ***BCC*** *metals are softer in an allotropic transformation where* ***FCC*** *and* ***HCP*** *metals have approximately the same strength.*

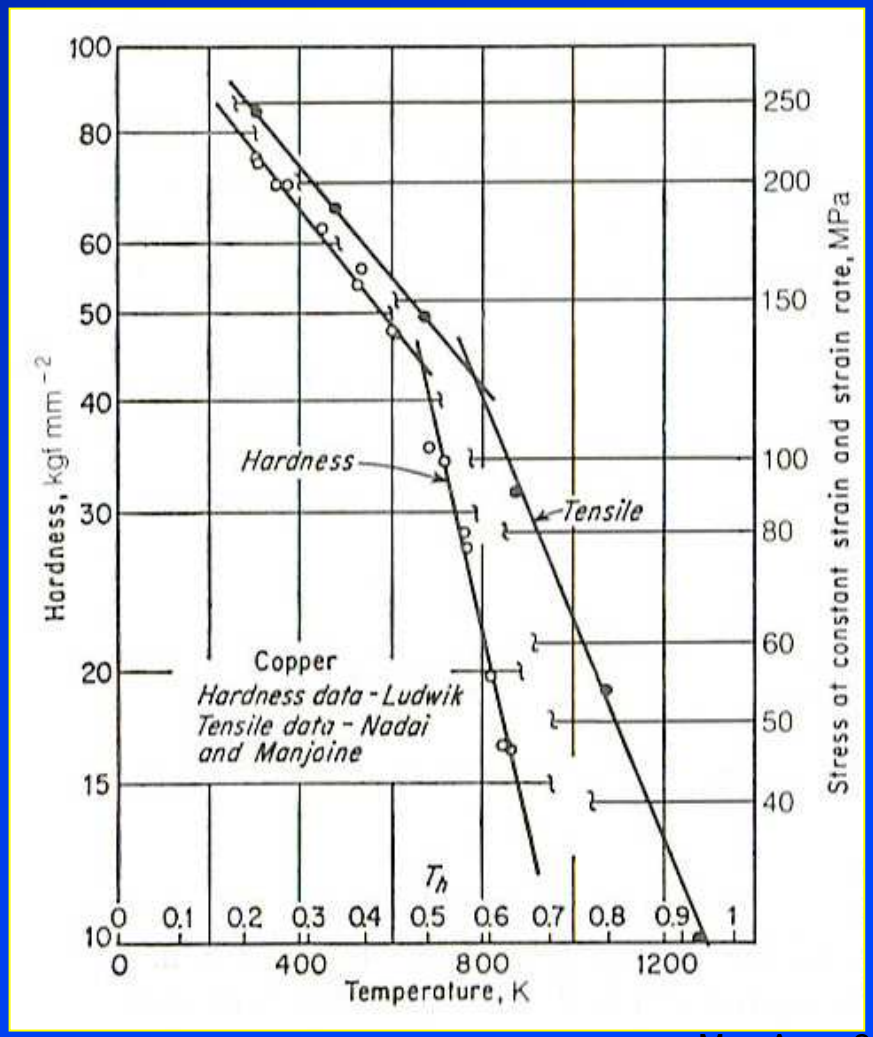

Temperature dependence of the hardness of copper

References

- Dieter, G.E., ***Mechanical metallurgy***, 1988, SI metric edition, McGraw-Hill, ISBN 0-07-100406-8.
- Walkerm P.M.B., ***Materials science and technology dictionary***, 1999, Chambers Harrap Publisher, ISBN 0 550 13249 x.

Torsion Tests

Subjects of interest

- *Introduction/Objectives*
- *Mechanical properties in torsion*
- *Torsional stresses for large plastic strains*
- *Type of torsion failures*
- *Torsion test vs.Tension test*
- *Hot torsion testing*

Objectives

- This chapter provides fundamental knowledge of torsion test and significant parameters such as torque, modulus of rupture in torsion and angle of rotation will be highlighted.
- Different types of torsion failures will be evaluated and differentiated from tension failures.

Introduction

- ***Torsion test*** is not widely accepted as much as tensile test.
- ***Torsion tests*** are made on materials to determine such properties as the ***modulus of elasticity in shear***, the ***torsion yield strength*** and the ***modulus of rupture***.
- Often used for testing brittle materials and can be tested in full-sized parts, i.e., shafts, axles and twist drills which are subjected to torsional loading in service.

Introduction

Examples:

• Driveshaft is subjected to torsion in service.

www.caradvice.com

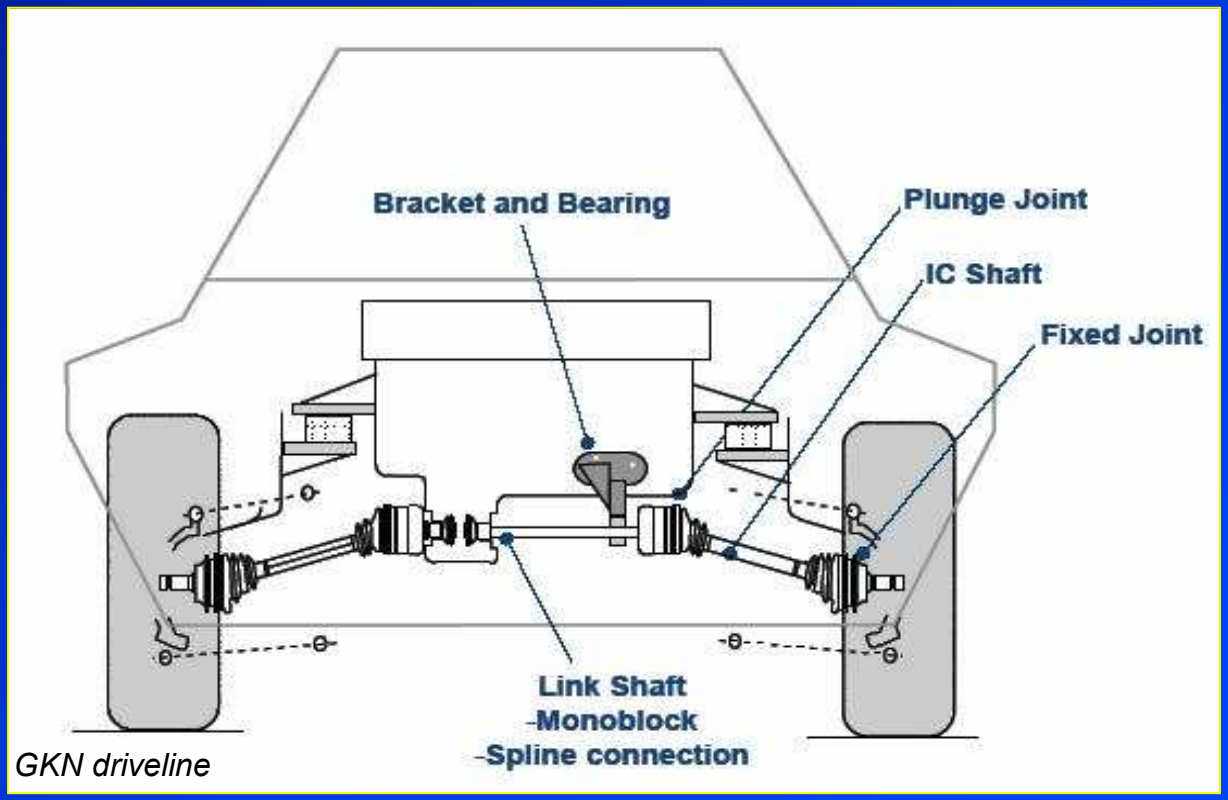

GKN driveline

Bar shaft

Torsion-testing equipment

Torsion-testing equipment consists of

1) ***A twisting head***, with a chuck for gripping the specimen and for applying the twisting moment to the specimen.
2) ***A weight head***, which grips the other end of the specimen and measures the twisting moment of torque.

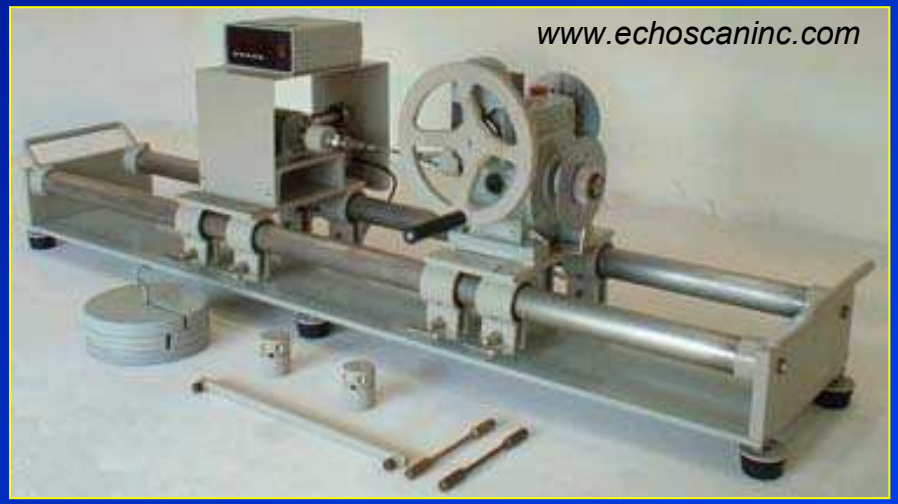

Specimen used

A circular cross section specimen is normally used since in the elastic range, shear stress varies linearly from a value zero at the centre of the bar to a maximum value at the surface.

Note: *Thin-walled tubular specimen is frequently used.*

Determination of torsion test

- Applying ***twisting moment*** to the specimen and measure the ***torque***.

- Determination is made of the ***angular displacement*** (or ***degree of rotation***) of a point near one end of the test section of the specimen with respect to a point on the same longitudinal element at the opposite end (using ***Troptometer***).

- The shear strain γ is given by

Where

$$\gamma = \tan\phi = \frac{r\theta}{L} \qquad \textit{Eq.1}$$

θ is the angle of twist or degree of rotation, radian

L is the test length of the specimen.

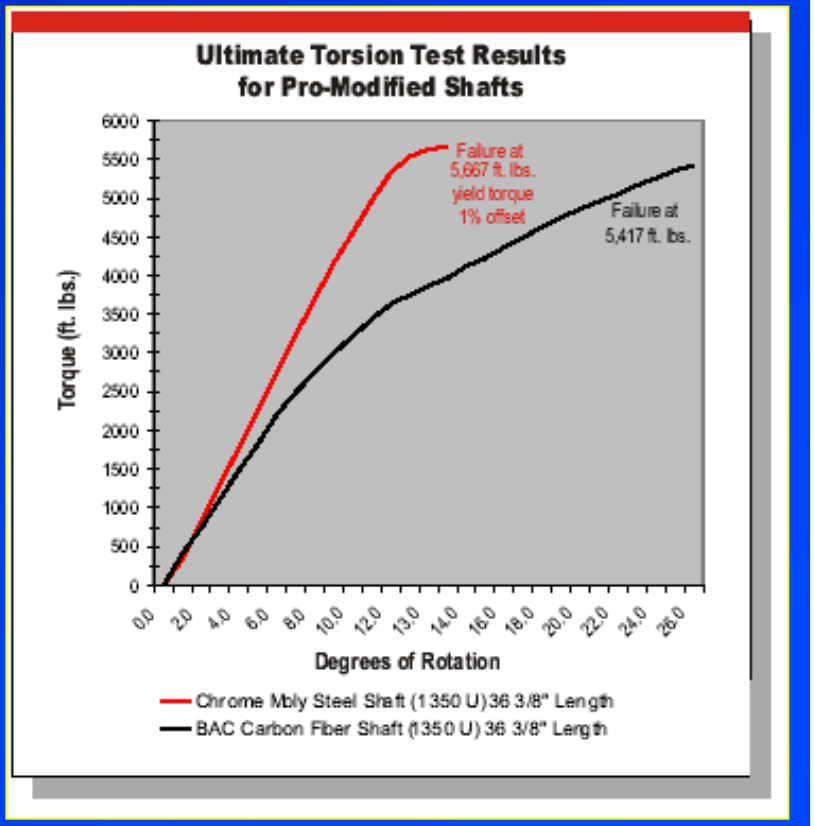

Torque-degree of rotation diagram

Mechanical properties in torsion

- Consider a cylindrical bar subjected to a ***torsional moment*** at one end.
- The ***twisting moment*** is resisted by shear stresses set up in the cross section of the bar. (zero at centre, max at surface)

$$M_T = \int_{r=0}^{r=a} \tau r dA = \frac{\tau}{r}\int_o^a r^2 dA$$

Eq.2

But $\int r^2 dA$ is the polar moment of inertia of the area with respect to the axis of the bar. Thus,

$$M_T = \frac{\tau J}{r}, or \ \tau = \frac{M_T r}{J}$$

Eq.3

Where τ = shear stress, Pa
M_T = torsional moment, Nm
r = radial distance measured from centre of bar, m
J = polar moment of inertia, m^4

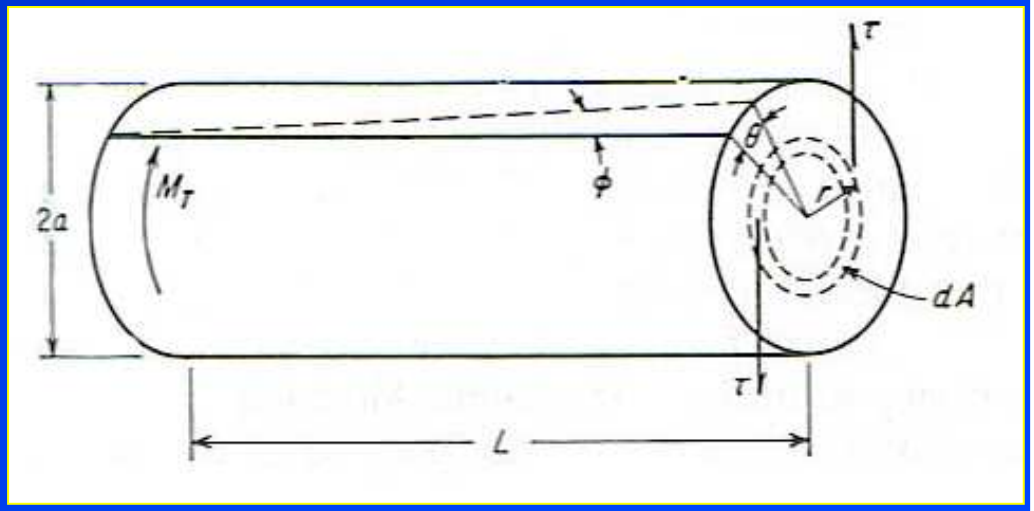

Torsion of a solid bar

Shear stress

- The ***maximum shear stress*** at the surface of the bar is

$$\tau_{\max} = \frac{M_T D/2}{\pi D^4/32} = \frac{16M_T}{\pi D^3} \qquad \textit{Eq.4}$$

- For a ***tubular specimen***, the shear stress on the outer surface is

$$\tau = \frac{16M_T D_1}{\pi(D_1^4 - D_2^4)} \qquad \textit{Eq.5}$$

Where D_1 = Outside diameter of tube
D_2 = Inside diameter of tube

Note: *Eq.4 and Eq.5 is applied only for a linear relationship.*

Elastic properties and yield strength

• The ***elastic properties*** in torsion can be obtained by using the torque at the ***proportional limit*** (~ 0.04 rad.m^{-1}) where the shear stress is calculated corresponding to the twisting moment from *Eq.4* or *Eq.5*.

• The ***torsional elastic limit*** or ***yield strength*** can be obtained from testing a ***tubular specimen*** since the stress gradient are practically eliminated.

Note: *To measure the shearing yield strength and modulus of elasticity*

$$\frac{\text{Length of reduced section}}{\text{Outside diameter}} \sim 10$$

$$\frac{\text{Diameter}}{\text{Thickness}} \sim 8\text{-}10$$

To prevent specimen to fail in bulking rather than in torsion:

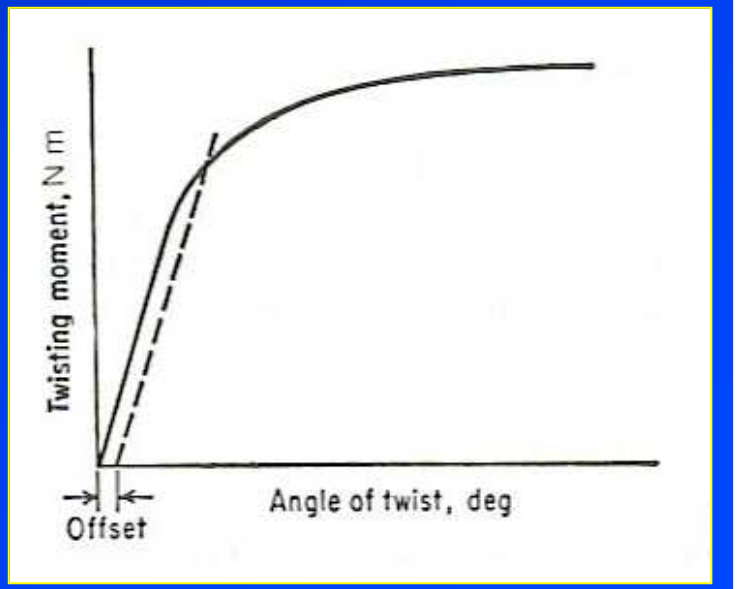

Torque-twist diagram

Modulus of rupture

- ***Modulus of rupture*** or the ***ultimate torsional shearing stress*** is determined by substituting shearing measured torque in to *Eq.4* or Eq.5. → slightly overestimate.
- The ***modulus of elasticity*** in shear ***G*** or the modulus of rigidity is addressed as follows:

$$G = \frac{\tau}{\gamma} \qquad \textit{Eq.6}$$

Or

$$G = \frac{M_T L}{J\theta} \qquad \textit{Eq.7}$$

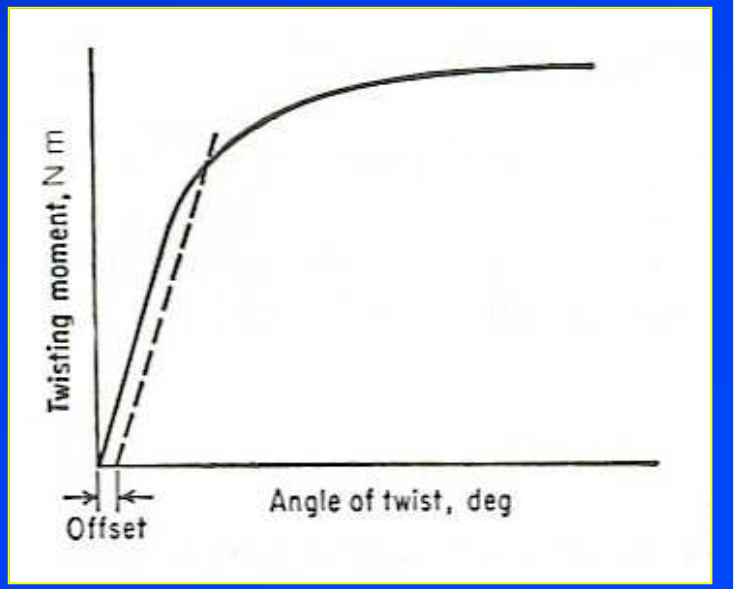

Torque-twist diagram

Torsional stresses for large plastic strains

• Beyond the ***torsional yield strength***, the torque-twist angle relationship is no longer linear and in the ***plastic range*** the ***shear stress*** in the bar at the outer fiber can be calculated from

$$\tau_a = \frac{1}{2\pi a^3}\left(\theta' \frac{dM_T}{d\theta'} + 3M_T\right) \qquad \textit{Eq.8}$$

Or

$$\tau_a = \frac{1}{2\pi a^3}\left(BC + 3CD\right)$$

Where $\theta' = \theta / L$

• At maximum point, $\frac{dM_T}{d\theta'} = 0$.

The ***ultimate torsional shear strength*** or ***modulus of rupture*** in the bar at the outer fibre is

$$\tau_u = \frac{3M_{\max}}{2\pi a^3} \qquad \textit{Eq.9}$$

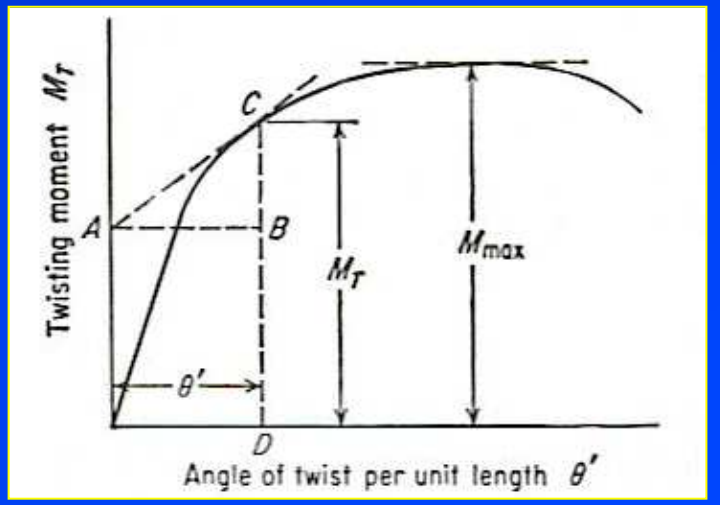

Method of calculating shear stress from torque-twist diagram.

Types of torsion failures

• ***State of stress*** in torsion on the surface of a bar occurs on two mutually perpendicular planes (longitudinal ***yy*** and transverse ***xx***).

• The principal stresses σ_1,(longitudinal) σ_3 (compressive) make an angle of 45° and $\sigma_3 = -\sigma_1$. (intermediate stress $\sigma_2 = 0$).

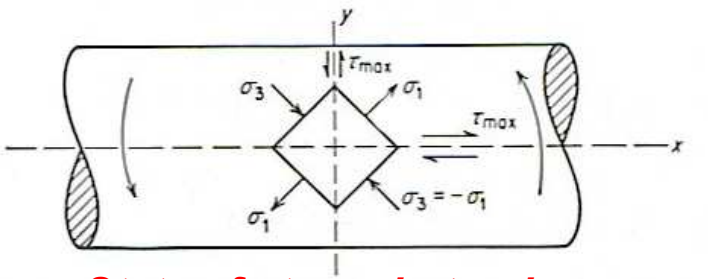

State of stress in torsion

(a) Shear (ductile) failure ***(b) Tensile (brittle) failure***

• ***Torsion failures*** are different from tensile failures in that there is ***little localised reduction of area or elongation***.

a) ***Shear (ductile) failure*** is along the maximum shear plane.

b) ***Tensile (brittle) failure*** is perpendicular to the maximum tensile stress (at 45°), resulting in a helical fracture.

Types of torsion failures

Brittle failure

Drive shaft failure

Torsion test vs. tension test

Tension test	*Torsion test*
$\sigma_1 = \sigma_{max};\ \sigma_2 = \sigma_3 = 0$	$\sigma_1 = -\sigma_3;\ \sigma_2 = 0$
$\tau_{max} = \frac{\sigma_1}{2} = \frac{\sigma_{max}}{2}$	$\tau_{max} = \frac{2\sigma_1}{2} = \sigma_{max}$
$\varepsilon_{max} = \varepsilon_1;\ \varepsilon_2 = \varepsilon_3 = -\frac{\varepsilon_1}{2}$	$\varepsilon_{max} = \varepsilon_1 = -\varepsilon_3;\ \varepsilon_2 = 0$
$\gamma_{max} = \frac{3\varepsilon_1}{2}$	$\gamma_{max} = \varepsilon_1 - \varepsilon_3 = 2\varepsilon_1$
$\bar{\sigma} = \frac{\sqrt{2}}{2}\left[(\sigma_1-\sigma_2)^2 + (\sigma_2-\sigma_3)^2 + (\sigma_3-\sigma_1)^2\right]^{1/2}$	
$\bar{\varepsilon} = \frac{\sqrt{2}}{3}\left[(\varepsilon_1-\varepsilon_2)^2 + (\varepsilon_2-\varepsilon_3)^2 + (\varepsilon_3-\varepsilon_1)^2\right]^{1/2}$	
$\bar{\sigma} = \sigma_1$	$\bar{\sigma} = \sqrt{3}\,\sigma_1$
$\bar{\varepsilon} = \sigma_1$	$\bar{\varepsilon} = \frac{2}{\sqrt{3}}\varepsilon_1 = \frac{\gamma}{\sqrt{3}}$

- There is better chance for ***ductile behaviour*** in torsion than in tension.

Critical τ_{max} ➡ **Plastic flow**

Critical σ_{max} ➡ **Fracture**

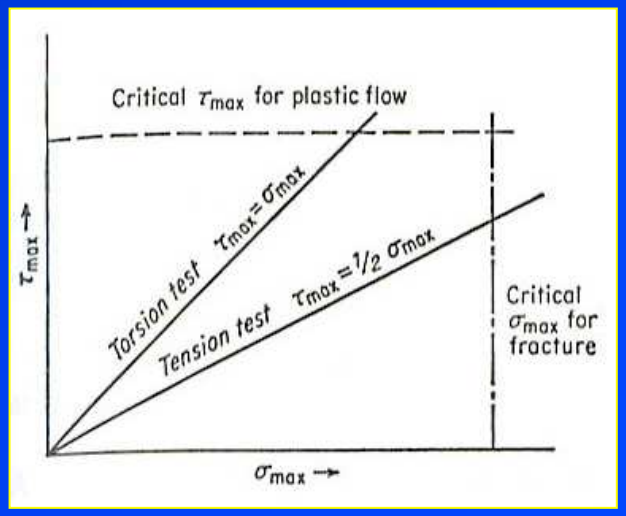

Effect of the ratio τ_{max}/σ_{max} in determining ductility.

Hot torsion testing

• Under ***hot-working condition*** (***T*** > 0.6T_m, ε *up to* 10^3 s^{-1}), torsion test is often used to obtain data on the ***flow properties*** and ***fracture***.

Hot torsion testing machine

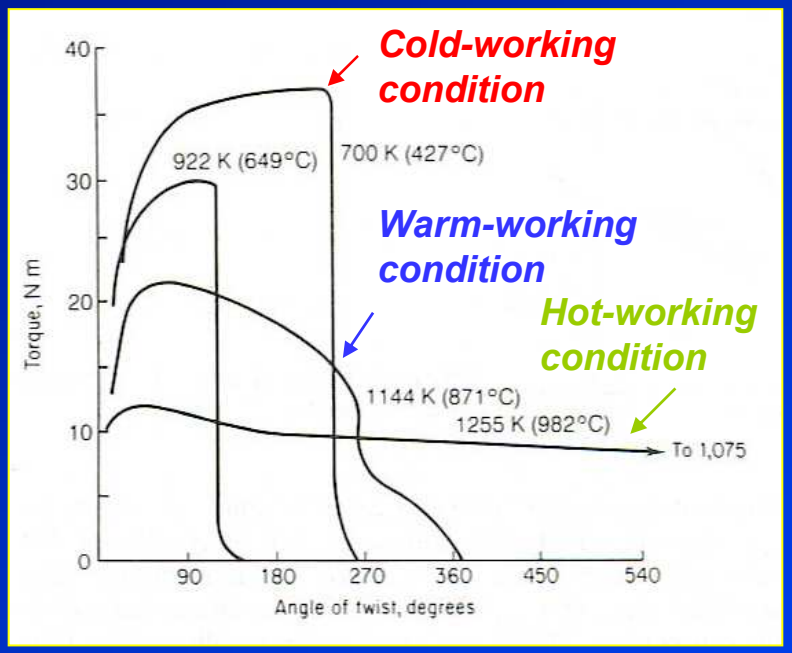

Torque-twist curves at different temperatures for a nickel-based alloy in torsion at ε =2.5 s^{-1}.

• In ***hot working condition (m>>n)***, the maximum shear stress is expressed as follows;

$$\tau_a = \frac{M_T}{2\pi a^3}(3+m+n) \qquad \textit{Eq.10}$$

Where

m is strain rate sensitivity

n is the strain hardening exponent.

References

- Dieter, G.E., ***Mechanical metallurgy***, 1988, SI metric edition, McGraw-Hill, ISBN 0-07-100406-8.

Fracture mechanics

Subjects of interest

- *Introduction/ objectives*
- *Stress intensity factor*
- *Determination of fracture toughness*
- *Fracture toughness and design*
- *Plasticity correction*
- *Crack opening displacement*
- *R curve*
- *Probabilistic aspects of fracture mechanics*

Objectives

- This chapter provides fundamental backgrounds of fracture mechanics and its use for the understanding of brittle fracture.
- Different approaches used for determining fracture toughness of materials will be discussed.
- The application of fracture mechanics are emphasised for the selection of materials for the required applications.

Introduction

***Griffith* proposed that an existing crack will propagate when the released elastic strain energy is at least equal to the energy required to create the new crack surface.**

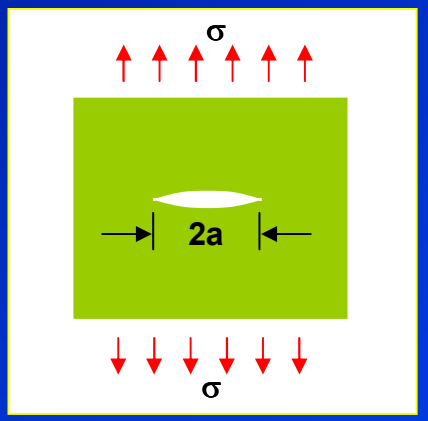

Griffith crack model

$$\sigma_f = \left(\frac{2E\gamma_s}{\pi a}\right)^{1/2}$$

Eq.1

• ***Irwin*** later modified the ***Griffith theory*** by replacing the term $2\gamma_p$ with the ***potential strain energy release rate*** ***G*** , giving the expression as follows;

$$\sigma_f = \left(\frac{EG}{\pi a}\right)^{1/2}$$

Eq.2

• ***Irwin*** showed that ***G*** is ***measurable*** and can be related to the ***stress intensity factor***, ***K***, obtained from the ***sharp crack fracture toughness test***.

• The ***critical condition*** to which the crack propagates to cause global failure is when this ***G*** value exceeds the ***critical value***, ***G***.

Fracture mechanics

Stress intensity factor

In ***mode I*** failure and ***plane-strain condition***, the relationship between G_{IC} and K_{IC} can be shown by an expression as follows;

$$G_{IC} = \frac{K_{IC}^2 (1-\upsilon^2)}{E} \qquad \text{Eq.3}$$

Where K_{IC} is the critical stress intensity factor for mode I failure.

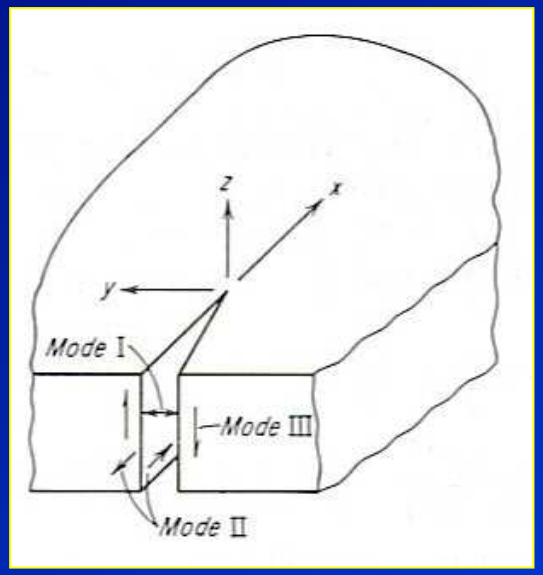

Crack deformation mode.

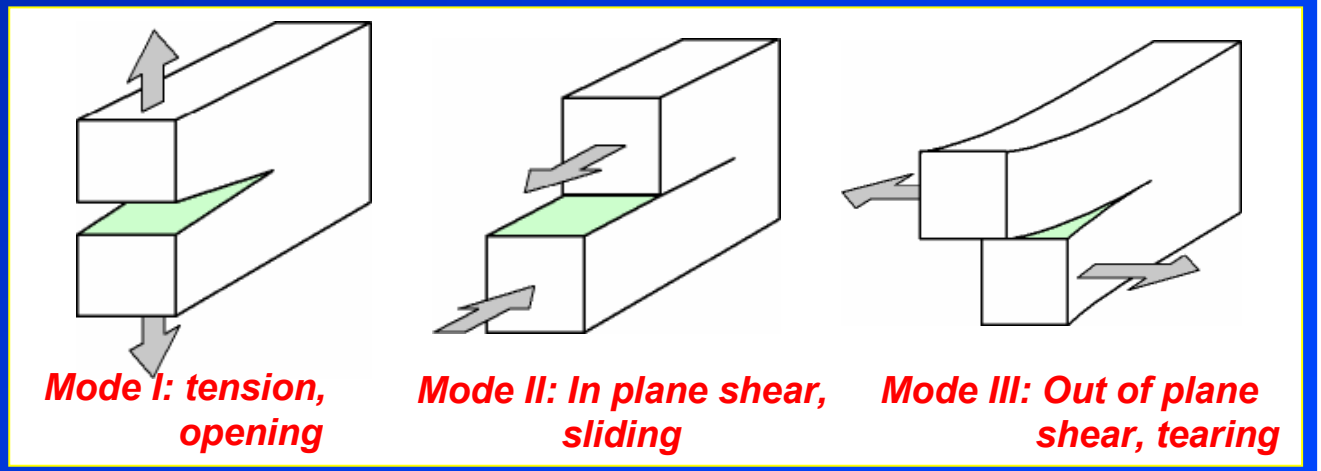

Mode I: tension, opening

Mode II: In plane shear, sliding

Mode III: Out of plane shear, tearing

Fracture modes

Note: ***K*** *value can be evaluated using* ***standard experimental approaches****, which is much more readily than values of* ***G****.*

Stress intensity factor

Stress intensity factor K_{IC} can be described as fracture toughness of materials (material resistance to crack propagation) under conditions of

1) *brittle fracture*
2) *in the presence of a sharp crack*
3) *under critical tensile loading*

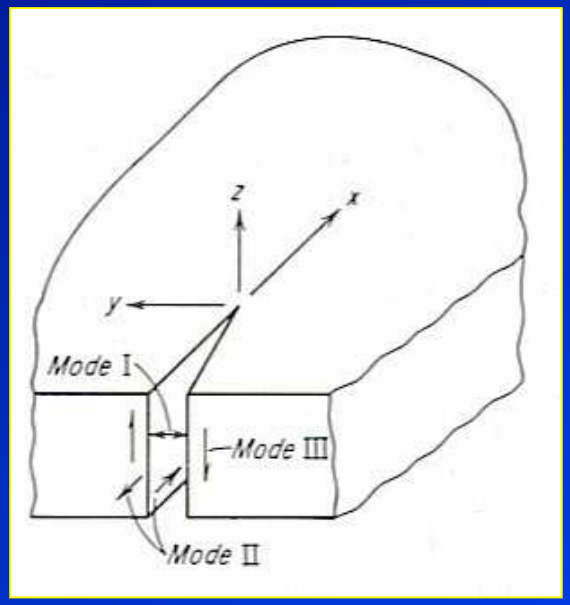

Crack deformation mode

$$K_{IC} = \alpha \sigma_{app} \sqrt{\pi a_c}$$ *Eq.4*

Where

K_{IC} is the critical stress intensity factor for plane strain condition in mode I failure.

a_c is the critical crack length in an infinite plate

σ_{app} is the applied stress

α is a parameter dependent on specimen and crack geometry

LEFM – Linear Elastic Fracture Mechanics

K values of various crack geometries

(a)

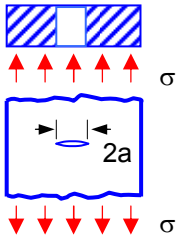

Through thickness crack

$$K = \sigma_{app}\sqrt{\pi a}$$

(d)

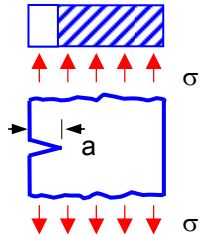

Edge crack

$$K = 1.12\sigma_{app}\sqrt{\pi a}$$

(b)

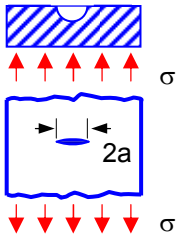

Semi circular crack

$$K = 0.6\sigma_{app}\sqrt{\pi a}$$

(e)

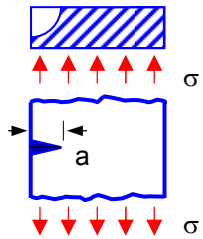

Corner crack

$$K = 0.8\sigma_{app}\sqrt{\pi a}$$

(c)

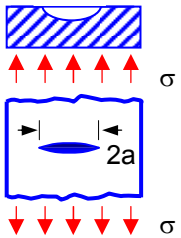

Semi elliptical crack

$$K = 0.8\sigma_{app}\sqrt{\pi a}$$

Determination of fracture toughness

Fracture toughness of material can be determined according to LEFM analysis

1) K_{IC} fracture toughness

works well for very high strength materials.
→ exhibiting brittle fracture

2) Crack tip opening displacement CTOD

Used for lower strength materials (σ_o < 1400 MPa), exhibiting small amount of plastic deformation before failure.

3) J-integral (J_{IC})

Used for lower strength materials, exhibiting small amount of plastic deformation before failure.

4) R-curve

The resistance to fracture of a material during slow and stable crack propagation.

K_{IC} fracture toughness

K_{IC} fracture toughness *of material is obtained by determining the* ***ability of material to withstand the load*** *in the presence of a sharp crack before failure.*

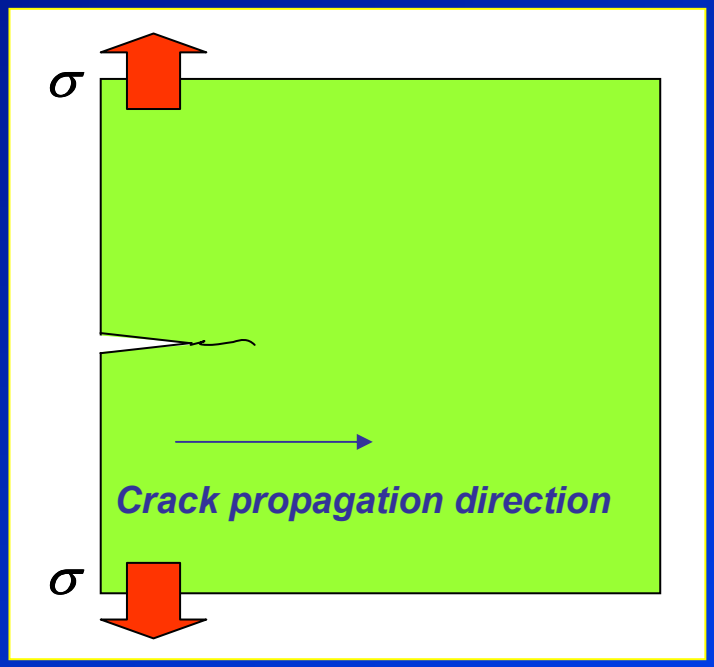

Fracture toughness → How long the existing crack will grow until the specimen fails

• ***Fracture toughness*** is required in the ***system of high strength and light weight***, i.e., high strength steels, titanium and aluminium alloys.

EX:

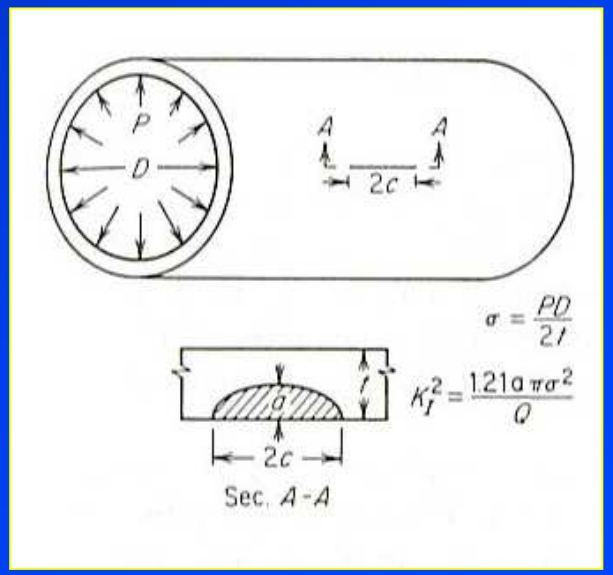

Flaw geometry and design of cylindrical pressure vessel

Stress distribution in the presence of a crack

The ***stress distribution*** in a thin plate for an elastic solid in terms of the coordinates (*fig*) is given by

$$\sigma_x = \sigma\left(\frac{a}{2r}\right)^{1/2}\left[\cos\frac{\theta}{2}\left(1-\sin\frac{\theta}{2}\sin\frac{3\theta}{2}\right)\right]$$

$$\sigma_y = \sigma\left(\frac{a}{2r}\right)^{1/2}\left[\cos\frac{\theta}{2}\left(1+\sin\frac{\theta}{2}\sin\frac{3\theta}{2}\right)\right]$$

$$\sigma_z = \sigma\left(\frac{2}{2r}\right)^{1/2}\left[\sin\frac{\theta}{2}\cos\frac{\theta}{2}\cos\frac{3\theta}{2}\right]$$

Eq.5

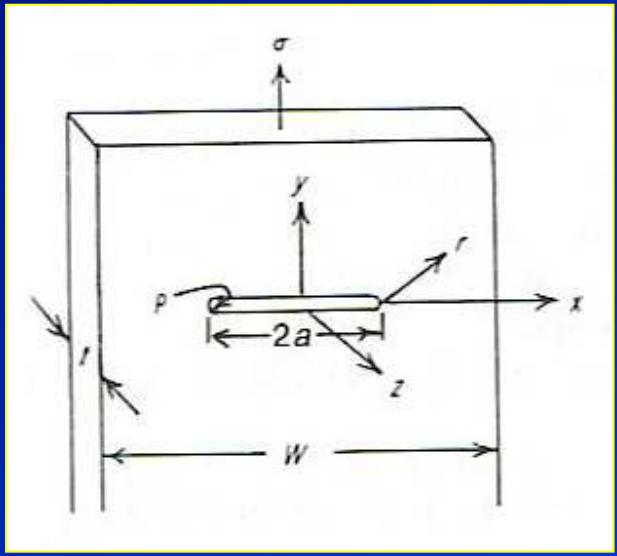

Model for equations for stresses at a point near a crack

Where σ is gross nominal stress = ***P/wt*** for ***a > r >*** ρ.

For an orientation directly ahead of the crack tip ($\theta = 0$)

$$\sigma_x = \sigma_y = \sigma\left(\frac{a}{2r}\right)^{1/2}, \tau_{xy} = 0$$

Eq.6

Stress distribution in the presence of a crack

- ***High local stress intensity*** is present in front of the sharp crack. → ***stress concentration leading to brittle failure***.
- σ_z is strongly dependent on specimen thickness and is negligible in thin specimen (***plane stress***).

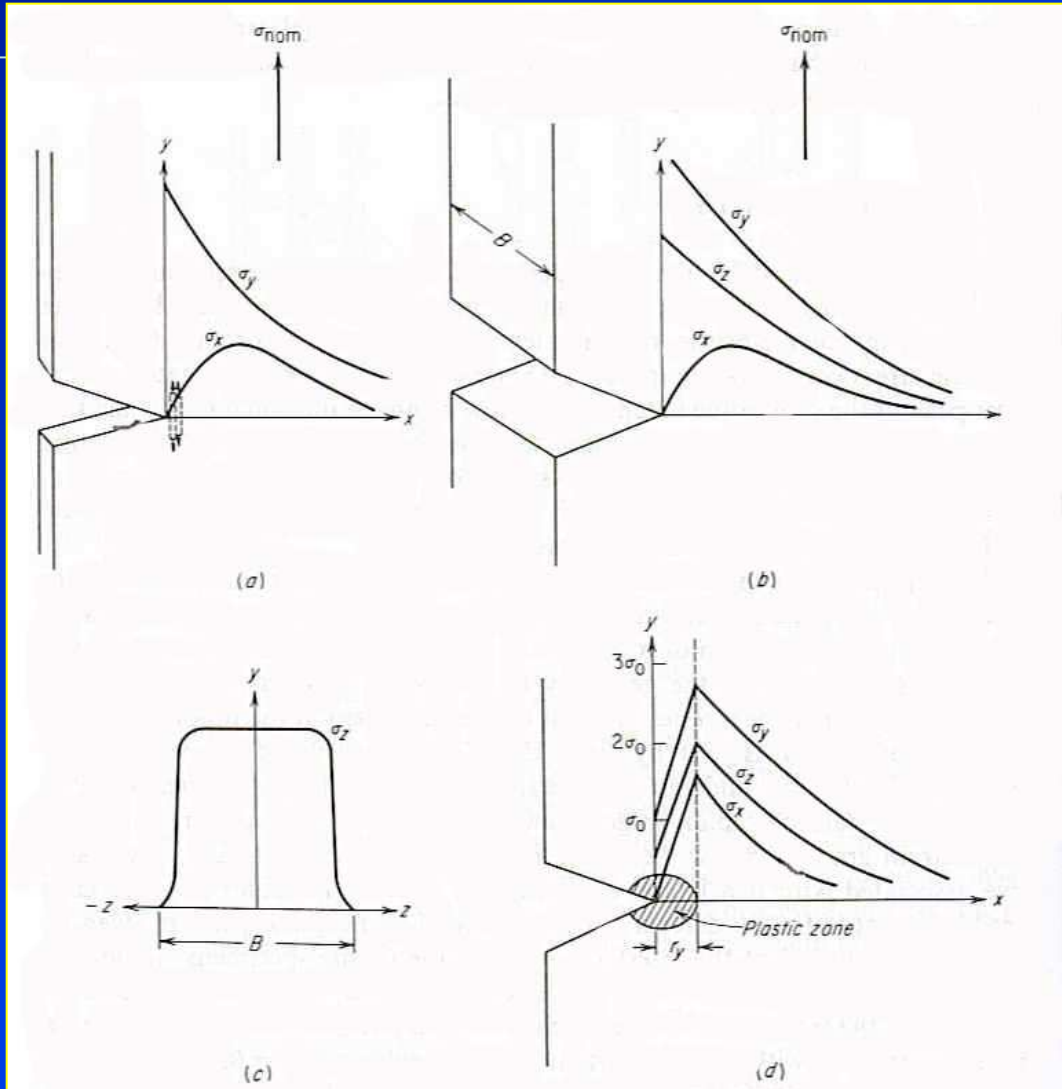

Figure 7-15 (*a*) Elastic stresses beneath a notch in a thin plate (planes stress); (*b*) elastic stresses beneath a notch in plane strain; (*c*) distribution of σ_z with z at $x = 0$ (plane strain); (*d*) distribution of stresses during local yielding (plane strain).

Determination of K_{IC} fracture toughness

- K_{IC} – the critical stress intensity in mode I fracture
- Need to make sure that the specimen is tested under mode I fracture and in a plane strain condition → brittle condition.

1) Validation of K_{IC} fracture toughness values
2) Specimen preparation
3) Testing procedure
4) Calculation of K_{IC} value

Validation of K_{IC} value

• Since the ***stress distribution under the notch*** varies due to specimen thickness, which also affect ***toughness of materials of different test specimen dimensions***.

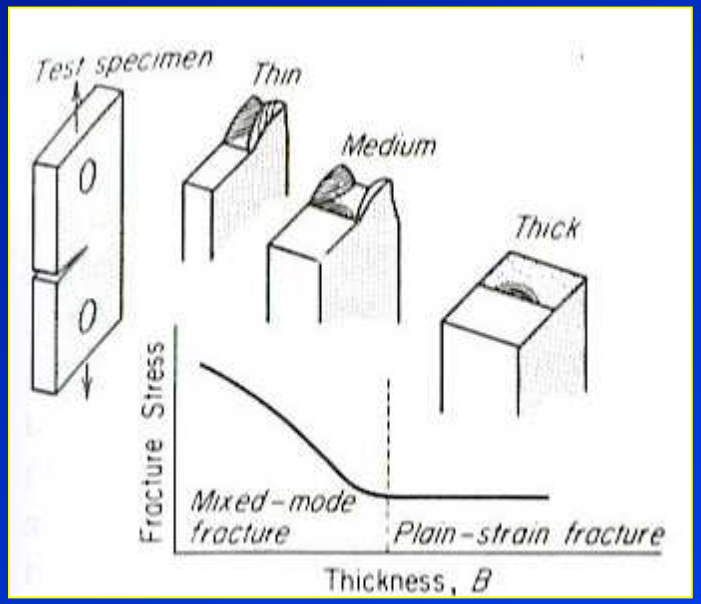

Effect of specimen thickness on stress and mode of fracture

• Due to the criterion for brittle fracture in the presence of the notch, the ***plane strain condition,*** is required for the validation of fracture toughness K_{IC} values.

$$B, W - a_o, a_o \geq 2.5\left(\frac{K_{IC}}{\sigma_o}\right)^2 \qquad \text{Eq.7}$$

Where
- B is specimen thickness
- W is specimen width
- a_o is the original crack length
- $W-a_o$ is the ligament
- σ_o is the yield strength

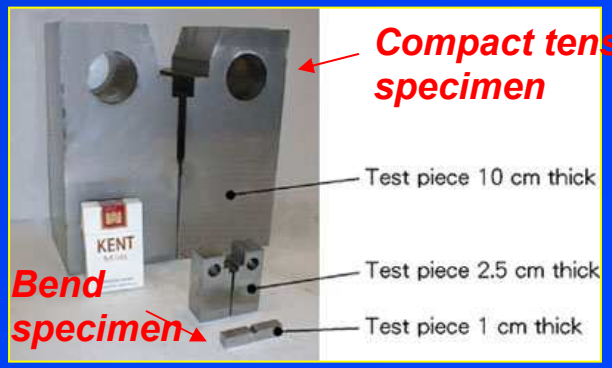

Specimen preparation

- Select the specimen dimensions.
- Select the crack propagation direction.
- ***Fatigue pre-cracking*** by applying fatigue load at a controlled condition of small load and amplitude to obtain a sharp fatigue pre-crack to ensure ***high stress distribution ahead of the crack tip.***

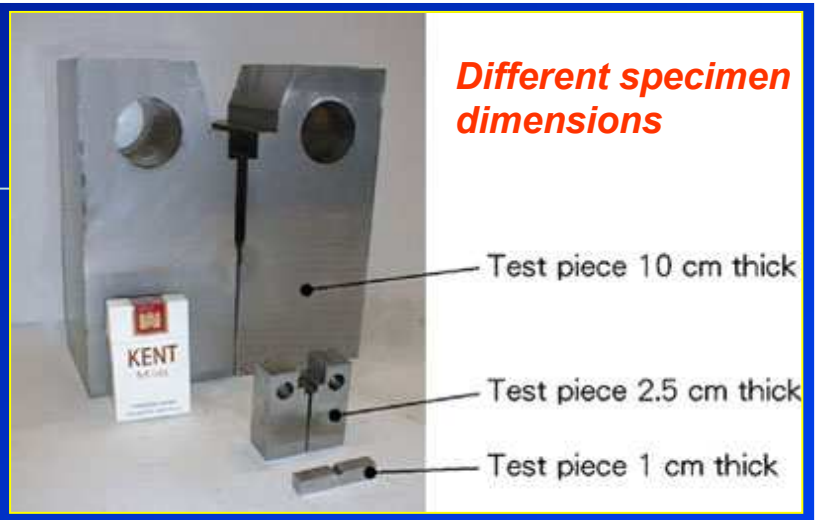

Different specimen dimensions

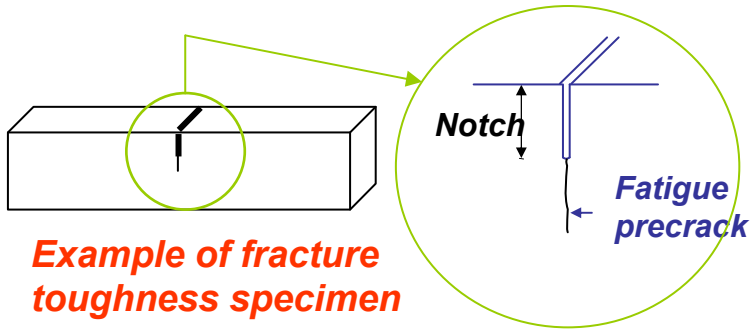

Example of fracture toughness specimen

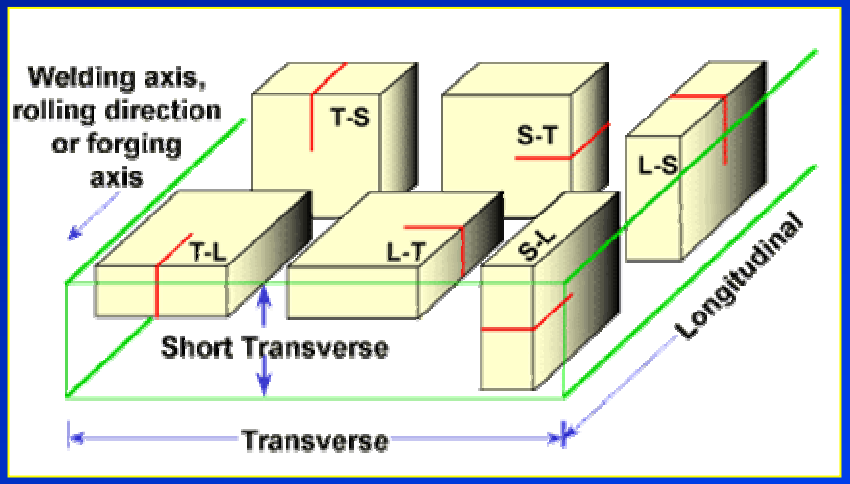

Directions of crack propagation

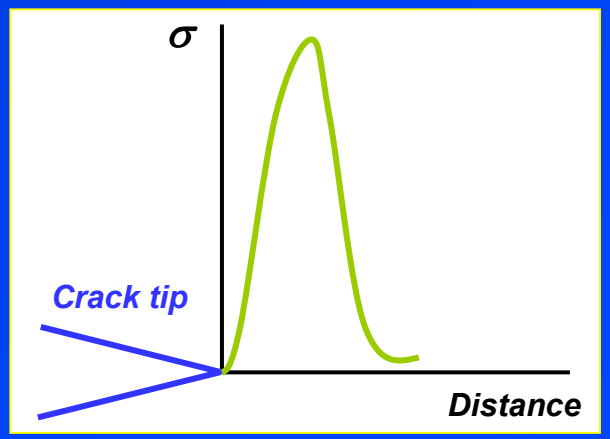

Stress distribution ahead of fatigue pre-crack

Test procedure for K_{IC} fracture toughness

- A ***pre-cracked specimen*** is arranged and monotonically loaded until failure.
- Load and clip gauge displacement are recorded during loading to give a graph, which will be used for calculation.

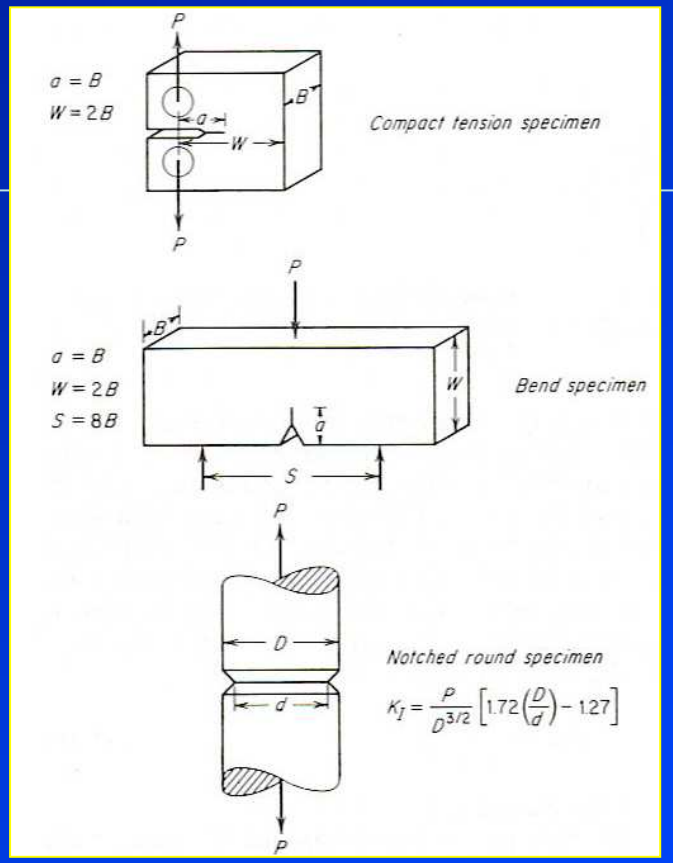

Three-point bend arrangement for fracture toughness test

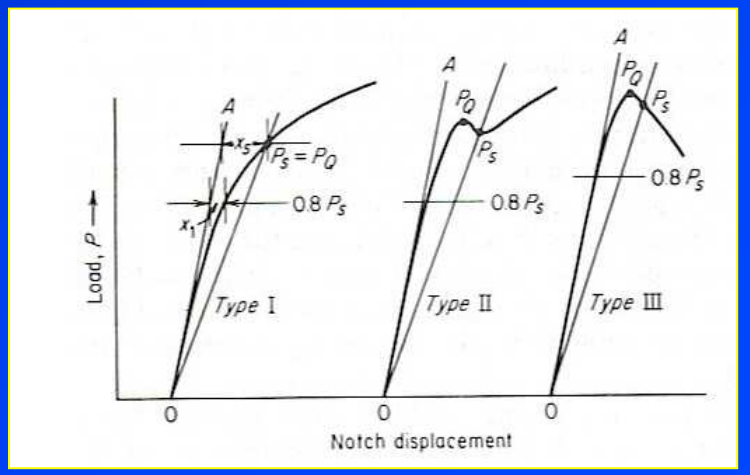

Load-clip gauge displacement curves

Calculation of K_{IC} fracture toughness

Fracture toughness K_Q is calculated using the following expression (for a bend specimen).

$$K_Q = \frac{PS}{BW^{1.5}} \times f\left(\frac{a}{W}\right)$$

Eq.8

Where
- ***P*** is the load
- ***S*** is the span length
- ***B*** is the specimen thickness
- ***W*** is the specimen width
- ***f(a/W)*** is the compliance function

For bend specimen

$$f\left(\frac{a_o}{W}\right) = \left[2.9\left(\frac{a_o}{W}\right)^{1/2} - 4.6\left(\frac{a_o}{W}\right)^{3/2} + 21.8\left(\frac{a_o}{W}\right)^{5/2} - 37.6\left(\frac{a_o}{W}\right)^{7/2} + 38.7\left(\frac{a_o}{W}\right)^{9/2}\right]$$

Eq.9

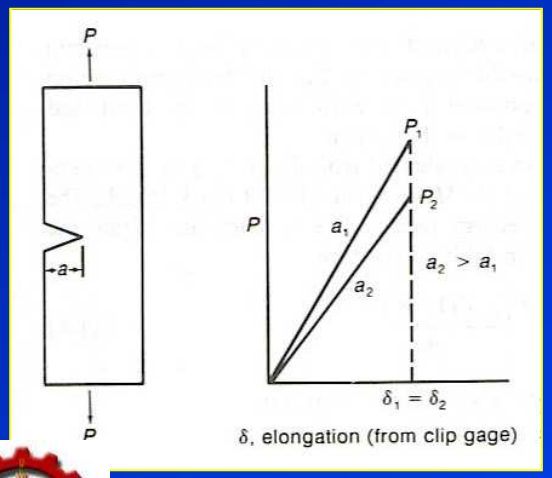

Compliance function depending on the crack length

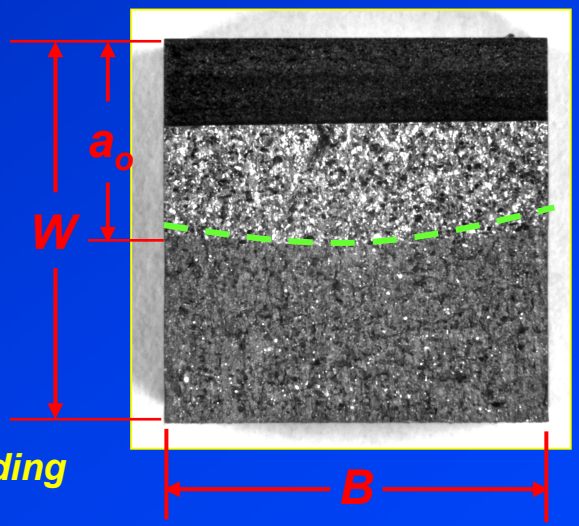

$$a_0 = \frac{1}{8}\left(\frac{a_1 + a_9}{2} + \sum_{i=2}^{i=8} a_i\right)$$

Eq.10

If the K_Q value obtained from Eq.8 is verified according to Eq 7, → K_{IC}.

Typical values of K_{IC}

Table 11-1 Typical values of K_{1c}

Material	Yield strength, MPa	Fracture toughness K_{1c}, MPa $m^{1/2}$
4340 steel	1470	46
Maraging steel	1730	90
Ti-6Al-4V	900	57
2024-T3 Al alloy	385	26
7075-T6 Al alloy	500	24

Fracture toughness and design

- *If the **K_{IC}** value of material is known and the presence of a crack is allowed, we can then monitor the crack propagation during service prior to failure. → **How long we can use the component before it fails.***
- ***Crack in the component** (in service) can be detected by using **Non Destructive Testing** (**NDT**), i.e., ultrasonic, dye-penetrant, X-ray, Eddy current, ferromagnetic inspection.*

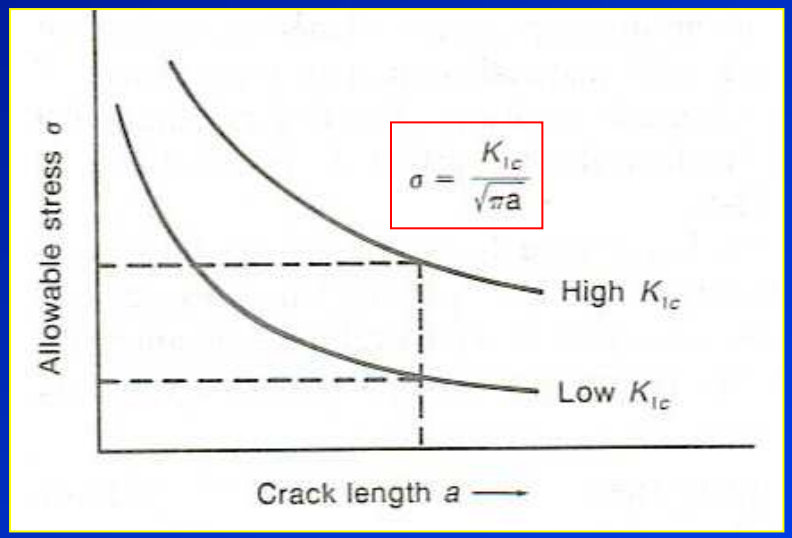

Relation between fracture toughness and allowable stress and crack size

$$K_{IC} = \alpha \sigma_{app} \sqrt{\pi a_c} \qquad \textit{Eq.11}$$

- From equation and figure, we can design the ***allowable stress*** σ at the presence of a given ***crack length a*** without failure.

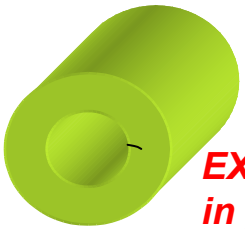

EX: Crack observed in pressure vessel

Example: *The stress intensity for a partial-through thickness flaw is given by* $K = \sigma\sqrt{\pi a}\sqrt{\sec \pi a / 2t}$ *where* ***a*** *is the depth of flaw penetration through a wall thickness* ***t****. If the flaw is 5 mm deep in a wall 12 mm thick, determine whether the wall will support a stress of 172 MPa if it is made from 7075-T6 aluminium alloy.*

K_{IC} of 7075-T6 ***Al alloy*** = 24 MPa.m$^{1/2}$,
a = 5 x 10^{-3} m
t = 12 x 10^{-3} m

$$\sec\frac{\pi a}{2t} = \sec\frac{\pi\left(5\times10^{-3}\right)}{2\left(12\times10^{-3}\right)} = \sec 0.6545 = \frac{1}{\cos 0.6545} = 1.260$$

$$\sigma = \frac{K_{IC}}{\sqrt{\pi a}\sqrt{\sec \pi a / 2t}} = \frac{24}{\sqrt{\pi\left(5\times10^{-3}\right)}\sqrt{1.260}} = \frac{24}{\sqrt{0.01979}} = 171 \ \ MPa$$

But the applied stress is 172 MPa.m$^{1/2}$. The flaw will therefore propagate as a brittle fracture.

Example: *A thin-wall pressure vessel is made from Ti-6Al-4V with* K_{IC} *= 57 MPa.m*$^{1/2}$ *and* σ_o *= 900 MPa. The internal pressure produces a circumferential hoop stress of 360 MPa. The crack is a semi-elliptical surface crack orientated with the major plane of the crack perpendicular to the uniform tensile hoop stress, see fig. For this type of loading and geometry the stress intensity factor is given by*

$$K_I^2 = \frac{1.21 a \pi \sigma^2}{Q}$$

a = *surface crack,*

σ = *the applied nominal stress*

Q = $\phi^2 - 0.212(\sigma/\sigma_o)^2$

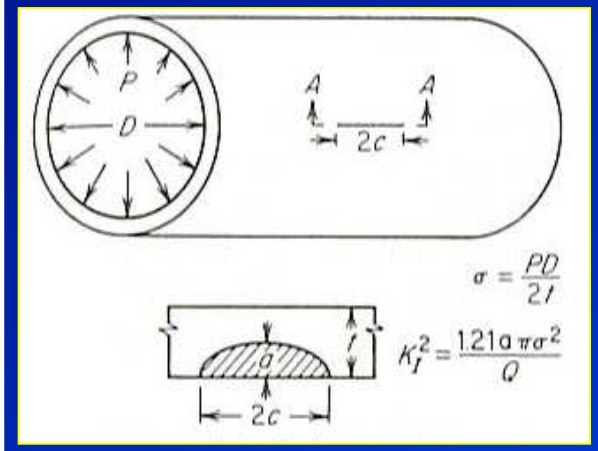

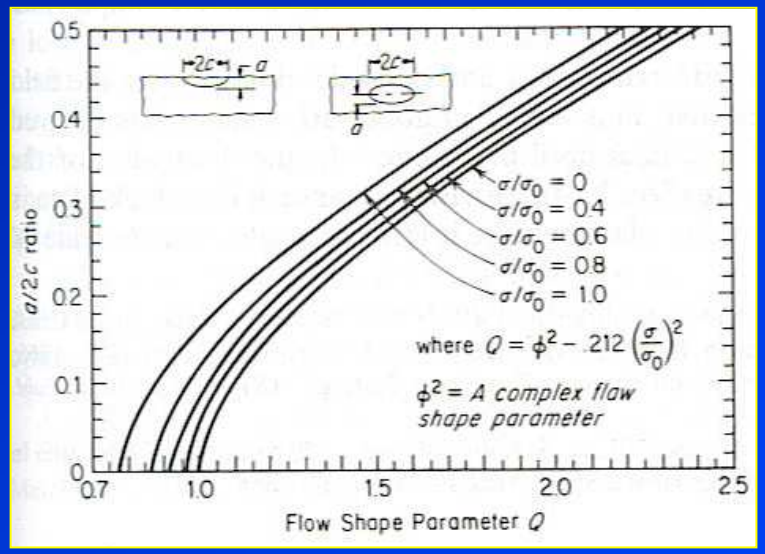

$$\frac{\sigma}{\sigma_0} = \frac{360}{900} = 0.4$$

For a 12 mm wall-thickness, we will find out the critical crack a_c that causes rupture. If **2a=2c**, then **Q** = 2.35.

$$a_c = \frac{K_I^2 Q}{1.21\pi\sigma^2} = \frac{(57)^2(2.35)}{1.21\pi(360)^2} = 15.5mm$$

Note:

a_c (15.5 mm) > wall thickness (12 mm),
→ leak before failure

If the crack is very elongate, e.g., ***a/2c*** *= 0.05, then* ***Q*** *= 1.0, and the critical crack length* a_c *is now 6.6 mm.*

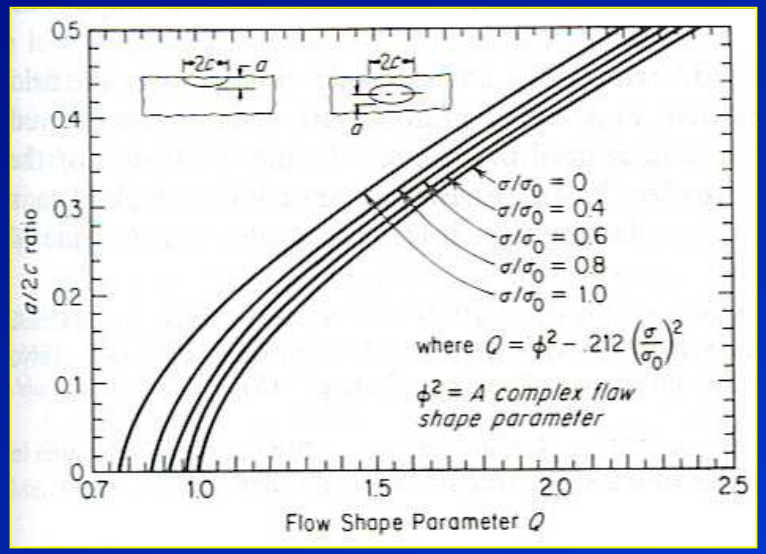

$$a_c = \frac{K_I^2 Q}{1.21\pi\sigma^2} = \frac{(57)^2(1.0)}{1.21\pi(360)^2} = 6.6 \ \ mm$$

In this case the vessel would fracture when the crack had propagated about half-way through the wall thickness

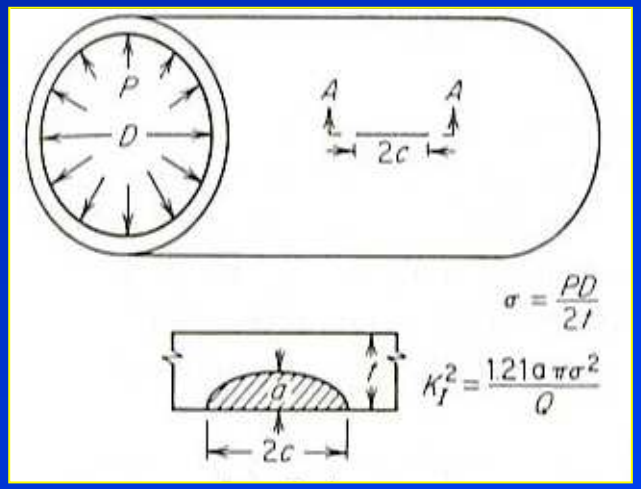

Variables affecting fracture toughness K

- **Metallurgical factors**

- Microstructure, inclusions, impurities
- Composition
- Heat treatment
- Thermo-mechanical processing

- **Test conditions**

-Temperature
- Strain rate
- Specimen thickness

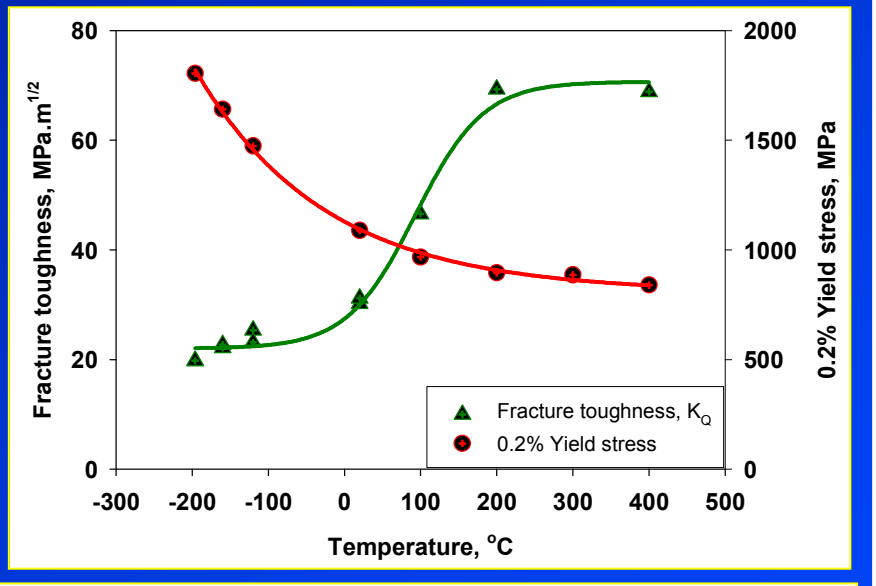

Temp ↓
Strain rate ↑
Specimen thickness ↑

K_{IC} ↓

Plasticity correction

From r → r_p, $\sigma_y > \sigma_o$

- *In reality, yielding occurs and is not allowed in the shaded area.*
- *This is compensated by extending the plastic zone to be larger than r_p.*

*In the presence of a sharp crack, the **plastic zone size** ahead of the **crack tip** varies dependent on the sharpness of the crack tip and the state of stresses.*

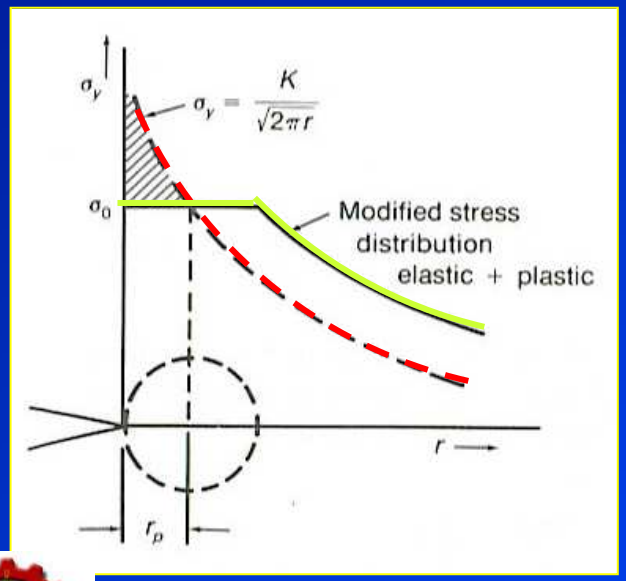

Estimation of plastic zone size

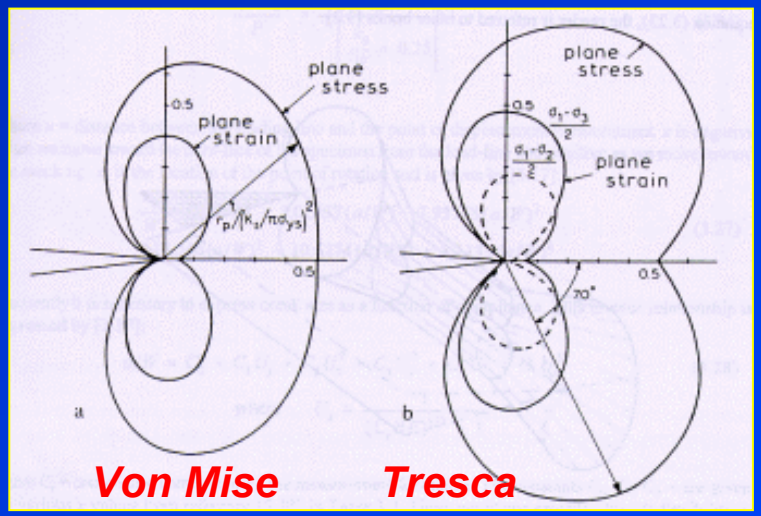

Plastic zone ahead of the crack tip

Plane stress

$$r_p = \frac{1}{2\pi}\frac{K^2}{\sigma_o^2}$$

Eq.12

Plane strain

$$r_p = \frac{1}{6\pi}\frac{K^2}{\sigma_o^2}$$

Eq.13

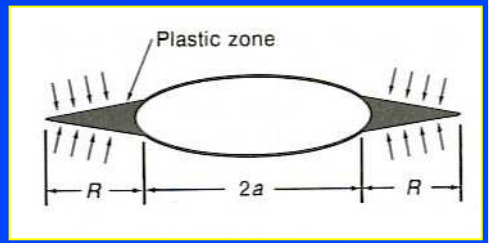

Dugdale's model of plastic zone

Crack tip opening displacement (CTOD)

For materials that exhibit certain extent of plasticity before failure.

The ***crack-tip displacement concept*** considers that the material ahead of the crack contains a series of miniature tensile specimen having a ***gauge length l*** and a ***width w***.

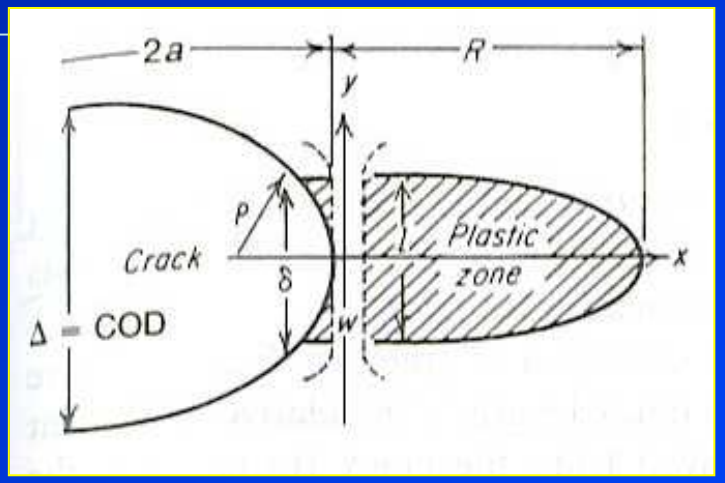

Model of crack-tip displacement

Under stable crack growth

Failure of specimen near the crack tip does not immediately causes failure in the adjacent one. → need to increase the load to further propagate the crack. → controllable → stable.

Under unstable crack growth

Specimen near the crack tip fails first and immediately causes the adjacent one crack further. → occur under decreasing stress.

Determination of CTOD

CTOD, δ, can be determined using the clip gauge which give an indirect measurement of ***displacement at the crack tip*** δ.

Specimen test arrangement

• If the origin of the measurement at the centre of a crack of length ***2a*** then,

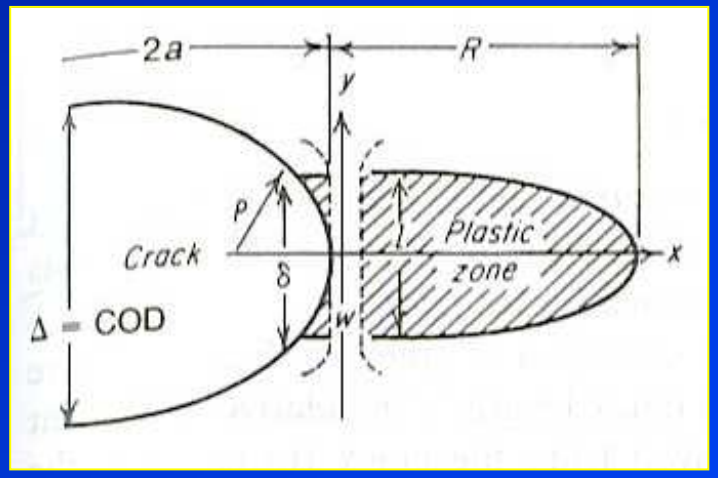

$$CTOD = \delta = \frac{4\sigma}{E}\left(2ar_p\right)^{1/2}$$

Eq.14

Where σ is the applied stress
r_p is the plastic zone size
E is the Young's modulus

J-integral

• ***J-integral*** is a more comprehensive approach to fracture mechanics of ***lower-strength ductile materials***.

• ***J-integral*** can be interpreted as the potential energy difference between two identically loaded specimens having slightly ***different crack lengths***.

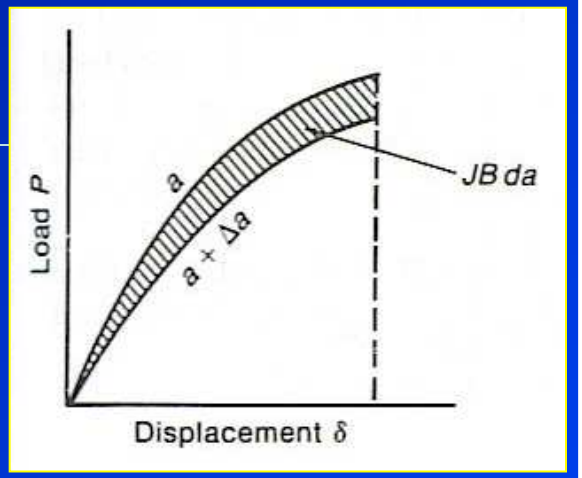

Physical interpretation of the J integral

• Testing is carried out in a similar manner to fracture toughness K_{IC} but using ***a series of identical specimens*** (the multi-specimen approach) or ***a single specimen***.

Three point bend specimen	***Compact tension specimen***
$J = \frac{2A}{Bb}$ *Eq.15*	$J = \frac{2A}{Bb}\left[\frac{(1+\alpha)}{(1+\alpha^2}\right]$ *Eq.16*

$$\alpha = \left[\left(\frac{2a}{b}\right)^2 + 2\left(\frac{2a}{b}\right) + 2\right]^{1/2} - \left(\frac{2a}{b} + 1\right)$$

Eq.17

Where ***A*** = area under load-displacement curve

B = specimen thickness

b = unbroken ligament (***W-a***)

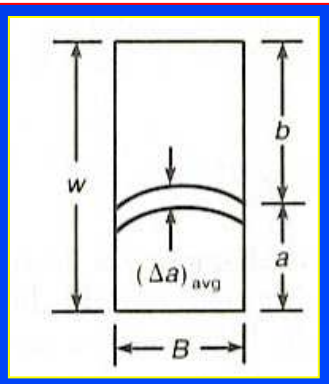

Specimen dimensions

J-integral

J-integral data is represented as a crack-resistance curve, ***J*** vs ***Δa***, *fig (a).*

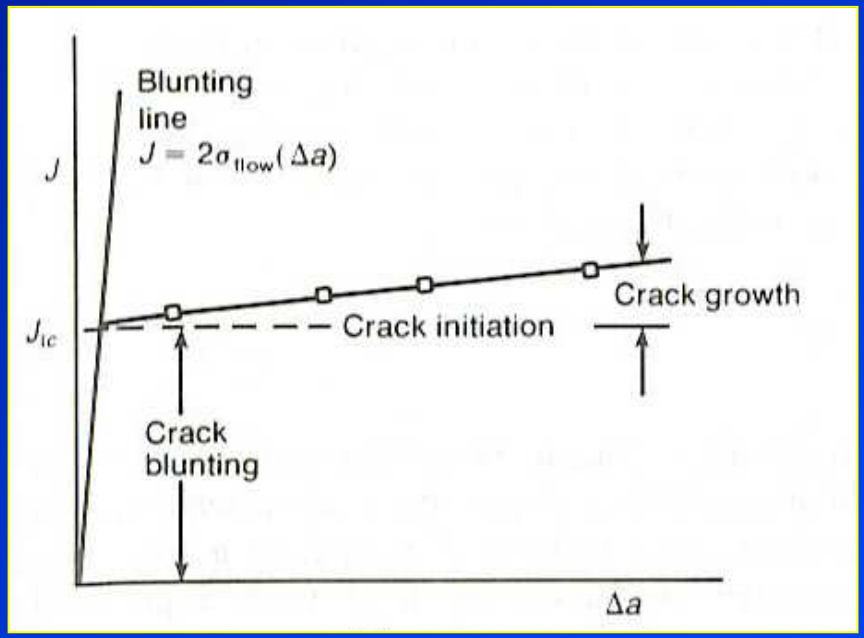

The blunting line is drawn from the origin through the curve where

$$J = 2\sigma_{flow}(\Delta a) \qquad \textit{Eq.18}$$

R-curve

- The ***R curve*** characterises the ***resistance to fracture of a material*** during slow and stable crack propagation as the plastic zone grows as the crack extends from a sharp notch.
- An ***R curve*** is a graphical representation of the ***resistance to crack propagation R*** versus ***crack length a***.

- ***Irwin*** suggested that failure (unstable crack growth) will occur when the rate of change of strain-energy release rate $\partial G / \partial a$ equals the rate of change in resistance to crack growth $\partial R / \partial a$.

$$\frac{\partial G}{\partial a} = \frac{\partial R}{\partial a} \qquad \textit{Eq.19}$$

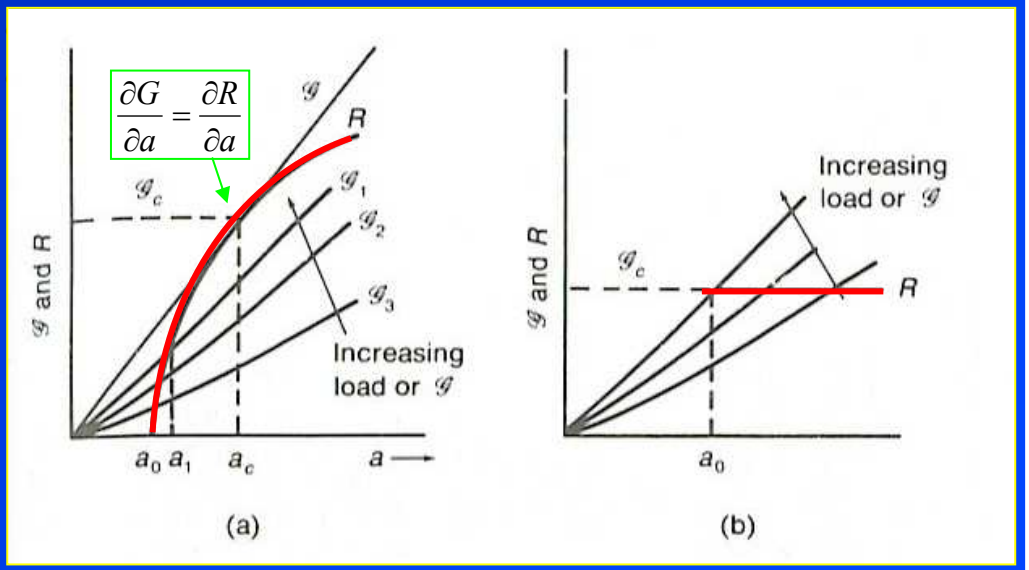

(a) R-curve for a ductile material,
(b) R-curve for a brittle material.

Probabilistic aspects of fracture mechanics

• ***Failures of brittle materials*** normally give ***a high variability of results*** which requires statistic analysis.

Ex: The fracture stress values can be achieved at different values.

• If specimen is divided into small elements each having a crack of different sizes, the strength of the material is determined by the element with the ***longest crack*** (***weakest-link concept***) not by the average values of the distribution of ***flaws***.

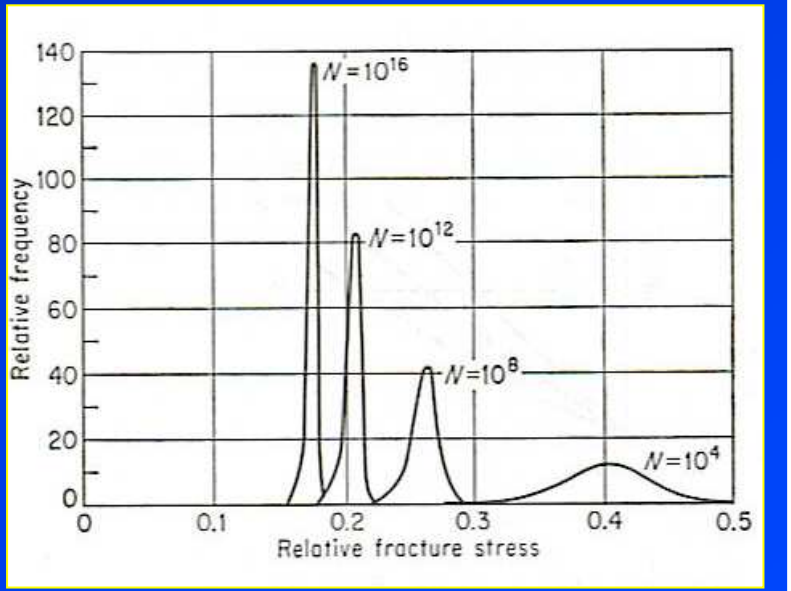

Calculated frequency distribution of fracture stress as a function of number of cracks N

*The initial crack size must be assumed to be the **largest crack size** that can be expected to be undetected by non destructive inspection and the fracture toughness might be assumed to be the **lowest possible value** to be expected in the material.*

Toughness of materials

The role of metallurgical variables on toughness of materials.

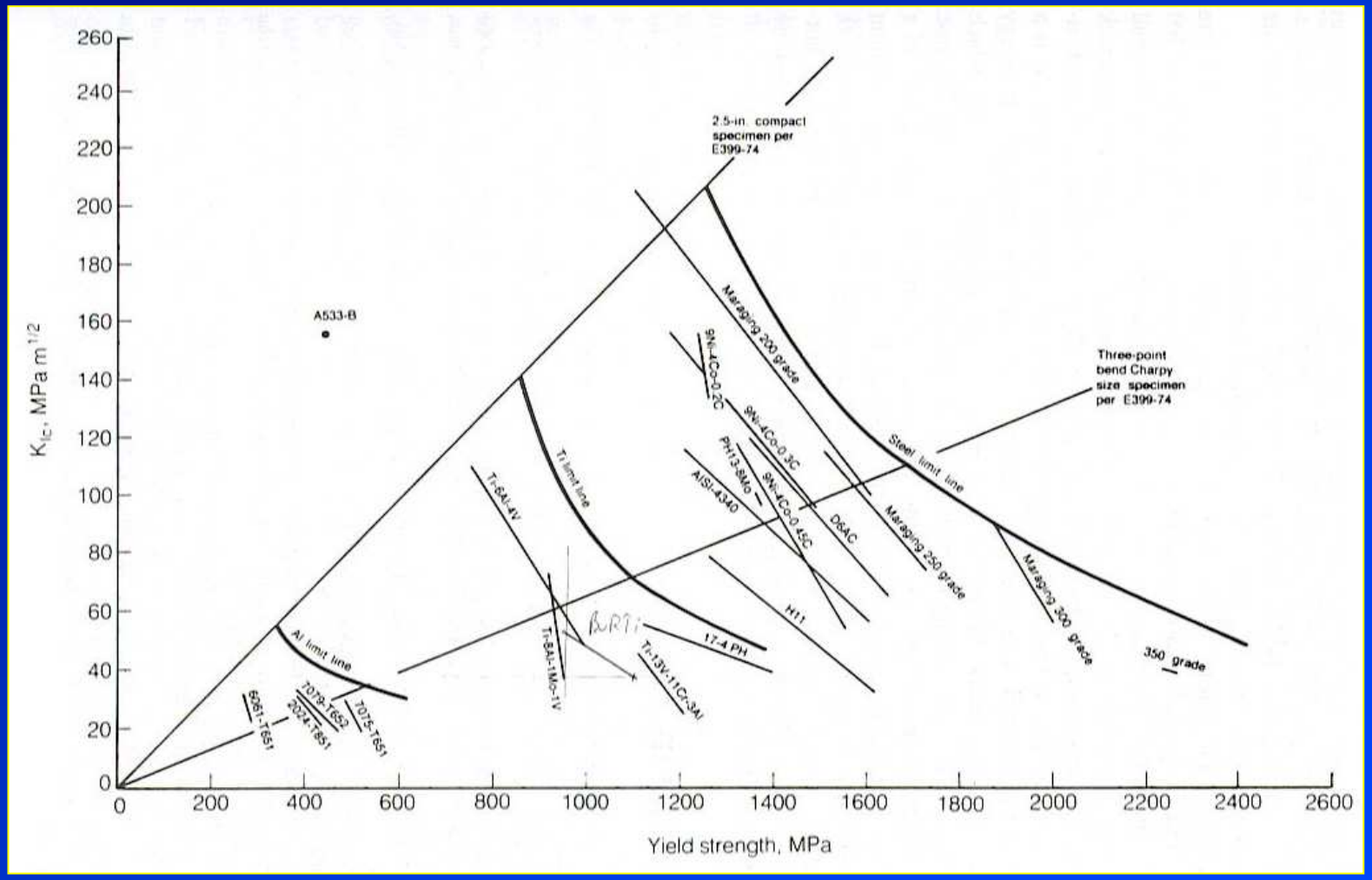

Strength ↑ **Toughness** ↓

Toughness of materials

To obtain material with high toughness

- ***Small and rounded particles → reduce pileup stress.***
- ***Should be widely spaced → proper volume fraction.***
- ***Inclusions should be avoid, or large widely spaced inclusions are less damaging.***
- ***Fine grain size → minimise dislocation pileup stress.***
- ***High crack deflection → more energy absorb during fracture.***

References

- Dieter, G.E., ***Mechanical metallurgy***, 1988, SI metric edition, McGraw-Hill, ISBN 0-07-100406-8.
- Sanford, R.J., ***Principles of fracture mechanics***, 2003, Prentice Hall, New Jersey, ISBN 0-13-092992-1.

Fatigue of metals

Subjects of interest

- *Objectives / Introduction*
- *Stress cycles*
- *The S-N curve*
- *Cyclic stress-strain curve*
- *Low cycle fatigue*
- *Structural features of fatigue*
- *Fatigue crack propagation*
- *Factors influencing fatigue properties*
- *Design for fatigue*

Objectives

- This chapter provides fundamental aspects of fatigue in metals and the significance of fatigue failure.
- Different approaches for the assessment of fatigue properties, i.e., fatigue S-N curve and fatigue crack growth resistance will be introduced.
- Discussion will be made on factors influencing fatigue properties of metals, for example, mean stress, stress concentration, temperature
- Finally design against fatigue failure will be highlighted.

Introduction

Fatigue failure in a bolt

Fatigue initiation

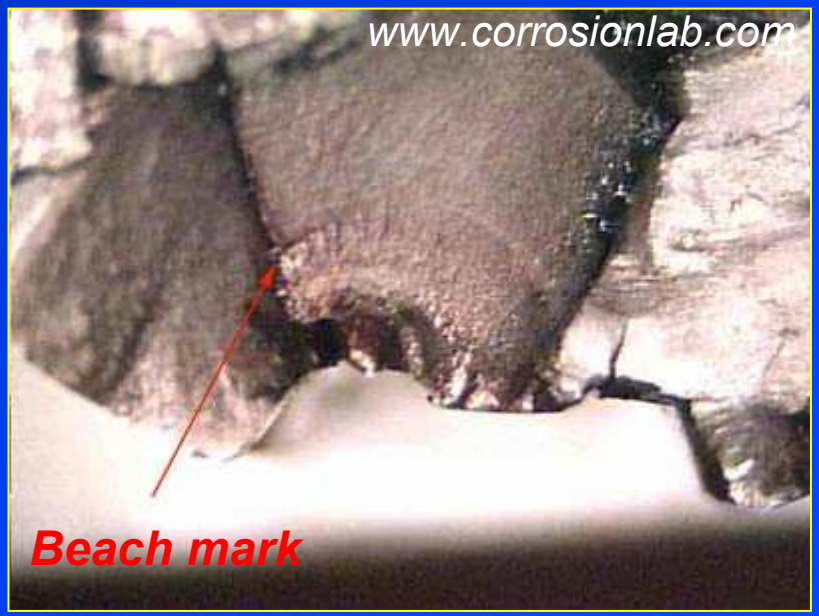

Introduction

Fatigue failure occurs at the outer rim of the wheel

Fatigue fracture area in a shaft caused by corroded inside area

Introduction

Fatigue failures are widely studies because it accounts for 90% of all service failures due to mechanical causes.

Characteristics

- Fatigue failures occur when metal is subjected to a ***repetitive or fluctuating stress*** and will fail at a ***stress much lower than its tensile strength***.
- Fatigue failures occur without any ***plastic deformation*** (no warning).
- Fatigue surface appears as a smooth region, showing ***beach mark*** or origin of fatigue crack.

Failure of crankshaft journal

Fatigue failure of a bolt

Factors causing fatigue failure

Basic factors

1) *A maximum tensile stress of sufficiently high value.*
2) *A large amount of variation or fluctuation in the applied stress.*
3) *A sufficiently large number of cycles of the applied stress.*

Additional factors

- Stress concentration
- Corrosion
- Temperature
- Overload
- Metallurgical structure
- Residual stress
- Combined stress

Stress cycles

Different types of fluctuating stress

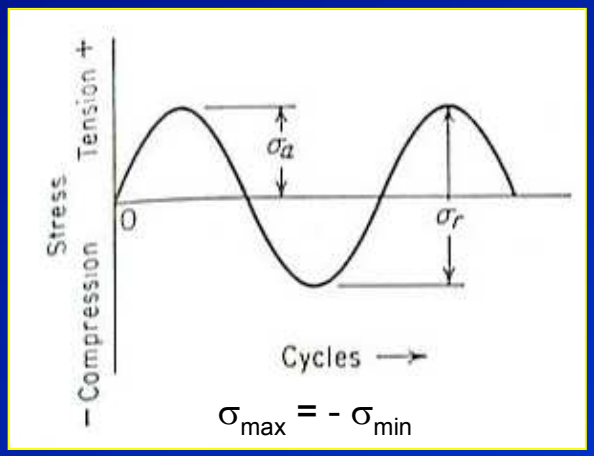

(a) Completely reversed cycle of stress (sinusoidal)

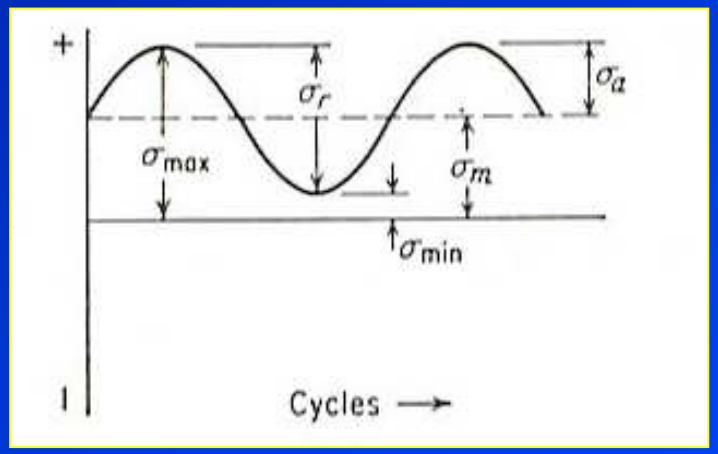

(b) Repeated stress cycle

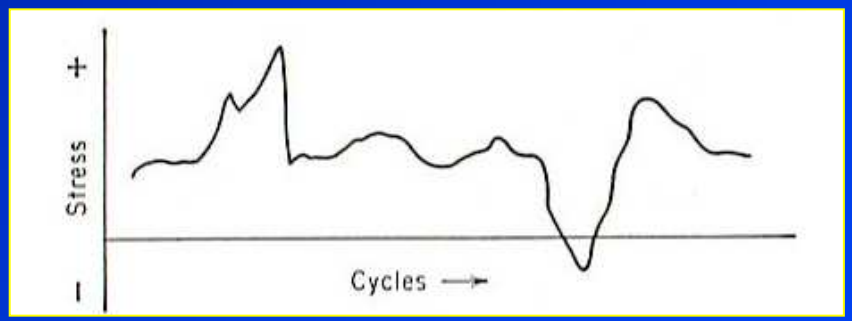

(c) Irregular or random stress cycle

Tensile stress +

Compressive stress -

Stress cycles

Nomenclature of stress parameter in fatigue loading

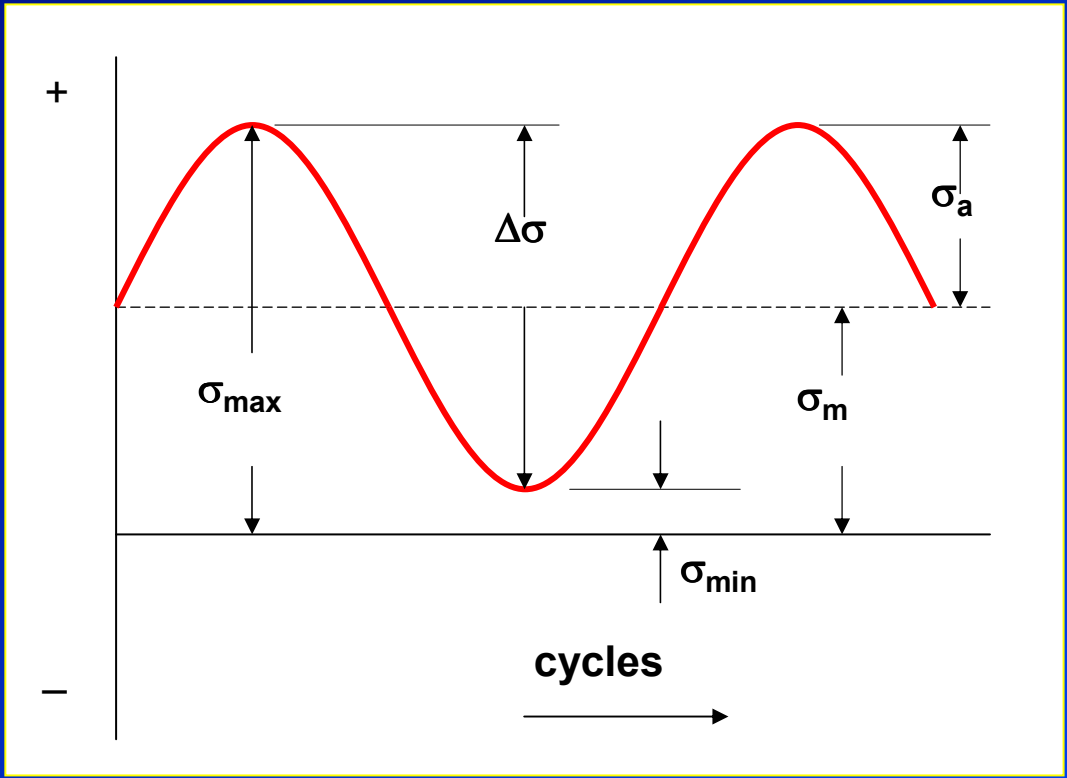

Fatigue stress cycle

Maximum stress, σ_{max}

Minimum stress, σ_{min}

Stress range

$$\Delta\sigma \ \ or \ \ \sigma_r = \sigma_{\max} - \sigma_{\min} \qquad \textit{Eq.1}$$

Alternating stress

$$\sigma_a = \frac{\Delta\sigma}{2} = \frac{\sigma_{\max} - \sigma_{\min}}{2} \qquad \textit{Eq.2}$$

Mean stress

$$\sigma_m = \frac{\sigma_{\max} + \sigma_{\min}}{2} \qquad \textit{Eq.3}$$

Stress ratio

$$R = \frac{\sigma_{\min}}{\sigma_{\max}} \qquad \textit{Eq.4}$$

Amplitude ratio

$$A = \frac{\sigma_a}{\sigma_m} = \frac{1-R}{1+R} \qquad \textit{Eq.5}$$

The S-N curve

- ***Engineering fatigue data*** is normally represented by means of ***S-N curve***, a plot of ***stress S*** against the ***number of cycle***, ***N***.
- *Stress can be* → σ_a, σ_{max}, σ_{min}
- σ_m , ***R or A*** *should be mentioned.*

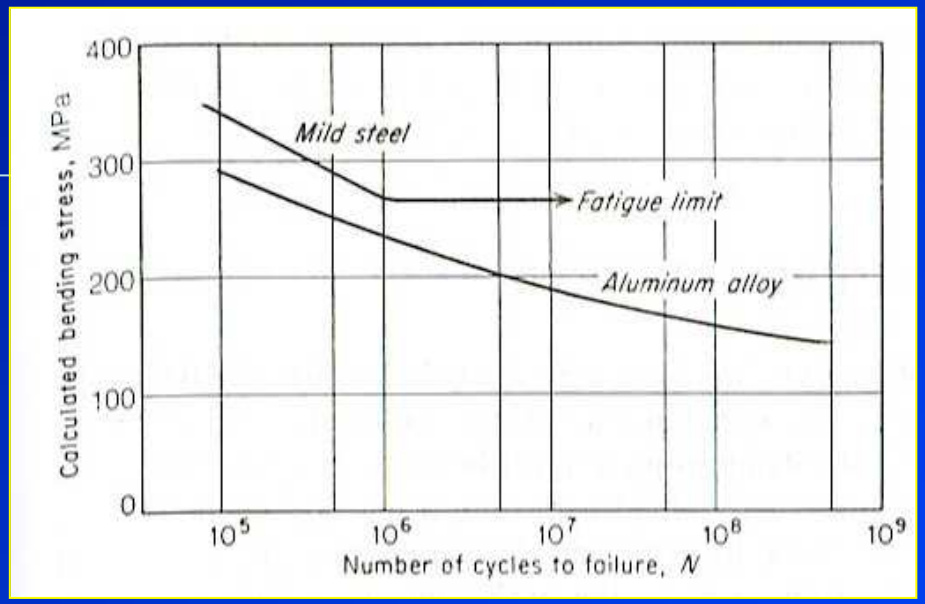

Typical fatigue curves

- ***S-N curve*** is concerned chiefly with ***fatigue failure at high numbers of cycles*** (N > 10^5 cycles) → high cycle fatigue (***HCF***).
- ***N*** < 10^4 or 10^5 cycles → low cycle fatigue (***LCF***).
- ***N*** increases with decreasing ***stress level***.
  - ***Fatigue limit or endurance limit*** is normally defined at 10^7 or 10^8 cycles. Below this limit, the material presumably can endure an infinite number of cycle before failure.
  - ***Nonferrous metal***, i.e., aluminium, do not have ***fatigue limit*** → fatigue strength is defined at ~ 10^8 cycles.

Basquin equation

• The ***S-N curve*** in the ***high-cycle region*** is sometimes described by the ***Basquin equation***

$$N\sigma_a^p = C \qquad \textit{Eq.6}$$

Where σ_a is the stress amplitude
p and ***C*** are empirical constants

HCF High cycle (low strain) fatigue

LCF Low cycle (high strain) fatigue

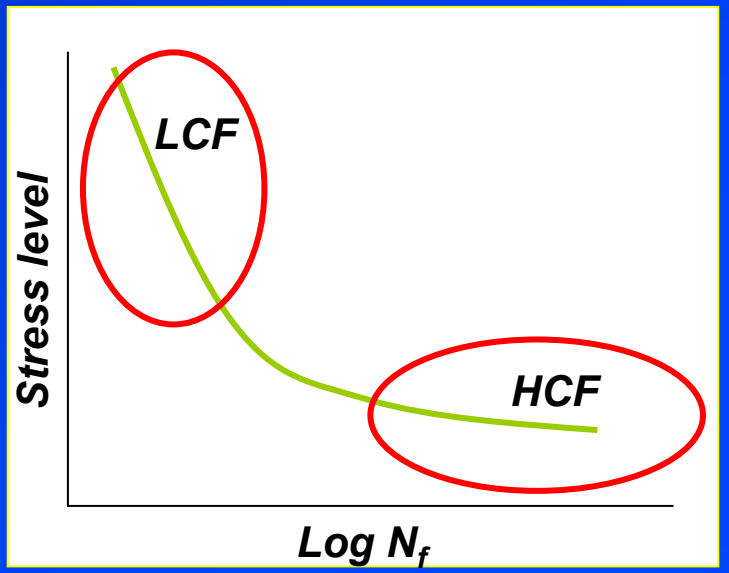

Construction of S-N curve

- The construction of ***S-N curve*** normally requires ~ 8-12 specimens by first testing at a high level of stress ~ 2/3 of the tensile strength of the material.
- The test is then carried out at lower levels of stress until ***runout***.

- The data obtained is normally ***scattered*** at the same stress level by using several specimens.
- This requires ***statistic approach*** to define the ***fatigue limit***.

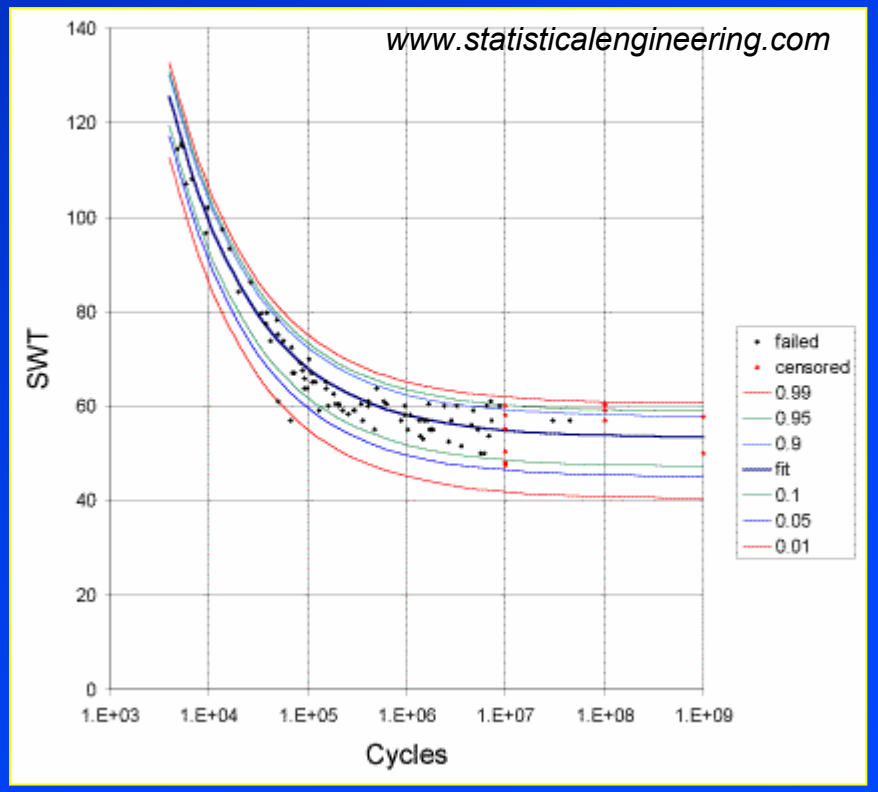

S-N fatigue curve

Statistical nature of fatigue

- Because the ***S-N fatigue data*** is normally scattered, it should be therefore represented on a ***probability basis***.
- Considerable number of specimens are used to obtain statistical parameters.
- At σ_1, 1% of specimens would be expected to fail at N_1 cycles.
- 50% of specimens would be expected to fail at N_2 cycles.

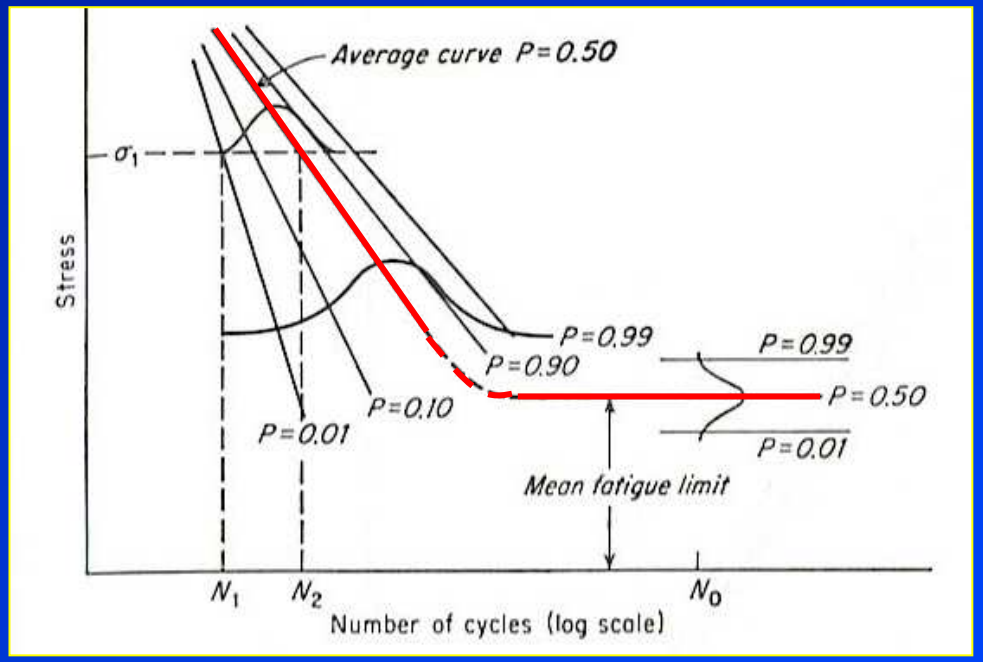

Fatigue data on a probability basis

Note: The S-N fatigue data is more scattered at lower stress levels. Each specimen has its own fatigue limit.

- For ***engineering purposes***, it is sufficiently accurate to assume ***a logarithmic normal distribution of fatigue life*** in the region of the probability of failure of P = 0.10 to P = 0.90.

Effect of mean stress, stress range and stress intensity (notch) on S-N fatigue curve

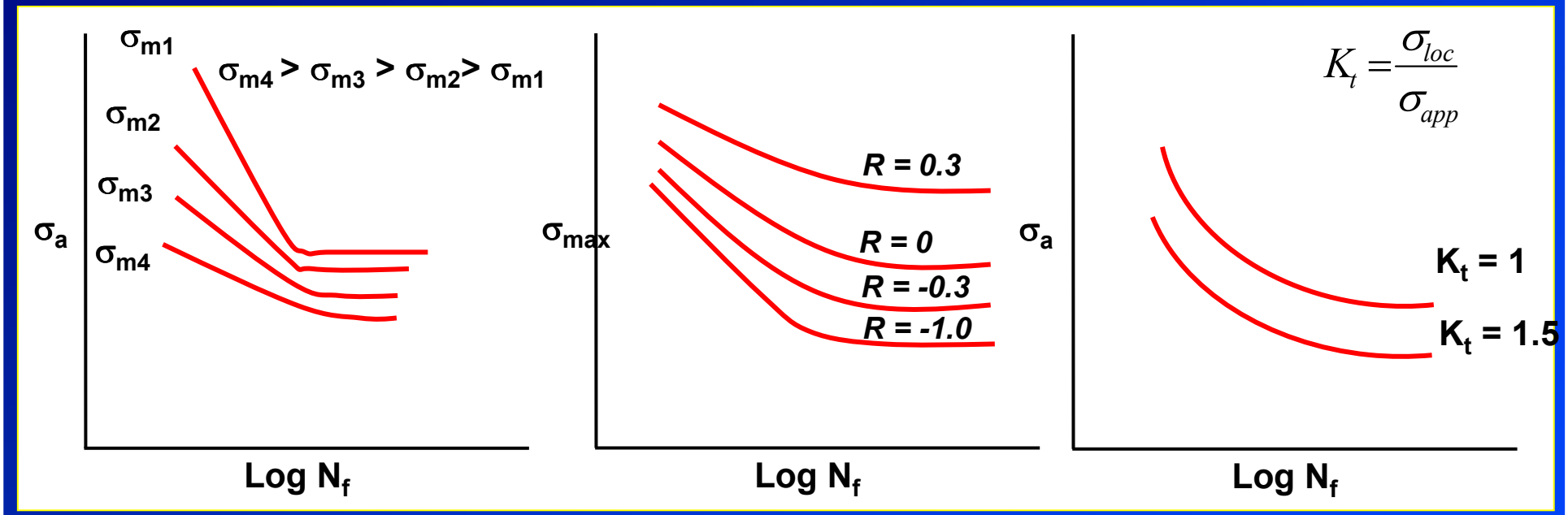

Mean stress ↑ **Fatigue strength** ↓

Stress range ↑ **Fatigue strength** ↓

Stress intensity ↑ **Fatigue strength** ↓

Goodman diagram

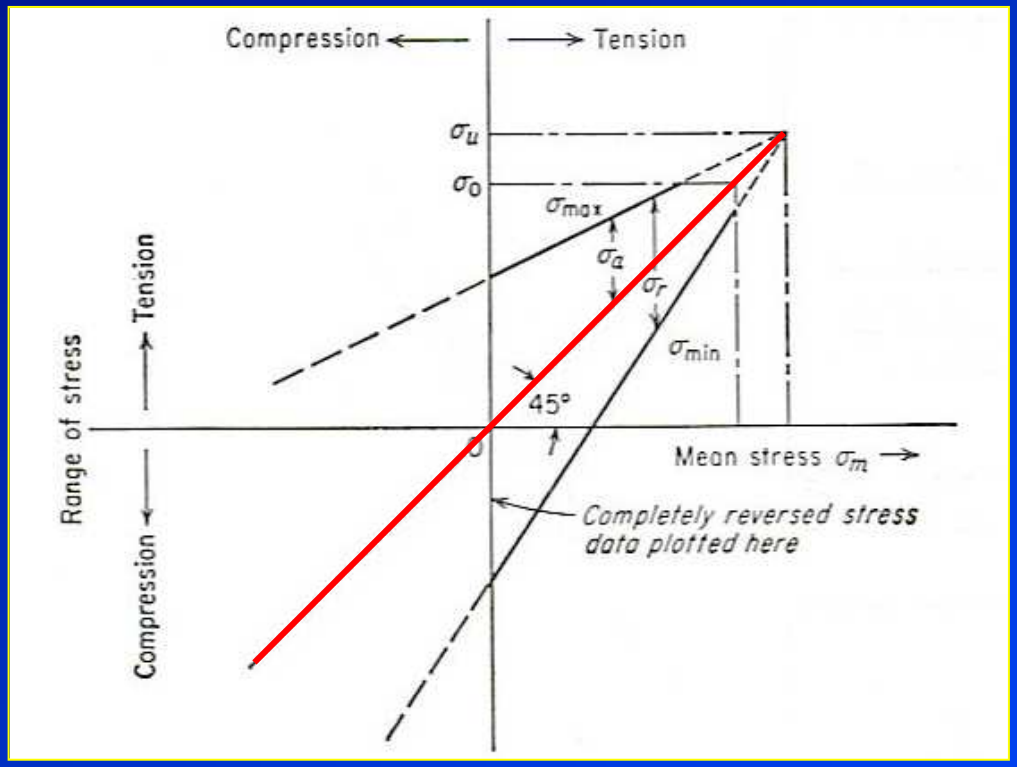

Goodman diagram

- ***Goodman diagram*** shows the variation of the limiting range of stress (σ_{max} - σ_{min}) on mean stress.
- As the ***mean stress*** becomes more tensile the ***allowable range of stress*** is reduced.
- At tensile strength, σ_u , the stress range is zero.

Haig-Solderberg diagram

- In ***Haig-Solderberg diagram*** is a plot of alternating stress σ_a and mean stress σ_m.
- The Goodman relationship may be expressed by

$$\sigma_a = \sigma_e \left[1 - \left(\frac{\sigma_m}{\sigma_u} \right)^x \right] \qquad \textit{Eq.7}$$

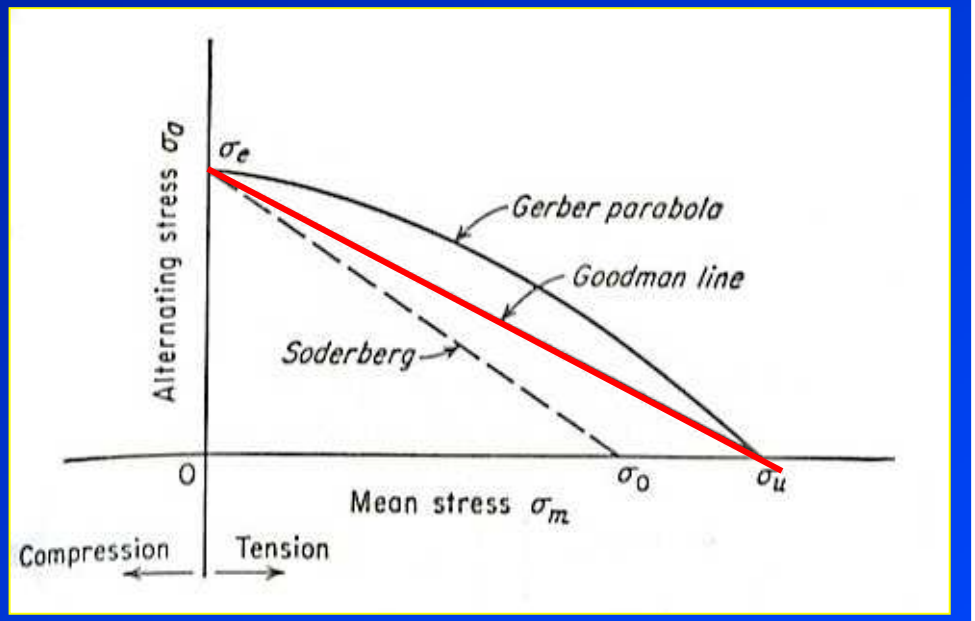

Haig-Solderberg diagram

Where ***x*** = 1 for the Goodman line,
x = 2 for the Gerber parabola,
σ_e = the fatigue limit for completely reversed loading.

- If the design is based on the ***yield strength*** σ_o, (based on ***Solderberg line***), then the σ_u is replaced by σ_o in this equation.

Master diagram for establishing influence of mean stress in fatigue

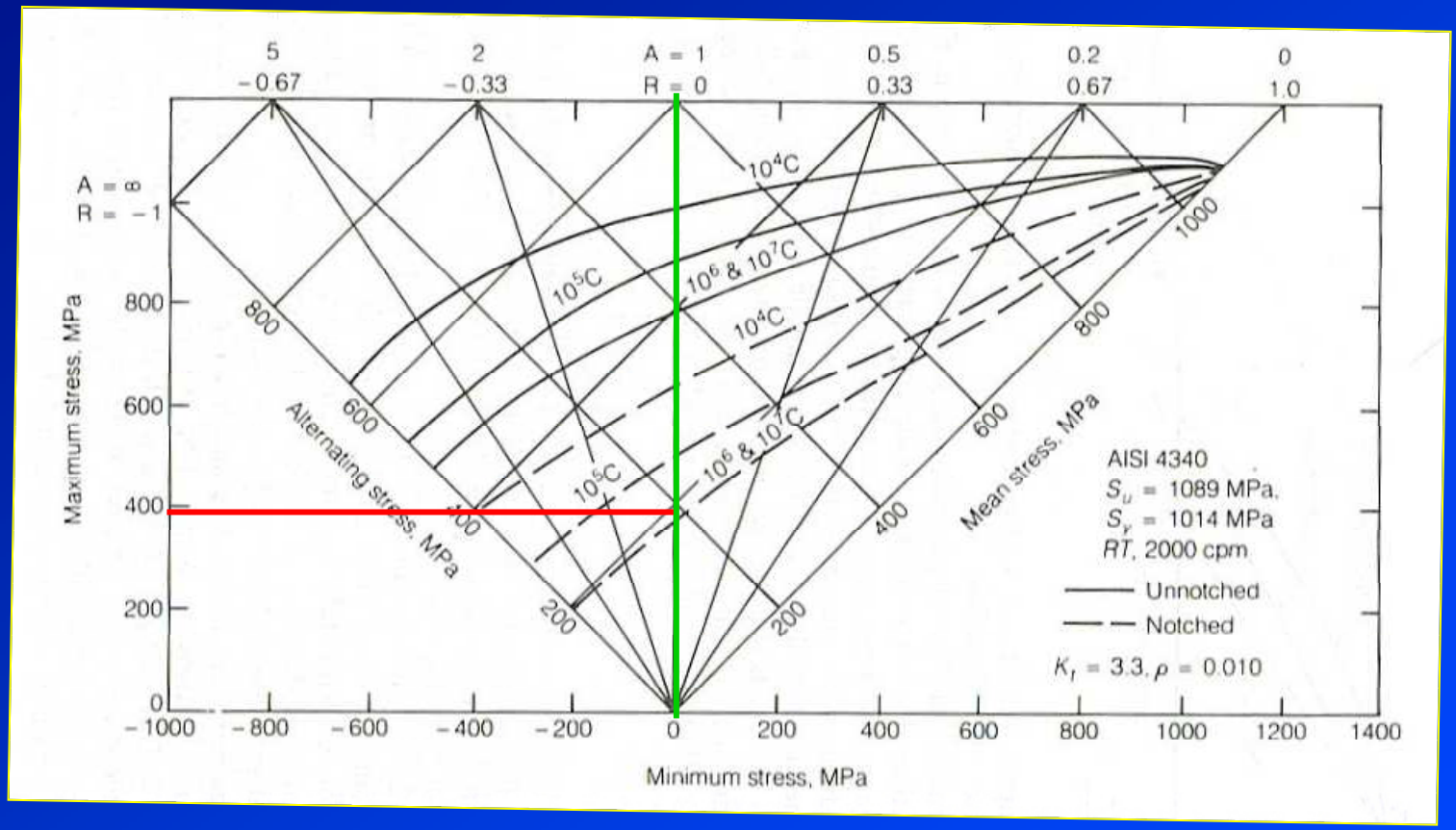

Ex: at σ_{max} = 400 MPa, σ_{min} = 0, a fatigue limit of the notched specimen is less than 10^6 cycles.

For the unnotched specimen is below the fatigue limit.

Example: *A 4340 steel bar is subjected to a fluctuating axial load that varies from a maximum of 330 kN tension to a minimum of 110 kN compression. The mechanical properties of the steel are:*

σ_u = 1090 MPa, σ_o = 1010 MPa, σ_e = 510 MPa

Determine the bar diameter to give infinite fatigue life based on a safety factor of 2.5.

Cylindrical cross section of the bar = ***A***, the variation of stress will be

$$\sigma_{\max} = \frac{0.330}{A} MPa, \quad \sigma_{\min} = -\frac{0.110}{A} MPa$$

$$\sigma_{mean} = \frac{\sigma_{\max} + \sigma_{\min}}{2} = \frac{0.330/A + (-0.110/A)}{2} = \frac{0.110}{A} MPa$$

$$\sigma_a = \frac{\sigma_{\max} - \sigma_{\min}}{2} = \frac{0.330/A - (-0.110/A)}{2} = \frac{0.220}{A} MPa$$

Using the ***conservative Goodman line*** and *Eq.7*.

$$\sigma_a = \sigma_e\left(1 - \frac{\sigma_m}{\sigma_u}\right), \quad \sigma_e = \frac{510}{2.5} = 204 \ MPa$$

$$\frac{0.220/A}{204} = 1 - \frac{0.110/A}{1090}$$

$$A = 1179 \ mm^2$$

$$D = \sqrt{\frac{4A}{\pi}} = 38.7 \ mm$$

Cyclic stress-strain curve

- Cyclic strain controlled fatigue occurs when the strain amplitude is held constant during cycling.
- Found in ***thermal cycling*** where a component expands and contracts in response to fluctuations in the operating temperature or in reversed bending between fixed displacements.

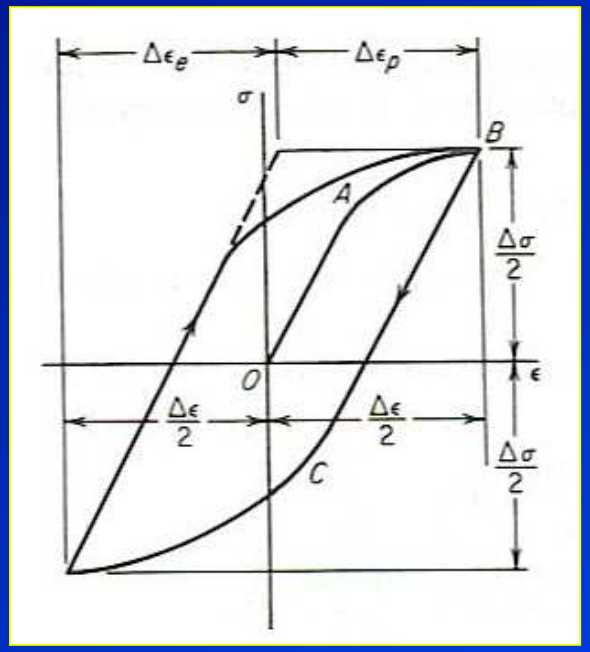

Stress strain loop for constant strain cycling

- During the initial loading, the stress-strain curve is ***O-A-B***.
- Yielding begins on unloading in compression at a lower stress ***C*** due to the ***Bauschinger effect***.
- A ***hysteresis loop*** develops in reloading with its dimensions of width, $\Delta\varepsilon$ and height $\Delta\sigma$.
- The ***total strain range*** $\Delta\varepsilon$ consists of the elastic strain component plus the plastic strain component.

$$\Delta\varepsilon = \Delta\varepsilon_e + \Delta\varepsilon_p \qquad \textit{Eq.8}$$

Cyclic hardening and cyclic softening

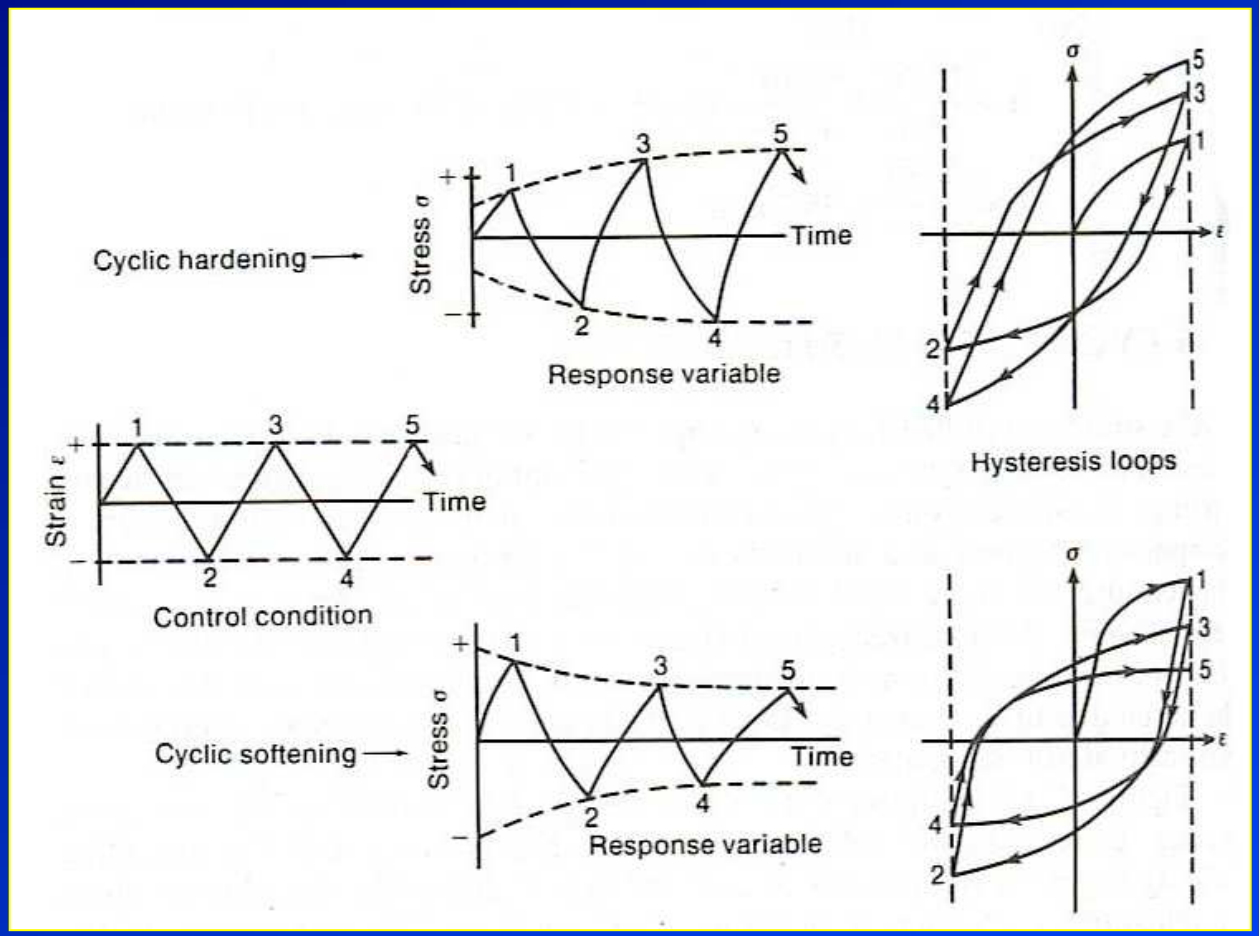

- ***Cyclic hardening*** would lead to a decreasing peak strain with increasing cycles. (***n>0.15***)
- ***Cyclic softening*** would lead to a continually increasing strain range and early fracture. (***n<0.15***)

Comparison of monotonic and cyclic stress-strain curves of cyclic hardened materials

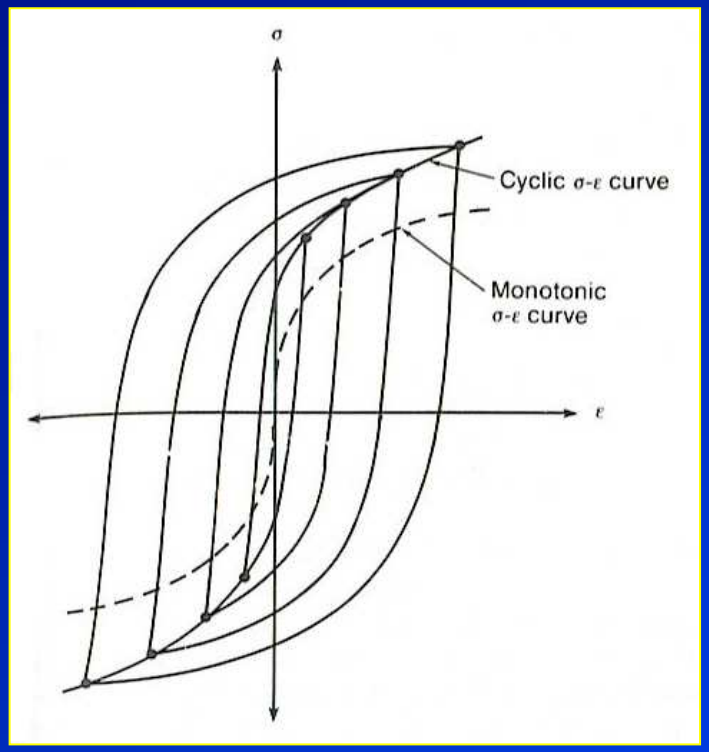

Monotonic and cyclic stress-strain curves

• The cycle stress-strain curve may be described by a power curve as follows

$$\Delta\sigma = K'\left(\Delta\varepsilon_p\right)^{n'} \qquad \textit{Eq.9}$$

Where ***n'*** is the cyclic strain-hardening exponent

K' is the cyclic strength coefficient

Since strain amplitude

$$\frac{\Delta\varepsilon}{2} = \frac{\Delta\varepsilon_e}{2} + \frac{\Delta\varepsilon_p}{2}$$

$$\frac{\Delta\varepsilon}{2} = \frac{\Delta\sigma}{2E} + \frac{1}{2}\left(\frac{\Delta\sigma}{K'}\right)^{1/n'}$$

For metals ***n'*** varies between 0.10 -0.20.

Low cycle fatigue

• ***Low cycle fatigue*** (***LCF***) (high strain) is concerned about fatigue failure at relatively ***high stress*** and ***low numbers of cycles*** to failure.

• ***Ex:*** in the nuclear pressure vessels, steam turbines and power machinery. Usually concerned with ***cyclic strain*** rather than ***cyclic stress***.

• ***LCF*** data is normally present as a plot of strain range $\Delta\varepsilon_p$ against ***N***.

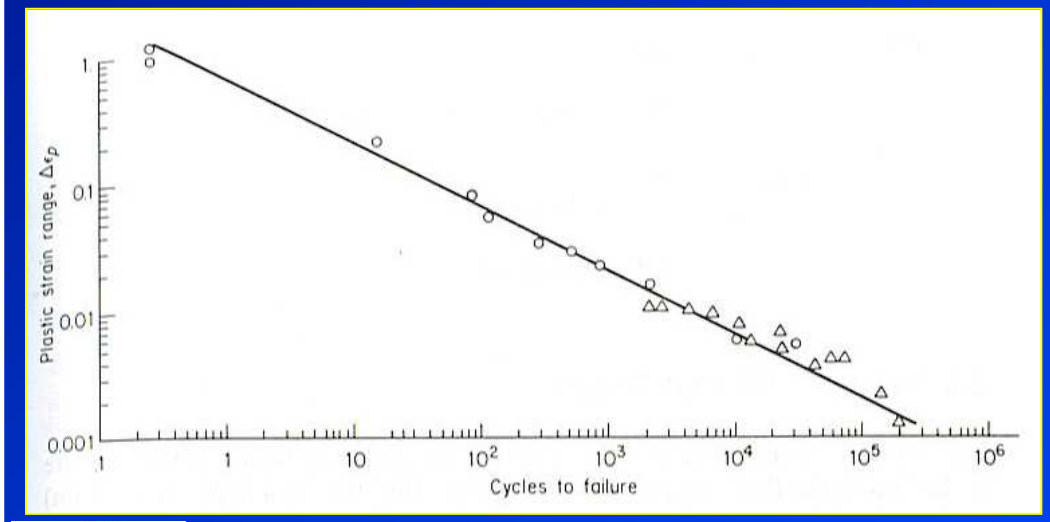

Low-cycle fatigue curve ($\Delta\varepsilon_p$ vs. N).

• On the log scale, this relation can be best described by

$$\frac{\Delta\varepsilon_p}{2} = \varepsilon'_f (2N)^c \qquad \textit{Eq.10}$$

Where

$\Delta\varepsilon_p/2$ = plastic strain amplitude

ε'_f = fatigue ductility coefficient

$2N$ = number of strain reversals to failure.

c = fatigue ductility exponent varies between -0.5 to -0.7.

Example: *For the cyclic stress-strain curve, σ_B =75 MPa and ε_B = 0.000645. If ε_f = 0.30 and **E** = 22x10⁴ MPa.*

Determine

(a) $\Delta\varepsilon_e$ and $\Delta\varepsilon_p$

$$\Delta\varepsilon_e = \frac{\Delta\sigma}{E} = \frac{2(75)}{22\times10^4} = 6.818\times10^{-4}$$

$$\Delta\varepsilon_p = \Delta\varepsilon - \Delta\varepsilon_e = (2\times0.000645) - 0.0006818 = 6.082\times10^{-4}$$

(b) The number of cycles to failure.

From the Coffin-Manson relation

$$\frac{\Delta\varepsilon_p}{2} = \varepsilon_f'(2N)^c$$

If **c** = -0.6 and $e_f \sim e'_f$

$$\frac{6.082\times10^{-4}}{2} = 0.30(2N)^{-0.6}$$

$$N = 49{,}000 \ \ cycles$$

Strain-life equation

• For the ***high-cycle (low strain) fatigue*** (***HCF***) regime, where the nominal strains are elastic, ***Basquin's equation*** can be reformulated to give

$$\sigma_a = \frac{\Delta\varepsilon_e}{2} E = \sigma_f' (2N)^b$$

Eq.11

$$\frac{\Delta\varepsilon}{2} = \frac{\Delta\varepsilon_e}{2} + \frac{\Delta\varepsilon_p}{2}$$

$$\frac{\Delta\varepsilon}{2} = \frac{\sigma_f'}{E}(2N)^b + \varepsilon_f'(2N)^c$$

Where
- σ_a = alternate stress amplitude
- $\Delta\varepsilon_e/2$ = elastic strain amplitude
- ***E*** = Young's modulus
- σ_f' = fatigue strength coefficient defined by the stress intercept at 2N=1.
- ***2N*** = number of load reversals to failure (N = number of cycles to failure)
- ***b*** = fatigue strength exponent, which varies between –0.05 and -0.12 for most metals.

Fatigue strain-life curve

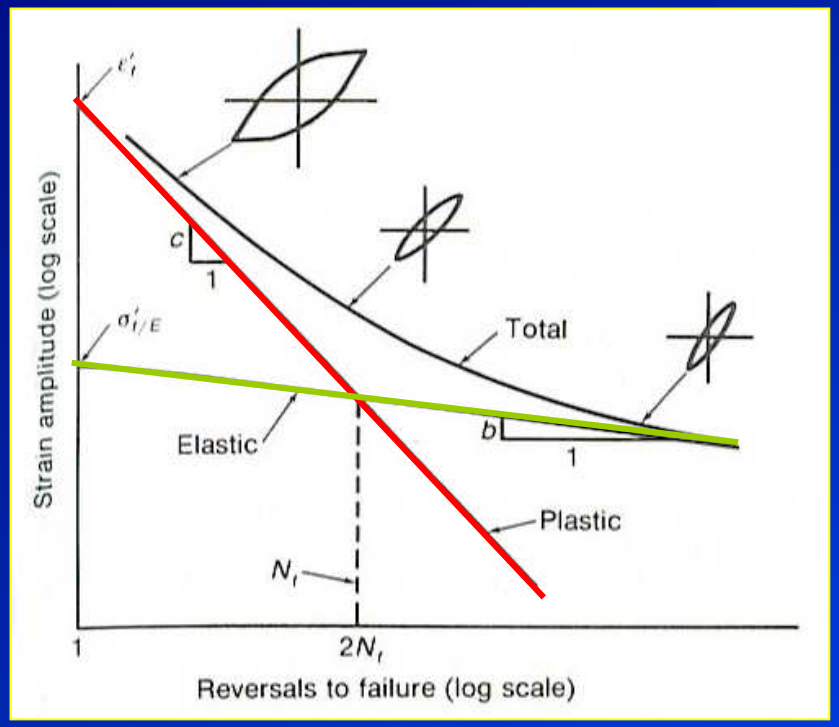

Ductile materials

➡ High cyclic strain condition

Strong materials

➡ Low cyclic strain condition

The fatigue life value at which this ***transition*** occurs is

$$2N_t = \left(\frac{\varepsilon_f' E}{\sigma_f'} \right)^{1/(b-c)}$$

Eq.12

The fatigue strain-life curve

- tends toward the plastic curve at large total strain amplitudes
- tends toward the elastic curve at small total strain amplitudes.

Structural features of fatigue

The fatigue process can be divided into the following processes;

1) ***Crack initiation:*** the early development of fatigue damage (can be removed by a suitable thermal anneal).
2) ***Slip band crack growth:*** the deepening of the initial crack on plane of high shear stress (stage I crack growth)
3) ***Crack growth on planes of high tensile stress:*** growth of well-defined crack in direction normal to maximum tensile stress
4) ***Ultimate ductile failure:*** occurs when the crack reaches sufficient length so that the remaining cross section cannot support the applied load.

Initiation of fatigue crack and slip band crack growth (stage I)

• ***Fatigue cracks*** are normally initiated at a ***free surface***. ***Slip lines*** are formed during the first few thousand cycles of stress.

• Back and forth fine slip movements of fatigue could build up notches or ridges at the surface. → act as ***stress raiser*** → initiate ***crack***.

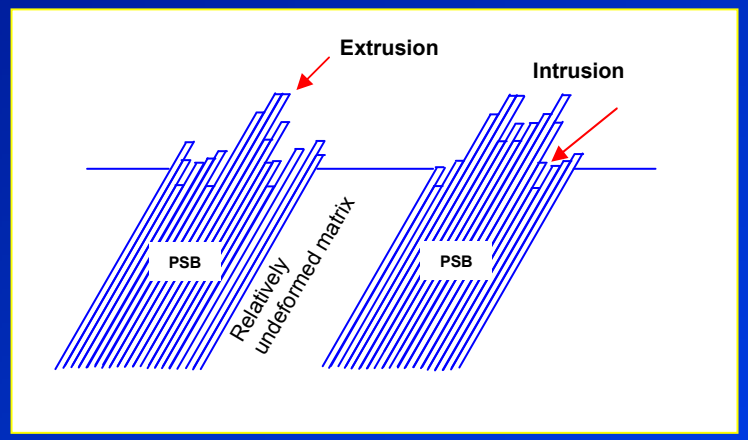

Model for fatigue initiation by extrusions and intrusions caused by cyclic slip during fatigue loading.

• In ***stage I***, the fatigue crack tends to propagate initially along slip planes (***extrusion*** and ***intrusion*** of ***persistent slip bands***) and later take the direction normal to the maximum tensile stress (***stage II***).

• The crack propagation rate in ***stage I*** is generally very low on the order of nm/cycles → giving ***featureless surface***.

Stable crack growth (stage II)

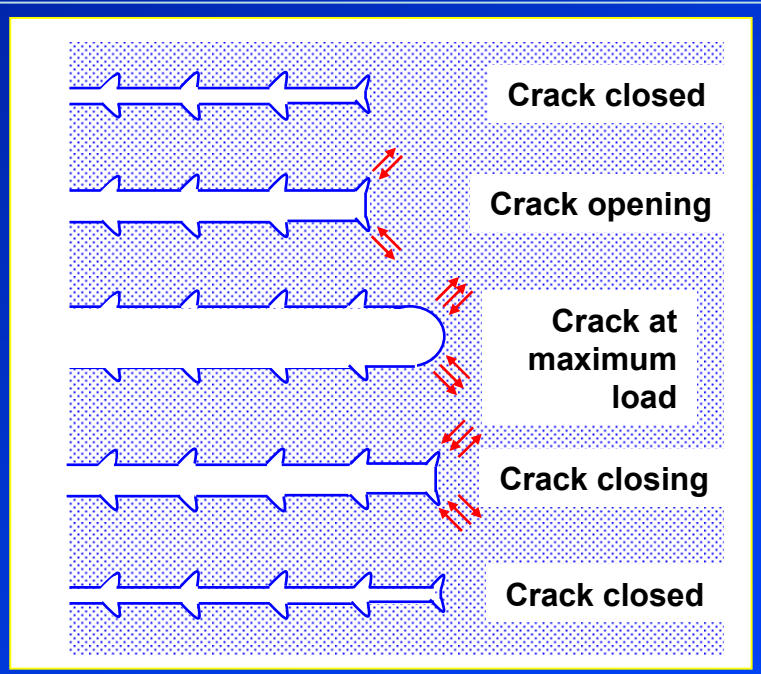

Plastic blunting model of fatigue striation

- The fracture surface of stage II crack propagation frequently shows a pattern of ripples or ***fatigue striations***.
- Each ***striation*** is produced by ***a single stress cycle*** and represents the successive position of an advancing crack front normal to the greatest tensile stress.

- ***Crack tip blunting*** occurs during ***tensile load*** at 45° and crack grows longer by ***plastic shearing***.
- ***Compression load*** reverses the slip direction in the end zones → crushing the crack surface to form a ***resharpened crack tip***.

Fatigue crack propagation

Fatigue crack propagation

- **Stage I** — Non-propagating fatigue crack (~0.25nm/cycle)
- **Stage II** — Stable fatigue crack propagation- widely study
- **Stage III** — Unstable fatigue crack propagation → failure

• For ***design against fatigue failure***, fracture mechanics is utilised to monitor ***the fatigue crack growth rate*** in the ***stage II*** Paris regime.

Eq.13

$$\frac{da}{dN} = A(\Delta K)^m$$

• Where the ***fatigue crack growth rate da/dN*** varies with ***stress intensity factor range ΔK***, which is a function of ***stress range Δσ*** and ***crack length a***.

Eq.14

$$\Delta K = K_{\max} - K_{\min}$$

$$\Delta K = \sigma_{\max}\sqrt{\pi a} - \sigma_{\min}\sqrt{\pi a}$$

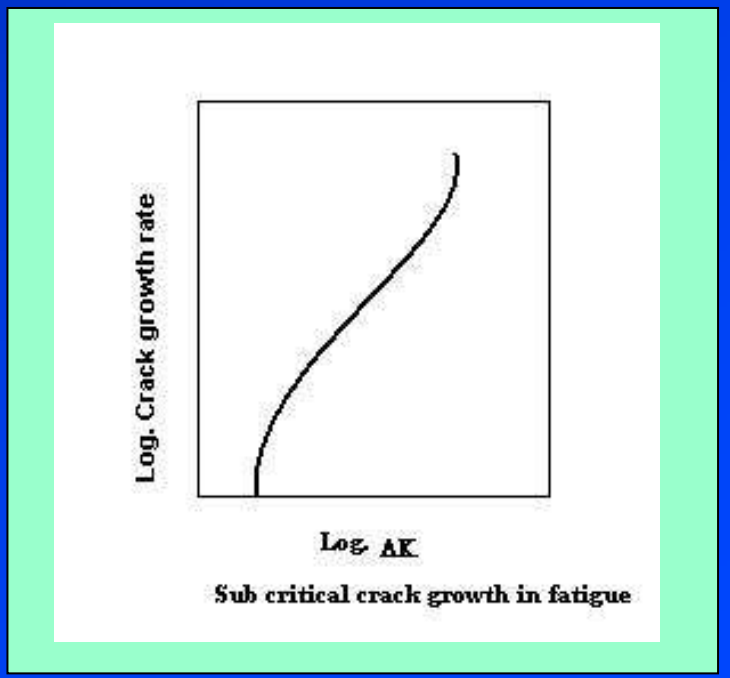

FCG curve

*A log scale plot gives **Paris exponent m** as the slope*

Fatigue crack propagation

Fatigue crack propagation

Stage I *Non-propagating fatigue crack (~0.25nm/cycle)*

Stage II *Stable fatigue crack propagation- widely study*

Stage III *Unstable fatigue crack propagation → failure*

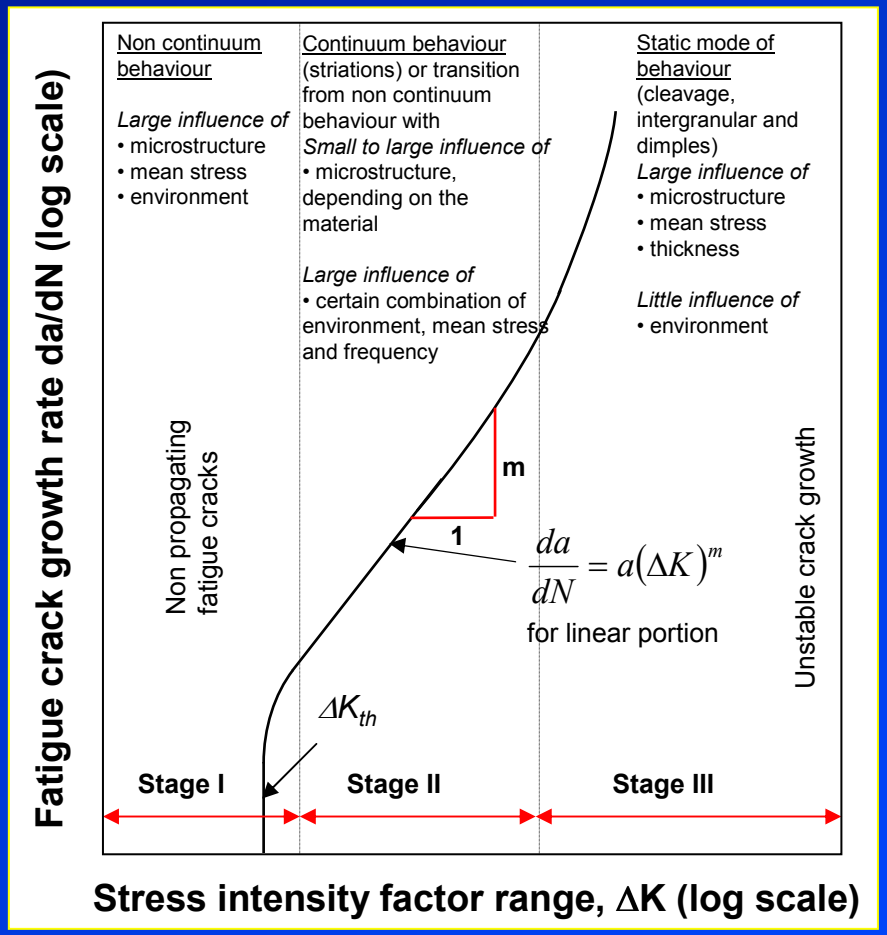

Fatigue crack growth behaviour

Fatigue crack growth propagation in stage II regime

Stage II fatigue crack growth propagation has been widely investigated in order to determine the ***fatigue crack growth life*** from the ***representing stable fatigue crack growth rate***.

$$\frac{da}{dN} = A(\Delta K)^m$$

m ↑

da/dN ↑

The ***fatigue crack growth life*** N_f (stage II) can be determined by

$$N_f = \int_0^{N_f} dN$$

$$N_f = \frac{a_f^{-(m/2)+1} - a_i^{-(m/2)+1}}{(-(m/2)+1) A \sigma_r^m \pi^{m/2} \alpha^m}$$

Eq.15

where ***m*** ≠ 2

α is the crack geometry factor

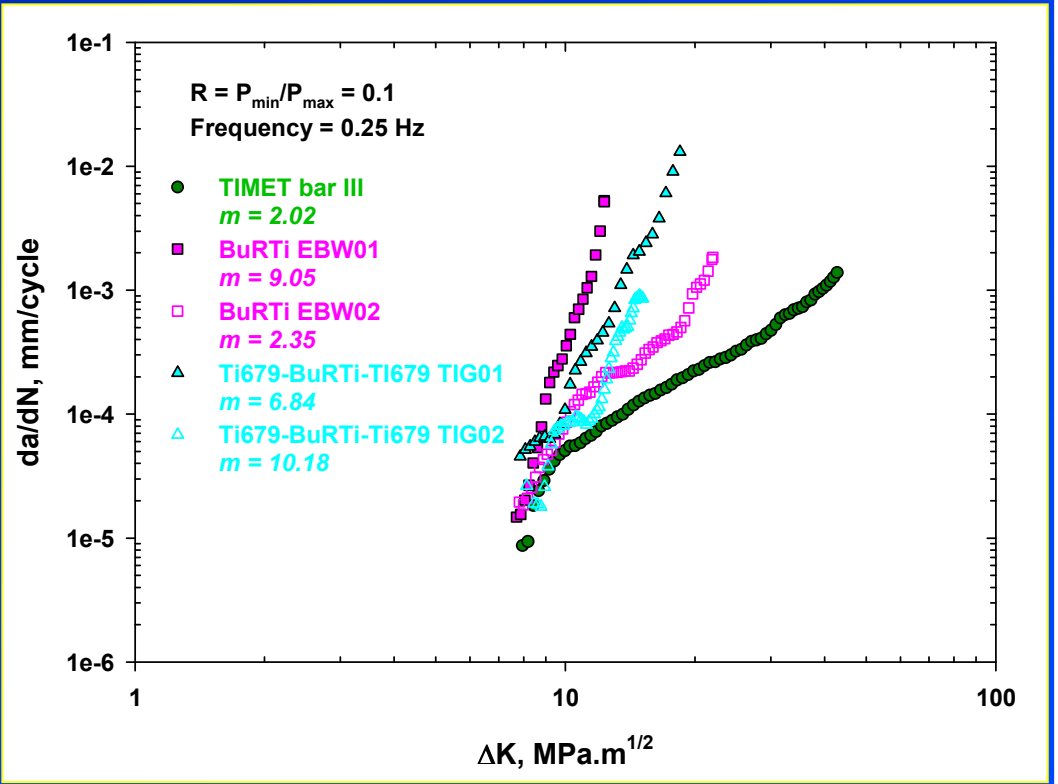

Fatigue crack growth in base metal and welded materials

Example: *A mild steel plate is subjected to constant amplitude uniaxial fatigue loads to produce stresses varying from* σ_{max} *= 180 MPa to* σ_{min} *= -40 MPa. The static properties of the steel are* σ_o *= 500 MPa,* σ_u *= 600 MPa,* E *= 207 MPa, and* K_c *= 100 MPa.m*$^{1/2}$*. If the plate contains an initial through thickness edge crack of 0.5 mm, how many fatigue cycles will be required to break the plate?*

For through thickness edge crack, α = 1.12, and for ferritic-pearlitic steels, A = 6.9 x 10^{-12} MPam$^{1/2}$ and m = 3.0.

σ_r = (180-0), since compressive stress are ignored, and neglect the influence of mean stress on the crack growth.

$$a_i = 0.0005 \ \ m, \ \ a_f = \frac{1}{\pi}\left(\frac{K_c}{\sigma_{\max}\alpha}\right)^2 = \frac{1}{\pi}\left(\frac{100}{180\times 1.12}\right)^2 = 0.078 \ \ m$$

From Eq.15

$$N_f = \frac{a_f^{-(m/2)+1} - a_i^{-(m/2)+1}}{(-(m/2)+1)A\sigma_r^m \pi^{m/2}\alpha^m}$$

$$N_f = \frac{(0.078)^{-(3/2)+1} - (0.0005)^{-(3/2)+1}}{(-(3/2)+1)(6.9\times 10^{-12})(180)^3(\pi)^{3/2}(1.12)^3} = 261{,}000 \ \ cycles$$

S-N curve fracture surfaces

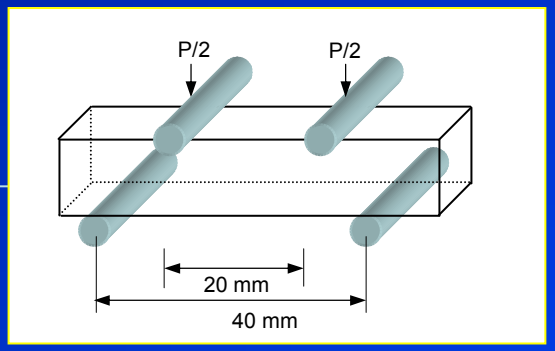

- ***S-N curve test*** involves crack initiation and crack propagation to failure. → overall fatigue life.
- Fatigue testing normally uses ***plain specimens*** of different specimen surface conditions, i.e., polished, ground, machined, etc. under tension or bending.
- Crack initiation might be due to inclusions, second phases, porosity, defects.

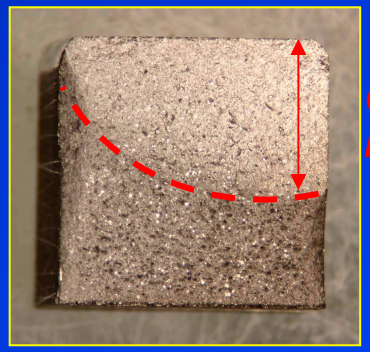

Crack length a

Corner crack

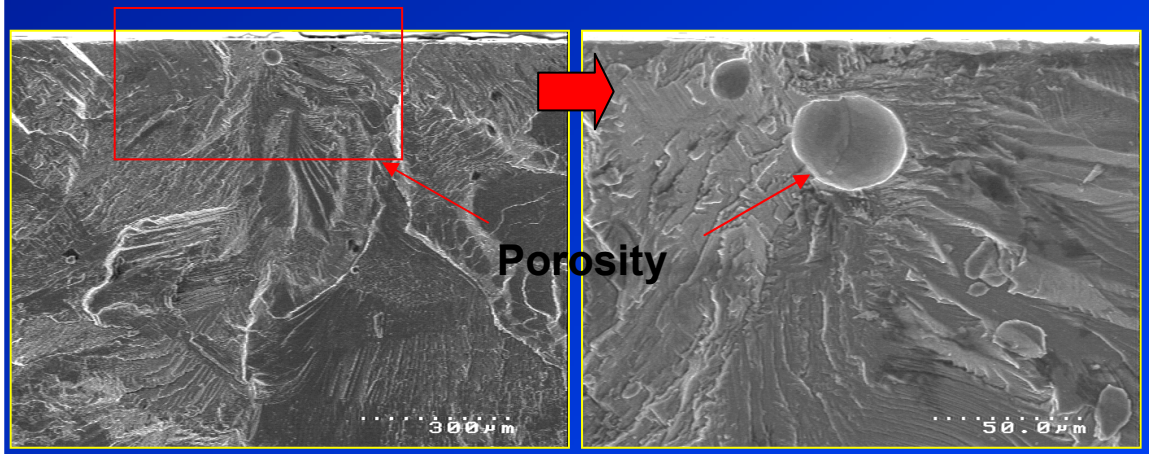

Fatigue crack initiation from porosity

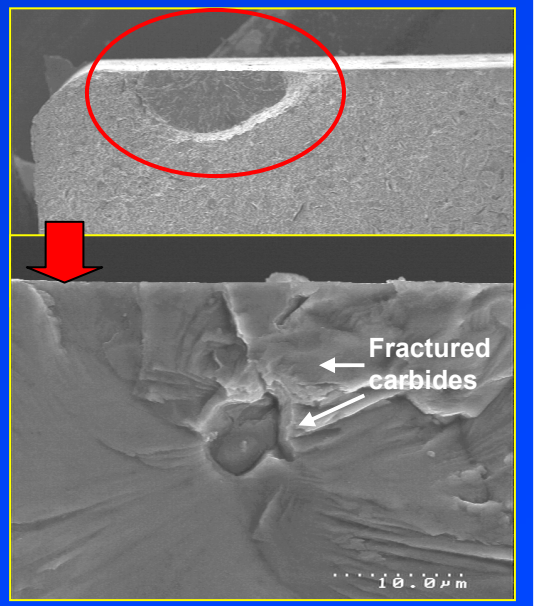

Fatigue crack initiation from inclusion/particle.

FCG fracture surfaces

- ***Fatigue crack growth*** (***FCG***) test involves only ***crack propagation*** stage but excludes ***crack initiation*** stage.
- Specimen has an ***initial short or small crack*** and this crack will propagate under cyclic loading.

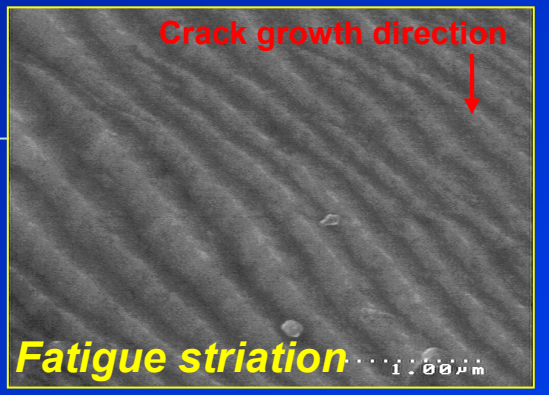

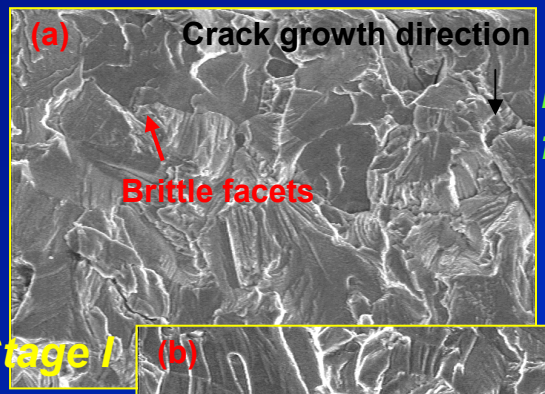

Brittle facet (slip) + fatigue striation

Stage I

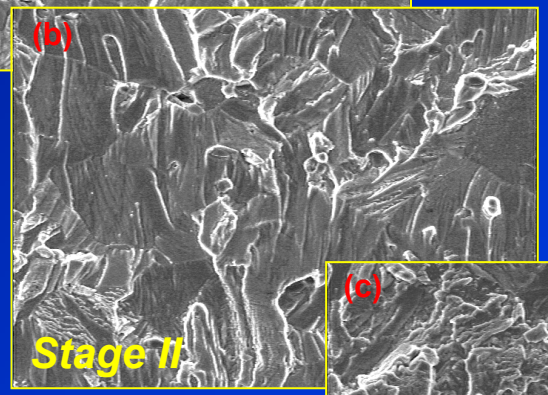

Fatigue striation

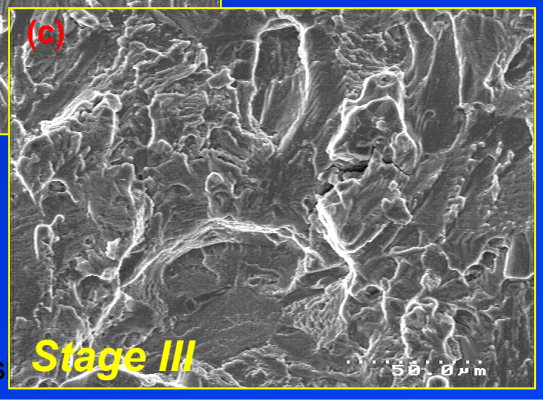

Brittle facets (cleavage) + microvoids

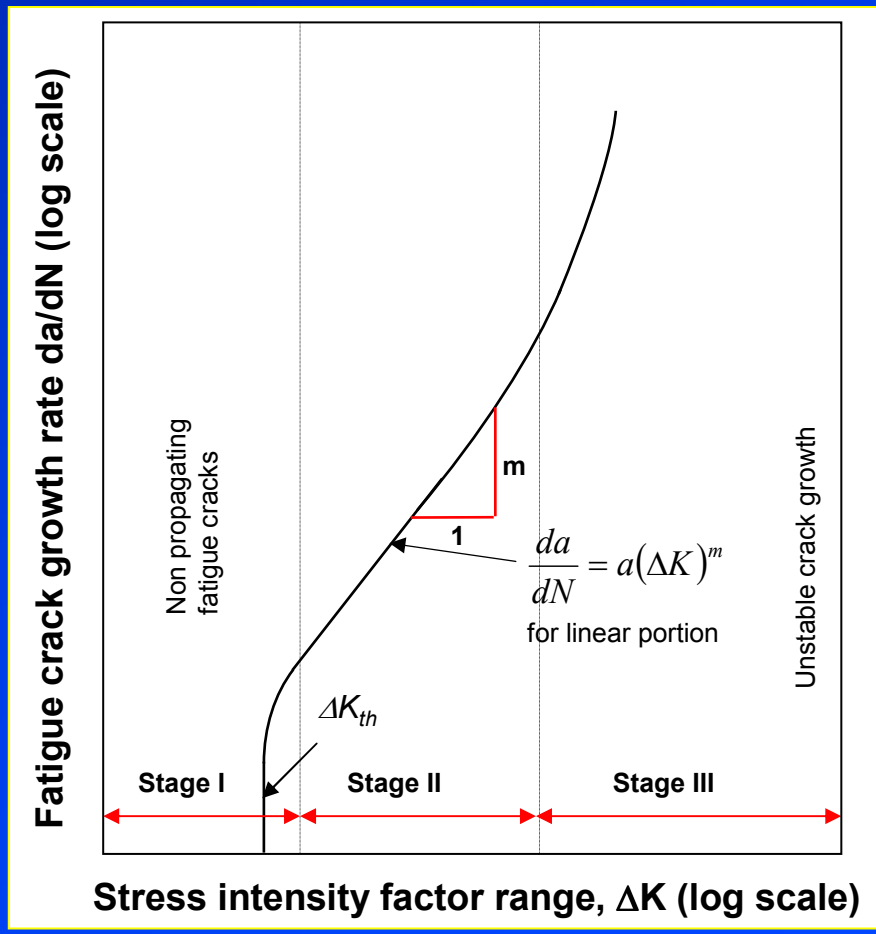

Factors influencing fatigue properties

- *Stress concentration*
- *Size effect*
- *Surface effects*
- *Combined stresses*
- *Cumulative fatigue damage and sequence effects*
- *Metallurgical variables*
- *Corrosion*
- *Temperature*

Effect of stress concentration on fatigue

Stress raiser ⬆ ***Fatigue strength*** ⬇⬇

➡ Should avoid stress raisers from machining and fabrication processes.

- The effect of ***stress raiser*** or notch on ***fatigue strength*** can be determined by comparing the ***S-N curve*** of ***notched*** and ***unnotched*** specimens. (based on the net section of specimen).
- The ***notch sensitivity factor q*** in fatigue is determined from

$$q = \frac{K_f - 1}{K_t - 1} \qquad \textit{Eq.16}$$

Where

K_t is theoretical stress-concentration factor, depending on elasticity of crack tip

K_f is fatigue notch factor, ratio of fatigue strength of notched and unnotched specimens.

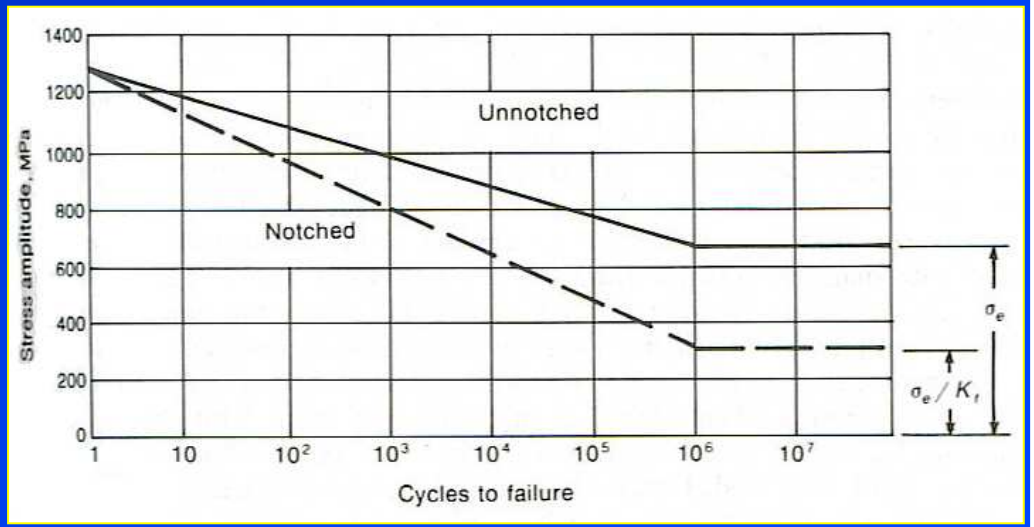

S-N curve of notched and unnotched specimens

Size effect on fatigue

Fatigue properties | **Experimental scale** ≠ **Industrial scale** | Due to size effect

- Fatigue property is ***better*** in the small sized specimens.
- Problem: the machine cannot accommodate ***large specimens***.
- ***Larger specimens*** → increases ***surface area*** subjected to cyclic load, higher possibility to find defects on surface.
  → decrease the stress gradient and increases the ***volume of material*** which is highly stressed.

Explain: It is usually impossible to duplicate the same ***stress concentration*** and ***stress gradient*** in a small-sized laboratory specimens.

Solution: Use statistic approaches, i.e., ***Weibull statistics.***

Surface effects on fatigue

- ***Fatigue properties*** are very sensitive to ***surface conditions***,
- ***Fatigue initiation*** normally starts at the surface since the ***maximum stress*** is at the surface.

The factors which affect the surface of a fatigue specimen can be roughly divided into three categories;

- ***Surface roughness***
- ***Changes in surface properties***
- ***Surface residual stress***

Surface roughness

- Different surface finishes produced by different ***machining processes*** can appreciably affect ***fatigue performance***.
- Polished surface (very fine scratches), normally known as '***par bar***' which is used in laboratory, gives the ***best fatigue strength.***

Table 12-3 Fatigue life of SAE 3130 steel specimens tested under completely reversed stress at 655 MPa†

Type of finish	Surface roughness, μm	Median fatigue life, cycles
Lathe-formed	2.67	24,000
Partly hand-polished	0.15	91,000
Hand-polished	0.13	137,000
Ground	0.18	217,000
Ground and polished	0.05	234,000
Superfinished	0.18	212,000

† P. G. Fluck, *Am. Soc. Test. Mater. Proc.*, vol. 51, pp. 584–592, 1951.

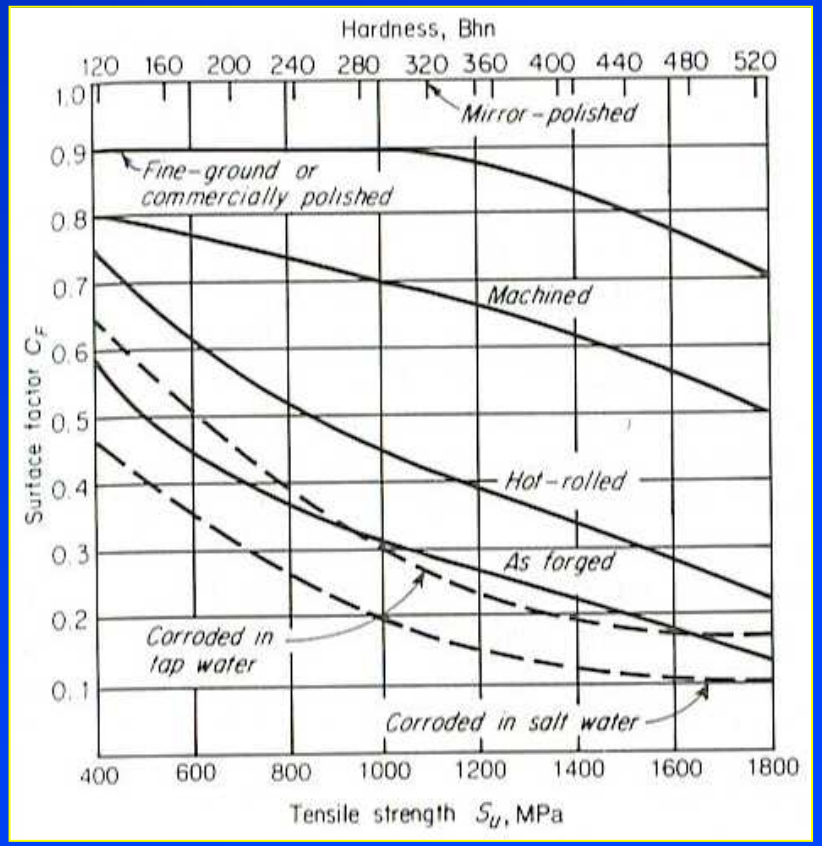

Reduction factor for fatigue limit of steel due to various surface treatments

Changes in surface properties

• Changes in surface properties due to surface treatments

Change in fatigue strength/properties.

Treatments which reduces fatigue performance

Decarburization — ***Ex:*** decarburization of surface of heat-treated steels.

Soft coating — ***Ex:*** Soft aluminium coating on an age-hardenable Al alloy.

Electroplating — Might reduces fatigue strength due to changes in residual stress, adhesion, porosity, hardness.

Treatments which improves fatigue performance

Carburizing

Nitriding

Flame hardening

Induction hardening

• Forming harder and stronger surface → introducing compressive residual stress.

• The strengthening effect depends on the diameter of the part and the depth of the surface hardening.

Surface residual stress

• ***Residual stresses*** arise when plastic deformation is ***not uniform*** throughout the entire cross section of the part being deformed.

Loading	Unloading
Part undergone plastically deformed in tension	Compressive residual stress
Part undergone plastically deformed in compression	Tensile residual stress

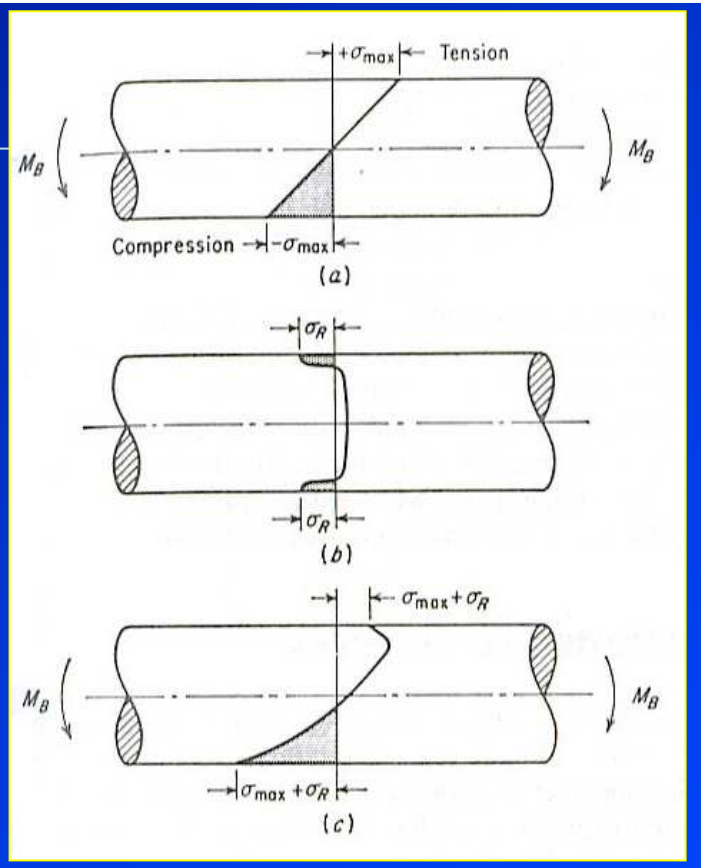

Superposition of applied and residual stresses

*(a) Shows the elastic stress distribution in a beam with **no residual stress**.*

*(b) Typical residual stress distribution produced by **shot peening** where the high compressive stress is balanced by the tensile stress underneath.*

(c) The stress distribution due to the algebraic summation of the external bending stress and the residual stress.

Commercial methods introducing favourable compressive stress

- ***Surface rolling***

  - Compressive stress is introduced in between the rollers during sheet rolling.

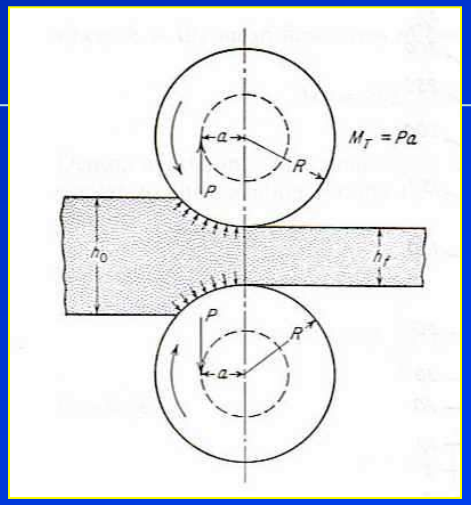

Sheet rolling

- ***Shot peening***

  - Projecting fine steel or cast-iron shot against the surface at high velocity.

- ***Polishing***

  - Reducing surface scratches

- ***Thermal stress***

  - Quenching or surface treatments introduce volume change → giving compressive stress.

Effect of combined stresses on fatigue

Few data has been made on ***fatigue test*** with ***different combinations of types of stresses***.

- ***Ductile metals*** under combined bending and torsion fatigue follow a distortion-energy (von Mises).
- ***Brittle materials*** follows the maximum principal stress theory (Tresca).

Sines has proposed expressions for

Low strain

$$\left[(\sigma_{a1}-\sigma_{a2})^2+(\sigma_{a2}-\sigma_{a3})^2+(\sigma_{a3}-\sigma_{a1})^2\right]^{1/2}+C_2(m_1+m_2+m_3)\geq\frac{\sqrt{2}\sigma_a}{K_f} \qquad \textit{Eq.17}$$

High strain

$$\varepsilon_q=\frac{\gamma_{oct}}{2}=\frac{1}{3}\left[(\varepsilon_1-\varepsilon_2)^2+(\varepsilon_2-\varepsilon_3)^2+(\varepsilon_3-\varepsilon_1)^2\right]^{1/2} \qquad \textit{Eq.18}$$

Note: *Effects of residual stress and triaxial stress are included.*

Cumulative fatigue damage and sequence effects on fatigue

Practically, ***levels of stress*** are not held constant as in ***S-N tests***, but can vary below or above the designed stress level.

- ***Overstressing*** : The initial applied stress level is higher than the fatigue limit for a short period of time beyond failure, then cyclic stressing below the fatigue limit. This overstressing ***reduces the fatigue limit***.

- ***Understressing*** : The initial applied stress level is lower than the fatigue limit for a period of time, then cyclic stressing above the fatigue limit. This understressing ***increases the fatigue limit*** (might be due to strain hardening on the surface.

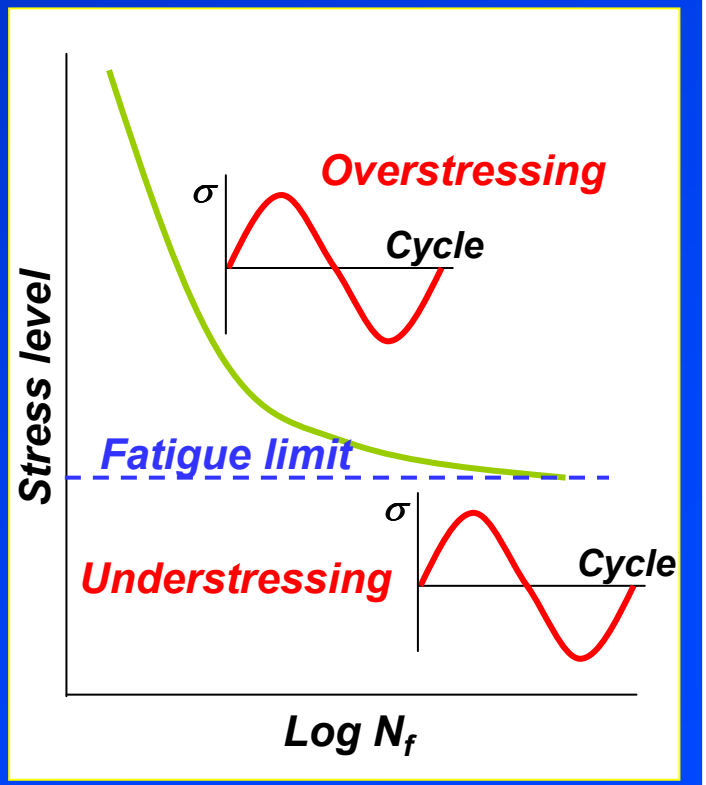

Cumulative damage rule

The percentage of fatigue life consumed by operation at one operating stress level depends on the magnitude of subsequent stress levels → ***the cumulative rule*** called ***Miner's rule***.

$$\frac{n_1}{N_1}+\frac{n_2}{N_2}+\ldots+\frac{n_k}{N_k}=1 \;\; or \;\; \sum_{j=1}^{j=k}\frac{n_j}{N_j} \qquad \textit{Eq.19}$$

Where $n_1, n_2,..n_k$ = the number of cycles of operation at specific overstress levels.

$N_1, N_2,..N_k$ = the life (in cycles) at this same overstress level.

Note: *for notched specimen, the fatigue strength is reduced much more than it would be predicted from the* ***Miner's linear damage rule.*** *This is due to the effect of residual stress produced at the notch by overload stresses in the plastic region.*

Example: *A plain sided specimen is subjected to $1x10^7$ cycles, at an applied stress range of 200 MPa. Estimate how many further cycles can be applied at a stress range of 500 MPa before failure is predicted to occur.*

Given information

Applied stress range (MPa)	*Number of cycles to failure*
600	*$1x10^4$*
500	*$2x10^4$*
400	*$5x10^4$*
300	*$3x10^5$*
250	*$3x10^6$*
200	*$8x10^7$*

From Miner's rule

$$\frac{n_1}{N_1}+\frac{n_2}{N_2}+\ldots+\frac{n_k}{N_k}=1$$

$$\frac{1\times10^7}{8\times10^7}+\frac{x}{2\times10^4}=1$$

$$\frac{x}{2\times10^4}=1-\frac{1}{8}$$

$$x=\frac{7}{8}\times2\times10^4=1.75\times10^4 \ \ cycles$$

Assumption: *the total life of a part can be estimated by adding up the percentage of life consumed by each overstress cycle.*

Therefore, the specimen can further withstand the fatigue load at 500 MPa for

Effects of metallurgical variables on fatigue

- ***Fatigue property*** is normally greatly improved by changing the designs or, reducing stress concentration, introducing compressive stress on the surface.
- Few attempts have paid on ***improving metallurgical structure*** to improve fatigue properties but it is still important.
- ***Fatigue property*** is frequently correlated with ***tensile properties***.

$$\text{Fatigue ratio} = \frac{\text{Fatigue strength}}{\text{Tensile strength}}$$

Tensile strength ↑

Fatigue strength ↑

Note: for smooth and polished specimen.
Ex: fatigue ratio ~ 0.5 for cast and wrought steels,
~ 0.35 for non-ferrous.

Fatigue strength improvement by controlling metallurgical variables

By increasing tensile strength

By strengthening mechanisms

- Grain boundary strengthening
- Fibre strengthening
- Second phase strengthening
- Cold working

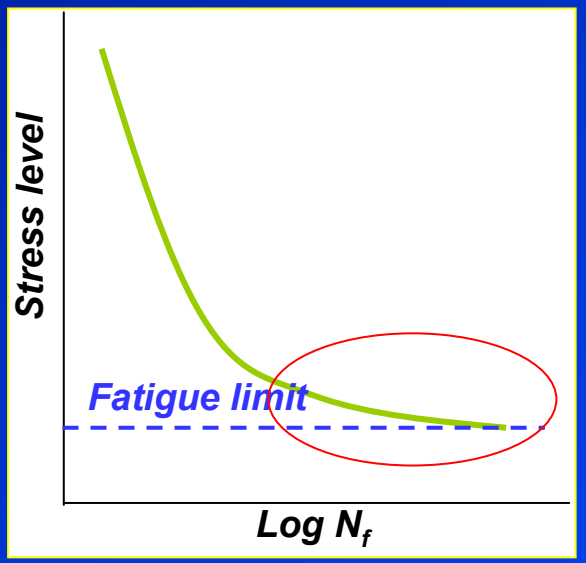

Note: *not for all cases and not proportionally.*

- Grain size has its greatest effect on fatigue life in the low-stress, high cycle regime.

Fatigue strength improvement by controlling metallurgical variables

By controlling microstructure

- ***Promote homogeneous slip /plastic deformation*** through thermomechanical processing → reduces residual stress/ stress concentration.
- ***Heat treatments*** to give hardened surface but should avoid stress concentration.
- ***Avoid inclusions*** → stress concentration → fatigue strength ↓↓
- ***Interstitial atoms*** increase yield strength , if plus ***strain aging*** → fatigue strength ↑↑

Table 12-4 Influence of inclusions on fatigue limit of SAE 4340 steel†

	Electric-furnace-melted	Vacuum-melted
Longitudinal fatigue limit, MPa	800	958
Transverse fatigue limit, MPa	545	827
Ratio transverse/longitudinal	0.68	0.86
Hardness, R_C	27	29

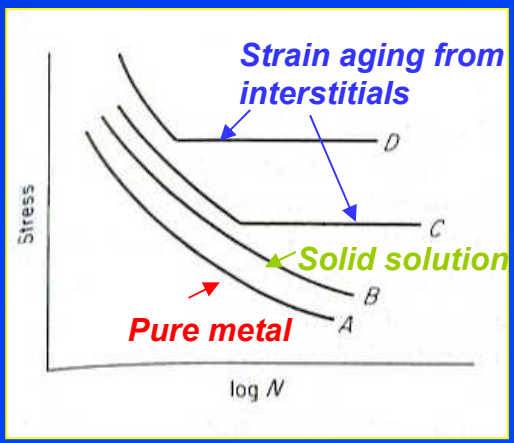

Effect of interstitial atoms

Effect of corrosion on fatigue

• ***Fatigue corrosion*** occurs when material is subjected to ***cyclic stress*** in a ***corrosive condition***.

• ***Corrosive attack*** produces ***pitting*** on metal surface. ***Pits*** act as notches → fatigue strength ⬇⬇.

• Chemical attack greatly ***accelerates*** the rate of fatigue crack propagation.

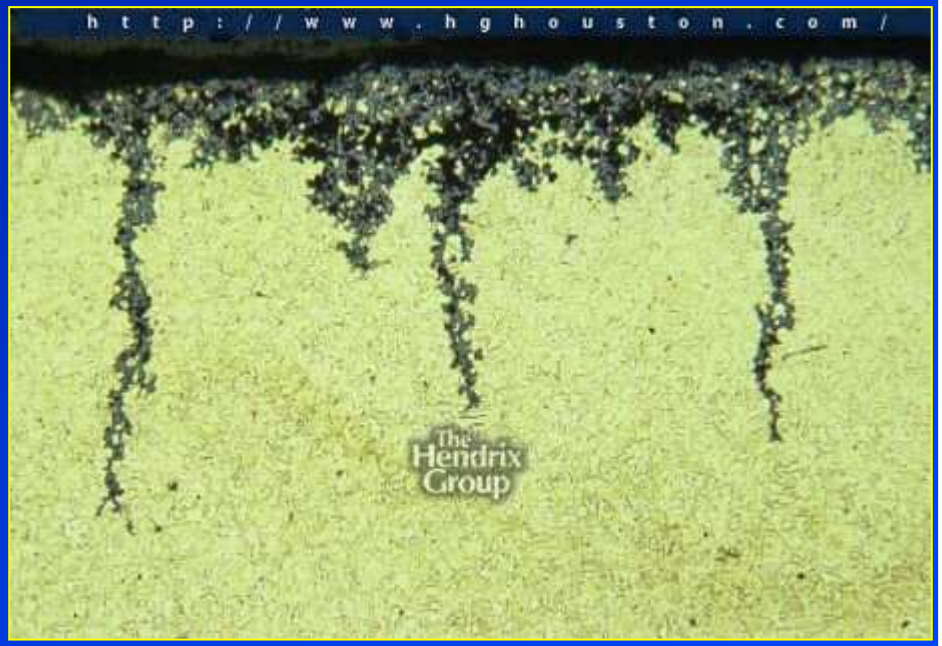

Corrosion fatigue of brass

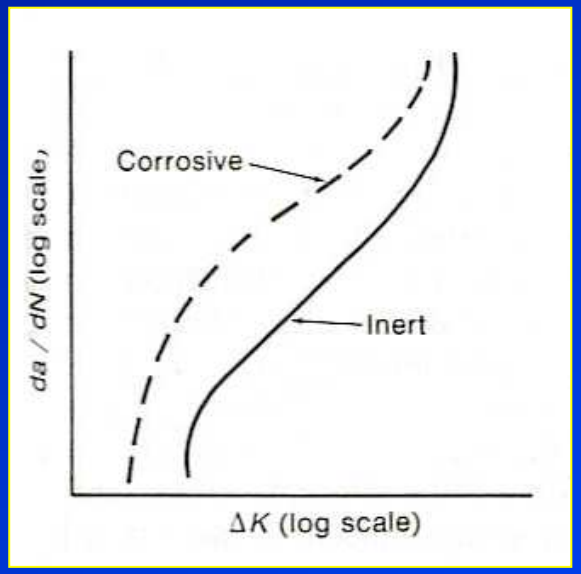

Role of a corrosive environment on fatigue crack propagation

Corrosion fatigue test

Corrosion fatigue test *can be carried out similar to fatigue test but in a controlled corrosive environment.*

• Since corrosion process is a ***time-dependent phenomenon***, the higher the ***testing speed*** (frequency), the smaller the ***damage due to corrosion***.

• The action of the cyclic stress causes ***localised breakdown of the surface oxide film*** → corrosion pits.

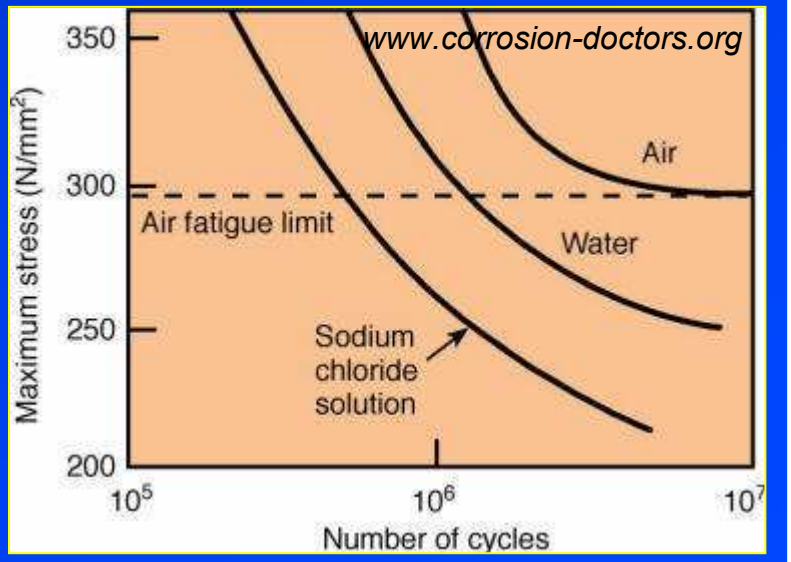

S-N curve in various condition

Minimization of corrosion fatigue

- ***Select corrosion-resistant materials*** for the desired application. ***Ex:*** stainless steel, bronze, would give better service than heat-treated steel.
- Protection of the metal from contact with the corrosive environment by ***protective metallic or non-metallic coatings***.
- ***Introducing compressive residual stresses*** by nitriding, shot peening → eliminating surface defects.

Effect of temperature on fatigue

Temperature ↓

(Increasing σ_{TS})

Fatigue strength ↑

If testing temp < ***RT*** → low temperature fatigue.

If testing temp > ***RT*** → high temperature fatigue.

- In high temperature fatigue, there is a transition from ***fatigue failure*** to ***creep failure*** as the temperature increases (creep dominates at high temperatures).
- ***Coarse grained metal*** has higher fatigue strength – where creep dominates.
- **Fine grained metal** has higher fatigue strength at low temperatures.

Temp →

Fatigue failure → ***Creep failure***

Transcrystalline fatigue failure

Intercrystalline creep failure

Thermal fatigue

Thermal fatigue occurs when metal is subjected to high and low temperature, producing fluctuating cyclic thermal stress.

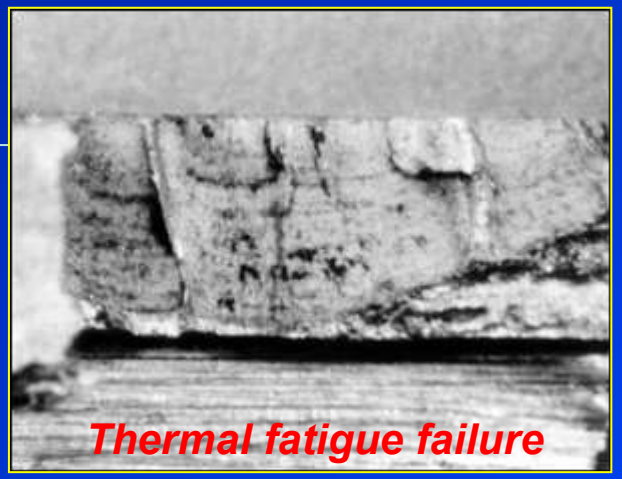
Thermal fatigue failure

Thermal cycle → **Volume change**

Cold

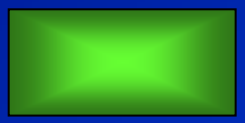

Hot

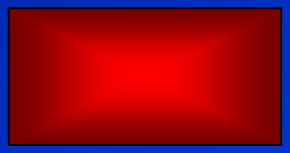

- Normally occurs in high temperature equipment.
- Low thermal conductivity and high thermal expansion properties are critical.

- The ***thermal stress*** developed by a temperature change ΔT is

$$\sigma = \alpha E \Delta T \qquad \text{Eq.19}$$

Where α is linear thermal coefficient of expansion
E is elastic modulus

If failure occurs by one application of thermal stress, the condition is called ***thermal shock***.

Design for fatigue

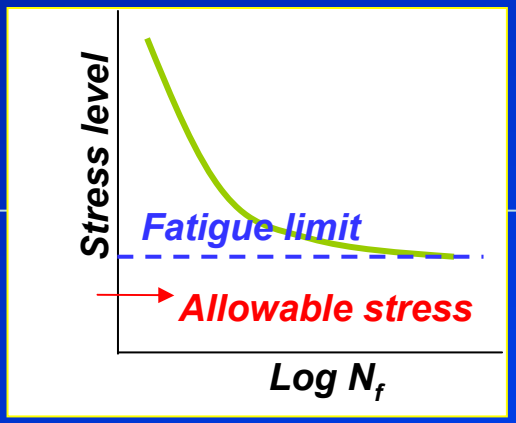

There are several distinct philosophies concerning for design for fatigue

1) ***Infinite-life design:*** Keeping the stress at some fraction of the fatigue limit of the material.
2) ***Safe-life design:*** Based on the assumption that the material has flaws and has finite life. Safety factor is used to compensate for environmental effects, varieties in material production/manufacturing.
3) ***Fail-safe design***: The fatigue cracks will be detected and repaired before it actually causes failure. For aircraft industry.
4) ***Damage tolerant design:*** Use fracture mechanics to determine whether the existing crack will grow large enough to cause failure.

References

- Dieter, G.E., ***Mechanical metallurgy***, 1988, SI metric edition, McGraw-Hill, ISBN 0-07-100406-8.
- Suresh, S., ***Fatigue of materials***, 1998, 2nd edition, Cambridge university press, ISBN 0-521-57847-7.
- Lecture note, MRes 2000, School of Metallurgy and Materials, Birmingham University, UK

Creep and stress rupture

Subjects of interest

- Objectives / Introduction
- The high temperature materials problem
- Temperature dependent mechanical behaviour
- Creep test
- Stress rupture test
- Structural change during creep
- Mechanisms of creep deformation
- Fracture at elevated temperature
- High temperature alloys

Objectives

- This chapter provides the understanding of deformation and fracture behaviour of material at high temperature.
- Creep and stress rupture tests will be compared such that the interpretation of test data will be discussed for engineering applications. This will lead to the selection of metal and alloys for desired uses at high temperature.

Introduction

High temperature applications

Steam power plant

Subjected to high stress at high temperature

Oil refinery

Steam turbine used in power plant

Process plant

High temperature materials problem

Temp ↑

- Atoms move faster → ***diffusion-controlled process***. This affects mechanical properties of materials.
- Greater mobility of dislocations (climb).
- Increased amount of vacancies.
- Deformation at grain boundaries.
- Metallurgical changes, i.e., phase transformation, precipitation, oxidation, recrystallisation.

High temperature materials/alloys

- Improved high temperature strength.
- Good oxidation resistance.

What is creep?

Creep ***occurs when a metal is subjected to a constant tensile load at an elevated temperature.*** → *Undergo a time-dependent increase in length.*

At which temperature that material will creep?

• Since materials have its own different melting point, each will creep when the homologous temperature > 0.5.

$$\text{Homologous temp} = \frac{\text{Testing temperature}}{\text{Melting temperature}} > 0.5$$

• ***The creep test*** measure the ***dimensional changes*** which occur when subjected to high temperature.

• ***The rupture test*** measures the effect of temperature on the long-time load bearing characteristics.

Creep test

The ***creep test*** is carried out by applying a ***constant load*** to a tensile specimen maintained at a ***constant temperature***, (according to ASTM E139-70).

Creep test setting

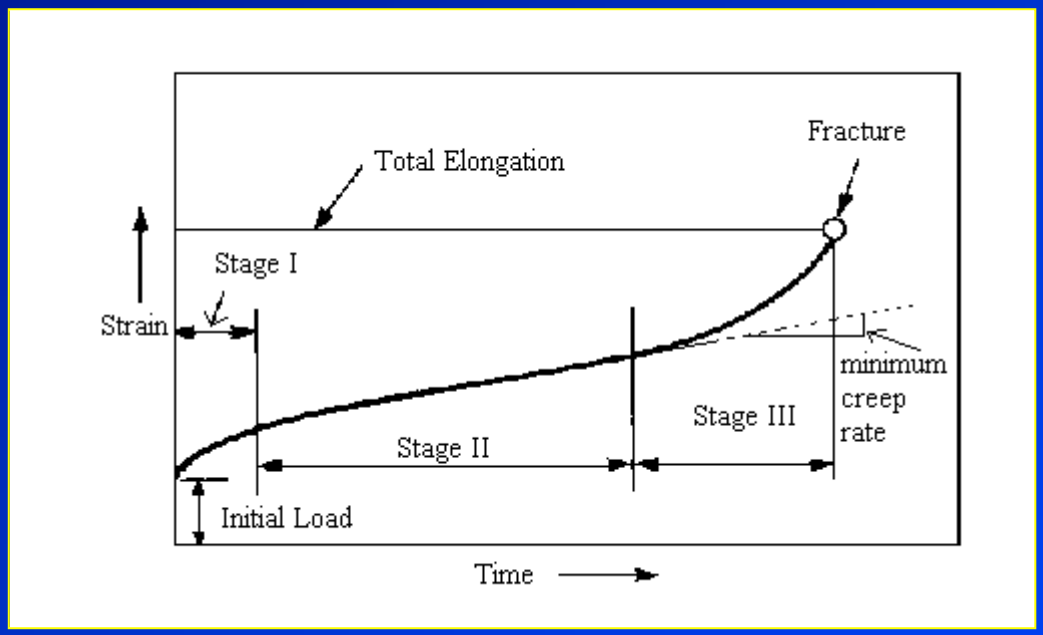

Typical creep curve

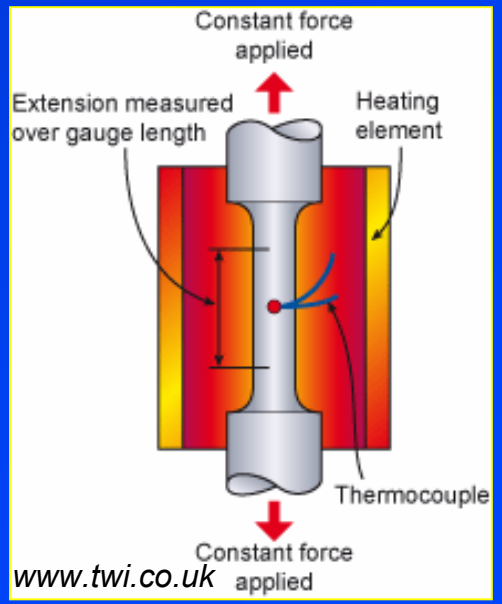

Schematic creep test

The creep curve

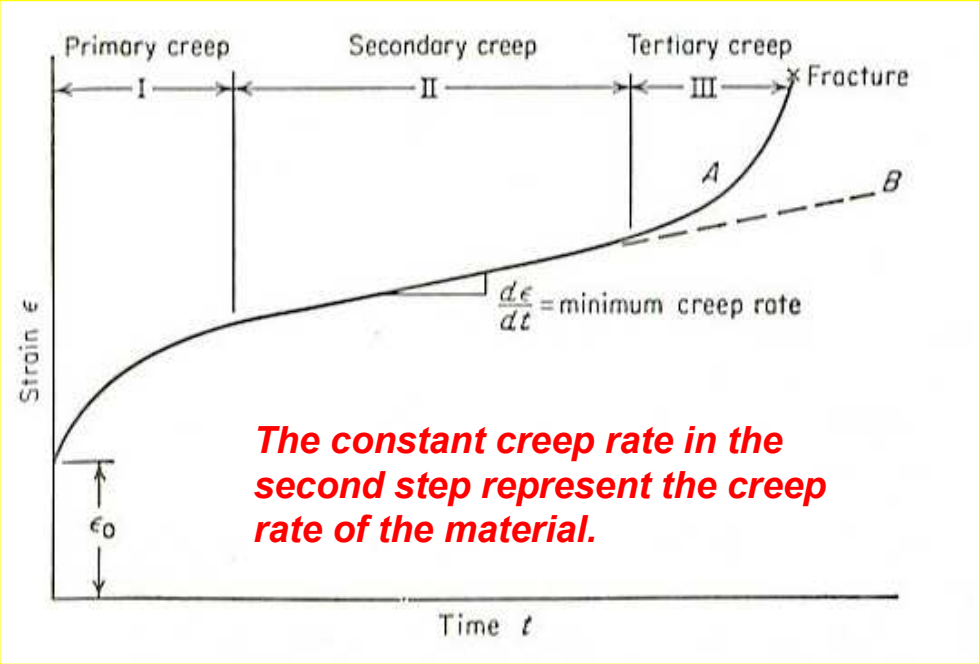

The constant creep rate in the second step represent the creep rate of the material.

Typical creep curve showing three stages of creep

Notes: B curve is obtained when the stress rather than the load is maintained.

A ***typical creep curve*** shows three distinct stages with different creep rates. After an initial rapid elongation ε_o, the creep rate decrease with time until reaching the steady state.

1) ***Primary creep*** provides decreasing creep rate.

2) ***Secondary creep*** gives the representing constant creep rate.

3) ***Tertiary creep*** yields a rapid creep rate till failure.

ε_o is instantaneous strain on loading which is partly ***recoverable*** with time (anelastic) and partly ***nonrecoverable*** with time (plastic).

Three stages of creep

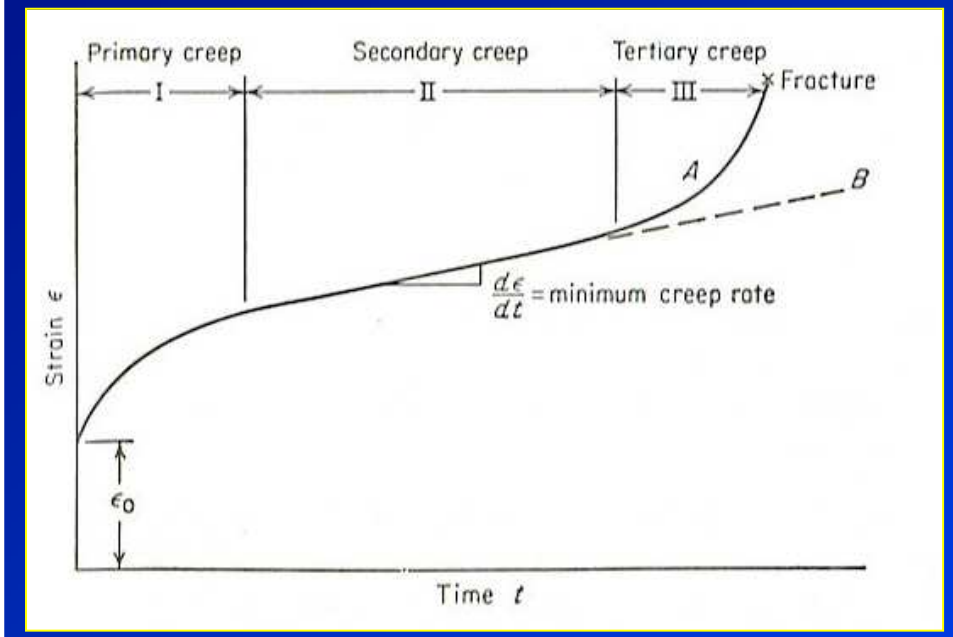

1) ***Primary creep*** is a period of transient creep. The creep resistance of the material increases due to material deformation. Predominate at low temperature test such as in the creep of lead at RT.

2) ***Secondary creep*** provides a nearly constant creep rate. The average value of the creep rate during this period is called the ***minimum creep rate***.

3) ***Tertiary creep*** shows a rapid increase in the creep rate due to effectively reduced cross-sectional area of the specimen.

Effect of stress on creep curves at constant temperature

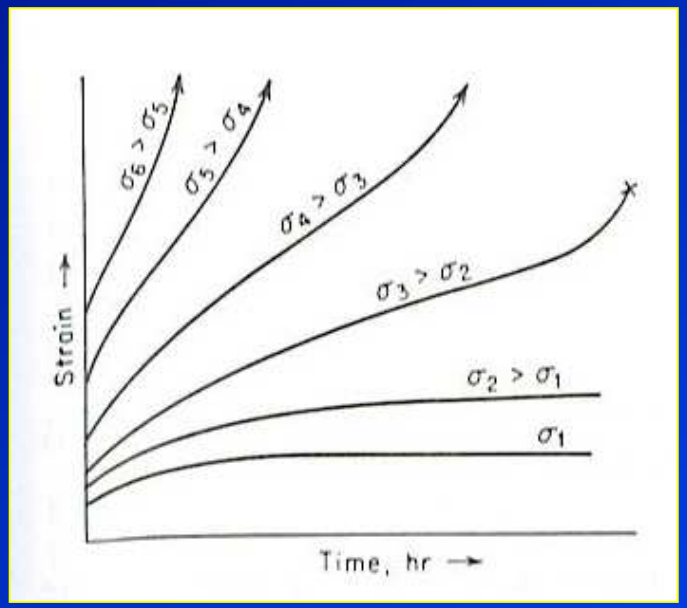

The shape of creep curve will slightly change according to the ***applied stress*** at a constant temperature.

Applied stress ↑ **Strain** ↑

Temp ↑ **Creep rate** ↑

The stress rupture test

	Creep test	Stress rupture test
Load	Low load	high load
Creep rate	minimum creep rate	high creep rate
Test period	2000-10000 h	1000 h
Total strain	0.5%	50%
Strain gauge	Good strain measuring devices	Simpler strain measuring devices

The ***rupture test*** in carried out in a similar manner to the ***creep test*** but at a ***higher stress level*** until the specimen fails and the ***time at failure*** is measured.

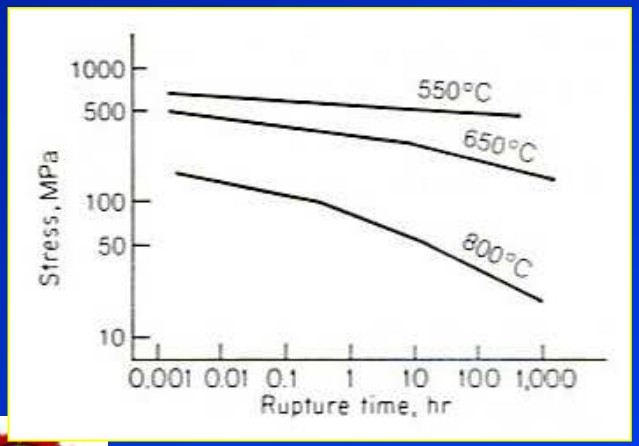

Stress rupture- time data on log-log scale

- ***Rupture strength*** and ***failure time*** are plotted, normally showing a ***straight line***.
- ***Changing of the slope*** indicates ***structural changes in the material***, i.e., transgranular → intergranular fracture, oxidation, recrystallisation, grain growth, spheroidization, precipitation.
- Direct application in ***design***.

Structural changes during creep

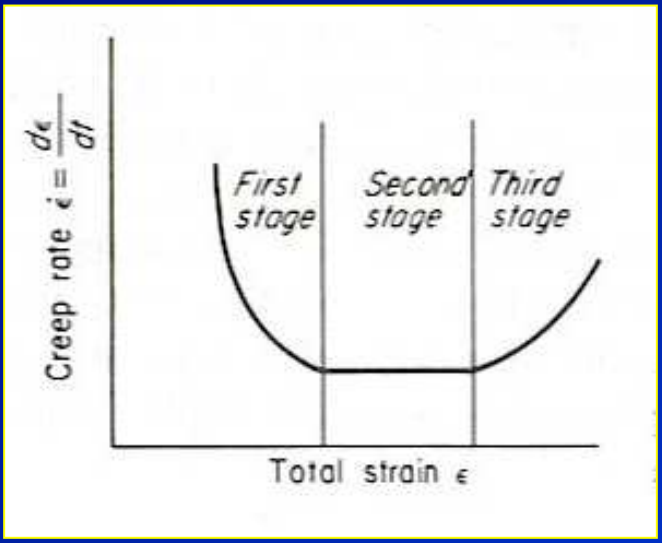

Creep rate and total strain relationship

Different creep rates result from ***changes in internal structure*** of the materials with creep rate and time.

There are ***three principal deformation processes*** at elevated temperature.

1) Deformation by slip

- More slip systems operate at high temperature
- Slip bands are coarser and widely spaced.

2) Subgrain formation

- Creep deformation produces imhomoginiety especially around grain boundaries, allowing dislocations to arrange themselves into a low-angle grain boundary. Easy for metals with high stacking false energy.

3) Grain boundary sliding

- Produced by shear process and promoted by increasing temperature/or decreasing strain rate.
- Results in grain boundary folding or grain boundary migration.

Mechanisms of creep deformation

The chief creep deformation mechanisms can be grouped into;

1) Dislocation glide

Involves dislocation moving along slip planes and overcoming barriers by thermal activation.
Occurs at high stress.

2) Dislocation creep

Involves dislocation movement to overcome barriers by diffusion of vacancies or interstitials.

3) Diffusion creep

Involves the flow of vacancies and interstitials through a crystal under the influence of applied stress.

4) Grain boundary sliding

Involves the sliding of grains past each other.

Deformation mechanism maps

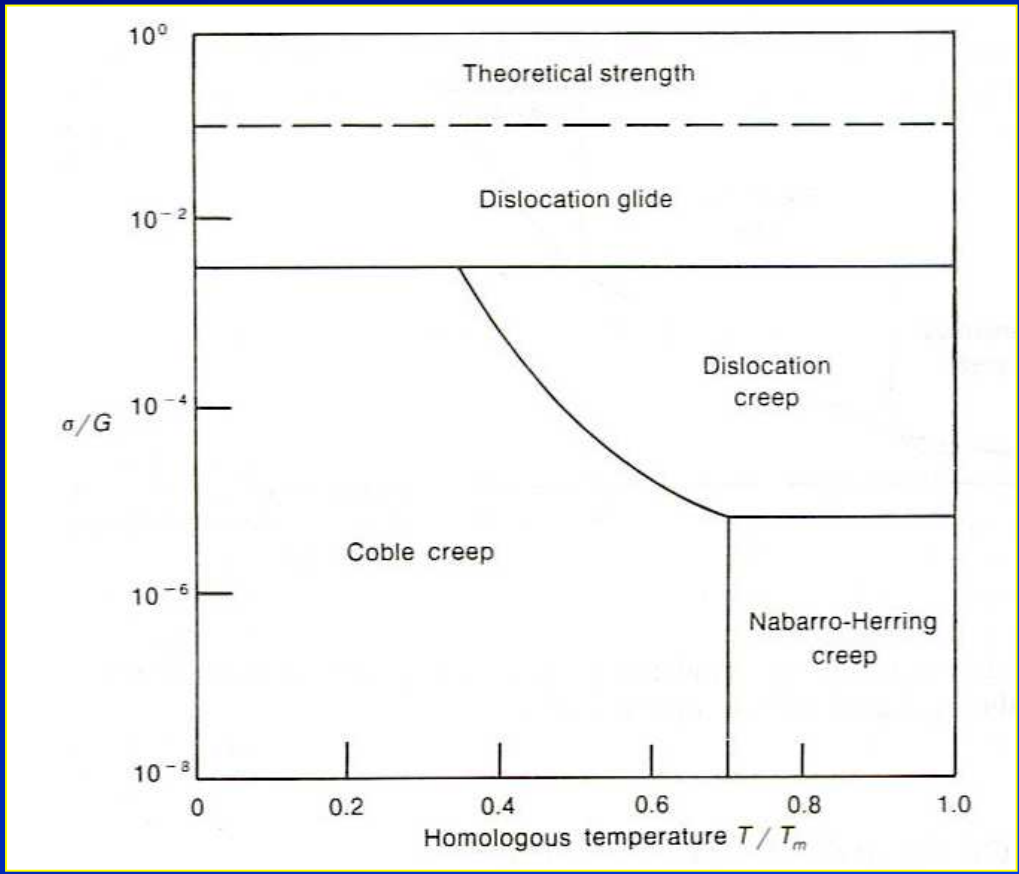

Simplified deformation mechanism map.

- *The various regions of the map indicate the **dominant deformation mechanism** for the combination of stress and temperature.*
- *At the **boundary**, two mechanisms occur.*

Note: *G is the shear modulus*

Activated energy for steady-state creep

- ***Steady-state creep deformation*** *predominates at temperatures above 0.5* T_m.

- Steady state creep can be expressed by

$$\dot{\varepsilon}_s = Ae^{-Q/RT} \qquad \textit{Eq.1}$$

Where ***Q*** = the activated energy for the rate-controlling process
A = the material structural constant
T = the absolute temperature
R = the universal gas constant

- The ***activated energy Q*** can be calculated by assuming the temperature interval is small so that the creep mechanisms is not expected to change.

$$A = \dot{\varepsilon}_1 e^{Q/RT_1} = \dot{\varepsilon}_2 e^{Q/RT_2}$$

$$Q = \frac{R\ln(\dot{\varepsilon}_1/\dot{\varepsilon}_2)}{(1/T_2 - 1/T_1)} \qquad \textit{Eq.2}$$

Superplasticity

- ***Superplasticity*** is the ability to withstand very large deformation in tension without necking.
- Give elongation > 1000%.
- Materials with high ***strain rate sensitivity*** (***m***) at high temperature ($T>0.5T_m$) → ***superplasticity***
- Materials characteristics: ***fine grain size*** (<10 μm) with the presence of ***second phase of similar strength to the matrix*** to inhibit grain growth and to avoid extensive internal cavity formation.
- Grain boundary should be ***high angle*** and ***mobile*** to promote grain boundary sliding and to avoid the formation of local stress concentration respectively.

Superplastic flow

The ***superplastic flow*** is given by

$$\dot{\varepsilon} = 10^{8}\left(\frac{\sigma}{E}\right)^{2}\frac{bD_{gb}}{\overline{L}^{3}}$$ *Eq.3* For grain boundary diffusion

$$\dot{\varepsilon} = 2\times 10^{9}\left(\frac{\sigma}{E}\right)^{2}\frac{D_{o}}{\overline{L}^{2}}$$ *Eq.3* For lattice self-diffusion

Where $\overline{L}$ is the mean linear intercept measure of grain size.
in this case ***n*** = 2, → ***m*** = 0.5

The predominant mechanism for superplasticity deformation is ***grain-boundary sliding*** accommodated by slip.

Fracture at elevated temperature

Temp

Transgranular fracture

Slip planes are weaker than grain boundaries

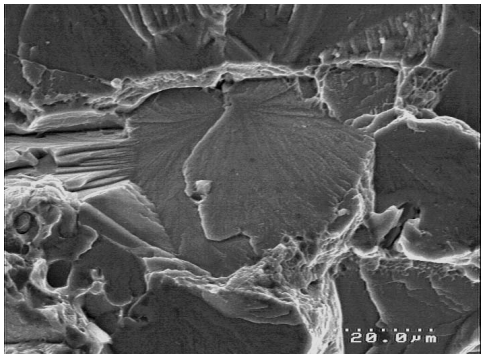

Transgranular cleavage fracture

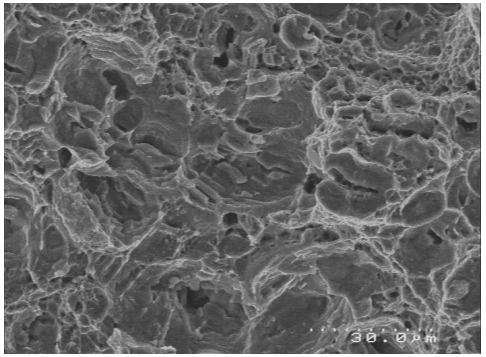

Transgranular microvoid coalescence

Intergranular fracture

Grain boundaries are weaker than slip planes.

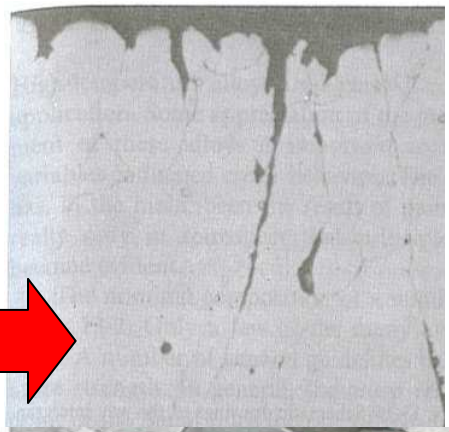

Grain boundary fracture

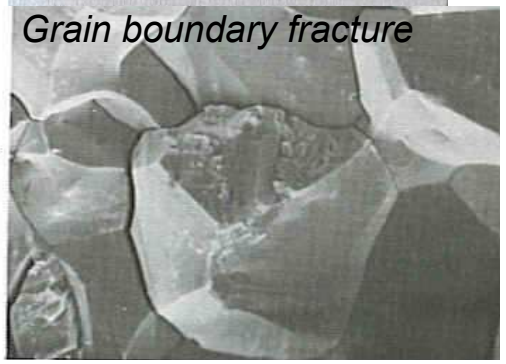

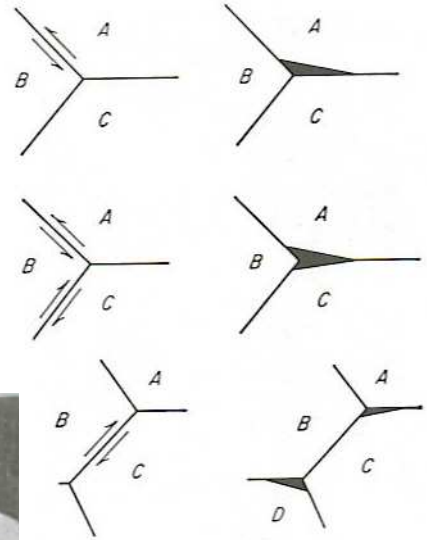

The formation of intergranular crack by grain boundary sliding

Note: at T just below T_{recrys}, ductility drops due to grain boundary sliding → intergranular failure.

Equicohesive temperature

• *Strength of **GB** = **grain** at the equicohesive temperature (**ECT**).*

Strain rate ↓ ***ECT*** ↓

Increasing the tendency for intergranular failure

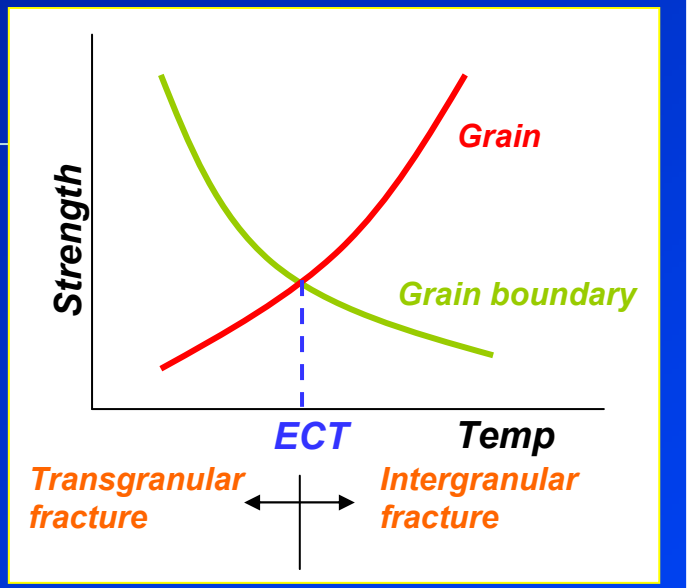

• Below ***ECT*** small grain sized material is stronger due to high density of grain boundaries to improve strength.

• Above ***ECT*** large grain sized material is stronger due to less tendency for grain boundary sliding.

Note: *Single crystal structure is therefore appreciable for high temperature applications, i.e., nickel base alloy single crystal turbine blade.*

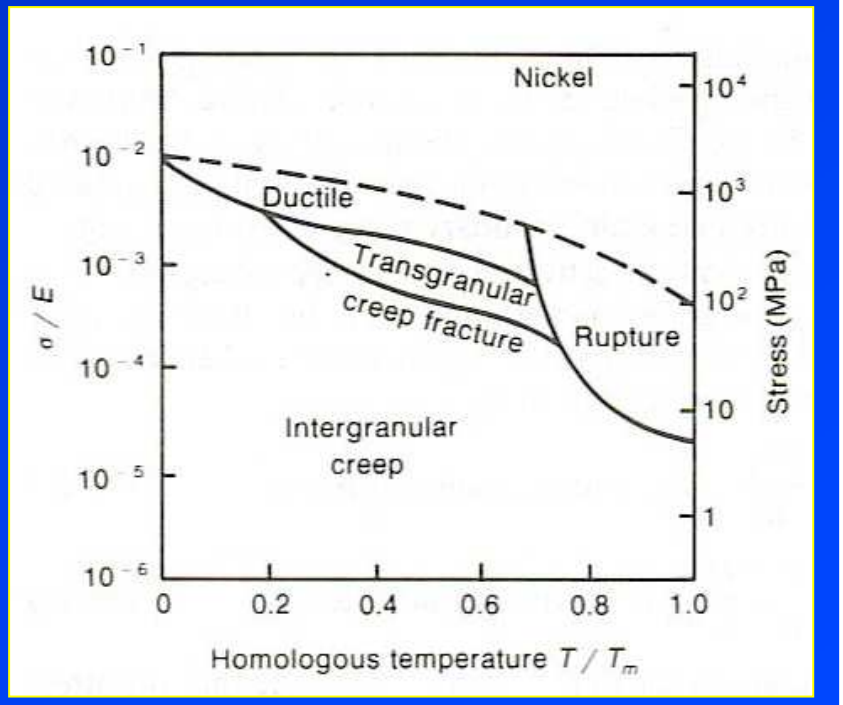

Fracture mechanism map for nickel

High temperature alloys

• ***High temperature alloys*** are ***complex in their microstructures*** to obtain the required properties at service temperatures.

• ***High melting point*** alloys normally has high creep resistance.

• Metals with ***high stacking false energy*** → easy for slip → ***creep***.

• ***Fine precipitates*** having high thermal stability are necessary for high creep resistance (prevent grain growth). ***Ex:*** (1) ***Nickel base alloy*** containing fine precipitates of intermetallic compounds ***Ni_3Al, NI_3Ti or $Ni_3(Al,Ti)$,*** (2) ***Creep resistance steels*** containing fine carbides ***VC, TiC, NbC, Mo_2C or $Cr_{23}C_6$.***

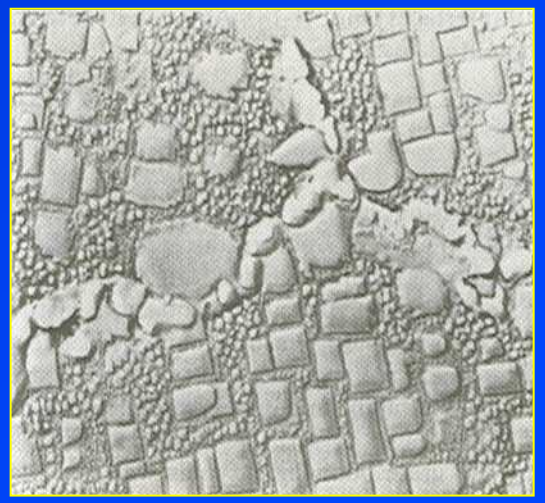

Microstructure of nickel base alloy

Drawbacks

• ***Difficult to fabricate*** by hot-working, cold working or welding.

• ***Highly alloyed metals*** are difficult to produced by precision casting.

Composition of some high temperature alloys

Table 13-2 Compositions of some high-temperature alloys

Alloy	C	Cr	Ni	Mo	Co	W	Cb	Ti	Al	Fe	Other
Ferritic steels											
1.25 Cr-Mo	0.10	1.25	—	0.50						Bal.	
5 Cr-Mo	0.20	5.00	—	0.50						Bal.	
Greek Ascoloy	0.12	13.0	2.0			3.0				Bal.	
Austenitic steels											
316	0.08	17.0	12.0	2.50						Bal.	
16-25-6	0.10	16.0	25.0	6.00						Bal.	
A-286	0.05	15.0	26.0	1.25				1.95	0.2	Bal.	
Nickel-based alloys											
Astroloy	0.06	15.0	56.5	5.25	15.0			3.5	4.4		
Inconel	0.04	15.5	76.0							7.0	
Inconel 718	0.04	19.0	Bal.	3.0			5.0	0.80	0.60	18.0	
René 41	0.10	19.0	Bal.	10.0	11.0			3.2	1.6	2.0	
Mar-M-200	0.15	9.0	Bal.	—	10.0	12.5	1.0	2.0	5.0		
TRW 1900	0.11	10.3	Bal.	—	10.0	9.0	1.5	1.0	6.3		
Udimet 700	0.15	15.0	Bal.	5.2	18.5			3.5	4.25	1.0	
In-100	0.15	10.0	Bal.	3.0	15.0			4.7	5.5		1.0 V
TD Nickel	—	—	Bal.								2.0 ThO_2
Cobalt-based alloys											
Vitallium (HS-21)	0.25	27.0	3.0	5.0	Bal.					1.0	
S-816	0.40	20.0	20.0	4.0	Bal.	4.0		4.0		3.0	

Presentation of engineering creep data

Creep strength is defined as the stress at a given temperature, which produces a ***steady-state creep rate*** (10^{-11} to 10^{-8} s^{-1}.)

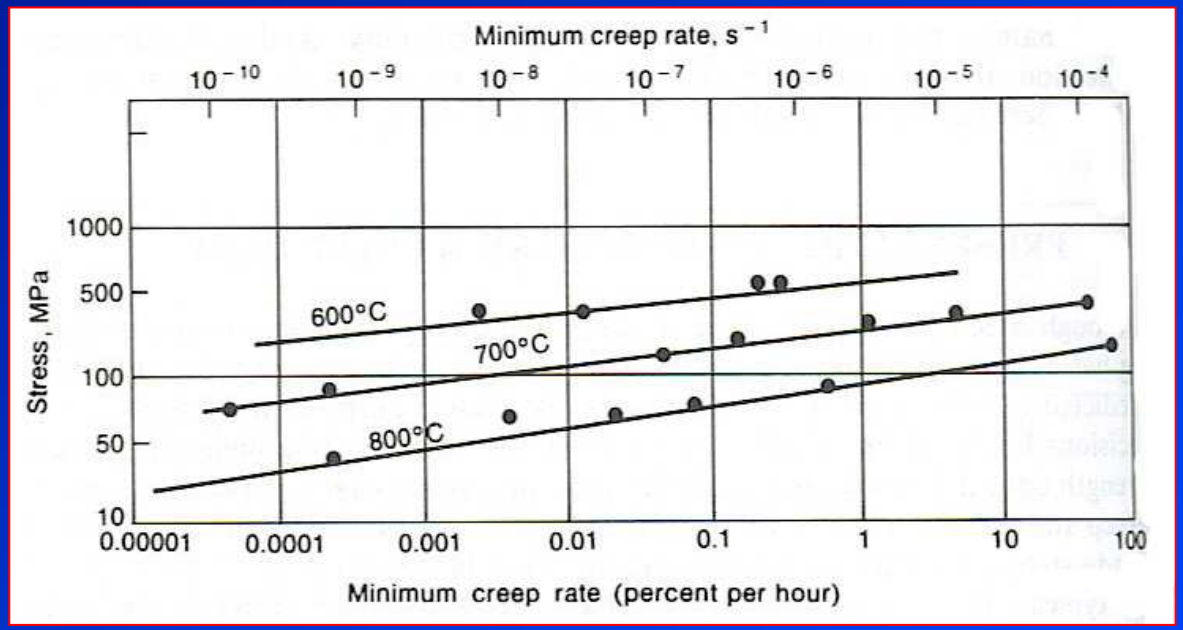

Stress vs minimum creep rate

• ***Log-log plot*** is used so that the extrapolation of one log-cycle represents a ***tenfold change***.

Creep data

Creep data can also be presented as ***a plot of stress and time*** to produce different amounts of total strain.

- The upper most curve is the ***stress rupture curve***.
- The percentage beside each data point is the ***percentage reduction at failure***.

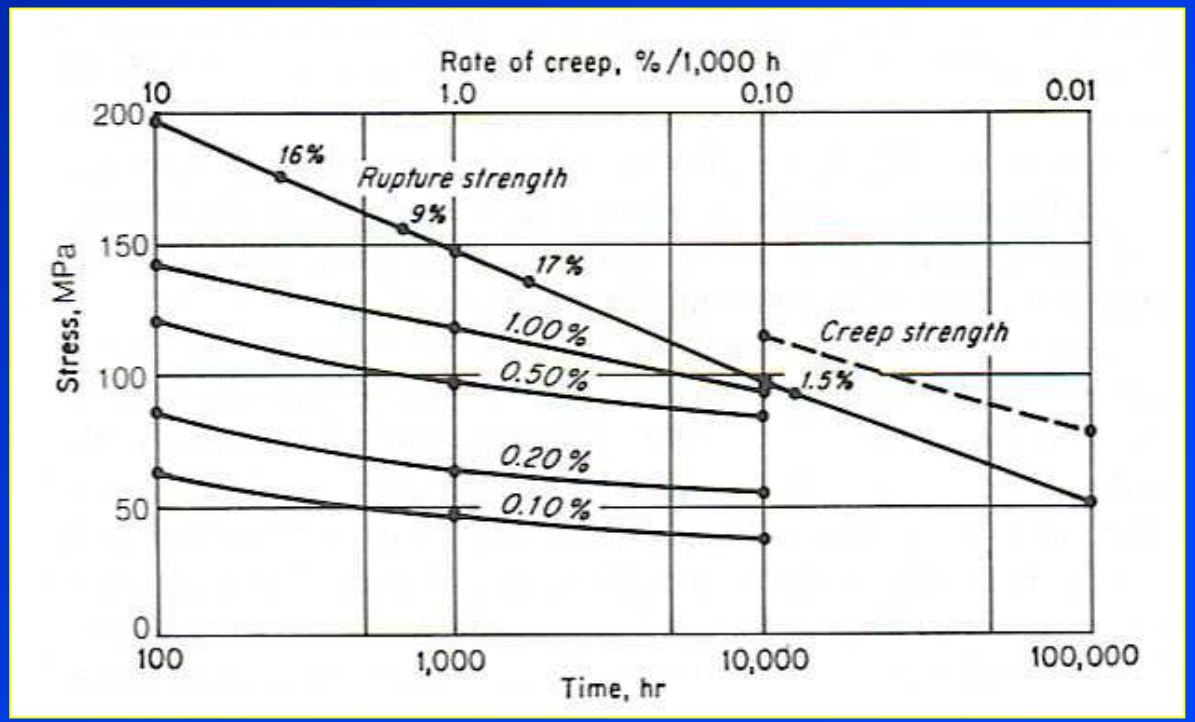

Deformation time curve

Example: *Determine the working stress at 600°C and 800°C for type 316 stainless steel if the design criterion is a creep strength based on 1 percent extension in 1000 hr. Use a factor of safety of 3.*

1% creep in 1000h $= 10^{-5}\,h^{-1} = \dfrac{10^{-5}}{3600}\,s^{-1} = 2.8\times10^{-9}\,s^{-1}$

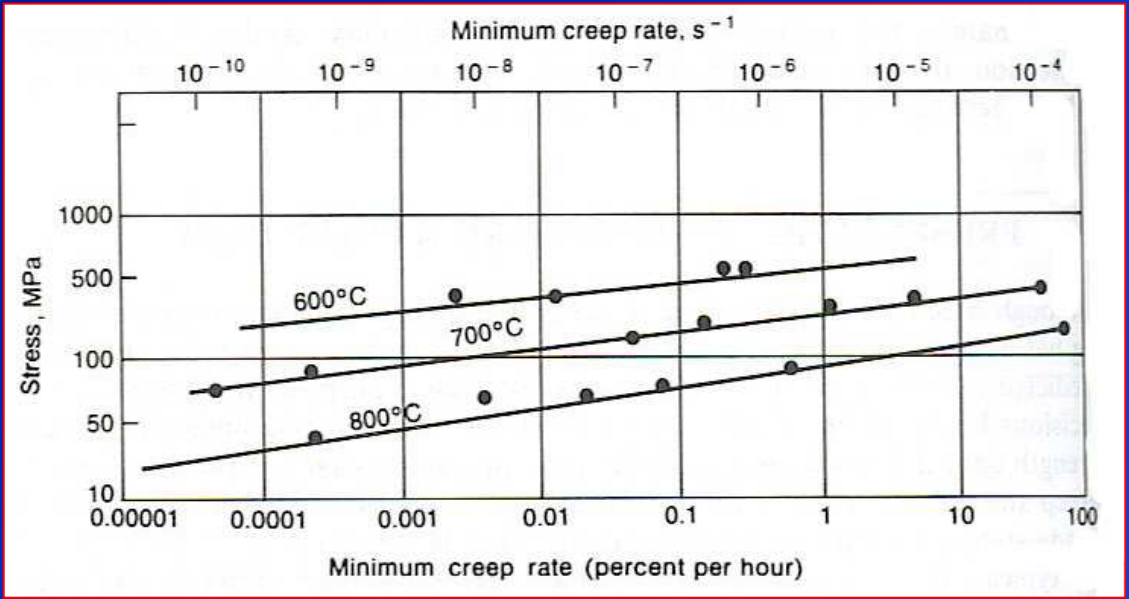

From stress and minimum creep rate curve, the ***working stress*** *using the safety factor of 3 can be obtained in the table below.*

Temperature	Creep strength, MPa	Working stress, MPa
600°C	210	70
800°C	30	10

Example: *For the stress-minimum creep rate curve, determine the activation energy for creep at a stress of 100 MPa.*

$$at\ T_2 = 700^o C = 973K;\ \dot{\varepsilon}_2 = 10^{-8} s^{-1}$$
$$at\ T_2 = 800^o C = 1073K;\ \dot{\varepsilon}_1 = 10^{-5} s^{-1}$$

From Eq.2

$$Q = \frac{R \ln(\dot{\varepsilon}_1 / \dot{\varepsilon}_2)}{(1/T_2 - 1/T_1)} = \frac{(8.3 Jmol^{-1} K^{-1}) \ln(10^3)}{1/973 - 1/1073} = 599 kJmol^{-1}$$

Reference

- Dieter, G.E., ***Mechanical metallurgy***, 1988, SI metric edition, McGraw-Hill, ISBN 0-07-100406-8.

Brittle fracture and impact tests

Subjects of interest

- *Objective*
- *The brittle-fracture problem*
- *Notch-bar impact tests*
- *Ductile to metal transition temperature curve*
- *Metallurgical factors affecting transition temperature.*
- *Drop-weight test and other large scale tests*
- *Embrittlement in metals*

Objectives

- *This chapter provides an understanding of characteristics and causes of brittle fracture and factors affecting brittle fracture will be indicated.*
- *The awareness of brittle fracture under service conditions will be made by the use of ductile to brittle transition temperature curve.*

The brittle-fracture problems

Failure of Liberty Ships during services in World War II.

The cause of failure was due to crack initiated from defects in the welded area and subjected to subzero temperature.

Three basic factors contribute to a brittle cleavage fracture.

1) Triaxial state of stress

2) Low temperature

3) High strain rate

Impact test

To determine the susceptibility of materials to brittle behaviour.

Notch bar impact test

- Notched bar test specimens are used in different sizes and designs.
- The ***Charpy impact specimen*** is the most widely used.
- The parameter (***energy absorption***) obtained are not readily expressed in terms of stress level, so it is difficult for design.
- Can use the test result to indicate how brittle the materials are.

The specimen is hit by a pendulum until fracture.

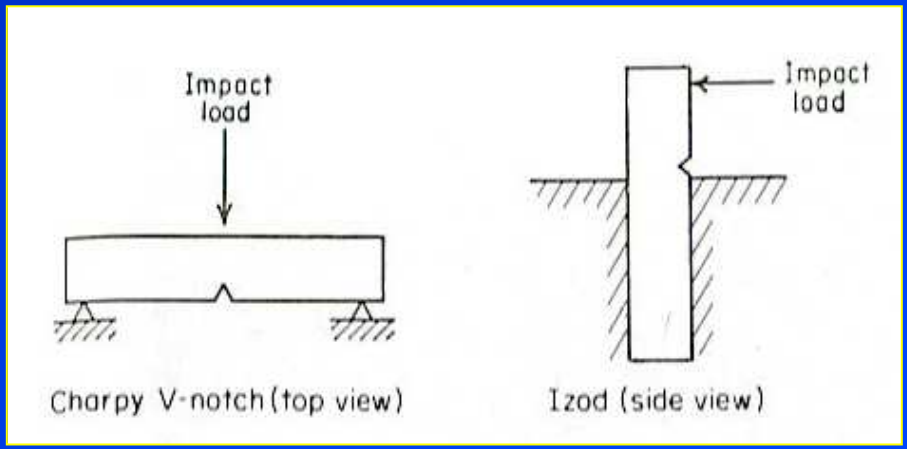

Method of loading in Charpy V notch and Izod tests.

The Charpy impact test

The Charpy test *measures the total energy absorbed during specimen fracture.*

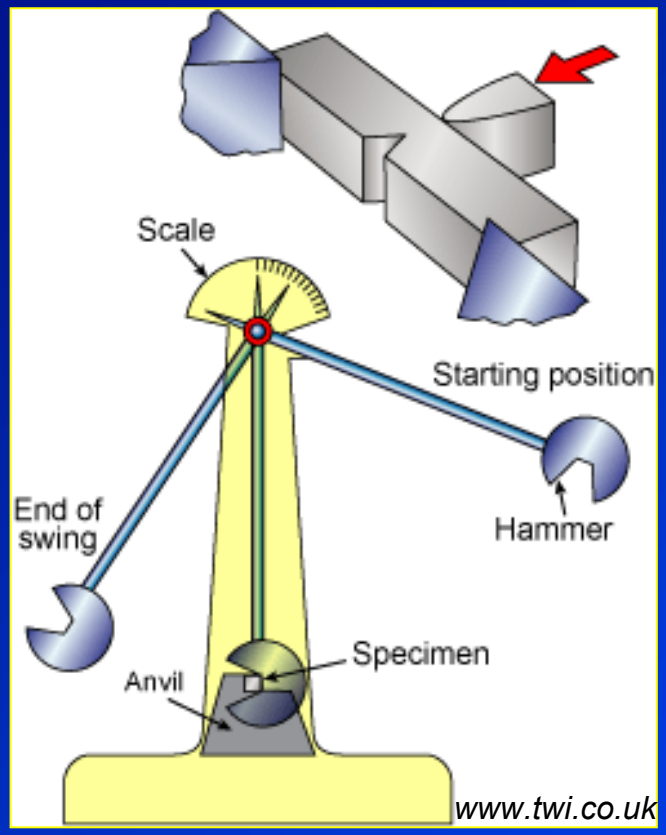

Charpy impact test diagram

- The standard Charpy specimen is hit by a ***pendulum*** at the opposite side of the notch and the ***energy required to break open is measured***.
- Standard specimen size is 10x10x55 mm^3 with a ***V notch*** of 2 mm deep, 45° angle and 0.25 mm root radius.

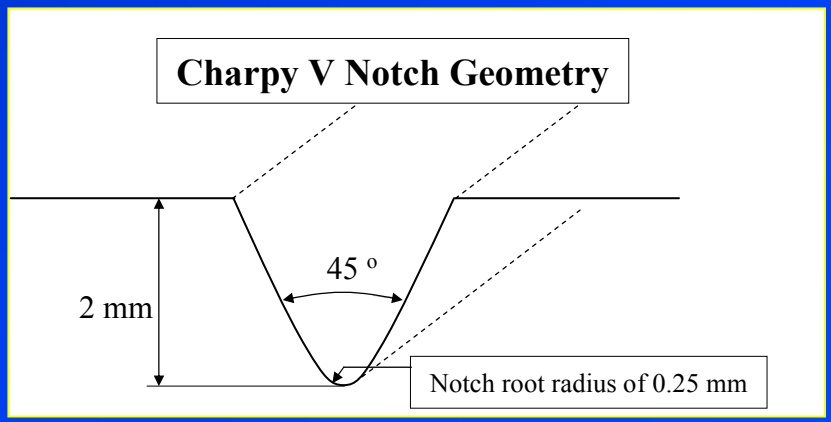

Absorbed energy ⬆ **Impact toughness** ⬆

Ductile to brittle transition temperature curve

- The ***absorbed energy (Joule)*** is plotted against testing temperature, giving a ductile to brittle transition temperature curve (***DBTT curve***).
- The curve represents a change in fracture behaviour from ***ductile at high temperature*** to ***brittle at lower temperature***.

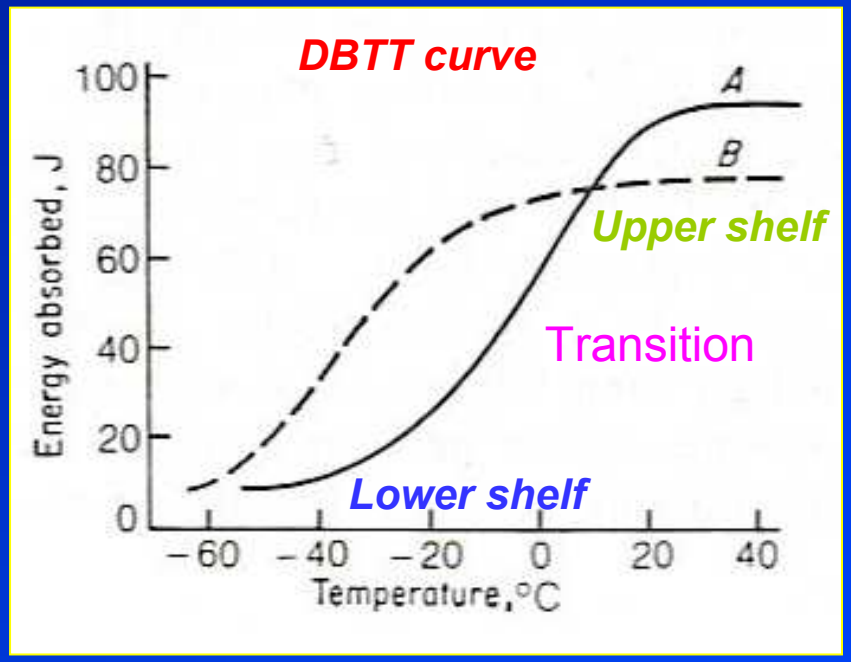

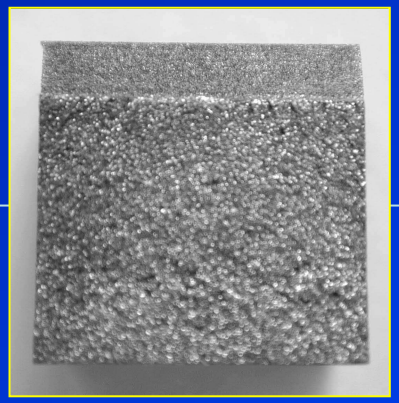

Lower shelf

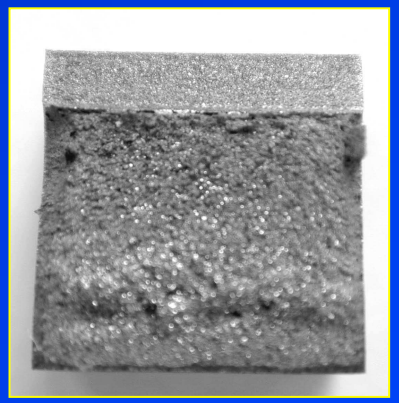

Transition – mixed mode

Upper shelf

Fracture surfaces of tested specimens

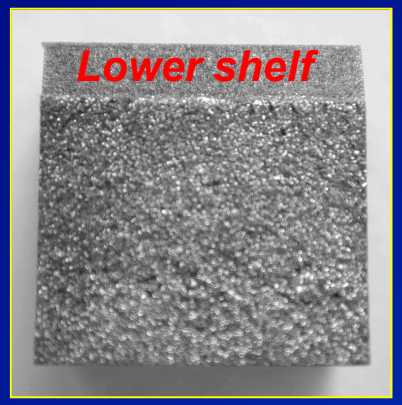

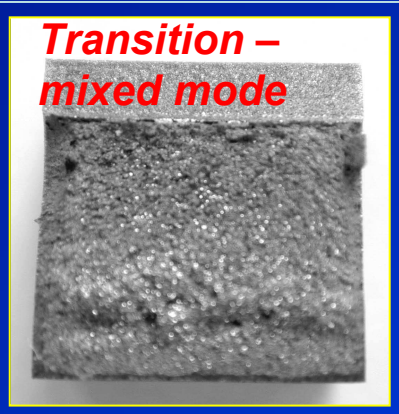

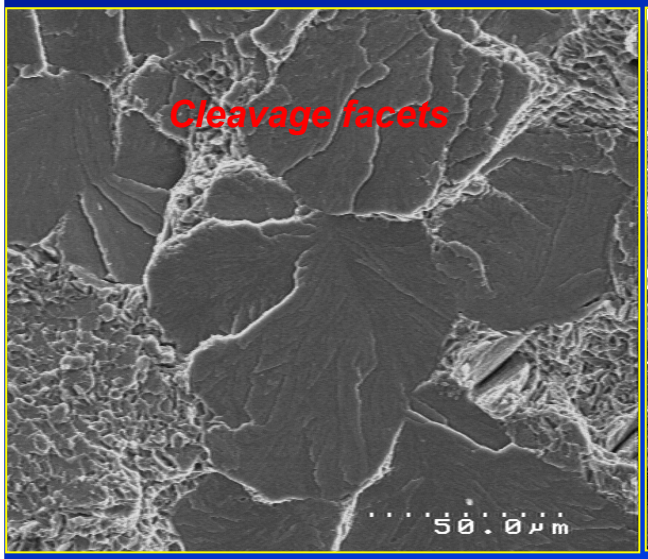

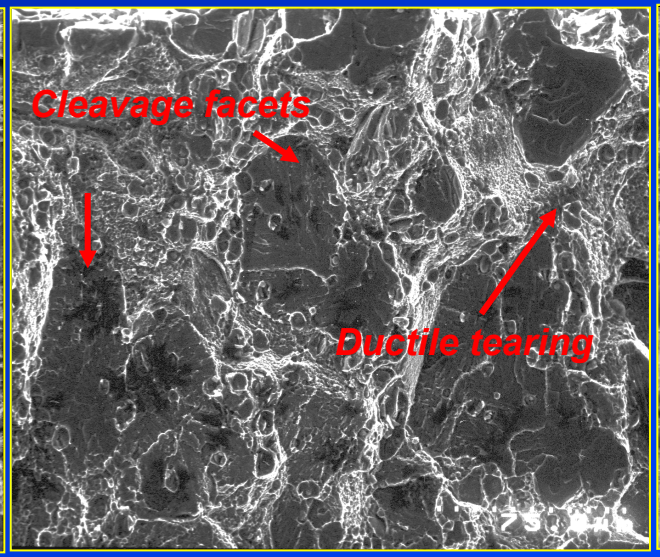

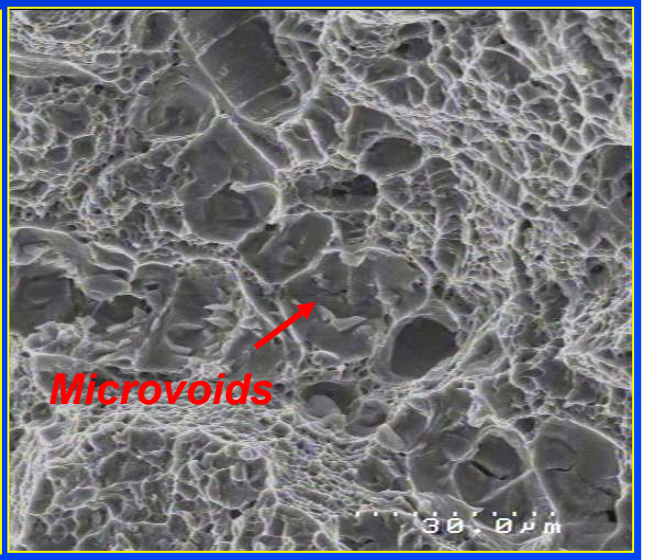

Brittle fracture

Mixed mode of brittle and ductile failures

Microvoid coalescence in ductile failure

Transition temperature

Different criteria are used to determine the ***transition temperature***, depending on the purpose of the application.

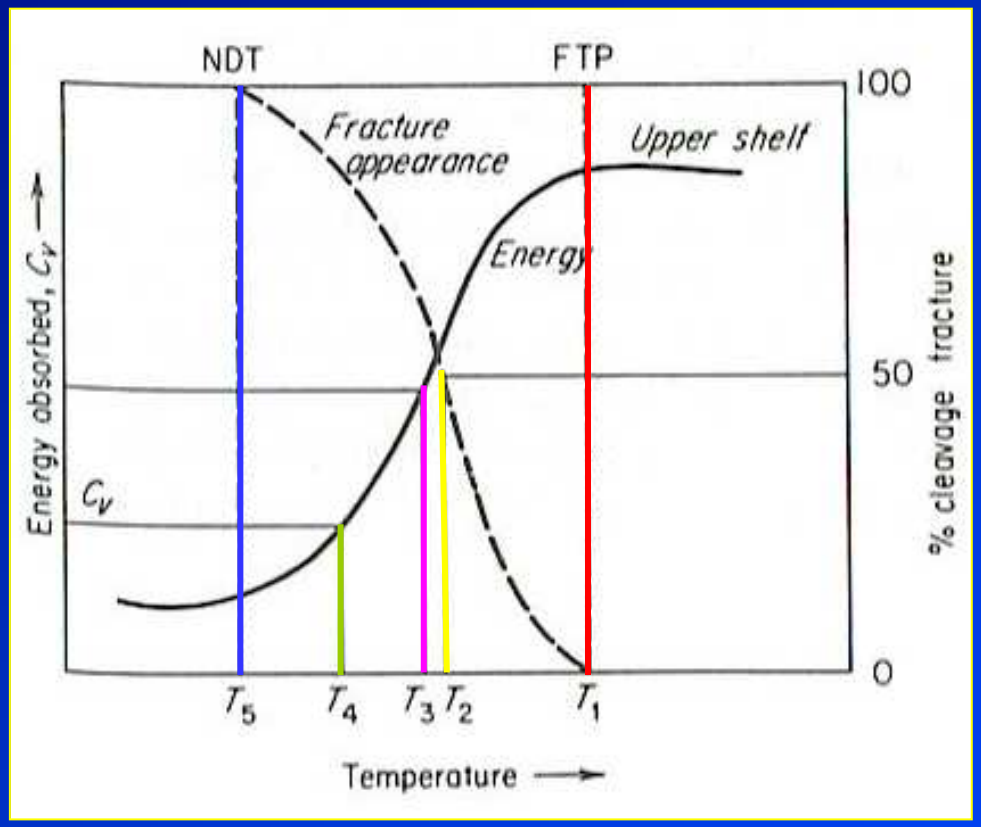

Various criteria of transition temperature obtained from Charpy test

1) ***T_1 transition temp*** is the ***Temp*** at which fracture is 100% ductile (fibrous).
2) ***T_2 transition temp*** is the Temp at which fracture is 50% cleavage and 50% ductile.
3) ***T_3 transition temp*** is the Temp at the average energy absorption of upper and lower shelves.
4) ***T_4 transition temp*** is the Temp defined at ***C_v*** = 20J.
5) ***T_5 transition temp*** is the Temp at which fracture is 100% cleavage.

Note: *FTP is fracture transition plastic*

Metallurgical factors affecting DBTT curves

- The ***shape and position*** of the ***DBTT curve*** is important because it determines the ***transition temperature,*** which indicates where it is safe to use for the required application.
- There are several factors affecting the ***DBTT curve.***

  - ***Crystal structure***
  - ***Interstitial atom***
  - ***Grain size***
  - ***Heat treatment***
  - ***Specimen orientation***
  - ***Specimen thickness***

Effect of crystal structure

• Only ***BCC structure materials*** experience ductile to brittle transition temperature. → be careful to select the ***service temperature***.

• This is due to limited active slip systems operating at low temperature. → ***very low plastic deformation***.

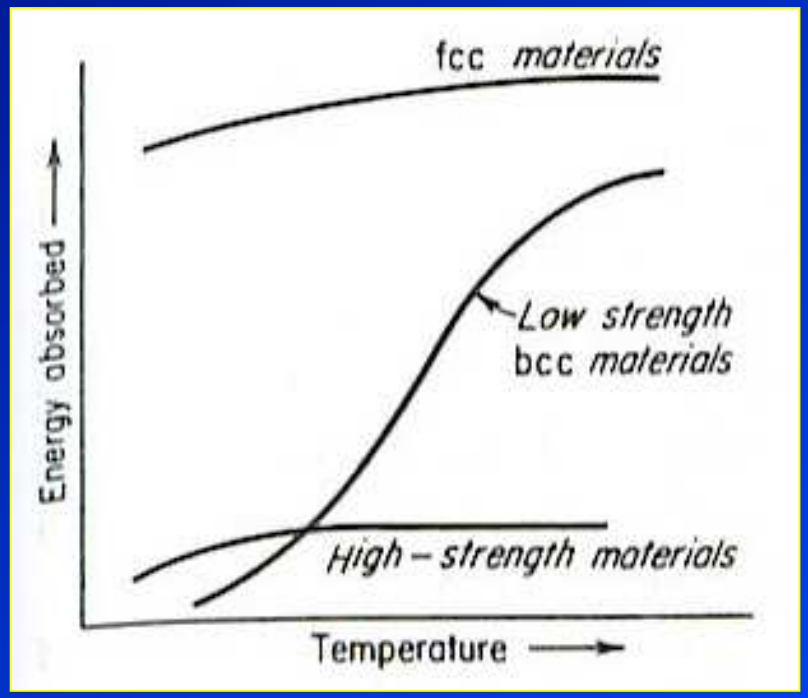

Relationship between energy absorption and test temperature

• ***Increasing temperature*** allows more slip systems to operate → more ***plastic deformation***.

• ***FCC*** and ***HCP*** metals do not experience ductile to brittle transition, therefore they give the same energy absorption at any temperatures.

Effect of interstitial atom

• ***Carbon*** and ***manganese*** contents have been observed to change the ***DBTT*** curve.

Carbon content → **Smoother curve** → **Higher Transition temp** → ***Become ductile at higher temperature***

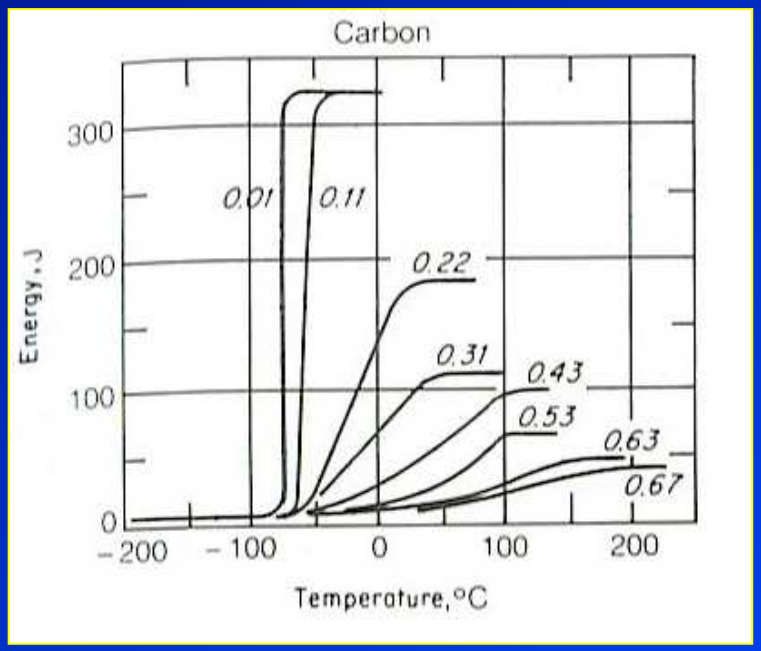

Effects of carbon content on DBTT curves for steel

Ex: in steel

• ***Mn: C ratio*** should be at least 3:1 to satisfy notch toughness.

• ***P, Si, Mo, O*** raise the transition temperature while ***Ni*** is beneficial to notch toughness.

Effect of grain size

- Grain size has a strong effect on transition temperature.

Grain size ↓ **Transition temperature** ↓

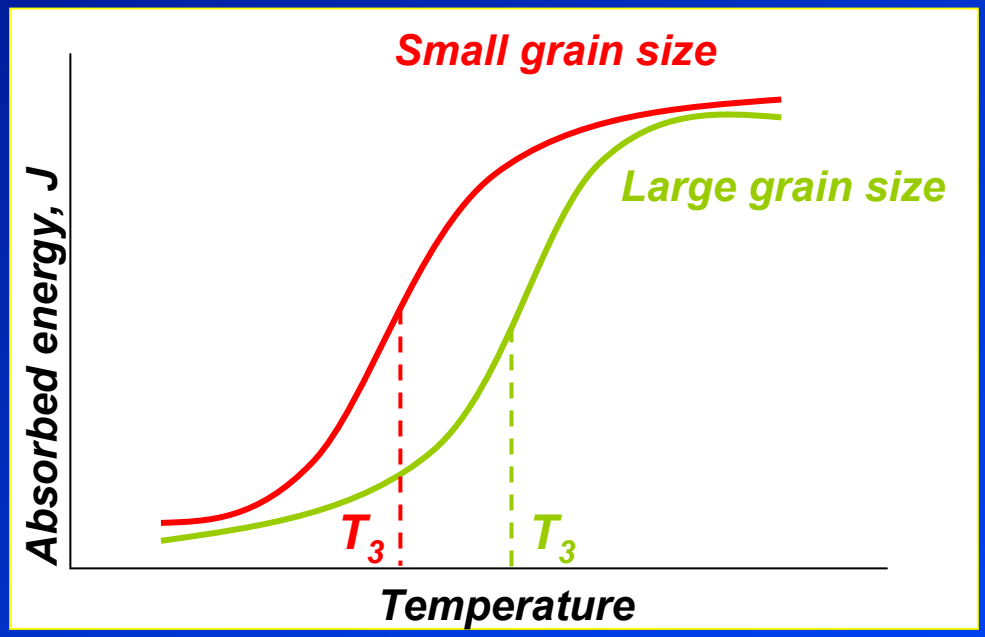

- *Reducing grain size shifts the DBTT curve to the left → has a wider range of service temperatures.*
- *Heat treatments that provide grain refinement such as air cooling, recrystallisation during hot working help to lower transition temperature.*

Effect of heat treatment

- ***Tempered martensitic structure steel*** produces the best combination of strength and impact toughness.

Tempering temperature ⬆

Energy absorption ⬆

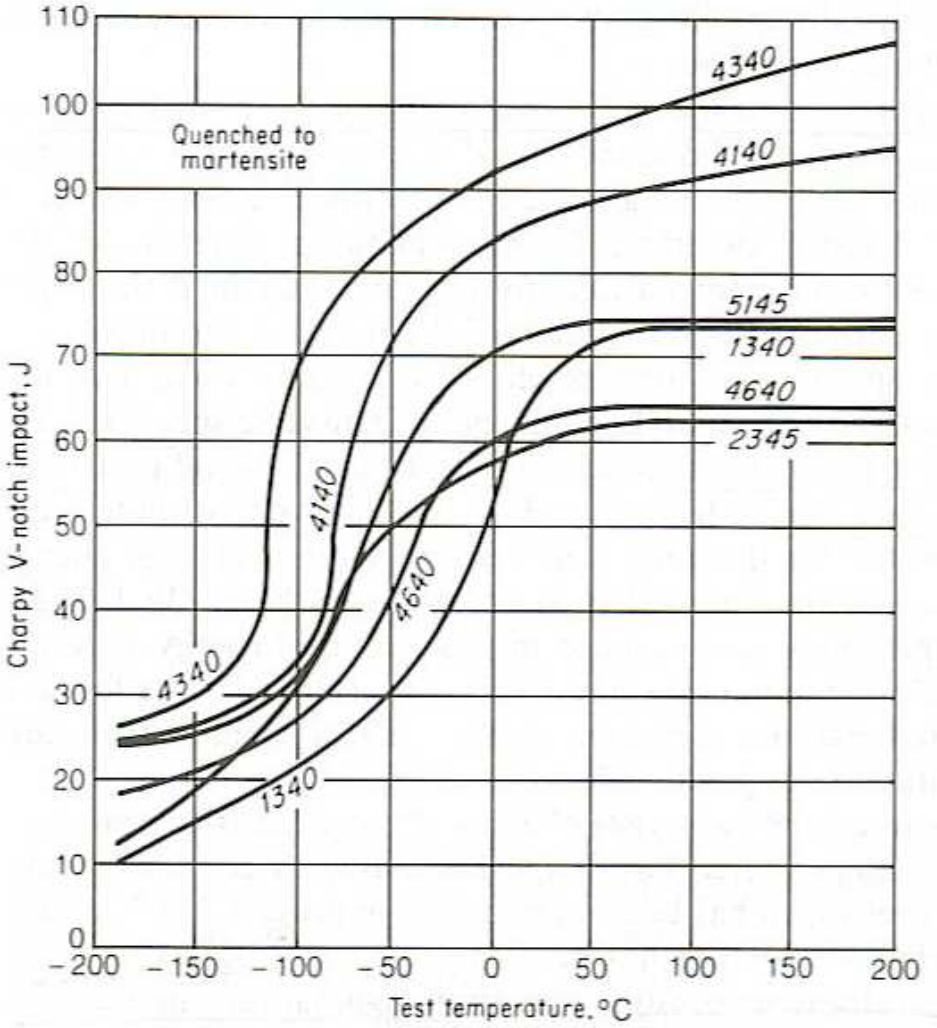

DBTT curves of different alloy steel, having tempered martensitic structure

Effect of specimen orientation

• For impact test, ***anisotropic properties*** are also observed in ***rolled or forged products***, giving different energy absorption according to ***specimen orientations***.

• ***Longitudinal (B)*** shows the best energy absorption because the crack propagation is across the fibre alignment.

• ***Transverse (C)*** gives the worst energy absorption because the crack propagates parallel to the rolling direction.

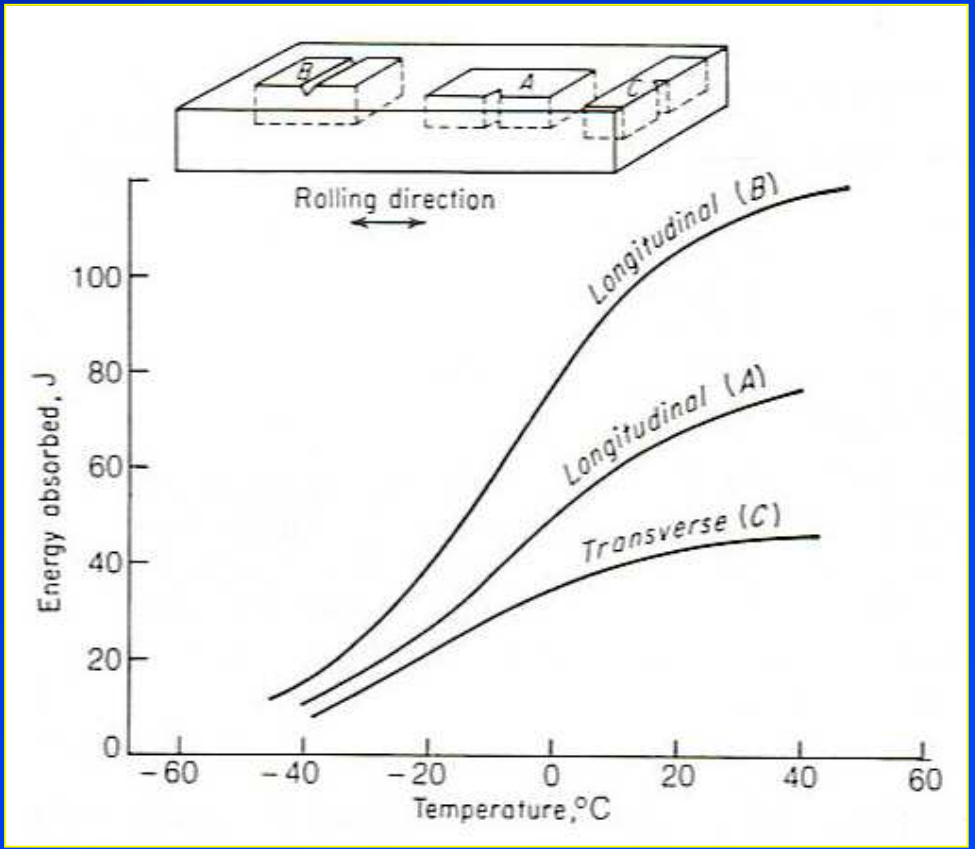

Effect of specimen orientation on DBTT curve

Effect of specimen thickness

• ***Larger specimen size*** (in-service components) provides higher constraint → ***more brittle***.

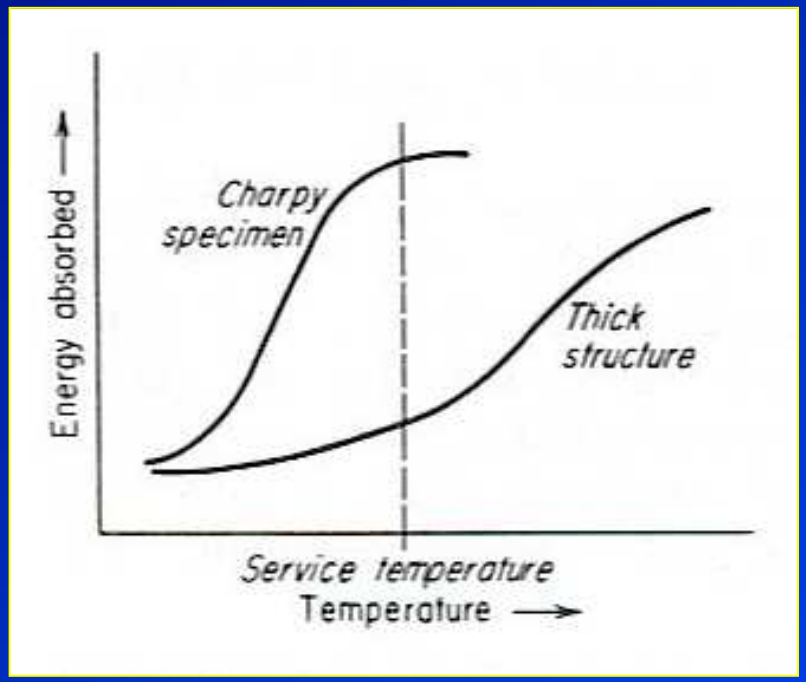

Effect of section thickness on transition temperature

If large size specimens are used, the transition temperature will increase.

Large scale tests

Drop-weight test and other large scale tests

- Several techniques have been developed to test specimens with different sizes to suit the applications.
- The ***specimen thickness*** is at least 25 mm.

1) Explosion-crack starter test

2) Drop-weight test (DWT)

3) Dynamic-tear test (DT)

4) Robertson crack-arrest test

Explosion crack starter test

- The plate was placed over a circular die and dynamically loaded with an ***explosive charge***.
- The **brittle weld bead** introduces a ***small natural crack*** in the test plate.
- The test is carried out over a temperature range, giving ***different fracture appearance***.

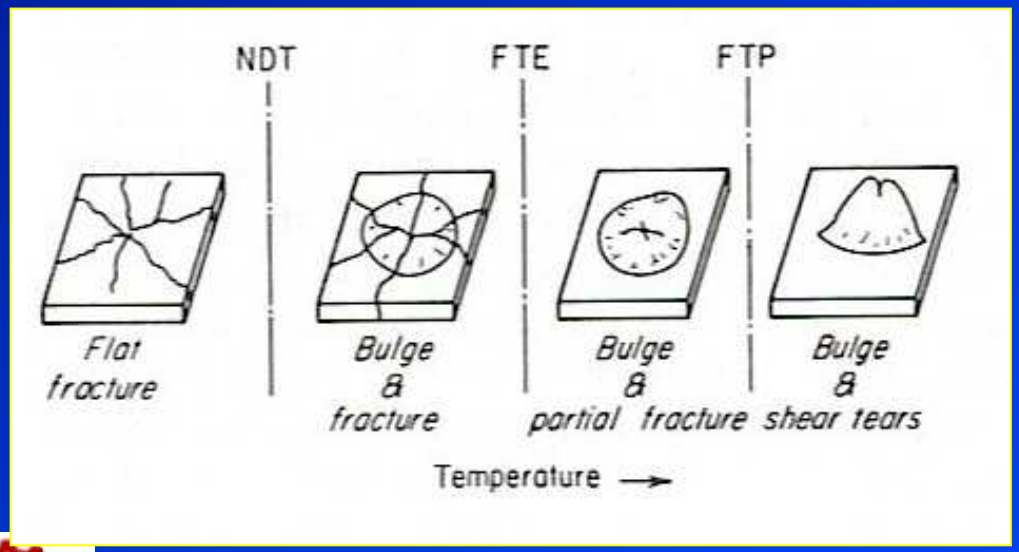

Fracture appearance vs temperature

NDT – nil ductility temperature

FTE – Fracture transition elastic

FTP – Fracture transition plastic

Plate dimensions : 350x350x25 mm^3

Drop weight test

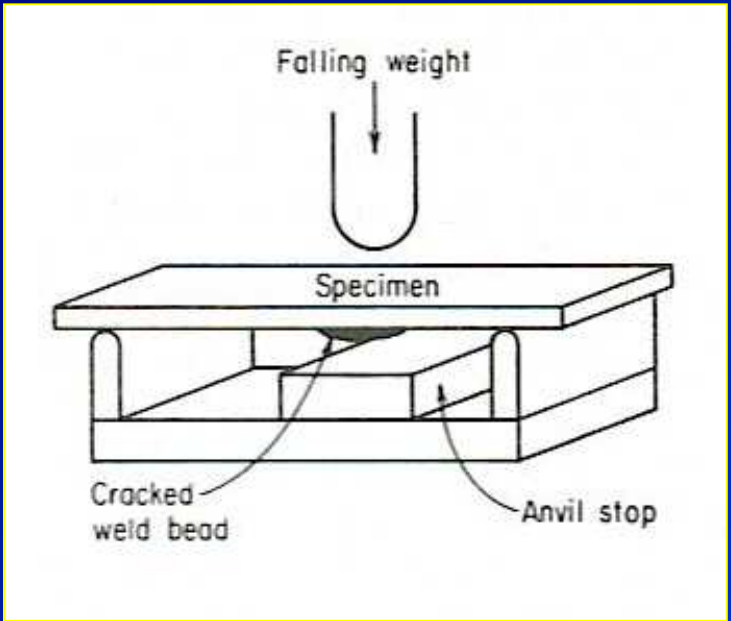

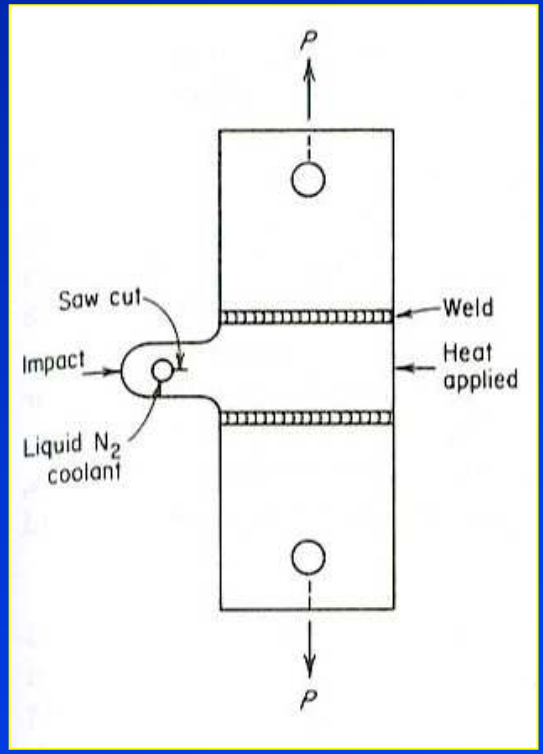

Robertson crack-arrest test.

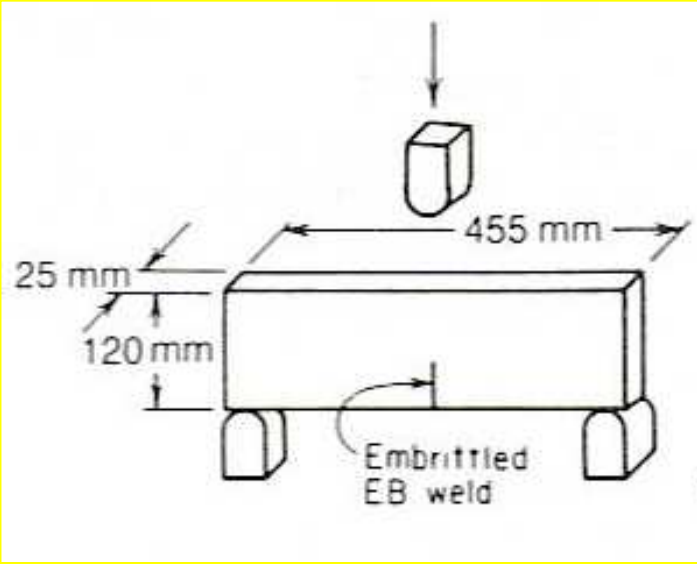

Dynamic tear test

Embrittlement in metals

- *Temper embrittlement*
- *Hydrogen embrittlement*
- *Stress corrosion cracking*
- *Liquid metal embrittlement*
- *Neutron embrittlement*

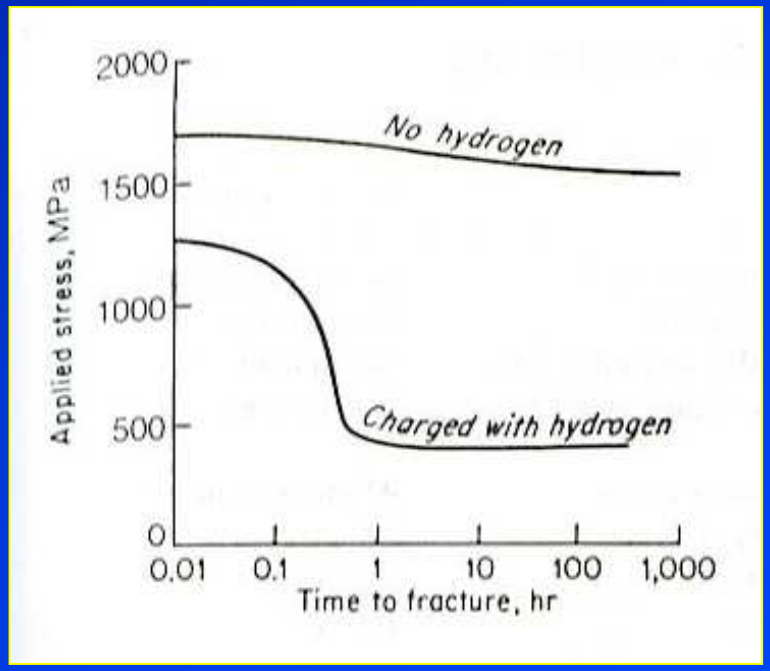

Delayed fracture curve

Reference

- Dieter, G.E., ***Mechanical metallurgy***, 1988, SI metric edition, McGraw-Hill, ISBN 0-07-100406-8.